8-1988

Paleoenvironmental Analysis and Test of Stratigraphic Cyclicity in the Nolichucky Shale and Maynardville Limestone (Upper Cambrian) in Central East Tennessee

Lawrence James Weber Jr.
University of Tennessee - Knoxville

Recommended Citation

Weber, Lawrence James Jr., "Paleoenvironmental Analysis and Test of Stratigraphic Cyclicity in the Nolichucky Shale and Maynardville Limestone (Upper Cambrian) in Central East Tennessee. " PhD diss., University of Tennessee, 1988.
https://trace.tennessee.edu/utk_graddiss/1379

To the Graduate Council:

I am submitting herewith a dissertation written by Lawrence James Weber Jr. entitled "Paleoenvironmental Analysis and Test of Stratigraphic Cyclicity in the Nolichucky Shale and Maynardville Limestone (Upper Cambrian) in Central East Tennessee." I have examined the final electronic copy of this dissertation for form and content and recommend that it be accepted in partial fulfillment of the requirements for the degree of Doctor of Philosophy, with a major in Geology.

Kenneth R. Walker, Major Professor

We have read this dissertation and recommend its acceptance:

Steven G. Driese, Thomas W. Broadhead, Edward E. Clebsch

Accepted for the Council:

Carolyn R. Hodges

Vice Provost and Dean of the Graduate School

(Original signatures are on file with official student records.)

To the Graduate Council:

I am submitting herewith a dissertation written by Lawrence James Weber, Jr. entitled "Paleoenvironmental Analysis and Test of Stratigraphic Cyclicity in the Nolichucky Shale and Maynardville Limestone (Upper Cambrian) in Central East Tennessee." I have examined the final copy of this dissertation for form and content and recommend that it be accepted in partial fulfillment of the requirements for the degree of Doctor of Philosophy, with a major in Geology.

Kenneth R. Walker

Kenneth R. Walker, Major Professor

We have read this dissertation
and recommend its acceptance:

Steven G. Driese

Thomas W. Broadhead

Edward E.C. Clebsch

Accepted for the Council:

CWMinkel

Vice Provost
and Dean of The Graduate School

PALEOENVIRONMENTAL ANALYSIS AND TEST OF STRATIGRAPHIC CYCLICITY IN THE NOLICHUCKY SHALE AND MAYNARDVILLE LIMESTONE (UPPER CAMBRIAN) IN CENTRAL EAST TENNESSEE

A Dissertation
Presented for the
Doctor of Philosophy
Degree
The University of Tennessee, Knoxville

Lawrence James Weber Jr.

August 1988

ACKNOWLEDGEMENTS

Special appreciation is given to Dr. Kenneth R. Walker, Carden Professor of the Department of Geological Sciences, for his close supervision and advice during the course of this work. This dissertation has benefited greatly from his scholarly and financial help. In addition, I would like to thank Ken for his friendship and his genuine concern for my well-being during my tenure at the University of Tennessee.

I am grateful to the members of my committee, Drs. T.W. Broadhead, E.E. Clebsch, and S.G. Driese, for their guidance and critical review of this study. I appreciate the aid given to me by Dr. C. Steven Haase. Also, I would like to thank M.L. McKinney and J.F. Read for their critical review of earlier drafts of Chapters 3 and 4.

It is a pleasure to acknowledge L. Foreman, G. Jernigan, E. Johnson, M. Kozar, K. Roberson, M. Steinhauff, and other past and present members of the Carbonate Research Group at the University of Tennessee for many enlightening and constructive discussions. I would like to thank L. Hardie, S. Moshier, and A.R. Palmer for allowing me to tap their knowledge of Cambrian rocks while in the field. Oak Ridge National Laboratory and S. Haase are acknowledged for allowing access to drill core. Field assistance was provided in part by D. Reeves, M. Kozar, and my wife, Teri, who also edited part of the manuscript.

The major source of funding for my research was a research fellowship from the Environmental Sciences Division of Oak Ridge

National Laboratory. This research has also been supported by grants from the Mobil Carbonate Fund, the Appalachian Basin Industrial Associates, Sigma Xi, the American Association of Petroleum Geologists, the Geological Society of America, and the Professors Honor Fund of the Department of Geological Sciences of the University of Tennessee. I especially thank Sun Exploration and Production Company for their generous financial support of this work.

ABSTRACT

The Upper Cambrian Nolichucky Shale and Maynardville Limestone (upper Conasauga Group) crop out along a succession of southeastward dipping imbricate thrust sheets, which trend northeast-southwest in the Valley and Ridge of eastern Tennessee. In the vicinity of Oak Ridge and Knoxville, Nolichucky and Maynardville outcrop and drill core have been examined at six localities. The Nolichucky contains an abundance of thick shale and thinly bedded shale and limestone, whereas the Maynardville is composed of very thick-bedded carbonate, predominantly limestone. In central east Tennessee fourteen major lithofacies are identified in the upper Conasauga Group. The Nolichucky/Maynardville sequence is subdivided into three parts representing: (1) a slightly "deeper" intracratonic basin (30-50 m water depth; lower Nolichucky, (2) a shallow intracratonic basin (5-30 m deep; upper Nolichucky), and (3) a peritidal platform (0-5 m deep; Maynardville).

The Nolichucky Shale was deposited in a storm-dominated paleoenvironmental setting, whereas the Maynardville Limestone is similar to other ancient tidally-influenced deposits. In the Nolichucky, the majority of carbonate production occurred in and around shoals and within cyanobacterial mats. Storms were effective in moving carbonate sediment off the shoals and mats into adjacent shale-dominated subtidal areas. The Maynardville represents small tidal flats that accreted vertically and migrated laterally. Sediment was produced in open-water subtidal areas, which were adjacent to tidal flats, and tides, storms, and fairweather waves transported sediment to nearby low-relief intertidal banks and supratidal islands. The distribution of facies along the Nolichucky/Maynardville bathymetric profile was much more irregular (mosaic-like) than predicted by the depositional model of earlier workers.

An integrated approach of overlying substitutability analysis, embedded Markov chain analysis, and modified autoassociation analysis to verify statistically the occurrence of cycles in stratigraphic sequences is applied to the upper Conasauga Group of central east Tennessee. Stratigraphic sections within the Nolichucky Shale and in the Maynardville Limestone show weakly developed cyclicity, which is probably a result of the storm- and tide-dominated paleoenvironmental setting. Local processes were more important in controlling lithologic repetition than were larger-scale processes (e.g., geoidal, tectonic, or glacioeustatic). Large-scale processes have been documented in modern and other ancient settings, but their record may be masked in many sequences by local events.

TABLE OF CONTENTS

CHAPTER PAGE

1. INTRODUCTION 1

  General Geologic Setting 1
  Paleogeography/Tectonic Setting 5
  Location/Stratigraphy 17
  Depositional Environment/Previous Work 20
  Biostratigraphy of Upper Conasauga Group 23
    Trilobites 25
    Conodonts 27
    Acritarchs 28
  Purpose 29

2. STRATIGRAPHY, SEDIMENTOLOGY, PETROLOGY, AND DEPOSITIONAL ENVIRONMENTS OF THE UPPER CONASAUGA GROUP (NOLICHUCKY SHALE AND MAYNARDVILLE LIMESTONE) IN EAST TENNESSEE 31

  Introduction 31
    Descriptive Stratigraphy 33
      Pumpkin Valley Shale 34
      Rutledge Limestone 35
      Rogersville Shale 35
      Maryville Limestone 36
      Nolichucky Shale 37
      Maynardville Limestone 38
      Post-Conasauga Group Strata 39
    Scope of Study 40
    Methods of Investigation 41
  Facies Analysis 43
    Introduction 43
    Cryptalgalaminate (CL) 52
      Description 52
      Interpretation 54
    Stromatolites (STROM) 58
      Description 58
      Interpretation 63
    Thrombolites (THROM) 64
      Description 64
      Interpretation 68
    Oncolitic-Oolitic Packstone/Grainstone (NOPG) 70
      Description 70
      Interpretation 74
    Peloidal Packstone/Grainstone (EPG) 76
      Description 76
      Interpretation 83

CHAPTER PAGE

Mudstone Interbedded With Shale (MWS) 85
  Description 85
  Interpretation 88
Oolitic Packstone/Grainstone (OPG) 89
  Description of Thick Lenticular Buildups 89
  Interpretation 96
  Description of Thin Sand Sheets 97
  Interpretation 98
Fossiliferous Packstone/Grainstone (FPG) 99
  Description 99
  Interpretation 103
Fossiliferous Packstone/Grainstone Interbedded with Shale (FPGWS) 103
  Description 103
  Interpretation 106
Laminated Peloidal Packstone/Grainstone (XPG) 108
  Description 108
  Interpretation 112
Laminated Peloidal Packstone/Grainstone Interbedded with Shale (XPGWS) 115
  Description 115
  Interpretation 120
Shale Interbedded with Laminated Peloidal Packstone/Grainstone (SWXPG) 121
  Description 121
  Interpretation 121
Shale (S) 125
  Description 125
  Interpretation 127
Intraclastic Packstone/Grainstone (IPG) 130
  Description 130
  Interpretation 133
Summary of Depositional Environments 139

3. USING MULTIPLE ANALYTICAL TECHNIQUES FOR THE RECOGNITION OF SEDIMENTARY CYCLES 141

Introduction 141
Discussion of Techniques 143
  Markov Chain Analysis 143
  Substitutability Analysis 150
  Auto-Association Analysis 152
  Runs Test 154
Integration of Techniques 156
Summary and Conclusions 159

CHAPTER PAGE

4. CYCLICITY IN THE UPPER CAMBRIAN OF THE SOUTHERN APPALACHIANS: A TEST OF OBJECTIVE STATISTICAL TECHNIQUES 161

Introduction 161
Geological Setting 163
Location/Stratigraphy 163
Lithology 164
Depositional Environment 173
Procedure 176
Classification of Lithologies 176
Categorizing Lithologies 177
Testing for Cyclicity 185
Results 187
Problems Involved in Analysis of Cyclicity 201
Conclusions 205

5. ENVIRONMENTAL SYNTHESIS AND MODEL FOR THE UPPER CONASAUGA NOLICHUCKY SHALE AND MAYNARDVILLE LIMESTONE SEQUENCE 207

Introduction 207
Stratigraphic Setting 209
Distribution of Lithofacies 209
Origin of Sedimentary Features and Structures 211
Depositional Model 221

6. SUMMARY AND CONCLUSIONS 229

LIST OF REFERENCES 234

APPENDICES 259

A. STANDARD MEASUREMENT CONVENTIONS 260
B. DESCRIPTION OF STRATIGRAPHIC SECTIONS 262
C. PETROGRAPHIC CONSTITUENT ANALYSIS 347
D. X-RAY DIFFRACTION ANALYSIS OF SHALE 381

VITA 388

LIST OF TABLES

TABLE PAGE

1.1. Representative Paleoenvironmental and Sedimentologic Studies of the Cambrian System in North America 3

2.1. Rock Classification Schemes Used to Describe the Nolichucky/Maynardville Sequence 44

2.2. The 14 Major Lithofacies Which Occur in the Upper Conasauga Group 45

2.3. Constituent Composition of Lithofacies 48

2.4. Characteristics of the CL Lithofacies 53

2.5. Characteristics of the STROM Lithofacies 59

2.6. Characteristics of the THROM Lithofacies 65

2.7. Characteristics of the NOPG Lithofacies 71

2.8. Characteristics of the EPG Lithofacies 77

2.9. Characteristics of the MWS Lithofacies 86

2.10. Characteristics of the OPG Lithofacies 90

2.11. Characteristics of the FPG Lithofacies 100

2.12. Characteristics of the FPGWS Lithofacies 104

2.13. Characteristics of the XPG Lithofacies 109

2.14. Characteristics of the XPGWS Lithofacies 116

2.15. Characteristics of the SWXPG Lithofacies 122

2.16. Characteristics of the S Lithofacies 126

2.17. Characteristics of Shale Matrix Conglomerates 134

2.18. Characteristics of Lime Mud and Coarse-grained Matrix Conglomerates 135

2.19. Characteristics of Coarse-grained Matrix Conglomerates 136

TABLE PAGE

2.20. Summary of Depositional Environments 140

C.1. Analysis of CL Lithofacies 348

C.2. Analysis of STROM Lithofacies 349

C.3. Analysis of THROM Lithofacies 350

C.4. Analysis of NOPG Lithofacies 351

C.5. Analysis of EPG Lithofacies 352

C.6. Analysis of MWS Lithofacies 354

C.7. Analysis of OPG Lithofacies 356

C.8. Analysis of FPG Lithofacies 362

C.9. Analysis of FPGWS Lithofacies 364

C.10. Analysis of XPG Lithofacies 366

C.11. Analysis of XPGWS Lithofacies 368

C.12. Analysis of SWXPG Lithofacies 370

C.13. Analysis of S Lithofacies 372

C.14. Analysis of IPG Lithofacies 375

D.1. Samples Used in XRD Analysis of Shale 384

D.2. D-Spacings in (Angstrom units) of the Observed X-Ray Diffraction Peaks 385

D.3. Identification of the Principal Clay Minerals and Quartz in the Nolichucky 386

LIST OF FIGURES

FIGURE PAGE

1.1. Present Outcrop and Subsurface Distribution of Cambrian Rocks in North America 2

1.2. Tectonic Framework of the Craton during Late Precambrian and Cambrian Time 4

1.3. Generalized Stratigraphic Nomenclature of Cambrian Strata in East Tennessee and Nearby Areas 6

1.4. Regional Lithofacies Distribution during the Late Early Cambrian 9

1.5. Key to Symbols Used to Indicate Environments of Deposition in the Series of Paleogeographic Maps 10

1.6. Regional Lithofacies Distribution during the Late Middle Cambrian 12

1.7. Regional Lithofacies Distribution during the Early Late Cambrian (Nolichucky Time) 14

1.8. Regional Lithofacies Distribution during the Early Late Cambrian (Maynardville Time) 15

1.9. Regional Lithofacies Distribution during the Late Late Cambrian 16

1.10. Exposures of Conasauga Group in East Tennessee and Locations of Measured Sections 18

1.11. Stratigraphic Relationships of the Formations within the Conasauga Group 19

1.12. Knoxville and Oak Ridge Vicinity Showing Measured Outcrop and Drill Core Used in This Study 21

1.13. Generalized Temporal Relationship of Cambrian Formations in East Tennessee 26

2.1. Palinspastic Base Map of East Tennessee Showing the Three Major Phases of Middle and Late Cambrian Sedimentation 32

2.2. Comparative Analysis between the Nolichucky Shale and Maynardville Limestone Showing the Relative Abundance of Each Lithofacies 46

FIGURE PAGE

2.3. Comparative Analysis between the Nolichucky Shale and Maynardville Limestone Showing the Rock-Unit Thickness and Bed Thickness of Each Lithofacies 47

2.4. Selected Features of the Cryptalgalaminate (CL) Lithofacies 55

2.5. Characteristics of Maynardville Stromatolites 61

2.6. Selected Features of the Thrombolite (THROM) Lithofacies 66

2.7. Selected Features of the Oncolitic-Oolitic (NOPG) Lithofacies 72

2.8. Selected Features of the Peloidal Packstone/Grainstone (EPG) Lithofacies 78

2.9. Selected Features of the Mudstone Interbedded with Shale (MWS) Lithofacies 81

2.10. Selected Features of the Oolitic Packstone/Grainstone (OPG) Lithofacies 91

2.11. Additional Features of the Oolitic Packstone/Grainstone (OPG) Lithofacies 93

2.12. Selected Features of the Fossil-dominated (FPG and FPGWS) Lithofacies 101

2.13. Selected Features of the Laminated Peloidal Packstone/Grainstone (XPG) Lithofacies 110

2.14. Selected Features of the Laminated Peloidal Packstone/Grainstone Interbedded with Shale (XPGWS) Lithofacies 117

2.15. Selected Features of the Shale-dominated (SWXPG and S) Lithofacies 123

2.16. Selected Features of the Intraclastic Packstone/Grainstone (IPG) Lithofacies 131

3.1. Transition Frequency Matrix of a Hypothetical Stratigraphic Column Composed of Four Distinct Lithologies 144

3.2. Transition Frequency Matrix 146

FIGURE PAGE

3.3. Difference Matrix 148

3.4. Lithologies Used to Show the Three Types of Substitutability 151

3.5. An Example of a Substitutability Matrix 151

3.6. Autoassociation Analysis using Hypothetical Stratigraphic Section and Repetitive Subset Described in Text 153

3.7. A Plot Showing the Thickness of Each Similar Cycle Versus the Number of Cycles in a Stratigraphic Section 155

3.8. Flow Diagram Summarizing the Procedure to Test for Presence of Cycles 158

4.1. Fourteen Recurring Lithologies within the Upper Conasauga Group 166

4.2. Distinguishing Features of the 10 Most Dominant Lithologies Recognized in the Nolichucky Shale 168

4.3. Distinguishing Features of the 9 Most Dominant Lithologies Recognized in the Maynardville Limestone 169

4.4. Bar Graph Showing the Distribution of the Ten Most Common Lithologies in the Nolichucky Shale at Five Different Localities 170

4.5. Bar Graph Showing the Distribution of the Nine Most Common Lithologies in the Maynardville Formation at Three Different Localities 172

4.6. Generalized Stratigraphic Section of the Nolichucky Shale and Maynardville Limestone Showing Overall Lithologic Character and Stratigraphic Distribution of Environmentally Sensitive Criteria 175

4.7. Lithologies Observed at I-75 before Grouping Similar Lithologies by Use of Substitutability Analysis 178

FIGURE PAGE

4.8. A 15 X15 Transition Frequency Matrix which Represents the Upper 94 Meters of the Late Cambrian Nolichucky Shale Located along Interstate 75 179

4.9. Downward Transition Probability Matrix 182

4.10. Overlying Substitutability Matrix 183

4.11. Overlying Substitutability Dendogram 184

4.12. Iterative Approach Used to Identify Most Complex Markov Chain 188

4.13. An 8 X 8 Transition Frequency Matrix for I-75 Outcrop of Nolichucky 189

4.14. Computer-generated Table Showing Results of Markov Chain Analysis for I-75 Outcrop of Nolichucky 190

4.15. Graphical Display of Lithologic Transitions which are Observed More Often than Expected in the Nolichucky Outcrop at I-75 191

4.16. Modified Autoassociation Analysis Showing the Stratigraphic Position and Range of Cycles for Nolichucky Shale at I-75 Outcrop 192

4.17. Transition Frequency Matrices That Reveal the Most Complex Markov Chain 194

4.18. Graphic Display of Cycles as Determined from Embedded Markov Chain Analysis of Transition Frequency Matrices in Figure 4.17 196

4.19. The Vertical and lateral Extent of Stratigraphic Intervals of Identical, Statistically Valid Cycles 197

4.20. Characteristics of Each Cycle Shown in Figure 4.19 199

5.1. Map of North America Showing the Location of the Equator during Middle and Late Cambrian Time 210

5.2. Columnar Sections of the Nolichucky Shale and Maynardville Limestone 212

5.3. Palinspastic Base Map Showing Each Locality 219

FIGURE PAGE

5.4. Generalized Block Diagram Showing Major Lithofacies Patterns and Environments of the Nolichucky Shale 222

5.5. Block Diagram Showing Three-Dimensional Reconstruction of the Maynardville Limestone 223

5.6. Detailed Block Diagram Showing Area "X" of Figure 5.4 225

5.7. Detailed Block Diagram Showing Area "Y" of Figure 5.4 226

5.8. Detailed Block Diagram Showing Area "Z" of Figure 5.4 228

D.1. Typical X-Ray Diffractogram of the Nolichucky Shale 387

CHAPTER 1

INTRODUCTION

General Geologic Setting

The Cambrian System records the first major episode of cratonic flooding on the North American continental plate (Sloss, 1963). Seas transgressed onto the Canadian Shield resulting in an onlap of predominantly fine-grained siliciclastics and carbonates during much of the Cambrian (Lochman-Balk, 1971). Remnants of these sedimentary rocks now occur as a discontinuous fringe around the shield area (Figure 1.1). Coeval rocks in areas such as Australia, Argentina, Siberia, and China were deposited in a similar depositional style (Ross, 1975; Scotese and others, 1979). In North America, Cambrian rock units have been studied extensively for at least a century. However, detailed paleoenvironmental and sedimentologic investigations have been conducted only during the past 25 years and have focused primarily on carbonate rocks (Table 1.1).

Along the southeastern margin of the North American craton (Figure 1.2), much of the Cambrian System represents shallow water deposition on a vast carbonate platform or rim complex (Palmer, 1971). Southeast of the platform margin a subsiding oceanic-type basin trapped deep water pelitic sediments (Rodgers, 1968; Bird and Dewey, 1970) (Figure 1.2). In a transect from the platform edge, northwestward onto the

Figure 1.1. Present outcrop and subsurface distribution (cross-hatched) of Cambrian rocks in North America, after Cook and Bally (1975).

Table 1.1. Representative paleoenvironmental and sedimentologic studies of the Cambrian System in North America (published citations focus on carbonate or integrated carbonate and fine-grained siliciclastic analyses).

Region	Citation
Southern Canadian Rocky Mts.	Aitken, 1966
	Aitken, 1967
	Aitken, 1978
Western United States	Palmer, 1971
	Kepper, 1972
	Lohmann, 1976
	Rees and others, 1976
	Taylor and Cook, 1976
	Cook and Taylor, 1977
	McIlreath, 1977
	Kepper, 1981
	Rees, 1986
Texas	Ahr, 1971
U. S. Appalachian Mts.	Harris, 1973
	Hubert and others, 1977
	Keith and Friedman, 1977
	Reinhardt, 1977
	Pfiel and Read, 1980
	Markello and Read, 1982
	Demicco, 1985
Canadian Appalachian Mts.	Chow and James, 1987a
	Chow and James, 1987b

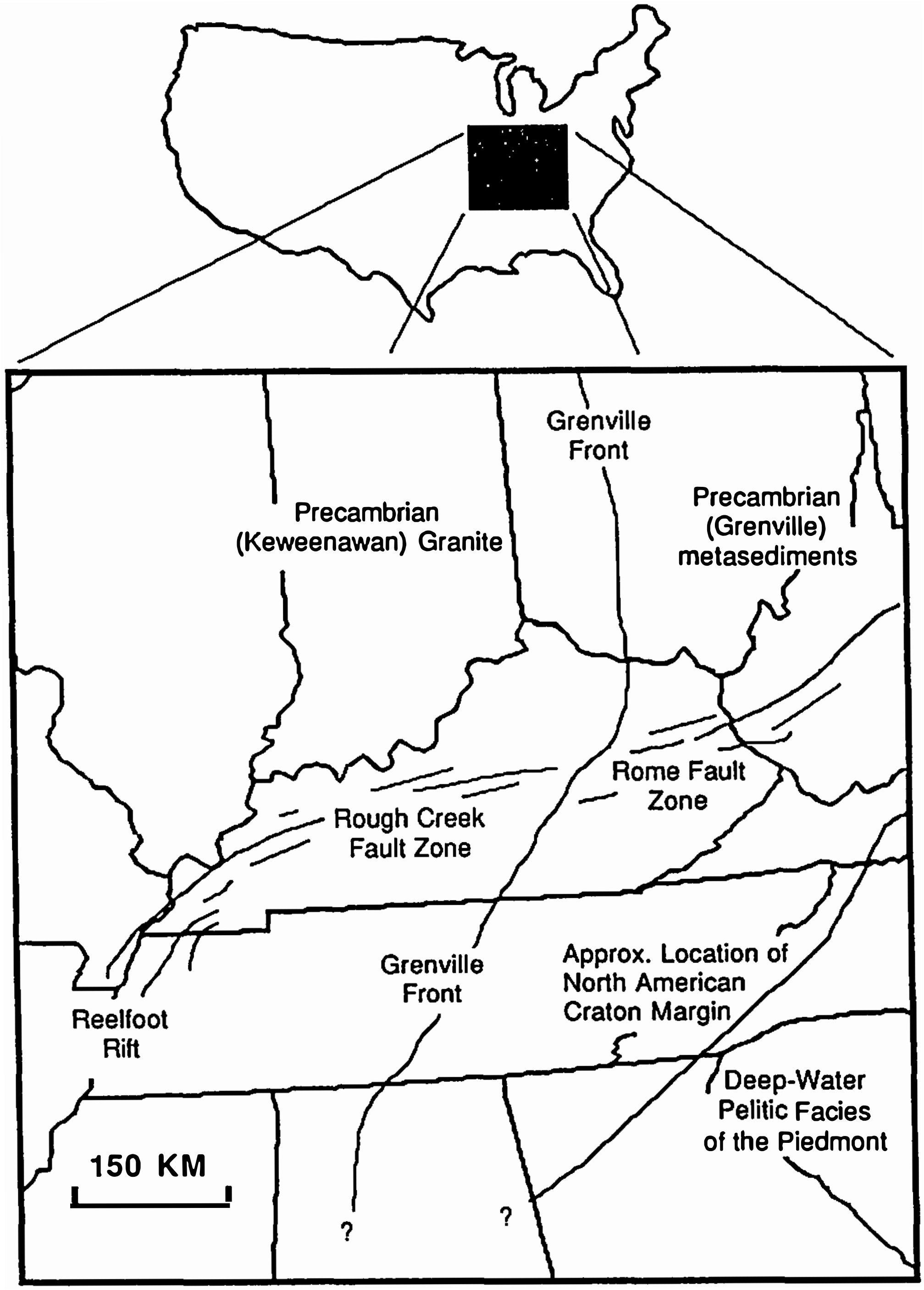

Figure 1.2. Tectonic framework of the craton during late Precambrian and Cambrian time (features presented on this map are derived from several sources; see reference list under paleogeography/tectonic setting).

craton, progressively younger Cambrian-aged sedimentary rocks onlapped the Precambrian Shield and older Cambrian deposits. Figure 1.3 shows generalized Cambrian stratigraphic nomenclature in Tennessee and nearby areas.

Paleogeography/Tectonic Setting

The following discussion (and associated paleogeographic maps) relies on the work of many investigators (Freeman, 1953; Rodgers, 1953; Calvert, 1962; Buschback, 1964 and 1970; Harris, 1964; Derby, 1965; Rodgers, 1968; Webb, 1969 and 1980; Colton, 1970; Lochman-Balk, 1971; Palmer, 1971; Janssens, 1973; Milici, 1973; Samman, 1975; Kidd and Neatherly, 1976; Bearce, 1977; Ammermann and Keller, 1979; Mack, 1980; Gilbert, 1981; Markello and Read, 1982; Beardsley and Cable, 1983; Denison and others, 1984; Howe and Thompson, 1984; Hasson and Haase, 1988). The quality of these investigations varies, and that coupled with the absence of established biostratigraphic markers throughout much of the Cambrian in the area of concern produce some disparity in regional stratigraphic relationships. As a result, only a generalized discussion is presented here. Yet, this discourse is necessary to establish a basic framework from which future work can build.

The Appalachian basin was extensive during the Cambrian and included much of the eastern and southern United States and portions of southeastern Canada. Cambrian sediments of the Appalachian basin were deposited on a Precambrian surface of two distinct terranes:

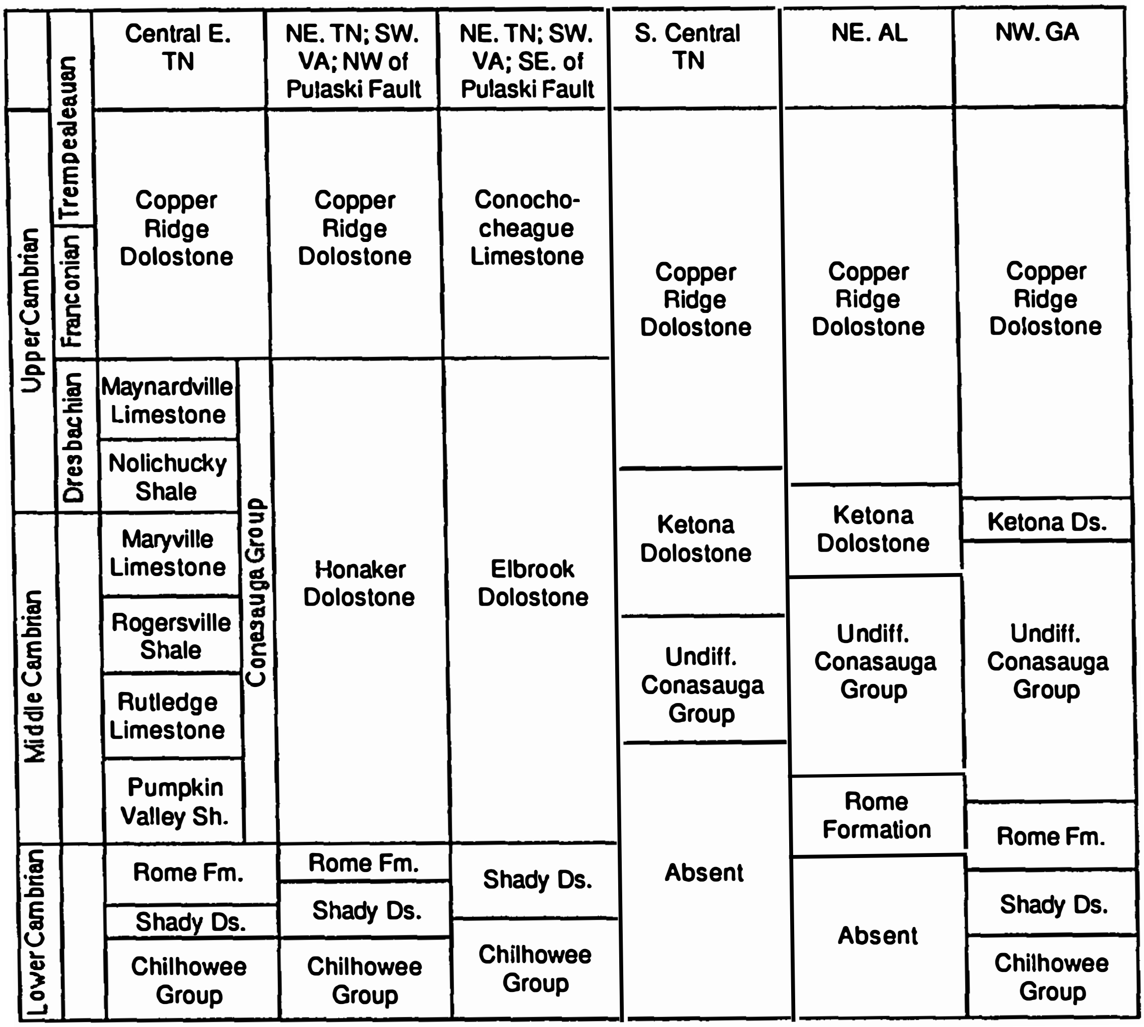

		Central E. TN		NE. TN; SW. VA; NW of Pulaski Fault	NE. TN; SW. VA; SE. of Pulaski Fault	S. Central TN	NE. AL	NW. GA
Upper Cambrian	Trempealeauan	Copper Ridge Dolostone		Copper Ridge Dolostone	Conococheague Limestone	Copper Ridge Dolostone	Copper Ridge Dolostone	Copper Ridge Dolostone
	Franconian							
	Dresbachian	Maynardville Limestone	Conasauga Group	Honaker Dolostone	Elbrook Dolostone			
		Nolichucky Shale				Ketona Dolostone	Ketona Dolostone	Ketona Ds.
Middle Cambrian		Maryville Limestone					Undiff. Conasauga Group	Undiff. Conasauga Group
		Rogersville Shale				Undiff. Conasauga Group		
		Rutledge Limestone						
		Pumpkin Valley Sh.				Absent	Rome Formation	Rome Fm.
Lower Cambrian		Rome Fm.		Rome Fm.	Shady Ds.		Absent	
		Shady Ds.		Shady Ds.				Shady Ds.
		Chilhowee Group		Chilhowee Group	Chilhowee Group			Chilhowee Group

Figure 1.3. Generalized stratigraphic nomenclature of Cambrian strata in east Tennessee and nearby areas. For references, see citation list under paleogeography/tectonic setting.

		SE. Missouri	Illinois; N. Indiana	S. Indiana	S. Ohio	N. Kentucky	Central Kenucky (rome trough)
Upper Cambrian	Trempealeauan	Eminence Ds.	Gunter Ss.	Knox Dolostone	Knox Dolostone	Rose Run Ss.	Copper Ridge Dolostone
			Eminence Ds.				
		Potosi Ds.	Potosi Ds.			Copper Ridge Dolostone	
	Franconian	Derby-Doe Run Ds.	Franconia Fm.				
		Davis Fm.	Ironton Fm.	Davis Fm.			
			Galesville Fm.				
	Dresbachian	Bonneterre Dolostone	Eau Claire Formation	Eau Claire Formation	Eau Claire Formation	Eau Claire Formation	Maynardville Fm.
		Lamotte Ss.	Mt. Simon Ss.	Mt. Simon Ss.	Mt. Simon Ss.	Mt. Simon Ss.	Conasauga Formation
Middle Cambrian		Absent	Basal Arkose	Basal Arkose	Basal Arkose	Basal Arkose	Rome Fm.
			Absent	Absent	Absent	Absent	
Lower Cambrian							Absent

Figure 1.3 (continued)

(1) unmetamorphosed rhyolitic and trachytic volcanic rocks and epizonal granitic rocks and (2) granite-gneiss, medium-grade metamorphic rock, and anorthosite (Keller and others, 1975; Denison and others, 1984). These terranes are separated by the Grenville Front, which trends along the eastern flank of the ancestral Cincinnati Arch then south through central Kentucky and Tennessee (Figure 1.2) (Ammerman and Keller, 1979). In the area of this study, two fault zones affected Cambrian deposition (Figure 1.2). The Rough Creek and the Rome fault zones are east-west trending and are part of a large continental transcurrent system, which extends northeast through West Virginia and Maryland (Webb, 1980). Although this fault system formed during late Precambrian rifting, periodic rejuvenation occurred when the region received sediment (Webb, 1969).

In east Tennessee and nearby areas the Precambrian craton has a southeast-facing basement slope (Webb, 1980), and during Early Cambrian time sea level transgressed this slope. According to Lochman-Balk (1971), great quantities of predominantly medium- to coarse-grained siliciclastic material was deposited along the craton margin in alluvial, beach, and marine shelf settings. These sediments are represented today by stratified rock units of the Chilhowee Group. Throughout the Early Cambrian, sea level rose further onto the craton, and in southwest Virginia, east Tennessee, and northwest Georgia upper Lower Cambrian deposits of sand, silt, clay, and carbonates (Rome Formation) graded southeastward into offshore platform-edge carbonates of the Shady Formation (Figures 1.4 and 1.5). Most of the Lower

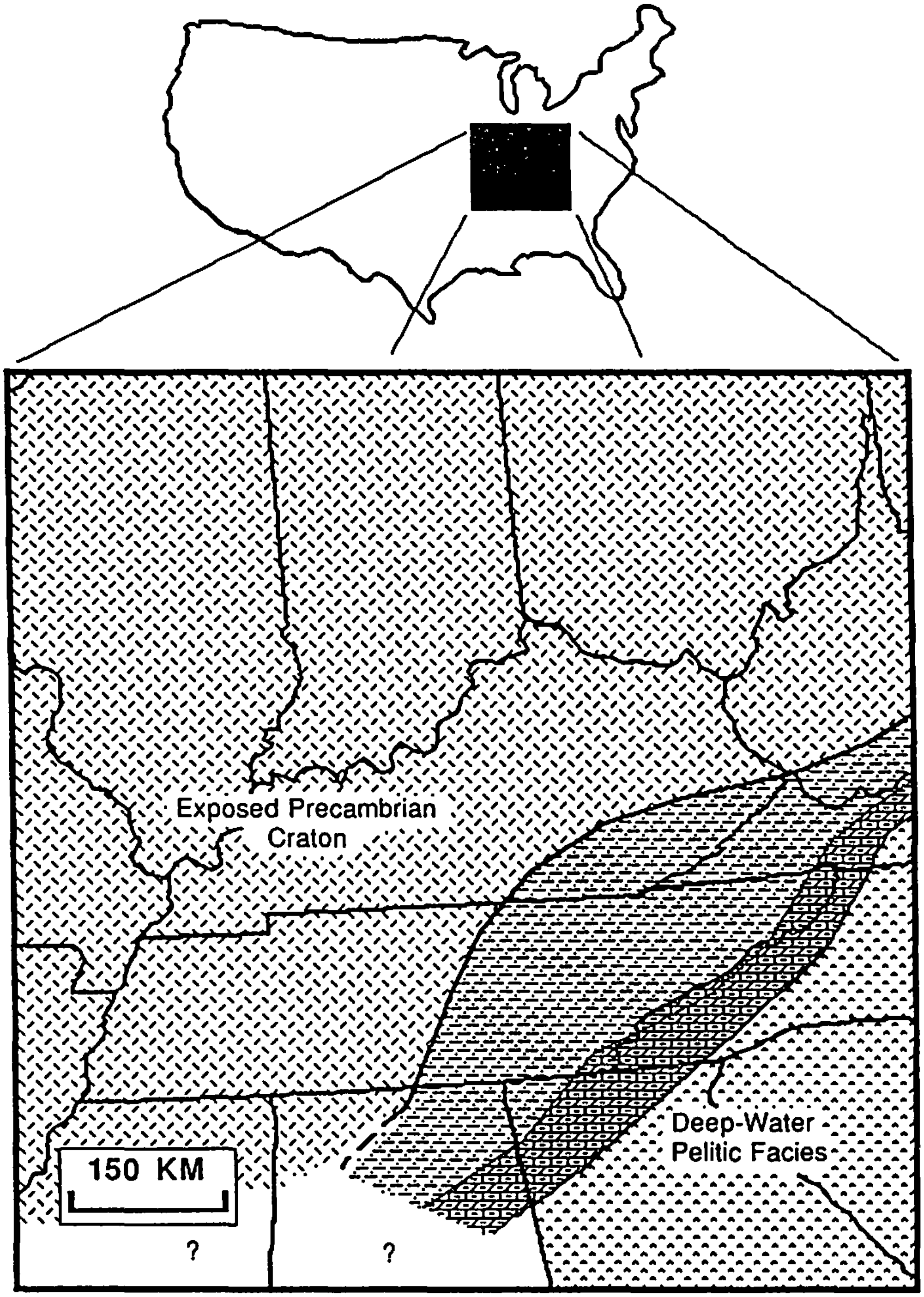

Figure 1.4. Regional lithofacies distribution during the late Early Cambrian (during deposition of the Rome Formation in east Tennessee). See Figure 1.5 for key to symbols used to indicate environments of deposition.

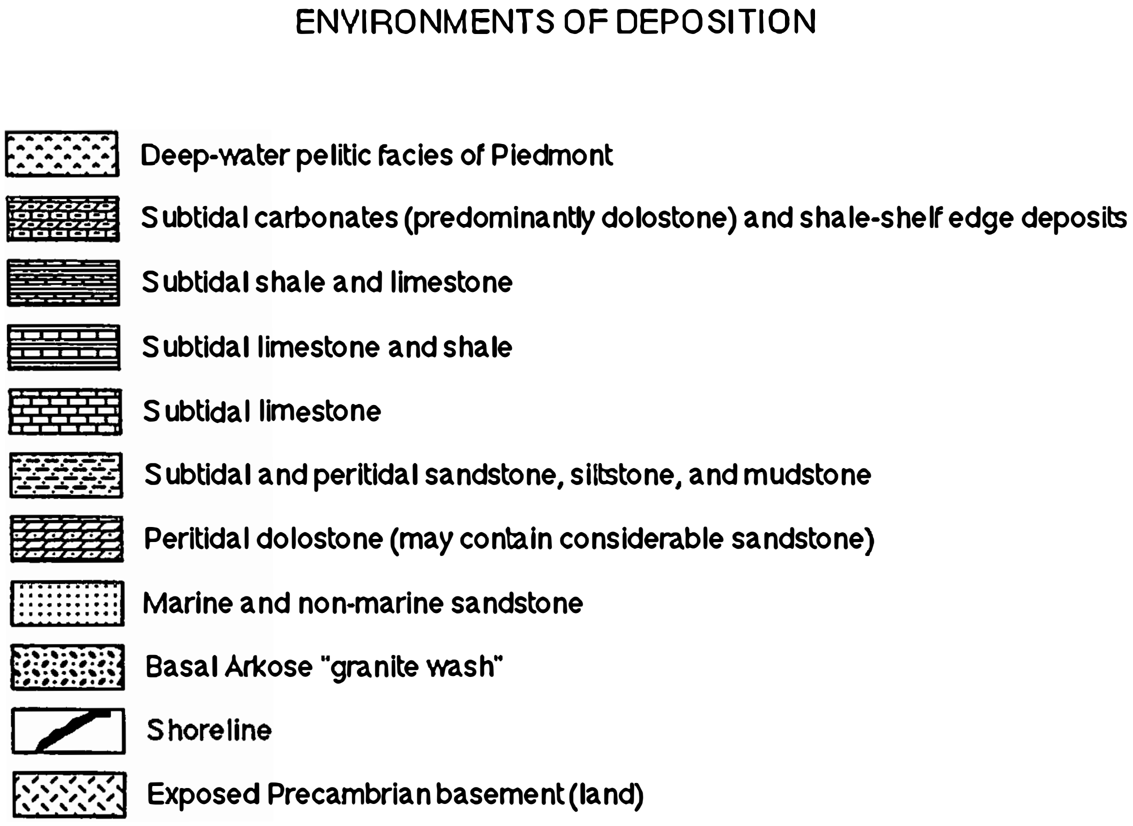

Figure 1.5. Key to symbols used to indicate environments of deposition in the series of paleogeographic maps (Figures 1.4, 1.6, 1.7, 1.8, and 1.9).

Cambrian sediments remained to the southeast of the Rough Creek and Rome fault zones (Ammerman and Keller, 1979).

As the sea encroached further inland during the Middle Cambrian, siliciclastics accumulated immediately offshore in central and southern Kentucky, eastern Tennessee, and in parts of Virginia, Alabama, and Georgia. This embayment received sediment from a delta system which drained northern Kentucky, Ohio, and perhaps southern Canada (Webb, 1980). In Kentucky and Tennessee the embayment, more specifically known as the Middle and Late Cambrian intrashelf basin, trapped primarily sand, silt, and clay (Rome Formation in Kentucky; Conasauga Group in Tennessee, Georgia, and Alabama; Nolichucky Formation in southwestern Virginia). Well-washed sand dominated nearshore areas in central Kentucky. Clay, silt, and rare sand are found offshore. In addition, periodic lowstands in sea level or decreased water turbidity (perhaps associated with channel lobe migration of the delta system or sea level highstands which trapped clastics in drowned river valleys) enabled limestone to be deposited offshore. By late Middle Cambrian the intrashelf basin was completely rimmed by peritidal dolostone along the seaward margin (Markello and Read, 1982) (Figure 1.6). According to Markello and Read (1982) the rim developed because sedimentation rates equalled or exceeded rates of sea level rise and/or platform subsidence.

The Rome Trough in east-central Kentucky (Figure 1.6) formed the northern boundary of the intrashelf basin. A thick clastic sequence accumulated within the trough. This depocenter was established by periodic downwarping of fault blocks, however, the absence of

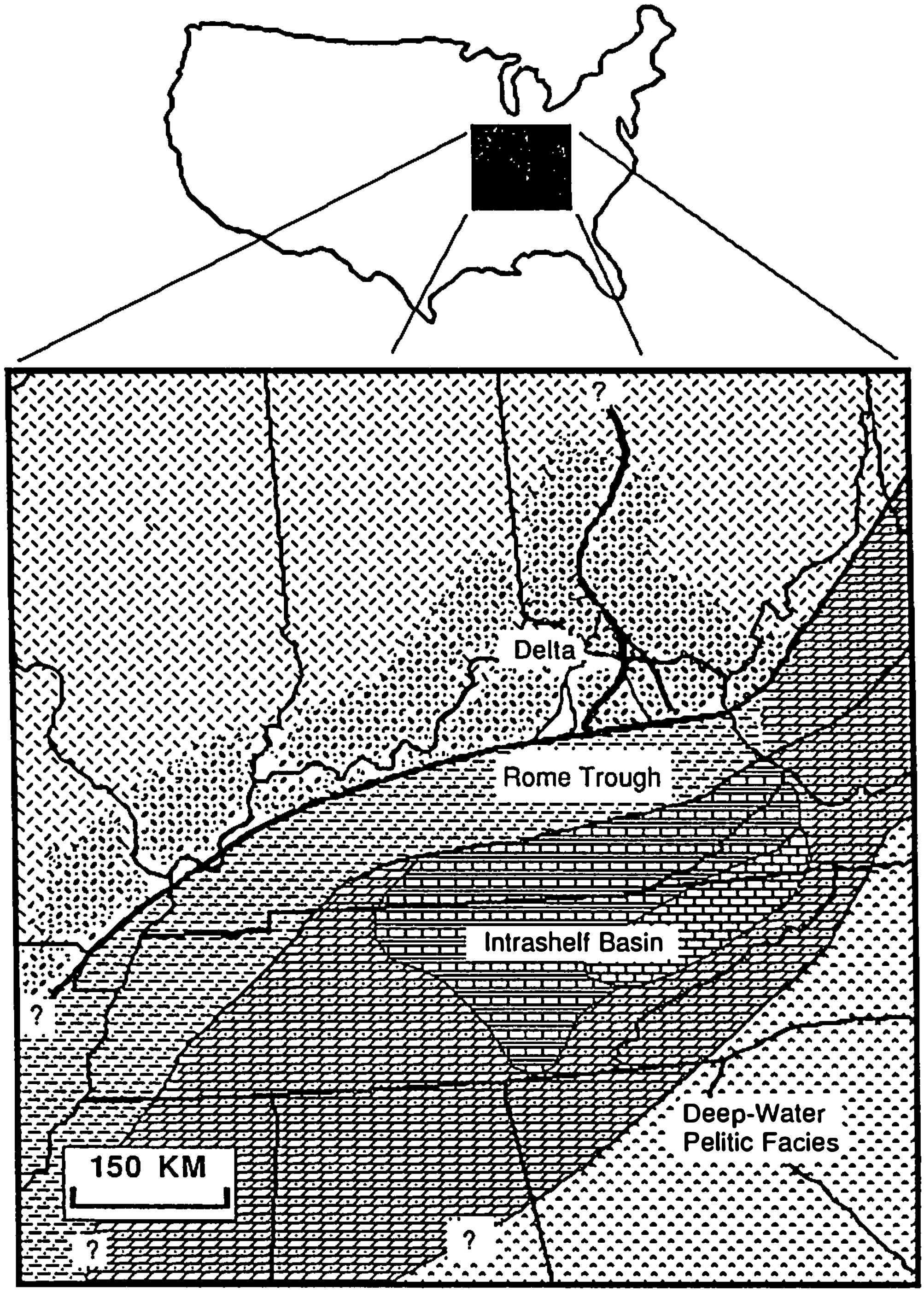

Figure 1.6. Regional lithofacies distribution during the late Middle Cambrian (during deposition of the Maryville Limestone in east Tennessee). See Figure 1.5 for key to symbols used to indicate environments of deposition.

conglomerates or unsorted detritus adjacent to the fault zone precludes the presence of a major fault scarp (Silberman, 1972). Active development of the Rome Trough was short lived; by the close of the Middle Cambrian, much of the Rome Trough had been filled. Only minor episodes of fault reactivation occurred after this time (Webb, 1980).

By Late Cambrian time, shallow seas covered parts of Ohio, Indiana, Illinois, and Missouri resulting in widespread deposition of clastics (Lochman-Balk, 1971) (see Figure 1.7). To the south and east, deltaic sediments (predominantly shale) were still being shed into the intrashelf basin (Webb, 1980). Limestone was the dominant depositional product along the southern and eastern portion of the intrashelf basin (Figure 1.7). Bordering much of the intrashelf basin was peritidal dolostone of the peritidal carbonate rim complex (Lochman-Balk, 1971; Markello and Read, 1982) (Figure 1.7).

During deposition of the Maynardville Limestone in east Tennessee (Figure 1.8), the intrashelf basin, now cut off from the clastic source, became greatly constricted in size as limestone filled the basin. By late Maynardville time the intrashelf basin had shoaled nearly to sea level. At this time and continuing throughout the remainder of the Cambrian, shallow epicontinental seas became so widespread that thick dolostone sequences were laid down over a wide geographic area (Figure 1.9). Although much of the dolostone may be secondary in origin, a considerable portion is believed to have formed penecontemporaneously with sedimentation, further supporting deposition under very shallow water (Laporte, 1971; Harris, 1973).

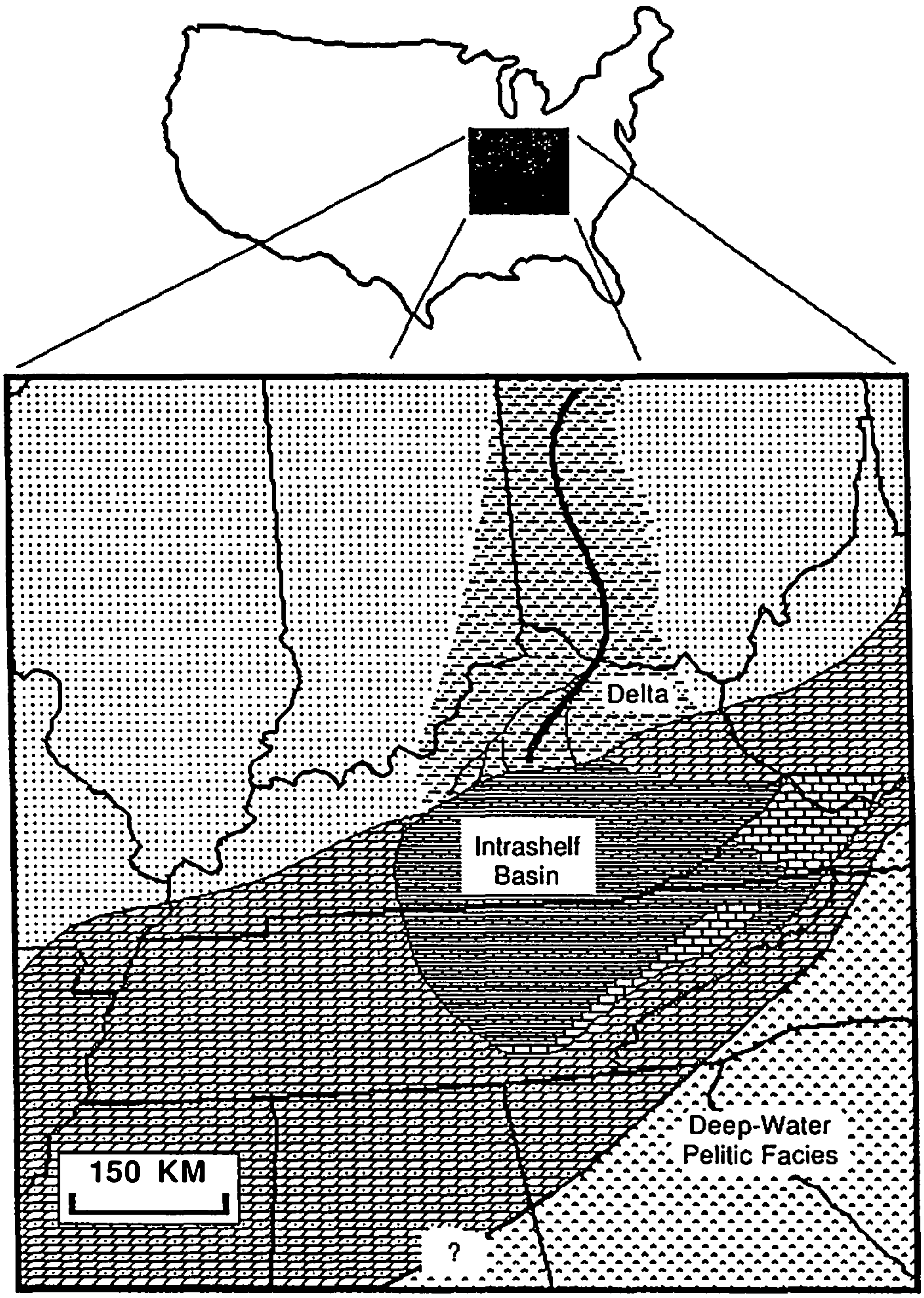

Figure 1.7. Regional lithofacies distribution during the early Late Cambrian (during deposition of the Nolichucky Shale in east Tennessee). See Figure 1.5 for key to symbols used to indicate environments of deposition.

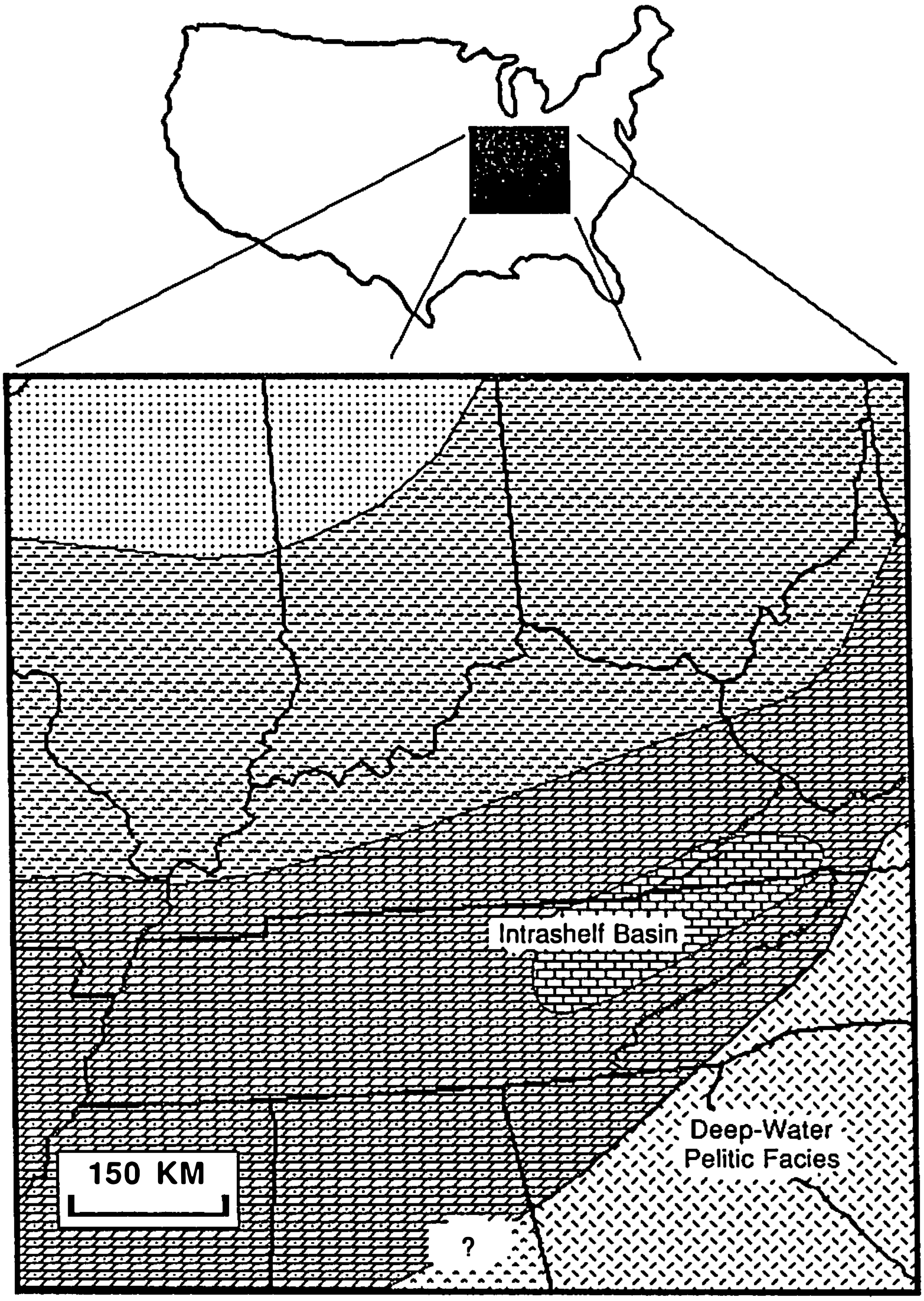

Figure 1.8. Regional lithofacies distribution during the early Late Cambrian (during deposition of the Maynardville Limestone in east Tennessee). See Figure 1.5 for key to symbols used to indicate environment of deposition.

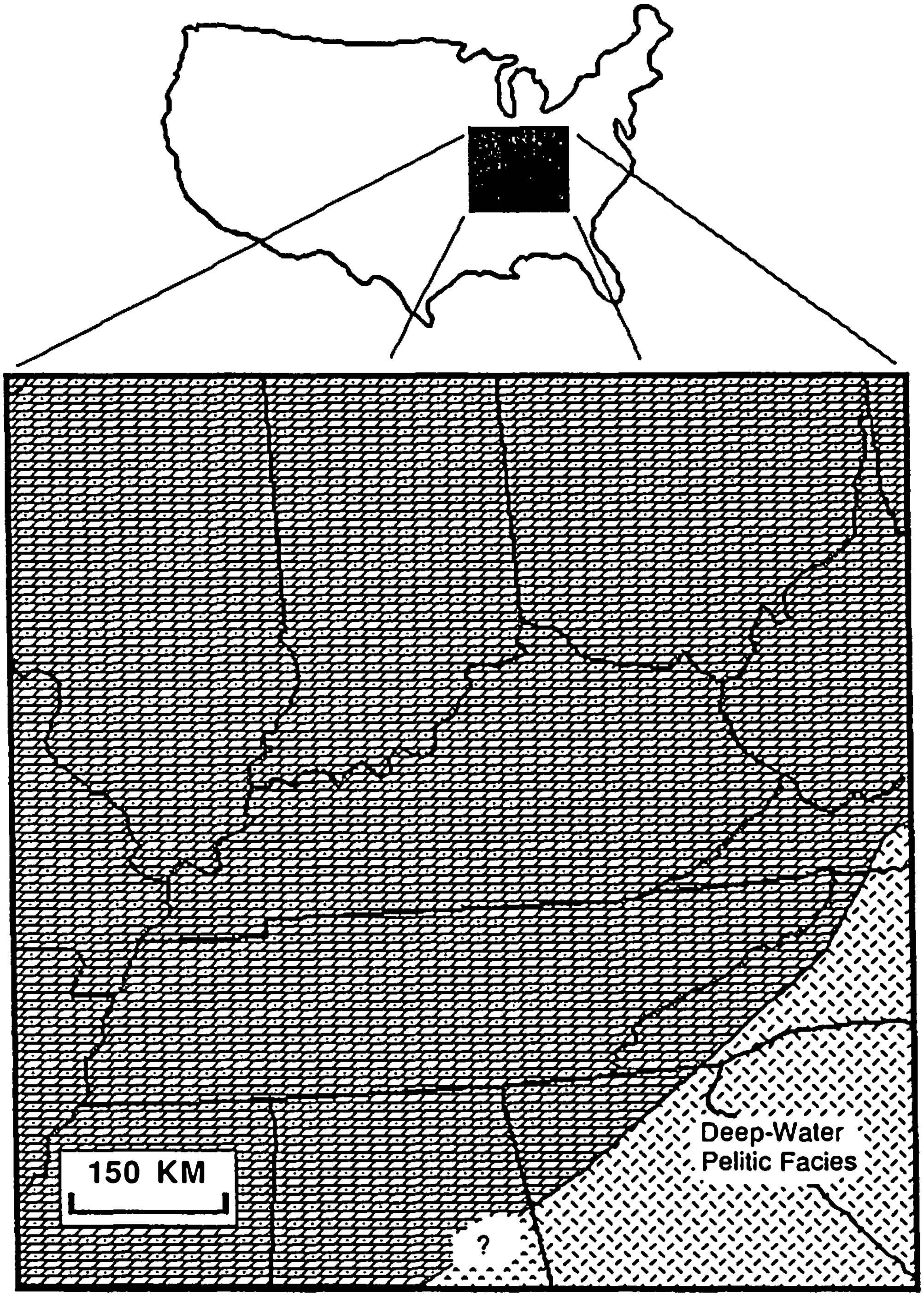

Figure 1.9. Regional lithofacies distribution during the late Late Cambrian (during deposition of the upper Copper Ridge Dolostone in east Tennessee). See Figure 1.5 for key to symbols used to indicate environment of deposition.

Location/Stratigraphy

Within the Valley and Ridge of east Tennessee, Middle and Late Cambrian rocks crop out along a succession of southeastward dipping imbricate thrust sheets, which trend northeast to southwest (Figure 1.10). The Valley and Ridge is from 90 to 140 kilometers wide. It is bounded on the northwest and southeast by the Cumberland Plateau and Southern Blue Ridge provinces, respectively.

In the vicinity of Knoxville, Middle and Upper Cambrian formations (excluding the Copper Ridge Dolostone) comprise the Conasauga Group (Figure 1.11). From base to top the Conasauga Group includes: the Pumpkin Valley Shale, Rutledge Limestone, Rogersville Shale, Maryville Limestone, Nolichucky Shale, and Maynardville Limestone. Only the Upper Cambrian Nolichucky Shale and Maynardville Limestone (subsequently referred to as upper Conasauga Group) are of primary concern here. The entire Group grades from dominantly dolostone in the east (northeastern Tennessee and southwestern Virginia), through intercalated carbonate and shale units in the Knoxville area to a sequence dominated by shale, west and southwest of localities D and F of Figure 1.10 (see Figure 1.11). The Conasauga Group is underlain by the Lower Cambrian, predominantly siliciclastic Rome Formation of tidal flat origin. Above the Group are very shallow subtidal and peritidal carbonates of the Upper Cambrian Copper Ridge Dolostone, the lowermost Formation of the Cambro-Ordovician Knox Group.

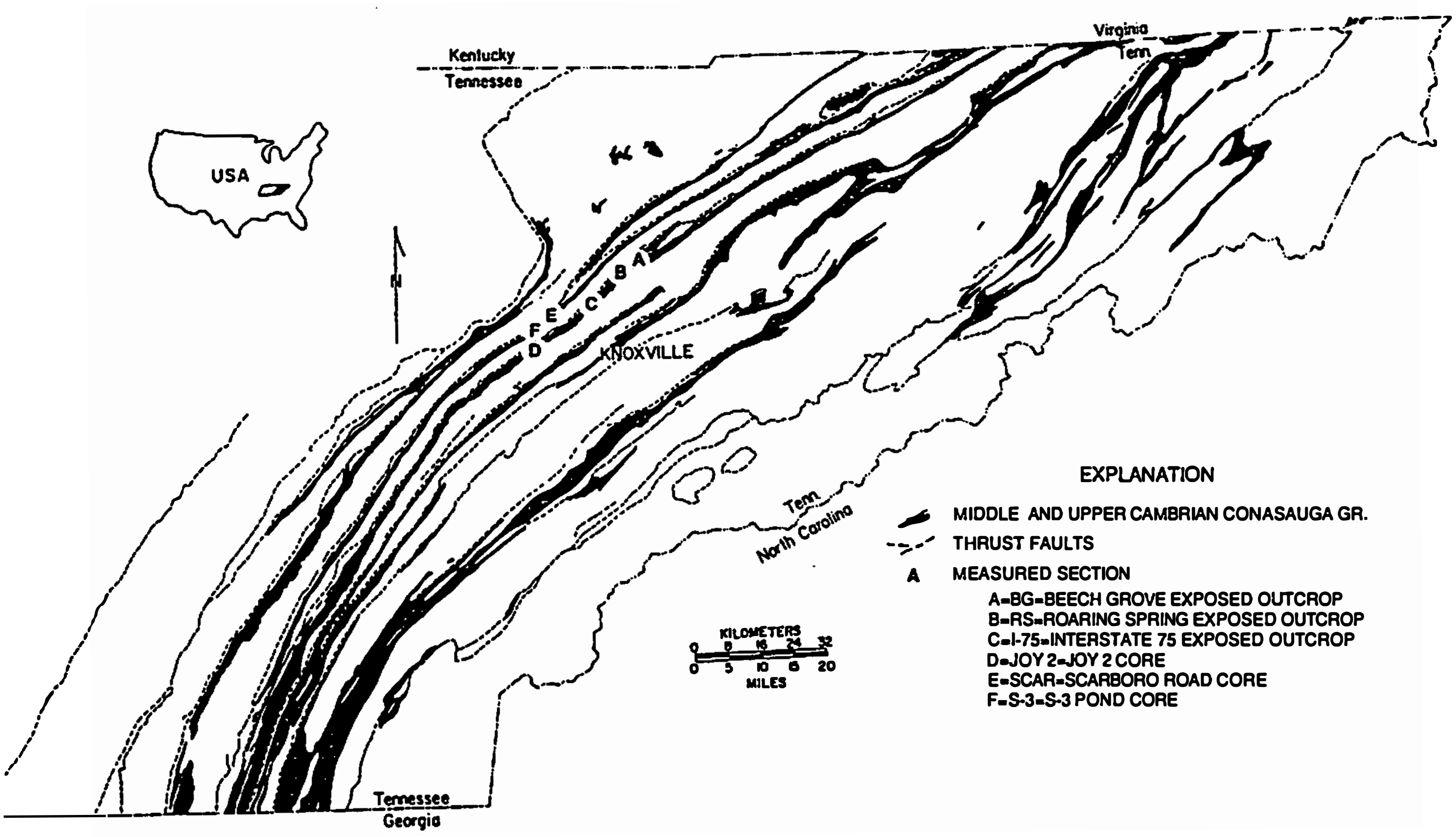

Figure 1.10. Exposures of Conasauga Group in east Tennessee and locations of measured sections.

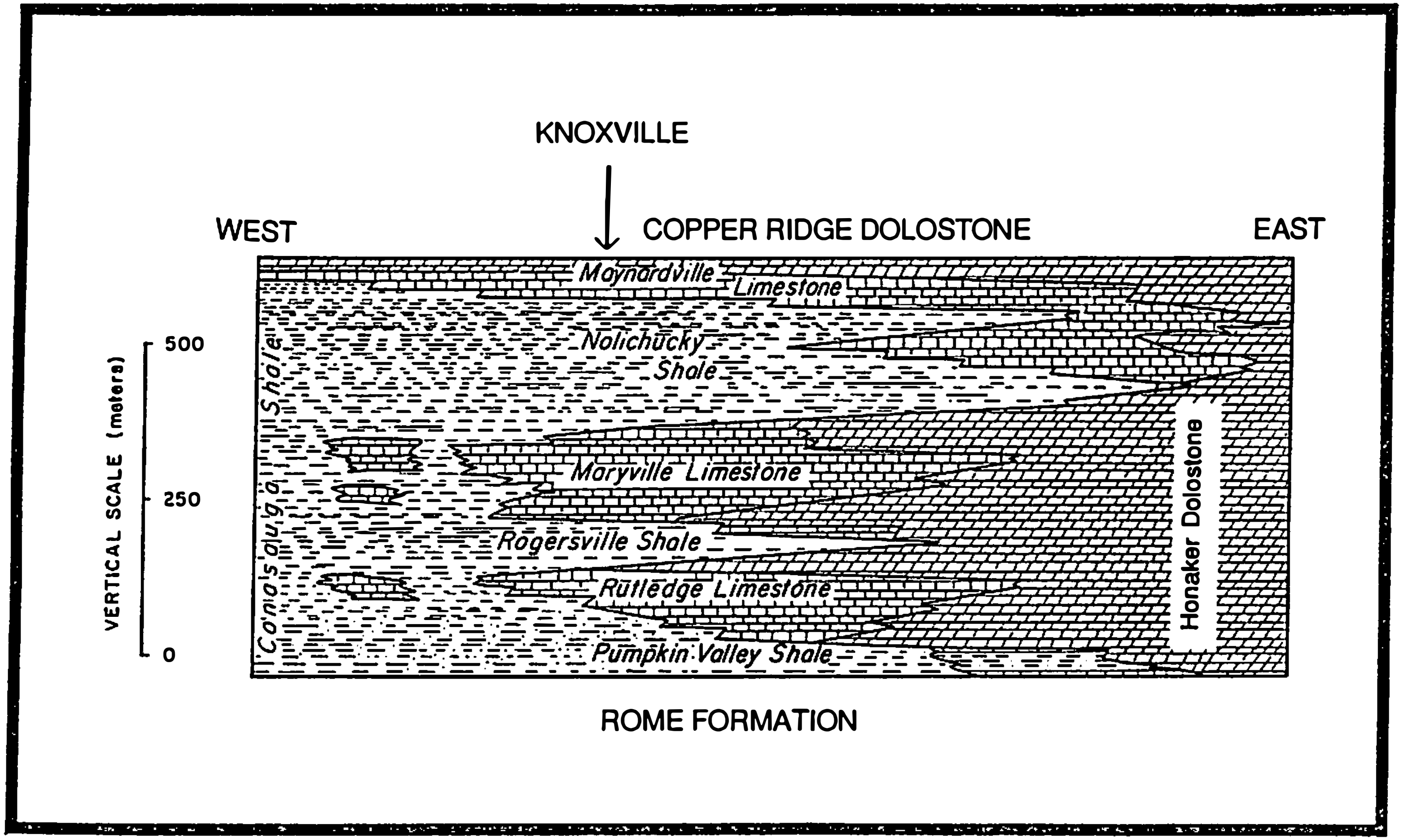

Figure 1.11. Stratigraphic relationships of the formations within the Conasauga Group (modified from Rodgers, 1953). Approximate position of the Nolichucky and Maynardville formations within the study area lies below and slightly on either side of the arrow corresponding to Knoxville, TN.

During the course of this research, six localities (Figure 1.12) have been examined in detail. Attention is focused on Nolichucky and Maynardville outcrop and drill core which are located in the vicinity of Knoxville and Oak Ridge, Tennessee. Detailed descriptions are found in Appendix B.

The localities analyzed were chosen after field reconnaissance because they represent the most well-preserved and complete stratigraphic intervals without significant structural complication in the Knoxville and Oak Ridge area. In addition, their geographic distribution is sufficiently broad to reveal environmental patterns or trends, but not too broad to prevent adequate correlation of stratigraphy, paleoenvironmental gradients, etc.

Depositional Environment/Previous Work

Prior to 1970, geologic investigations of the Nolichucky Shale and Maynardville Limestone within Tennessee and Virginia stressed generalized lithologic descriptions and paleontologic data (e.g., Hall and Amick, 1934; Butts, 1940; Rodgers and Kent, 1948; Raymond, 1959; Oder and Bumgarner, 1961; Havryluk, 1963; Harris, 1964; Rasetti, 1965; Derby, 1965; Helton, 1967; McConnell, 1967; Tarkoy, 1967). In recent years, several workers have inferred depositional models for upper Conasauga strata in east Tennessee and southwest Virginia (see Milici and others, 1973; Markello, 1979; and Markello and Read, 1981 and 1982). Milici and others (1973) conducted an examination of the Nolichucky

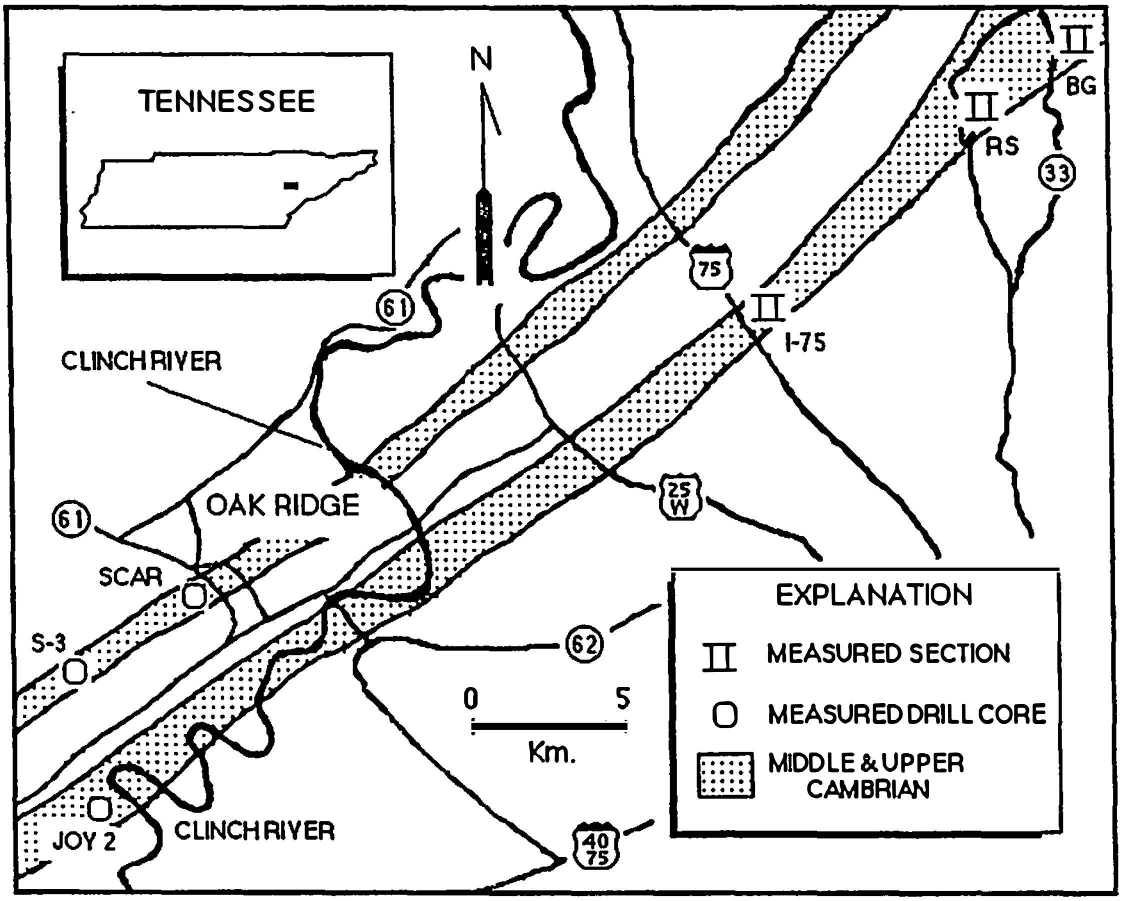

Figure 1.12. Knoxville and Oak Ridge vicinity showing measured outcrop and drill core used in this study.

Shale and Maynardville Limestone exposed along U.S. Interstate 75 (locality C of this study) on Copper Ridge. They discerned several lithofacies: (1) stromatolitic bioherms, (2) thin, irregularly bedded algal limestones, (3) cobbly weathering limestones, (4) banded argillaceous limestones, (5) oolitic calcarenites, (6) intraclastic and oolitic washover beds, and (7) subaerially exposed limestones and dolostones. In general, strata from this locality were interpreted as "lagoonal" sediments, protected from oceanic currents and waves, bounded to the east by an extensive carbonate bank and to the west by siliciclastic sediment.

Markello and Read (1981 and 1982) studied the Nolichucky Shale and Maynardville Formation in Virginia. They defined three major depositional environments: an intrashelf basin (Nolichucky Shale), a carbonate ramp with subtle westward slopes (Maynardville Limestone), and a peritidal carbonate platform (Elbrook and/or Honaker Formations). Deposition in the intrashelf basin, as described by Markello and Read (1981), resulted in a complex interbedded assemblage of storm-generated calcareous shale, laminated calcareous siltstone, intraformational flat-pebble conglomerate, bioclastic limestone, and oolitic limestone. The carbonate ramp is characterized by subwave base accumulations of fossil-rich "ribbon" carbonates, thin intraclastic limestone, and oolitic shoals.

Biostratigraphy of Upper Conasauga Group

In the southern Appalachians very few stratigraphic studies have used paleontologic information from the Middle and Late Cambrian as a basis for chronologic determination (McLaughlin, 1973). Although biostratigraphic investigations have been conducted in this region (Raymond, 1959; Derby, 1965; Palmer, 1971; Gilbert, 1981), more commonly, only generalized fossil lists are encountered in the literature (e.g., McCalley, 1897; Butts, 1926, 1940, and 1941; Woodward, 1929; Howell and Mason, 1938; Resser, 1938; Palmer, 1962; McKinney, 1977; Bearce and McKinney, 1977; Bell, 1978). Reasons for the paucity of biostratigraphic investigations in the southern Appalachian region are:

1. Good quality exposure of thick stratigraphic intervals is necessary to establish a working biostratigraphic reference section. Most Cambrian outcrops are vegetated.
2. Many of the generalized fossil lists which have been published are difficult to evaluate because of inadequate location, incomplete description, or questionable identification (see McLaughlin, 1973 for further discussion).
3. Many stratigraphic horizons lack fossils because Cambrian marine life, relative to other Phanerozoic time periods, exhibits low diversity. Also, pervasive diagenetic replacement is common and tends to destroy fossil remains.

4. Few Cambrian macrofossil groups serve as useful biostratigraphic indicators because of strong environmental controls on their distribution.
5. Cambrian-aged microfossils (acritarchs and conodonts) have only recently been recognized as potentially useful biostratigraphic indicators and regional biostratigraphic zonations are as yet unavailable.

Solutions to these and other biostratigraphic problems are beyond the scope of the present research.

In east Tennessee, siliciclastic and carbonate beds of the Lower Cambrian Rome Formation are generally devoid of megascopic fossil remains (Samman, 1975). In addition, within the thick, Upper Cambrian Knox dolostone section, the poor state of knowledge concerning intra-Knox Group biostratigraphy results from the scarcity of shelly fossils. Stressful shallow marine environments represented by most of the pre- and post-Conasauga Group lithologies (of Cambrian age) apparently precluded the development of diverse shelly communities. Within the Conasauga Group faunally and florally impoverished strata abound, but certain limestone and rare shale horizons do display a rich and abundant megascopic biota (McLaughlin, 1973). Trilobites, echinoderms, inarticulated brachiopods, gastropods, and various taxa of unknown affinities occur within the upper portion of the Conasauga Group (Nolichucky Shale and Maynardville Limestone). With the exception of trilobites, these fossils are not useful biostratigraphically (McLaughlin, 1973). In recent years, two microfossil groups (conodonts and acritarchs) have been increasingly studied on a world-wide basis because of their biostratigraphic potential in the Cambrian (Brasier, 1980). Detailed examination of these groups has not been conducted in east Tennessee. The usefulness of trilobites, conodonts, and acritarchs as biostratigraphic indicators in upper Conasauga strata is briefly discussed below.

Trilobites

Worldwide biostratigraphic zonation of Middle and Late Cambrian sequences is based almost entirely on trilobites. Fossil evidence indicates that trilobites were the most abundant, diverse, and widespread macrofauna inhabiting Cambrian seas. Many trilobite taxa have short ranges and thus serve as excellent "index" fossils.

Trilobites in the Nolichucky Shale and Maynardville Limestone parallel the uppermost Middle to early Late Cambrian (Dresbachian) trilobite zonation proposed by Lochman-Balk and Wilson (1958) for the mid-continent region (Figure 1.13). Three complete trilobite zones are present in the upper Conasauga sequence. *Cedaria* and *Crepicephalus* Zones occur through much of the Nolichucky Shale, while the base of the overlying *Aphelaspis* Zone occurs in the upper portion of the Nolichucky Shale and continues through the Maynardville Limestone (Figure 1.13).

Comparison of stratigraphic and time boundaries along a transect from the Knoxville area northeast into southwest Virginia reveals a discrepancy between lithostratigraphic and biostratigraphic subdivision (Raymond, 1959; Derby, 1965; McLaughlin, 1973). It is possible that the

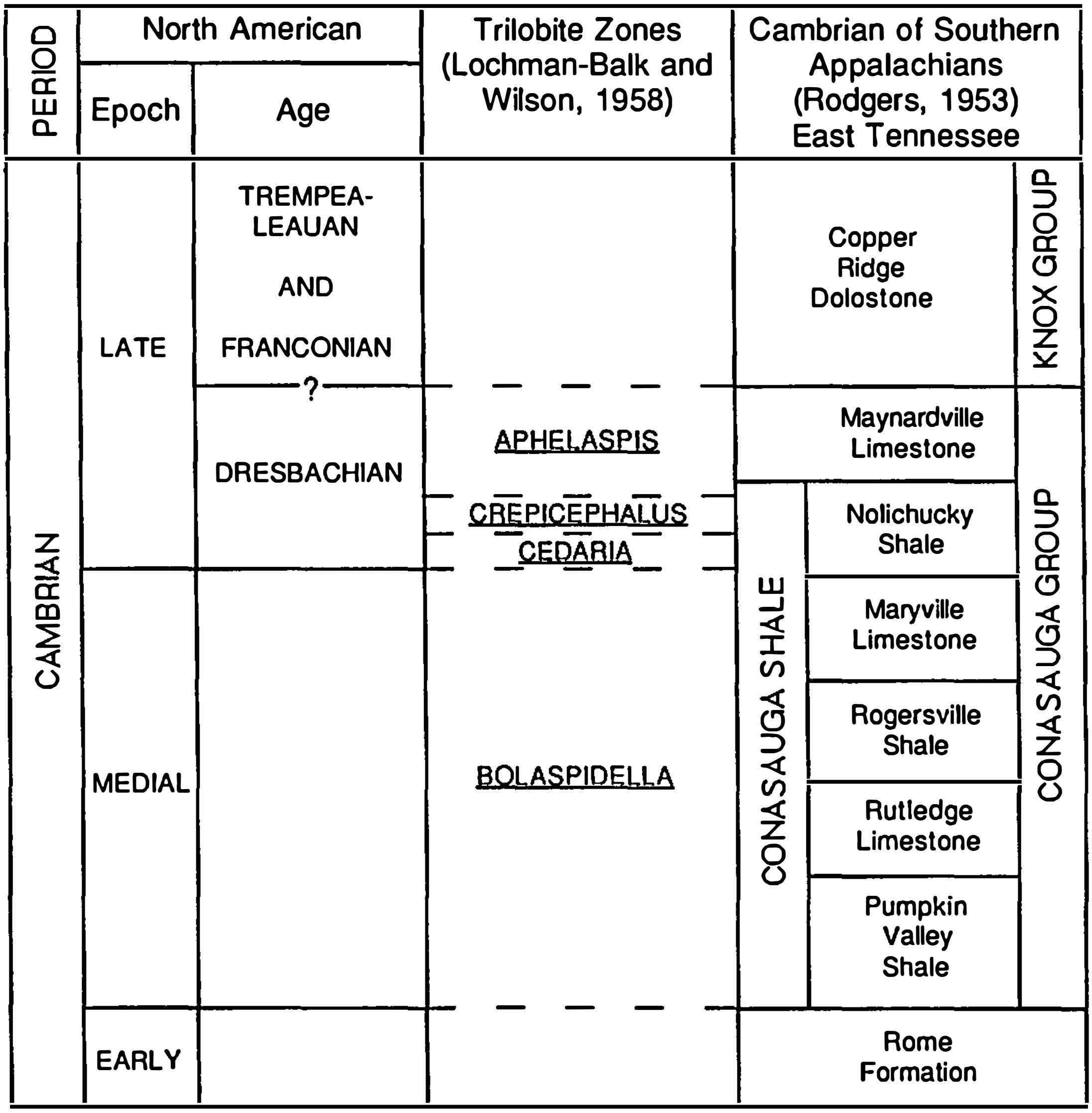

Figure 1.13. Generalized temporal relationship of Cambrian formations in east Tennessee (modified from Kozar, 1986).

environment rather than time succession exerted the dominant control over the observed faunal associations. When describing trilobite zonation in the Conasauga of Virginia, Markello and others (1979) noted that individual zones were assemblage zones and thus, were likely to show some degree of environmental control. Additional work is necessary to determine precise age relationships within the upper Conasauga Group in east Tennessee.

Conodonts

Although the biostratigraphic potential of conodonts in the upper Conasauga Group has not been evaluated to date, a pilot study by the present author revealed that conodonts are present in the Nolichucky Shale. Four 1 kg limestone samples (BG-6-65.2, I-61-2.0, I-62-1.2, and I-81-1.4) were dissolved in formic acid, but only sample I-61-2.0 contained conodonts. The total of 32 conodonts represented 6 form species (*Furnishina furnishi*, *Prosagittodontus dunderbergiae*, *Prooneotodus tenuis*, *Prooneotodus* n. sp. A of Miller (1981), *Nogamiconus cambricus*, and *Muellerodus pomeranensis*). Apparently, all three major types of conodonts are represented. The most abundant protoconodont is *Prooneotodus tenuis*, which has also been found in great numbers from Upper Cambrian strata in Nevada and eastern California (Miller, 1981). *Furnishina furnishi*, a paraconodont, is the most common form species from the Nolichucky sample and represents approximately 60% of the total population. Euconodonts may be represented by *Prooneotodus* n. sp. A of Miller (1981), which closely resembles the euconodont genus, *Oneotodus*.

These results suggest the need for further investigation. The occurrence of euconodonts in the Nolichucky is unlikely because the earliest euconodonts are not known to appear until mid to upper Franconian (J.F. Miller, verbal communication, 1985), and the Nolichucky Shale is Dresbachian (early Late Cambrian) in age (see Figure 1.13). It is possible that the specimen in question has been misidentified or that R.H. Miller's interpretation relating euconodonts to Prooneotodus n. sp. A is invalid.

It has been suggested by Miller (1984) that Cambrian conodont taxa are too long-ranging and not presently useful for precise biozonation. This is especially true for mid-Franconian and older rocks (Miller, 1984). Upper Dresbachian and lower Franconian conodonts have been studied from southern Nevada (Miller and others, 1981), and the distribution of these conodonts is primarily controlled by paleoenvironment and geographic position on the shelf. Despite these preliminary findings which suggest conodont biostratigraphy is not currently possible throughtout much of the Cambrian, Chinese workers have developed conodont zones to the base of the Middle Cambrian (An, 1981 and 1982).

Acritarchs

Acritarchs are microscopic marine planktonic algae which existed primarily during the Paleozoic (Tappan, 1980). In the Cambrian a rich and abundant flora of acritarchs is found in most marine deposits (Downie, 1984). According to Downie (1984), a substantial amount of research has been conducted in Great Britain where stratigraphic ranges of Cambrian acritarch species are constrained in well-dated sections. Ultimately, biostratigraphic zonation in the Cambrian will be based on acritarchs (a personal assessment), but knowledge of acritarchs is still very incomplete.

There are as yet no published reports of acritarchs from the upper Conasauga Group in the Knoxville and Oak Ridge vicinity. It is important to note that acritarchs have been identified from the Nolichucky Formation in extreme eastern Tennessee and southwestern Virginia (Clendening, 1978).

Purpose

The objectives of this investigation are as follows: (1) to achieve an integrated interpretation of depositional environments based on examination of stratigraphy, sedimentology, petrography, and petrology, (2) to present a new statistical approach in order to objectively analyze stratigraphic sequences for cyclic trends and to apply this approach to the Nolichucky Shale and Maynardville Limestone, (3) to propose a model for the evolution of the Late Cambrian intrashelf shale basin to shallow carbonate succession by examining lateral and vertical facies relationships, basin morphology, and paleoenvironmental information, (4) to compare results of this investigation to the model developed by Markello and Read (1982), (5) to provide a framework on which subsequent work in the upper Conasauga Group may build, and (6) to provide information which might aid Oak Ridge National Laboratories and the Department of Energy in their hazardous materials disposal work.

CHAPTER 2

STRATIGRAPHY, SEDIMENTOLOGY, PETROLOGY, AND DEPOSITIONAL ENVIRONMENTS OF THE UPPER CONASAUGA GROUP (NOLICHUCKY SHALE AND MAYNARDVILLE LIMESTONE) IN EAST TENNESSEE

Introduction

The Conasauga Group is a thick sequence of lower Paleozoic rocks which were deposited during Middle and Late Cambrian time. Today, this stratigraphic interval crops out in northeast to southwest trending belts (Figure 1.10) in the thrust faulted Valley and Ridge physiographic subprovince of the Southern Appalachian Major Highland Division. In east Tennessee Middle and Late Cambrian strata are recognized as having three distinct phases of sedimentation, as revealed by regional lithofacies patterns (Rodgers, 1953; modified by Hasson and Haase, 1988) (Figure 2.1). Between the Holston Mountain and Pulaski faults (southeastern phase), Conasauga Group equivalents (Honaker and Elbrook formations) crop out in a series of anticlinal folds (Hardeman and others, 1966) and are composed of dolostone and less abundant limestone. Northwest of the the Pulaski thrust fault, Conasauga rocks are exposed along southeasterly dipping imbricate thrust sheets. In a wide belt extending from the Pulaski Fault to the Wallen Valley Fault (Central phase), the Conasauga Group is divided into six formations (Figure 1.11)

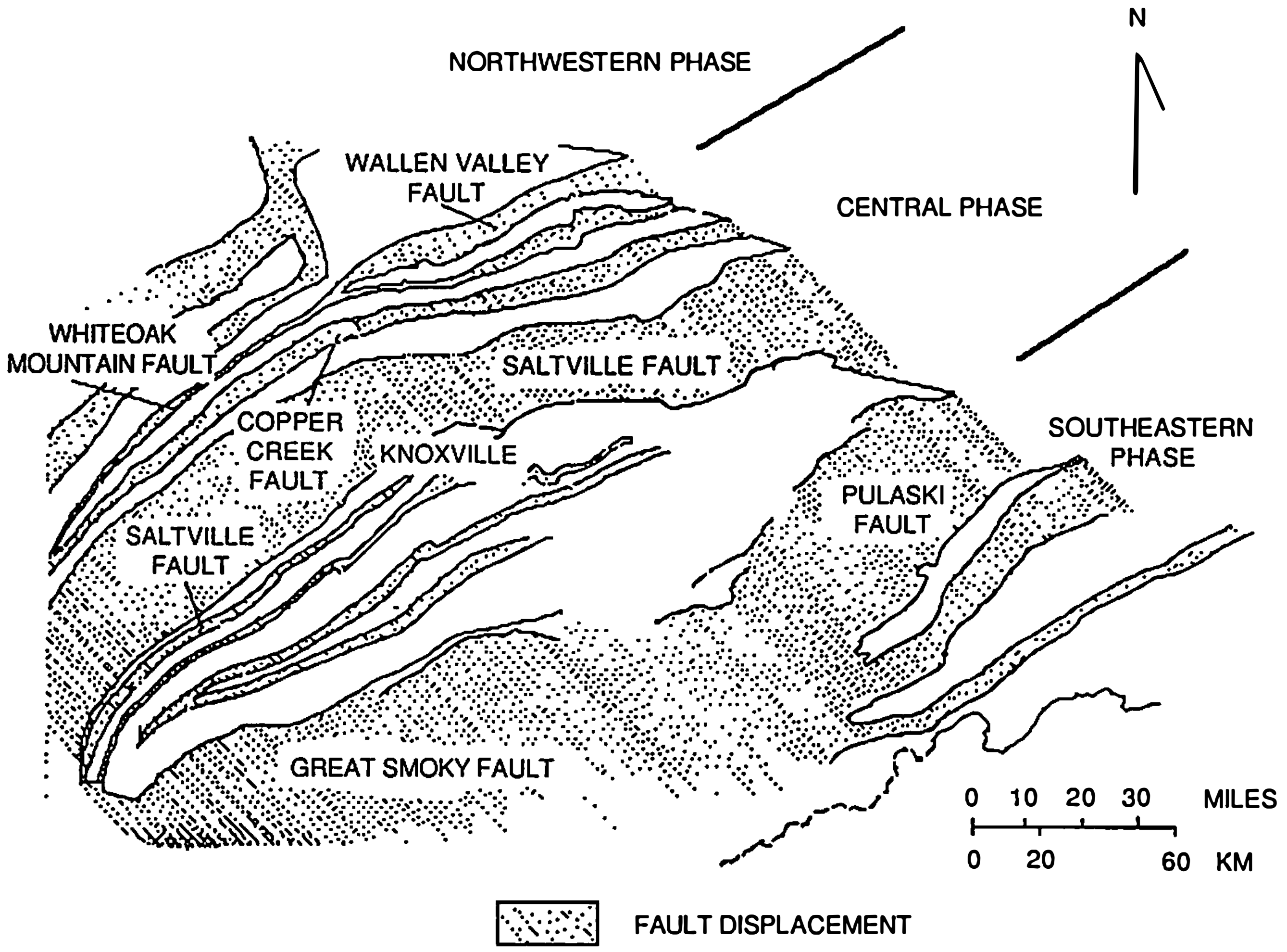

Figure 2.1. Palinspastic base map of east Tennessee showing the three major phases of Middle and Late Cambrian sedimentation (modified after Hasson and Haase, 1988). Faults are labeled within the area of displacement.

alternately dominated by shale and limestone. Northwest of the Wallen Valley Fault and presumably of the Whiteoak Mountain Fault (northwestern phase), Middle and Late Cambrian Conasauga strata are predominantly shale (Hasson and Haase, 1988).

Descriptive Stratigraphy

During Middle and Late Cambrian time a major transgression occurred over a subsiding, aggrading, and rimmed carbonate shelf (Rodgers, 1968; Palmer, 1971; Samman, 1975; Markello and Read, 1981 and 1982). The carbonate shelf rim complex located in extreme east Tennessee and in southwest Virginia is made up of the Early Cambrian Shady Dolomite (Pfeil and Read, 1980). Southeast or seaward of the Shady, deep-water pelitic sediments were deposited in the Proto-Atlantic Ocean. The Shady thins northwestward and intergrades in that direction with the Rome Formation. Throughout much of east Tennessee the Rome Formation is overlain by the Middle and Upper Cambrian Conasauga Group (Samman, 1975). In this area the Rome and Shady formations underwent deposition primarily in intertidal and supratidal environments (Samman, 1975). The Shady is composed of dolostone with locally abundant red shale and siltstone. The Rome is principally dolostone and shale where it intergrades with the Shady, but toward the craton, red and green sandstone, mudstone, shale, and dolostone occur which exhibit halite crystal casts and mudcracks (Samman, 1975).

A brief discussion follows concerning Conasauga Group stratigraphy. This section focuses on our knowledge of these formations within the central phase of sedimentation (as previously defined) near Knoxville and Oak Ridge, Tennessee. In particular, the northwestern extreme of the central phase is of primary interest here. For a more regional treatment of the stratigraphy, the interested reader is referred to Rodgers (1953), Derby (1965), Milici (1973), and Hasson and Haase (1988).

Pumpkin Valley Shale

The lowermost Formation of the Conasauga Group is the Pumpkin Valley Shale. It is characterized by maroon and gray-green shale, burrow-mottled siltstone, and planar-laminated to microhummocky cross-stratified subarkosic siltstone (Haase and others, 1985). Limestone and sandstone lithologies are observed occasionally. Haase and others (1985) subdivided the Pumpkin Valley Shale into two informal members. The lower member is separated from the upper member midway through the Formation where the rocks above tend to be more shale rich. The contact at the base of the Pumpkin Valley Shale is conformable and sharp. It is placed just above the uppermost sandstone bed in the Rome Formation at the bottom of a several meter thick shaly, gray siltstone (Hasse and others, 1985).

Because the Pumpkin Valley Shale is not well-exposed and is commonly faulted, estimates of formational thickness are not trustworthy (Hasson and Haase, 1988). In addition, the environment of deposition is not well understood, however, subtidal sedimentation is proposed due to an absence of features suggestive of subaerial exposure (Walker and Simmons, 1985).

Rutledge Limestone

The Rutledge Limestone conformably overlies the Pumpkin Valley Shale. This contact is gradational over several meters, but is placed where carbonate becomes consistently more abundant than shaly siltstone or silty shale (Haase and others, 1985). The Rutledge limestone is made up of nodular to thinly bedded lime mudstone with subordinant fossiliferous and peloidal packstone. Quartz silt is significant at some localities and forms graded sequences capped by microhummocky cross-stratification. The Rutledge Limestone varies considerably in thickness; available data indicate a range from 30 m to 100 m (Milici, 1973; Haase and others, 1985).

Rogersville Shale

Overlying the Rutledge Limestone is the Rogersville Shale. The Rogersville consists of maroon and gray-green massive to laminated noncalcareous mudstone, and wavy-bedded current-rippled calcarenite and subarkosic siltstone which display basal scoured surfaces and mud-draped tops (Haase and others, 1985). According to Haase and others (1985), glauconite is ubiquitous throughout the Rogersville shale and may comprise as much as 30% of the rock. Although Formation thickness may exceed 70 m at some localities, 30 m to 50 m is common throughout central east Tennessee (Knoxville and Oak Ridge vicinity) (Milici, 1973;

Haase and others, 1985; Hasson and Haase, 1988). Within the middle and upper portion of the Rogersville Shale, a carbonate unit of variable thickness called the Craig Limestone Member is observed. The Craig Limestone Member consists primarily of mottled, fine-grained limestone and dolostone, to coarse-grained intraclastic and oolitic limestone (Walker and Simmons, 1985). The Craig is locally stromatolitic (Hasson and Haase, 1988).

Maryville Limestone

The lower contact of the Maryville Limestone is conformable with the Rogersville Shale and is placed at the base of the first thick limestone bed, where limestone becomes more abundant than shale (Simmons, 1984). The Maryville contains a diverse assemblage of carbonate lithologies. Whereas lenticular- to nodular-bedded lime mudstone and fossiliferous, oolitic, and peloidal packstone are commonly observed, limestone clast conglomerates account for the majority of the sequence (Haase and others, 1985; Kozar, 1986). Within the Whiteoak Mountain and Hunter Valley strike belts, calcareous siltstone is abundant and displays current ripples, climbing ripples, and micro-hummocky cross-stratification (Kozar, 1986). Southwest and northwest of Knoxville, maroon and gray-green shale becomes significant, especially at the base and top of the Formation. Thickness values for the Maryville range from 75 m to 150 m (Milici, 1973; Kozar, 1986).

Based on the work of Simmons (1984) and Kozar (1986), much is known about the depositional environments of the Maryville in this area.

Generally, deposition took place above storm wave-base, but below normal wave-base along a gently sloping surface. According to Kozar (1986), in central east Tennessee deposition took place within a transition between fine-grained siliciclastics to the northwest and carbonates to the southeast.

Nolichucky Shale

The lower boundary of the Nolichucky Shale occurs at the base of the lowest thick shale unit which overlies thinly interbedded limestone and shale of the upper Maryville (Derby, 1965). Although the Nolichucky contains many of the same lithologies as found in the Maryville Limestone, a major difference between the two Formations is apparent. Shale dominates the Nolichucky accounting for 40% to 70% of the total thickness. Shale is maroon to dark gray-green and is commonly interbedded with intraclastic, oolitic, peloidal, and fossiliferous limestone. Rare calcareous siltstone interbeds are present within the lower 30 m to 50 m and are present toward the top of the unit.

The Nolichucky Shale has been subdivided into a lower and upper shale (Haase and others, 1985; Hasson and Haase, 1988). Between the shale intervals is a regionally traceable unit known as the Bradley Creek Limestone Member (Helton, 1967; Hasson and Haase, 1988). In central east Tennessee this member is not always present; where it is present, it is generally less than 20 m thick. The Bradley Creek Member consists predominantly of algal (Renalcis and Girvanella) wackestone and packstone with interstratified lime mudstone and oolitic limestone

(Haase and others, 1985). The total thickness of the Nolichucky Shale is variable, but ranges from 140 m to 180 m (Milici, 1973).

A prime objective of the present investigation is to derive an environmental interpretation for the Nolichucky Shale. This discussion will be presented later in this chapter. However, Markello and Read (1981 and 1982) have implied that much of the Nolichucky underwent deposition below normal wave-base but above storm wave-base in an intracratonic basin.

Maynardville Limestone

Prior to 1953, the Maynardville was regarded as a transitional sequence between thick shale below (Nolichucky Shale) and thick dolostone above (Knox Group). As a result, some workers treated the Maynardville as a member of the Nolichucky, while others considered the Maynardville to more closely resemble the Knox (for a detailed summary, see Bridge, 1956). More recently, the Maynardville has been elevated to formational status (Rodgers, 1953). The lower contact is placed at the base of the first thick, predominant limestone unit which is present above the last thick shale (Tarkoy, 1970). The contact between the Maynardville Limestone and the overlying Knox Group is placed approximately 100 meters up section at the base of a massive dolostone (Copper Ridge Dolostone), which may exceed several hundred meters in thickness (Milici, 1973).

The Maynardville is divided into two regionally persistent members: the Low Hollow Limestone Member and the Chances Branch Dolostone Member

(Harris, 1965; Harris and Mixon, 1970; Hasson and Haase, 1988). While this subdivision may be possible and appropriate in some areas of east Tennessee, in the Knoxville and Oak Ridge vicinity (central east Tennessee), placement of the contact between these members is extremely subjective. Generally, the Chances Branch Member is characterized by an increase in the abundance of dolostone and fine-grained carbonate lithologies (stromatolites and cryptalgalaminates). Although an increase in dolostone is noted up-section, this increase is gradual and varies significantly among localities. Thus, the formal subdivision is not used in this investigation.

The Maynardville consists primarily of thick-bedded oncolitic and oolitic packstone and grainstone as well as thrombolites, stromatolites, and cryptalgalaminates. According to the model presented by Markello and Read (1982), in southwestern Virginia the Maynardville Limestone was deposited downslope from peritidal facies (Elbrook and/or Honaker Dolostone) in a subwave-base, subtidal setting. In central east Tennessee this paleoenvironmental interpretation is in need of revision. Paleoenvironmental analysis of the Maynardville is presented later.

Post-Conasauga Group Strata

The Cambro-Ordovician Knox Group conformably overlies the Maynardville Limestone. The Knox has been divided into four widely recognized formations (Copper Ridge, Chepultepec, Kingsport, and Mascot, in ascending order) which span from Late Cambrian through Early Ordovician time. This sequence is primarily dolostone, deposited within a broad peritidal setting. The occurrence of desiccation features, oolitic and oncolitic lithologies, stromatolitic structures, and thick accumulations of finely crystalline dolostone substantiates this paleoenvironmental interpretation (Rodgers, 1953; Harris, 1969 and 1973; Weber, 1985).

Scope of Study

Descriptive stratigraphy of the Conasauga Group is well-established (e.g., Haase and others, 1985; Walker and Simmons, 1985; Hasson and Haase, 1988), but the processes that control lithofacies development and distribution are not as clearly understood. Recently, new quantitative techniques of stratigraphic analysis and a refined understanding of sedimentary processes have increased our ability to decipher the rock record in terms of process or dynamic stratigraphy (Mathews, 1984). This process-oriented approach is applied here to the Upper Cambrian Nolichucky/Maynardville sequence of east Tennessee. Reconstruction of dynamic processes is based on hierarchical three-tiered analysis (after Aigner, 1985). At the lowest level, individual strata are examined. This level involves reconstruction of depositional dynamics. Such criteria as erosional and depositional processes, mode of transport, and substrate changes, all of which occur over relatively short periods of time are of interest. Paleoenvironmental reconstruction (i.e., the identification and characterization of facies types) is accomplished through detailed field work, slab analysis, and petrographic investigation. Facies dynamics (facies sequences) represents an intermediate, more comprehensive level of analysis. At this scale stratigraphic sequences are analyzed for lateral and vertical development of facies. This sequential approach provides information concerning extent of cyclicity and significance of described facies. Basin dynamics, the most inclusive level, incorporates facies dynamics from various localities and regions. Here, such aspects as applicability of regional facies models, eustacy, and tectonics are considered. This hierarchical analysis is not restricted in application. Other basins have been modelled in a similar way (e.g., Shanmugam and Walker, 1980; Walker and others, 1983; Aigner, 1985)

This chapter focuses on paleoenvironmental reconstruction (depositional dynamics). Subsequent chapters will address aspects of facies and basin dynamics.

Methods of Investigation

Any dependable facies analysis requires detailed evaluation of the rocks in the field. In this study over 1300 meters of section from six localities (Figure 1.10) were examined on a centimeter by centimeter scale. Each change in lithology as well as the thickness of each lithology was recorded. Every practical precaution was taken to objectively measure and consistently define each lithology. Initially, a large number of lithologies was identified in the field. In order to reduce the original number of lithologies to a manageable level, a statistical procedure was used to systematically recategorize subordinant lithologies into geologically similar lithologies (details of this procedure are presented in Chapter 3). After completing the reduction process, 14 major lithologies remained. Next, special consideration was given to facies criteria, such as fossil content, sedimentary texture and structure, stratigraphic relationship, and geometry. This Chapter documents the integration of facies criteria to reach an understanding of each major lithology.

During the course of this study, 402 samples were collected from carbonate and shale units which appeared conspicuous because of their gross lithologic character. In the laboratory, hand specimens were cut and polished, and later examined using a hand lens and binocular microscope. More than 50 acetate peels were prepared from polished slabs. Approximately 370 thin-sections were made from rock samples. Each thin-section was examined, and characteristic features were identified under cathodoluminescent and/or transmitted light microscopy. Most thin-sections were stained using the Dickson (1966) technique for determination of carbonate and noncarbonate mineralogy.

Because quantification of recognizable features in thin-sections is important when characterizing facies, 152 thin-sections were point-counted (400 to 500 points per slide) using the method described by Chayes (1956). The total number of points counted per slide varied depending on average grain size and grain distribution. The composition of each thin-section is given in Appendix C (note that values have been rounded to the nearest 0.25%).

A wide variety of rock types are present in the upper Conasauga Group. As a result, various rock classification schemes are employed to adequately describe the rocks (Table 2.1). Because many of the limestone lithologies of the Nolichucky Shale contain appreciable amounts of siliciclastic material, adjectives such as argillaceous and silty are appropriate to further define the rock. In addition, limestone in the Maynardville is partially to pervasively dolomitized. Modifiers such as dolomitized, argillaceous, silty, sandy, etc. precede the main rock name if the abundance of these components exceeds 10 volume percent of the rock. Also, this investigation uses other standard conventions; bedding terminology and grain size nomenclature is outlined in Appendix A.

Facies Analysis

Introduction

As a result of this investigation, fourteen major lithofacies (Table 2.2) are identified in the upper Conasauga Group. The assemblage of facies within the Nolichucky Shale differs significantly from that of the Maynardville Limestone (Table 2.2). The Nolichucky contains an abundance of thick shale and thinly bedded shale and limestone lithologies, whereas the Maynardville is composed of very thick-bedded carbonate, predominantly limestone (compare Figures 2.2 and 2.3; see Table 2.2 for geological meaning of symbols). Data presented in Figures 2.2 and 2.3 are based on megascopic criteria which have been observed in the field. Further discrimination of lithofacies is possible through petrographic analysis. Table 2.3 summarizes petrographic

Table 2.1. Rock classification schemes used to describe the Nolichucky/Maynardville sequence.

Rock Type	Classification Used
Field classification of carbonate rocks (excludes stromatolites, thrombolites, cryptalgalaminates)	Dunham, 1969
Stromatolites and Thrombolites	Kennard and James, 1987
Cryptalgalaminates	Aitken, 1967
Petrographic classification of carbonate rocks	Folk, 1959; 1962
Siltstone	Picard, 1971
Shale*	Blatt, Middleton, and Murray, 1980

*Shale refers to fine-grained, fissile siliciclastic material predominantly composed of clay- and silt-sized particles

Table 2.2. The 14 major lithofacies which occur in the upper Conasauga Group. Symbols are used commonly in the text.

Symbol	Rock Name
CL	Cryptalgalaminates
STROM	Stromatolites
THROM	Thrombolites
NOPG	Oncolitic-oolitic packstone/grainstone
EPG	Peloidal packstone/grainstone
MWS	Mudstone interbedded with shale
OPG	Oolitic packstone/grainstone
FPG	Fossiliferous packstone/grainstone
FPGWS	Fossiliferous packstone/grainstone interbedded with shale
XPG	Laminated peloidal packstone/grainstone
XPGWS	Laminated peloidal packstone/grainstone interbedded with shale
SWXPG	Shale interbedded with laminated peloidal packstone/grainstone
S	Shale
IPG	Intraclastic packstone/grainstone

	NOLICHUCKY SHALE						MAYNARDVILLE LIMESTONE					
LITHOFACIES	NP	VR	R	C	A	VA	NP	VR	R	C	A	VA
CL	▨						▨	▨	▨	▨		
STROM	▨						▨	▨	▨	▨		
THROM	▨	▨	▨				▨	▨	▨	▨	▨	▨
NOPG	▨	▨					▨	▨	▨	▨		
EPG	▨	▨					▨	▨	▨	▨		
MWS	▨	▨	▨				▨	▨	▨			
OPG	▨	▨	▨	▨			▨	▨	▨			
FPG	▨	▨	▨				▨					
FPGWS	▨	▨	▨				▨					
XPG	▨	▨	▨				▨					
XPGWS	▨	▨	▨	▨	▨		▨	▨	▨			
SWXPG	▨	▨	▨	▨			▨	▨				
S	▨	▨	▨	▨	▨	▨	▨	▨				
IPG	▨	▨	▨	▨			▨	▨				

Figure 2.2. Comparative analysis between the Nolichucky Shale and Maynardville Limestone showing the relative abundance of each lithofacies (NP=Not Present; VR=Very Rare, <1%; R=Rare, 1-5%; C=Common, 5-15%; A=Abundant, 15-25%; VA=Very Abundant, >25%). For example, a lithofacies that is indicated as "abundant" accounts for between 15 to 25 meters of a stratigraphic section 100 meters thick. The abundance of each lithofacies is calculated for each locality.

	NOLICHUCKY SHALE				MAYNARDVILLE LIMESTONE			
	Rock-unit tkn. (cm.)		Bed tkn. (cm.)		Rock-unit tkn. (cm.)		Bed tkn. (cm.)	
Lithofacies	Mean	Range	Mean	Range	Mean	Range	Mean	Range
CL	0	---	---	---	221	28-716	221	28-716
STROM	0	---	---	---	120	45-210	120	45-210
THROM	134	13-275	134	13-275	417	11-2371	417	11-2371
NOPG	54	6-169	54	6-169	152	12-548	152	12-548
EPG	18	8-46	18	8-46	282	45-1100	282	45-1100
MWS	26	1-432	---	---	66	4-330	---	---
-M	---	---	2	<1-5	---	---	2	<1-5
-S	---	---	2	<1-5	---	---	2	<1-5
OPG	19*	2-115*	19*	2-115*	6	3-8	6	3-8
FPG	28	2-211	28	2-211	0	---	0	---
FPGWS	53	15-265	---	---	0	---	---	---
-FPG	---	---	3	<1-5	---	---	0	---
-S	---	---	2	<1-5	---	---	0	---
XPG	24	2-208	24	2-208	0	---	0	---
XPGWS	33	2-369	---	---	37	8-188	---	---
-XPG	---	---	3	<1-5	---	---	3	<1-5
-S	---	---	2	<1-5	---	---	2	<1-5
SWXPG	40	3-308	---	---	16	3-27	---	---
-S	---	---	5	<1-10	---	---	3	<1-5
-XPG	---	---	1	<1-2	---	---	1	<1-2
S	38	2-287	38	2-287	19	4-57	19	4-57
IPG	9	2-45	9	2-45	7	3-25	7	3-25

Figure 2.3. Comparative analysis between the Nolichucky Shale and Maynardville Limestone showing the rock-unit thickness and bed thickness of each lithofacies. Astericks (*) indicate that thick ooid shoal units observed at the I-75 and the Roaring Spring sections have not been factored into these values.

Table 2.3. Constituent composition of lithofacies. Values are expressed in percent (TR=trace=<0.5%).

Constituent	CL		STROM		THROM		NOPG	
	ave.	range	ave.	range	ave.	range	ave.	range
Echinoderms	---	---	---	---	2	TR-3	1	TR-3
Inarticulate brachs.	---	---	---	---	---	---	------	
Trilobites	TR	0-1	TR	0-TR	1	TR-2	3	TR-8
Girvanella	1	0-4	---	---	6	4-11	1	0-3
Chancelloria	---	---	---	---	---	---	---	---
Sponge spicules	---	---	---	---	3	2-6	TR	0-2
Skeletals, Total	1	0-4	TR	0-TR	18	9-44	6	1-15
Intraclasts, Total	TR	0-2	---	---	2	0-8	6	0-25
Mudstone	TR	0-2	---	---	1	0-7	1	0-3
Peloidal pckst.	---	---	---	---	TR	0-TR	3	0-16
Fossil. pckst.	---	---	---	---	---	---	TR	0-2
Oolitic pckst.	---	---	---	---	---	---	2	0-9
Qtz. siltstone	---	---	---	---	---	---	---	---
Ooids, Total	1	0-5	---	---	1	0-4	16	4-33
Fibrous/Pris.	TR	0-1	---	---	---	---	9	4-20
Polycrystalline	---	---	---	---	1	0-4	4	0-8
Monocrystalline	---	---	---	---	---	---	2	0-6
Superficial	1	0-5	---	---	---	---	---	---
Oncoids	---	---	---	---	---	---	22	14-31
Peloids	6	0-8	28	22-35	1	0-6	8	4-13
Micrite/Microspar	23	12-51	23	16-31	58	38-68	14	0-32
Cement, Total	7	0-21	7	5-9	3	0-8	20	TR-39
Fibrous/bladed	---	---	---	---	---	---	19	0-39
Syntaxial	---	---	---	---	---	---	1	0-2
Blocky	7	0-21	7	5-9	3	0-8	1	0-4
Qtz./feld. silt	1	0-4	---	---	1	0-6	---	---
Clay/Mica	---	---	---	---	2	0-12	---	---
Glauconite	---	---	---	---	---	---	---	---
Dolomite/Stylolite	47	23-71	41	25-58	12	3-23	6	0-14
Phosphate	---	---	---	---	---	---	---	---
No. of thin-sections	4		2		5		6	

Table 2.3. (continued).

Constituent	EPG		MWS		OPG		FPG	
	ave.	range	ave.	range	ave.	range	ave.	range
Echinoderms	2	0-13	TR	0-TR	3	0-33	12	TR-47
Inarticulate brachs.	---	---	TR	0-1	TR	0-TR	1	0-5
Trilobites	1	0-5	2	0-6	2	0-9	13	2-46
Girvanella	---	---	5	2-9	1	0-7	3	0-11
Chancelloria	---	---	---	---	TR	0-6	7	0-18
Sponge spicules	---	---	TR	0-1	---	---	TR	0-3
Skeletals, Total	4	0-18	7	2-14	6	TR-35	35	25-50
Intraclasts, Total	4	0-14	2	0-8	3	0-23	1	0-5
Mudstone	3	0-14	2	0-8	1	0-12	---	---
Peloidal pckst.	TR	0-1	TR	0-4	1	0-9	1	0-5
Fossil. pckst.	TR	0-3	---	---	---	---	---	---
Oolitic pckst.	---	---	---	---	1	0-23	---	---
Qtz. siltstone	---	---	---	---	---	---	---	---
Ooids, Total	7	0-34	---	---	44	27-57	3	0-12
Fibrous/Pris.	TR	0-2	---	---	22	3-47	1	0-4
Polycrystalline	---	---	---	---	15	0-43	---	---
Monocrystalline	---	---	---	---	7	0-40	2	0-12
Superficial	7	0-34	---	---	---	---	TR	0-2
Oncoids	---	---	---	---	---	---	---	---
Peloids	45	22-64	9	0-24	4	0-14	12	0-34
Micrite/Microspar	7	0-27	56	35-76	16	0-50	19	0-36
Cement, Total	22	7-33	2	0-7	22	0-52	15	0-32
Fibrous/bladed	3	0-21	TR	0-3	18	0-52	7	0-27
Syntaxial	1	0-3	TR	0-2	1	0-23	5	0-20
Blocky	18	3-33	1	0-3	2	0-11	3	0-8
Qtz./feld. silt	---	---	TR	0-3	TR	0-2	TR	0-1
Clay/Mica	---	---	12	5-32	TR	0-5	---	---
Glauconite	---	---	TR	0-1	TR	0-8	TR	0-2
Dolomite/Stylolite	10	0-23	8	3-12	4	0-13	13	3-31
Phosphate	---	---	---	---	---	---	TR	0-5
No. of thin-sections	7		9		32		10	

Table 2.3. (continued).

Constituent	FPGWS		XPG		XPGWS		SWXPG	
	ave.	range	ave.	range	ave.	range	ave.	range
Echinoderms	12	0-36	3	0-11	4	1-11	2	0-15
Inarticulate brachs.	1	0-3	1	0-2	TR	0-2	2	0-6
Trilobites	11	0-21	3	0-9	11	3-17	3	0-6
Girvanella	2	0-8	1	0-4	1	0-3	---	---
Chancelloria	2	0-13	---	---	1	0-7	---	---
Sponge spicules	---	---	---	---	TR	0-1	---	---
Skeletals, Total	29	18-37	8	TR-20	14	10-23	6	TR-22
Intraclasts, Total	---	---	1	0-7	3	0-9	3	0-29
Mudstone	---	---	1	0-7	1	0-4	---	---
Peloidal pckst.	---	---	TR	0-TR	2	0-7	3	0-29
Fossil. pckst.	---	---	---	---	---	---	---	---
Oolitic pckst.	---	---	---	---	---	---	---	---
Qtz. siltstone	---	---	---	---	---	---	---	---
Ooids, Total	---	---	2	0-11	TR	0-2	---	---
Fibrous/Pris.	---	---	2	0-11	TR	0-2	---	---
Polycrystalline	---	---	---	---	---	---	---	---
Monocrystalline	---	---	TR	0-TR	---	---	---	---
Superficial	---	---	TR	0-TR	---	---	---	---
Oncoids	---	---	---	---	---	---	---	---
Peloids	14	4-28	35	3-60	23	14-31	20	0-52
Micrite/Microspar	11	0-27	3	0-7	14	5-34	10	0-25
Cement, Total	18	0-54	12	0-32	18	6-34	5	0-12
Fibrous/bladed	12	0-35	2	0-6	1	0-3	2	0-12
Syntaxial	4	0-19	3	0-9	3	0-20	---	---
Blocky	2	0-7	7	0-22	13	6-25	3	0-12
Qtz./feld. silt	1	0-3	11	0-55	1	0-4	6	0-22
Clay/Mica	10	0-31	5	0-20	12	6-26	36	14-62
Glauconite	3	0-17	2	0-8	TR	0-1	1	0-4
Dolomite/Stylolite	7	0-15	19	0-71	8	1-19	10	0-21
Phosphate	2	0-9	---	---	TR	0-2	1	0-10
No. of thin-sections	7		10		8		9	

Table 2.3. (continued).

Constituent	S		IPG	
	ave.	range	ave.	range
Echinoderms	1	0-4	5	TR-17
Inarticulate brachs.	4	TR-13	TR	0-1
Trilobites	1	0-5	5	TR-15
Girvanella	---	---	1	0-7
Chancelloria	---	---	TR	0-3
Sponge spicules	---	---	TR	0-2
Skeletals, Total	6	TR-14	11	2-27
Intraclasts, Total	TR	0-4	54	27-92
Mudstone	TR	0-3	14	0-67
Peloidal pckst.	TR	0-2	21	0-65
Fossil. pckst.	TR	0-TR	13	0-92
Oolitic pckst.	---	---	TR	0-3
Qtz. siltstone	---	---	5	0-78
Ooids, Total	---	---	1	0-10
Fibrous/Pris.	---	---	1	0-10
Polycrystalline	---	---	---	---
Monocrystalline	---	---	---	---
Superficial	---	---	---	---
Oncoids	---	---	---	---
Peloids	30	9-61	8	0-23
Micrite/Microspar	---	---	5	0-21
Cement, Total	---	---	8	0-24
Fibrous/bladed	---	---	2	0-8
Syntaxial	---	---	4	0-12
Blocky	---	---	3	0-10
Qtz./feld. silt	2	TR-9	TR	0-6
Clay/Mica	55	31-82	3	0-28
Glauconite	1	0-3	TR	0-1
Dolomite/Stylolite	4	0-29	7	0-27
Phosphate	---	---	---	---
No. of thin-sections	16		27	

composition for 152 thin-sections which have been point-counted. Figures 2.2 and 2.3 and Table 2.3 should serve as general reference throughout the remainder of this Chapter.

Temporal and spatial variability of facies and environments will be addressed in Chapter 5. Thus, columnar sections are displayed more appropriately in that chapter.

Cryptalgalaminate (CL)

Cryptalgalaminate (after Aitken, 1967) is used here to refer to planar-laminated stromatolites. Stromatolites are defined as laminated organosedimentary structures built by trapping and binding of detrital sediment and/or mineral precipitation in association with microbial communities (Kennard and James, 1987). Recently, it has been established that sediment-forming microbial communities are dominated by cyanobacteria (blue-green algae of earlier authors) (for a complete discussion, see Bauld, 1981; Krumbein, 1983). Thus, the term "cryptalgal" (meaning hidden algae) is not literally correct. Revised classification schemes have been proposed (Kennard and James, 1987; Burne and Moore, 1987), but at present, cryptalgalaminate is preferred because it conveys precise meaning and is widely adopted.

Description (Table 2.4)

Cryptalgalaminates are distinctive features of the Maynardville Limestone, but are entirely absent within the Nolichucky Shale (Figure 2.2). Interlayered laminae that are smooth, wavy, and crinkly

Table 2.4. Characteristics of the CL Lithofacies.

Features		Characteristics
Lithology (Folk, 1959; 1962)		-Dolomitized pelmicrite -Fenestral dolomicrite -Dolomitized fenestral micrite
Bed Thickness		-Medium- to very thick-bedded -Laterally continuous
Sedimentary Texture and Structure		-Thinly laminated -Irregular, planar, wavy laminations -Cross-laminated -Small-scale truncation -Mudcracks -Microtepee structures -Fenestral fabric -Spar-filled pseudomorphs (?)
Bed Contacts		
	Upper	-Sharp
	Lower	-Sharp
Fossils		-Rare; finely comminuted trilobites, *Girvanella* tubules
Other		-Quartz silt -Superficial ooids -Algal peloids
No. of Thin-Sections Examined		-6
No. of Thin-Sections Point-Counted		-4

are the most distinguishing characteristic of this Facies (Figure 2.4A and B). Each individual lamina is made up of dolomicrite, dolomitized peloidal packstone/grainstone (Figure 2.4C), or intraclastic packstone with local accumulation of quartz silt and superficial ooids. The former two types of laminae are most commonly interlayered. Because laminae are thin, typically less than 0.5 mm thick, numerous laminae are bundled to form individual beds. Bed thickness averages about 2 m, but may exceed 7 m (Figure 2.3). Cross-stratified and truncated laminae are commonly observed where lateral exposure is sufficient (Figure 2.4D). Truncation of laminae forms micro-unconformities and reveals small-scale channels (?). Also, erosion is apparent where large platy clasts of laminated rock have been fragmented and locally transported. Other diagnostic features of this facies include: rare shallow mudcracks, microtepee structures, fenestral fabric, chert, and spar-filled pseudomorphs (?).

Interpretation

The cryptalgalaminates described above are similar in many respects to smooth mat-like sheets currently forming in lower to upper intertidal zones from Shark Bay (Logan and others, 1974) and the Persian Gulf (Kendall and Skipwith, 1968; Purser and Evans, 1973; Kinsman and Park, 1976). These modern cyanobacterial sheets resemble the Maynardville cryptalgalaminates in the following ways: (1) planar or smooth laminae prevail over highly crenulated or pustular laminae, (2) individual laminae are thin (usually several millimeters or less), (3) laminae are

Figure 2.4. Selected features of the Cryptalgalaminate (CL) Lithofacies.

A. Outcrop of smooth and wavy laminae which overlie a thin and laterally discontinuous interval dominated by laterally-linked hemispheroids (LLH) or domal stromatolites. LLH structures occur just above the tape measure. Base of tape is 5 cm in length. Roaring Spring section.

B. Polished slab of alternating light and dark laminae. Smooth and wavy laminae are dominant. Low-amplitude stylolites should not be confused with crinkly laminae. Rock is entirely dolomite. Interstate 75 section. Sample I-82-0.3.

C. Photomicrograph of dolomicrite (dark bands) and dolomitized peloidal packstone (light bands). Field of view is 6.5 mm in long dimension. Interstate 75 section. Sample I-80-1.3.

D. Outcrop of buckled, truncated, and ripped-up laminated rock. Note that intraclasts are angular and irregular in shape; this suggests that clasts were locally transported. Pencil is 14 cm long. Interstate 75 section.

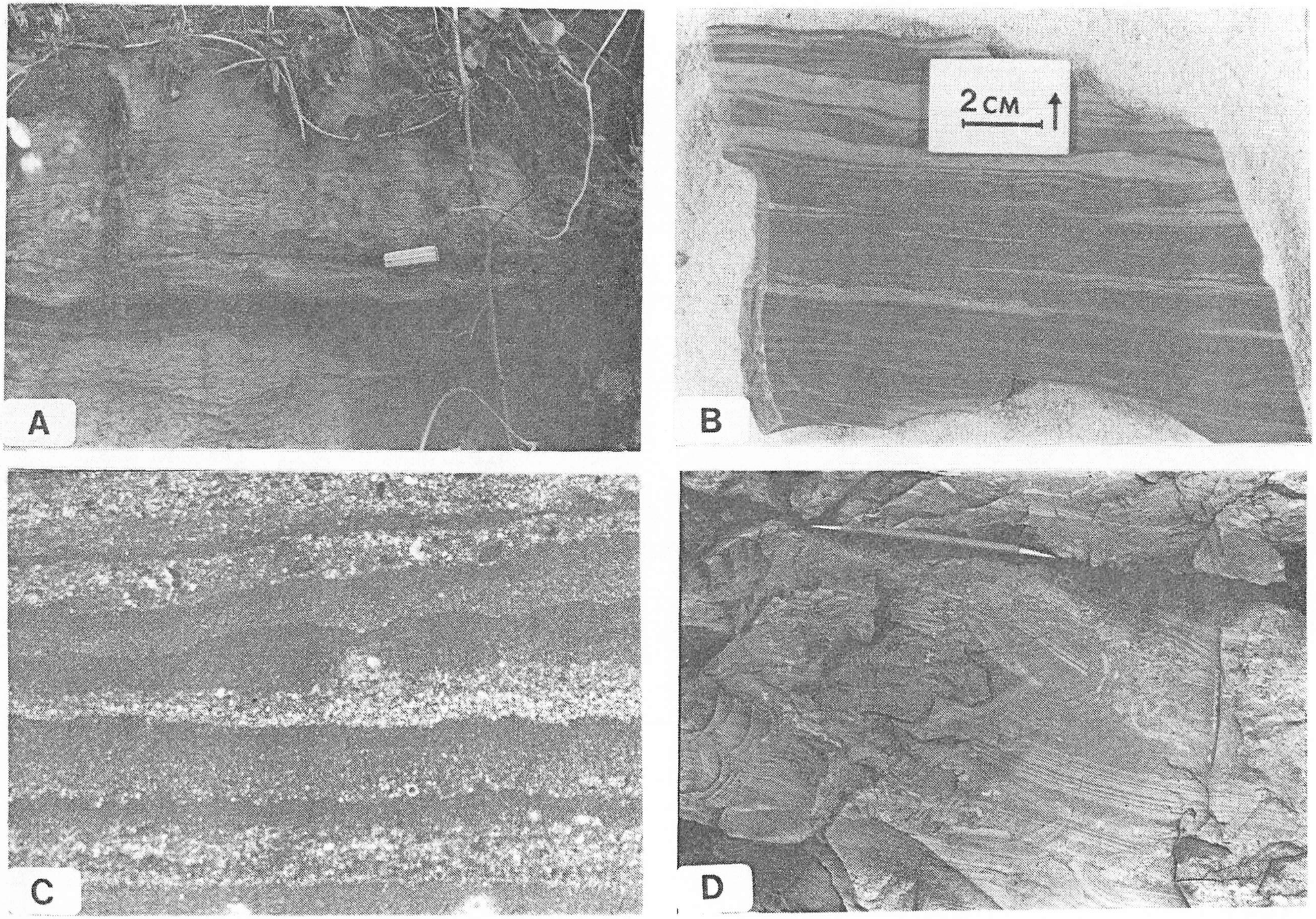
A
2 см
B
C
D

composed of alternating lime mud (micrite) and peloids, and (4) thin intraclastic beds may interrupt normal alternation of laminae. In addition, mudcracks, microtepee structures, fenestrae, and erosion are common to both modern and ancient low-energy tidal flat settings (James, 1979; Shinn, 1983).

Trapping and binding of detrital sediments by cyanobacteria are the primary mechanisms that form Shark Bay and Persian Gulf "cryptalgal" laminations. According to Logan and others (1974) and Davies (1970), sediment is transported from subtidal areas onto the tidal flats (e.g., trilobites and peloids in the Maynardville). During exceptional storms, intraclastic layers are deposited, and algal mats are locally scoured, eroded, and reworked (Logan and others, 1974; Shinn, 1983).

The occurrence of quartz silt and fine-grained superficial ooids in the Maynardville is enigmatic. Although superficial ooids are recognized in facies down depositional dip and could be transported onto the tidal flat by tides (probably storm tides), quartz silt is not ubiquitous anywhere within the Maynardville. However, certain laminae on the tidal flat reveal microlenses of silt-sized ooids and quartz. These locally abundant accumulations probably represent wind-transported sediment that were either reworked by tidal water or deposited in slight topographic depressions.

Flat-laminated sediments (grossly similar to the Maynardville) occur in upper intertidal and supratidal environments in the Bahamas (Hardie, 1977). Differences in composition and thickness of laminae as well as the absence of fresh water carbonate (algal tuffa) may rule out the Bahaman modern analogue. In addition, the Bahaman tidal flat is situated in a humid, tropical climate. Markello (1979) infers that the southern Appalachians were under the influence of a semiarid climate during the Late Cambrian. He cites the following to support his claim: the occurrence of collapse breccia, pseudomorphs after evaporites, the paucity of burrowing in very shallow sublittoral facies, the presence of calcitized anhydrite, and the preservation of stromatolites. Harris (1973), Alberstadt and Reesman (1978), Friedman and Radke (1979), Friedman (1980), Erwin (1981), and Demicco (1985) provide additional evidence to suggest that much of the Middle Cambrian to Lower Ordovician sequence along the Appalachian chain was deposited in an arid to semiarid climate.

Planar stromatolites in the Maynardville are interpreted to have formed in lower to upper intertidal zones of low-energy tidal flats. Mudcracks, uniformity of laminae, and buckling and brecciation of layers support this interpretation. The evidence presented here supports deposition from suspension, scour, and subaerial exposure, all processes active in intertidal regimes.

Stromatolites (STROM)

Description (see Table 2.5)

In this study three types of stromatolites have been observed, but only two varieties are considered important to this lithofacies. The Stromatolite Facies is composed of interstratified domal and planar

Table 2.5. Characteristics of the STROM Lithofacies.

Features	Characteristics
Lithology (Folk, 1959; 1962)	-Dolomitized fenestral pelmicrite -Dolomitized pelmicrite -Dolomitized biolithite -Dolostone
Bed Thickness	-Thick- to very thick-bedded -Laterally continuous
Sedimentary Texture and Structure	-Thinly laminated -Fine-grained algal peloids (pellets?) -Algal peloids rounded to subrounded -Fenestral fabric
Bed Contacts	
Upper	-Sharp
Lower	-Sharp
Fossils	-Rare; finely comminuted trilobites
Other	-Domal stromatolites are interstratified with cryptalgalaminates -Digitate stromatolites are interstratified with thrombolites
No. of Thin-Sections Examined	-7
No. of Thin-Sections Point-Counted	-2

stromatolites which form stratiform units (beds), ranging in thickness from 45 cm to 210 cm (Figure 2.3). Domal stromatolites are observed only in the Maynardville Limestone (Figure 2.2). Individual domes range from 1 cm to 10 cm in length and are less than 10 cm in vertical dimension (see Figure 2.4A). Sediment infilling interdomal regions includes dolomitized peloidal packstone/grainstone, intraclastic packstone, and mudstone. Also, cryptalgalaminates (similar in composition to the previously described lithofacies) are juxtaposed to domal stromatolites. Laminae which make up these stromatolites are composed primarily of alternating bands of peloids and micrite (now dolomicrite) (Figures 2.5A and B). Individual laminae are planar to curved, rarely more than several millimeters thick. Although this lithofacies may resemble the Cryptalgalaminate Lithofacies, significant differences exist. Irregular and wavy laminae, mudcracks, microtepee structures, and truncation features are not prevalent here. Fenestral fabric is locally important (Figure 2.5C).

Digitate stromatolites (the third type of stromatolite) are recognized in the Nolichucky Shale and the Maynardville Limestone as low relief hemispheroidal finger-like protrusions which tend to coalesce upward into thin wavy and planar-laminated bedfoms (Figure 2.5D). Digitate stromatolites are observed in association with thrombolites, and commonly form caps that never exceed a few centimeters in thickness. Because of the close association of digitate stromatolites with thrombolites, both rock types are included in the Thrombolite Lithofacies and will be discussed later.

Figure 2.5. Characteristics of Maynardville stromatolites.

A. Photomicrograph of domal and planar stromatolites. Fine-grained, curved laminae of dolomicrite (darker bands) are interlayered with coarsely crystalline dolomitic peloid grainstone. Domal stromatolite (to right) is overlain by smooth/irregular laminae and peloidal carbonate. Field of view is 6.5 mm in long dimension. Joy 2 section. Sample J-2 307.5.

B. Photomicrograph is similar to A except much finer grained. Field of view is 6.5 mm in long dimension. Roaring Spring section. Sample R-19.

C. Photomicrograph of irregular fenestrae in partially dolomitized mudstone. Fenestral voids are filled with blocky calcite and dolomite cement. Field of view is 6.5 mm in long dimension. Interstate 75 section. Sample I-81-5.9.

D. Polished slab of digitate stromatolite. Abundant spar-filled laminoid fenestral voids occur within the stromatolite. Micrite is located between adjacent digitate "fingers". Irregular vugs are apparent in this area and are filled with blocky calcite cement. Also note "peaked" stylolites. Stratigraphic up is toward top of page in this sample. Interstate 75 section. Sample I-81-5.9.

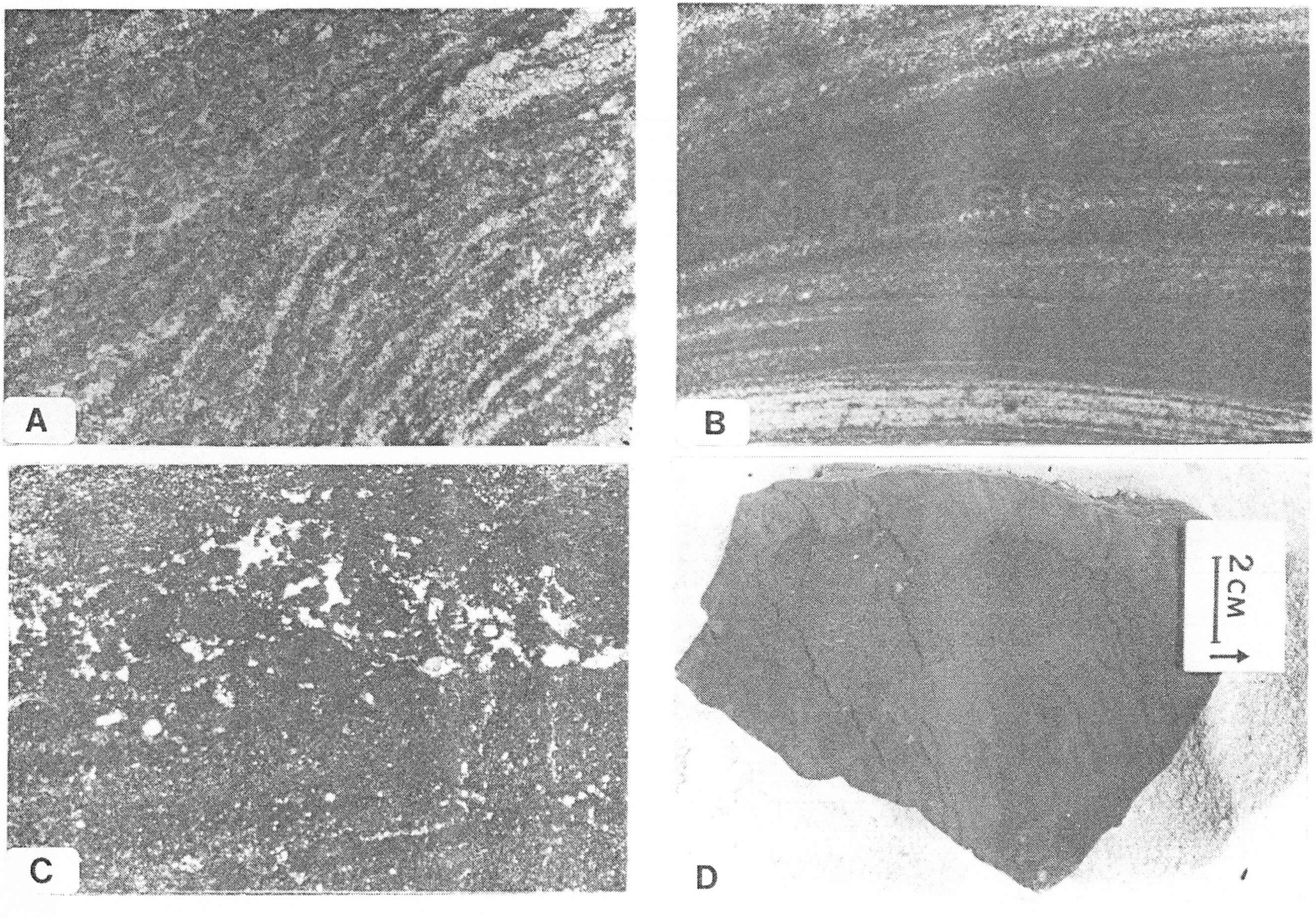
A
B
C
D
2 CM

Interpretation

Rapid microbial growth and effective binding are requisites for the development of domal stromatolites (laterally linked hemispheroids or LLH structures, after Logan and others, 1964). Mats of colloform cyanobacterial which resemble LLH structures occur in modern subtidal and lower intertidal settings (Kendall and Skipwith, 1968; Logan and others, 1974; Playford and Cockbain, 1976). Ginsburg and others (1954), Logan and others (1964), Aitken (1967), and Bathurst (1975) documented the occurrence of domal stromatolites on intermittently exposed tidal flats.

Deposition of the Stromatolitic Facies took place in the lower intertidal regime. This interpretation is supported by an absence of sedimentary features which suggest long-term exposure. Smooth flat laminations, crinkly lamination, shallow mudcracks, and microtepee structures are not found. The paucity of burrows and biotic constituents in this Lithofacies, as well as the occurrence of fenestral fabric and close stratigraphic association with cryptalgalaminates suggests that deposition occurred in an intertidal rather than subtidal setting.

Energy levels were somewhat higher in the Stromatolitic environment, as compared to the Cryptalgalaminatic environment. However, the small size of domal stromatolites as well as the absence of columnar stromatolites precludes deposition in high-energy. Hoffman (1976) suggests that low-relief and laterally discontinuous domal stromatolites are diagnostic of lower energy (protected shoreline) low intertidal settings.

Thrombolites (THROM)

Thrombolites are microbial structures that are related to stromatolites but lack internal lamination (Aitken, 1967). Thrombolites exhibit a megascopic clotted or mottled fabric of primary origin. The abundant, finely crystalline, and closely spaced mesoclots are easily distinguished from mottling caused by bioturbation, tectonism, or pressure solution. According to Kennard and James (1987) clots within thrombolites represent individual and/or colonial growth forms of microbial communities. These growth forms may be poorly differentiated but tend to be coccoid-dominated. Stromatolites, on the other hand, result from episodic sediment trapping and binding, and/or carbonate precipitation of mat-like or filamentous microbial communities (Kennard and James, 1987).

Description (Table 2.6)

In this study biohermal and biostromal thrombolites are similar in external appearance to stromatolites, but the internal composition of thromboids is strikingly different (Figure 2.6A). Internal megascopic structure consists of microcrystalline, nonlaminated, upward directed network of millimeter- to centimeter-scale fingers (mesoclots) which are separated by patches of carbonate mud (now burrowed mudstone) and coarse sediment (fossiliferous, oolitic, and peloidal wackestone to grainstone) (Figure 2.6B). Mesoclots make up between 25% and 75% of the volume of a thrombolite, and display a wide range of geometric shapes (e.g., arborescent, digitate, cerebral) and spatial patterns (e.g., isolated,

Table 2.6. Characteristics of the THROM Lithofacies.

Features	Characteristics
Lithology (Folk, 1959; 1962)	-Dolomitized biolithite -Biolithite
Bed Thickness	-Medium- to very thick-bedded -Non-bedded internally -Laterally continuous
Sedimentary Texture and Structure	-Mottled or clotted fabric -Burrows and bioturbation -Fine- to coarse-grained allochems -Rare fenestral pores
Bed Contacts	
Upper	-Sharp
Lower	-Sharp
Fossils	-Abundant and diverse; <u>Girvanella</u>, sponge spicules, echinoderms, trilobites, <u>Renalcis</u>, gastropods, pelecypods, <u>Epiphyton</u>, hyolithids
Other	-<u>Girvanella</u>, <u>Renalcis</u>, and lime mud make up some mesoclots -Vuggy porosity
No. of Thin-Sections Examined	-23
No. of Thin-Sections Point-Counted	-5

Figure 2.6. Selected features of the Thrombolite (THROM) Lithofacies.

A. Outcrop of thrombolitic bioherms. Note that internal lamination is distinctly absent from these buildups. Rock hammer is 25 cm in long dimension. Interstate 75 section.

B. Outcrop of upward directed mesoclots in a thrombolitic buildup. Adjacent to darker colored mesoclots is lime mudstone and grainstone. Field notebook is 11 cm in width. Roaring Spring section.

C. Photomicrograph of Epiphyton in a clotted micrite matrix. Field of view is 6.5 mm in long dimension. Interstate 75 section. Sample I-3-1.0.

D. Outcrop of planar-laminated stromatolites which cap a thrombolitic interval. Stromatolites are approximately 0.5 m thick. Interstate 75 section.

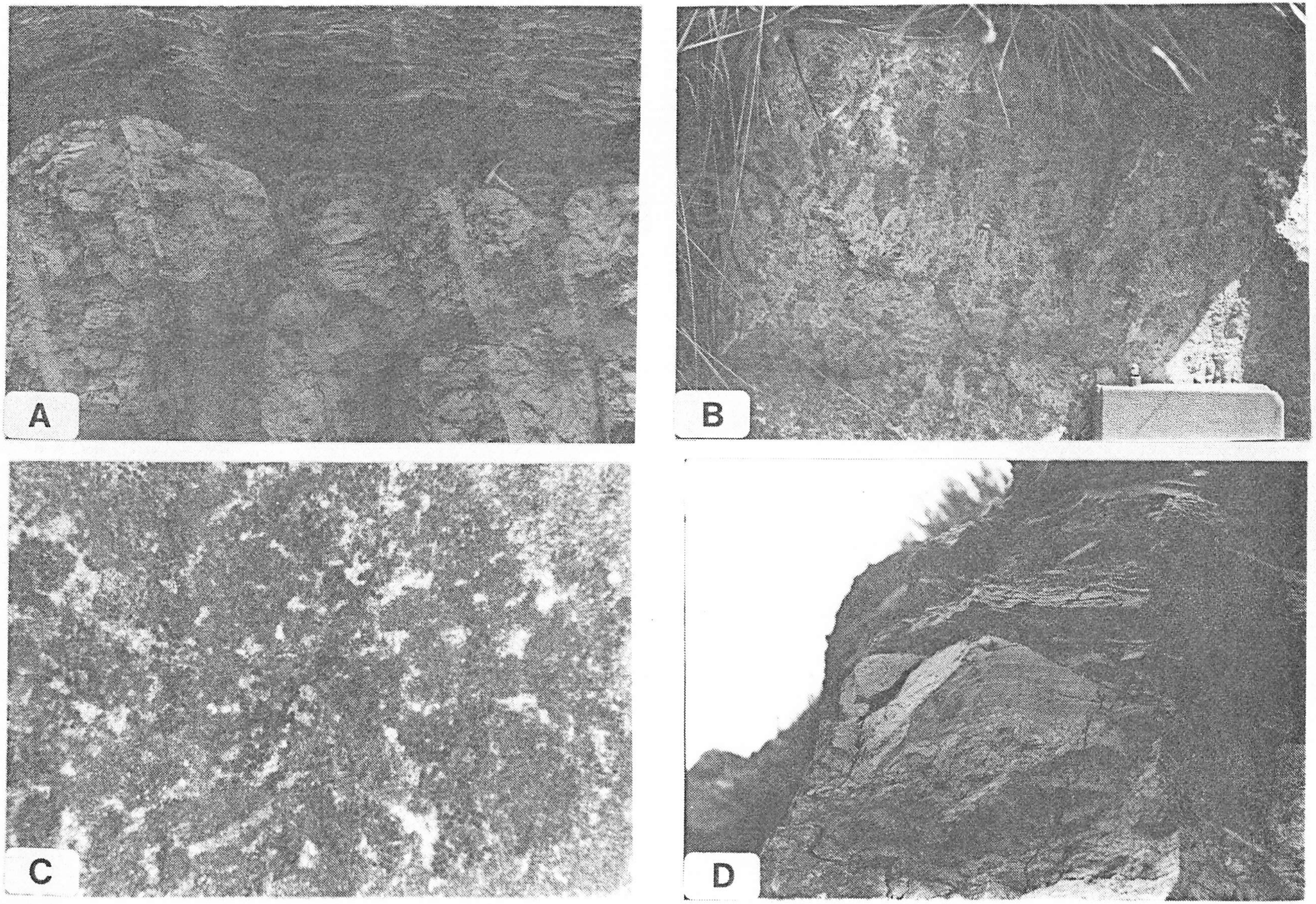
A
B
C
D

interconnected, coalesced). Biotic constituents associated with thrombolites are diverse and fairly abundant for the Cambrian (Table 2.3). *Girvanella*, *Renalcis*, and *Epiphyton* (Figure 2.6C) occur in association with the clotted micritic matrix.

The Thrombolite Lithofacies is composed primarily of thrombolites, but digitate stromatolites are also included here. Digitate stromatolites, which grade upward into thin wavy-laminated stromatolites, cap many thrombolitic horizons (Figure 2.6D and see Figure 2.11A). The stromatolites reveal fenestral fabric, irregular lamination, fine-grained dolomite replacement, and preserved *Girvanella* tubules.

This Facies is recognized in the Nolichucky Shale and Maynardville Limestone. Thrombolites are a subordinant component of the rock in the Nolichucky, while in the Maynardville, thrombolites are the dominant facies type (Figure 2.2). This Facies ranges from 11 cm to more than 23 m in thickness (Figure 2.3).

Interpretation

Thrombolites are essentially a lower Paleozoic phenomenon. Lack of recognition of these features in the Recent prevents the use of a uniformitarian approach, and thus, offers a potential interpretative problem. Fortunately, thrombolites have been studied thoroughly (Aitken, 1967; Ahr, 1971; James and Kobluk, 1978; Pratt and James, 1982; Demicco, 1985), and these studies indicate that thrombolites were deposited within a narrow zone extending from very shallow subtidal to low intertidal settings. Aitken (1967) studied thrombolites from the Cambro-Ordovician sequence in Alberta, Canada and concluded that deposition took place in water less than 2 m deep.

In the upper Conasauga Group, biohermal and biostromal thrombolites represent very shallow subtidal conditions based on the following features (no one feature indicates a particular depositional environment):

1. Irregular distribution of sediment on microbial mat surfaces
2. Irregular surface topography of thromboid "fingers"
3. Disruption by burrows
4. Abundant and diverse in situ fossil assemblages
5. Capping digitate and planar stromatolites
6. Fenestral fabric
7. Close stratigraphic association with the Cryptalgalaminate and Stromatolite Facies
8. Absence of features which indicate subaerial exposure

It is likely that the tops of many thrombolites shoaled to the lowermost intertidal zone. This is supported by the presence of digitate and planar stromatolite caps which display laminoid fenestrae. Based upon previous work (see citations above), thrombolites developed in mildly to strongly agitated water. The occurrence of grain-supported fabric and intraclasts in inter-thromboid regions of the Nolichucky/Maynardville thrombolites suggests at least moderately high-energy levels during certain periods.

Oncolitic-Oolitic Packstone/Grainstone (NOPG)

Description (Table 2.7)

Oncolitic carbonates range from 0.06 m to 5.48 m in thickness (Figure 2.3). They are observed most commonly in the Maynardville Limestone (Figure 2.2) as massive beds which average about 1.5 m in thickness (Figure 2.7A). In polished hand specimens and in thin-sections, this Facies is composed of packstone and poorly washed grainstone. Oncoids are the most abundant allochemical grain type, but skeletal debris, peloids, intraclasts, and ooids represent significant components of the rock (Table 2.3). Oncolitic lithologies are composed of abundant subelongate to elongate oncoids (14-31%), some of which measure up to 5 mm in long dimension. Girvanella sheaths, Renalcis, molluscs, trilobites, echinoderm ossicles, superficial ooids, peloids and small oncoids serve as nuclei.

Using the classification of Logan and others (1964), three morphologic types of oncoids are discerned in this study:

1. Type "C" oncoids: shape of oncoid is dependent on the shape of the nucleus. Individual laminae are irregular, even, and traced around the oncoid.
2. Type "R" oncoids: irregular and dome-shaped oncoids, where differential growth of microbes has produced laminae which pinch and swell and do not necessarily conform to nucleus shape. Individual laminae are irregular, uneven, and traced around the nucleus.

Table 2.7. Characteristics of the NOPG Lithofacies.

Features	Characteristics
Lithology (Folk, 1959; 1962)	-Oolitic, oncolitic intramicrudite -Fossiliferous, oncolitic oomicrite -Dolomitized oolitic oncosparrudite -Peloidal, oncolitic oosparite -Dolomitized peloidal oncosparrudite
Bed Thickness	-Thin- to very thick-bedded -Laterally continuous
Sedimentary Texture and Structure	-Coarse-grained ooids and oncoids (commonly exceed 2 mm. in diameter); rounded to subelongate and well-sorted -Hardgrounds -Aggregate grains -Spar-filled burrows
Bed Contacts	
Upper	-Sharp
Lower	-Sharp
Fossils	-Trilobites and rare echinoderms, *Girvanella* tubules, and sponge spicules
Other	-Stylolites -Pores filled with fibrous cement
No. of Thin-Sections Examined	-6
No. of Thin-Sections Point-Counted	-6

Figure 2.7. Selected features of the Oncolitic-Oolitic Packstone/Grainstone (NOPG) Lithofacies.

A. Outcrop of the upper portion of a thick oncolitic bed. Oncoids are several mm long. Also note other coarse-grained allochems such as ooids and coated trilobite grains. Rock hammer for scale. Beech Grove section.

B. Photomicrograph of normal (C) and irregular dome-shaped (R) oncoids. See text for explanation of types of oncoids. Field of view is 6.5 mm in long dimension. Interstate 75 section. Sample I-74-9.8.

C. Photomicrograph of interrupted oncoid. This type of oncoid reveals irregular, wavy laminae which are truncated. Field of view is 6.5 mm in long dimension. Interstate 75 section. Sample I-62-1.2.

D. Photomicrograph of hardground surfaces (arrows). Notice the micritic crust (C) which occurs on the uppermost hardground surface. In general, hardgrounds are laterally discontinuous. Many times they display some evidence of pressure solution, and thus grade into stylolites. Field of view is 6.5 mm in long dimension. Interstate 75 section. Sample I-29-5.7.

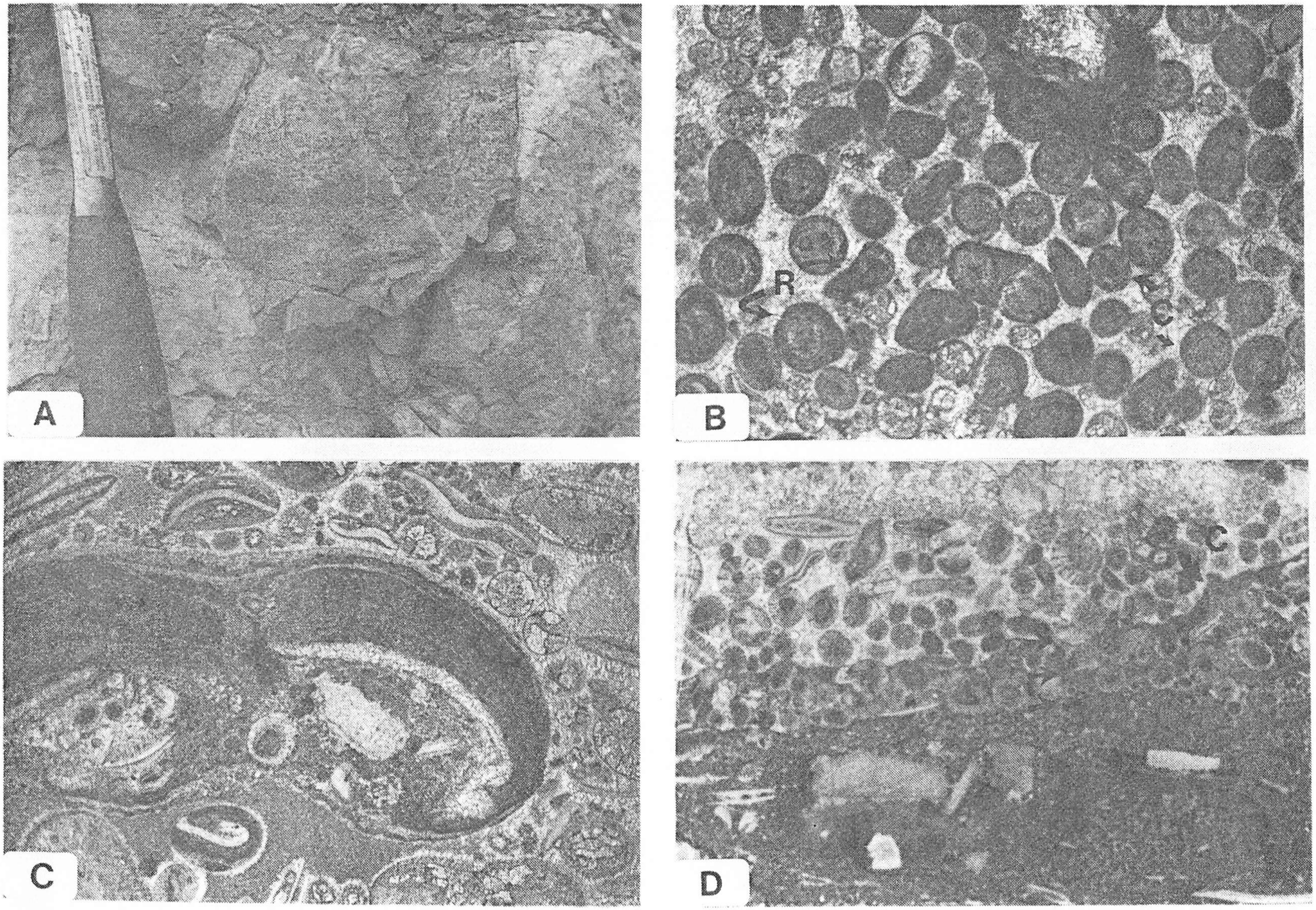
A
B
R
C
C
C
D

3. Type "I" oncoids: interrupted oncoids, where initial oncoid formation takes place, and later redeposition, dissolution, erosion, and/or reorientation occurs. Then, the surface undergoes renewed oncoid formation. Individual laminae are truncated and thus are not traceable around the oncoid.

Each type of oncoid is commonly observed in the upper Conasauga sequence Figure 2.7B and C).

Hardgrounds and scoured surfaces of this Facies are not restricted in locality. Hardground surfaces are planar and undulatory and are identified by the presence of truncated grains and/or micritic crusts, usually iron-stained, phosphatized, or pyritized (Figure 2.7D). Where closely spaced hardgrounds cut down through previously cemented hardgrounds, anastomosing hardgrounds occur.

Interpretation

All three major oncoid types (C, R, and I) occur in subequal abundance in any given oncolitic horizon. These oncoids formed in quiet- to moderately agitated-water conditions, but they were intermittently reworked by high-energy events, such as currents and/or storms (e.g., see Ball, 1967; Shinn, 1969; Hagan and Logan, 1974; Hine, 1977; Flugel, 1982). Based on our knowledge of modern oncoid-forming environments (Ginsburg, 1960; Flugel, 1982), this Facies probably underwent deposition in water no more than 3 m deep . Gebelein (1976) reports that optimum development of oncoids takes place in water less than 1 meter deep at Joulters Cay, Bahamas. Based upon evidence presented below, a very shallow subtidal origin is proposed for the Oncolitic Facies.

1. This Facies has a grain-supported framework (grainstone and packstone), where porefilling marine cement is volumetrically more abundant than micrite. Thick oncoid wackestone beds have been identified by Markello (1979), Erwin (1981), and Kozar (1986) as deeper water subtidal deposits.
2. In this study all three types of oncoids occur in about the same proportion. Greater abundance of Type "R" oncoids has been used to imply a deeper subtidal origin (Erwin, 1981).
3. An abundant and diverse biota is lacking here. Kozar (1986) described a wide variety of biotic constituents within his deeper-water subtidal oncolitic facies. In addition, Erwin (1981) was able to distinguish a shallow subtidal and a deeper subtidal oncolitic facies based largely on the richness of the biota.
4. Quartz silt and sand are not observed in the Oncolitic Facies. Erwin (1981) and Kozar (1986) described abundant detrital quartz from their "deeper" oncolitic facies.
5. Abraded, mechanically fragmented, and spalled oncoids are not present in the Oncolitic Facies. The presence of these features would imply greater current intensity, capable of transporting oncoids into deeper water environments.

6. The absence of subaerial exposure features such as mudcracks, fenestral fabric, microtepee structures, etc. precludes tidal flat deposition.
7. Periods of submarine exposure (substrate stability), as implied by numerous hardgrounds throughout this Facies, and moderate agitation enabled cyanobacteria to develop well-formed oncoids. Periodic currents and storms transported peloids, ooids, intraclasts, and skeletal debris from adjacent areas into this oncoid-forming environment.

Peloidal Packstone/Grainstone (EPG)

Description (Table 2.8)

The Peloidal Packstone and Grainstone Lithofacies is observed often in the Maynardville Limestone (very rare in the Nolichucky); it ranges from 0.5 m to 11 m in thickness, averaging almost 3 m (Figures 2.2 and 2.3). This Facies is composed of two end-member, nonintergrading subfacies. The Peloidal-Intraclastic Grainstone Subfacies is composed of reworked and rounded pieces of consolidated calcareous mud (Figure 2.8A and C) which coincides with very small intraclasts (intraclasts are greater than 2 mm, Folk, 1970). Peloids and intraclasts are made up of either calcite (micrite) or dolomite (dolomicrite). Also, fenestral fabric and blocky porefilling dolomite cement are observed in thin-section. Biotic constituents are rare. In outcrop low-angle cross-stratification is present in some beds. This Subfacies

Table 2.8. Characteristics of the EPG Lithofacies.

Features	Characteristics
Lithology (Folk, 1959; 1962)	-Pelsparite -Dolomitized pelsparite -Dolomitized oosparite (superficial ooids)
Bed Thickness	-Thin- to very thick-bedded -Laterally continuous
Sedimentary Texture and Structure	-Moderate sorting; fine-to medium-grained; rounded to angular peloids -Discontinuous hardgrounds -Low-angle cross-stratification -Burrows
Bed Contacts	
Upper	-Sharp
Lower	-Sharp
Fossils	-Rare echinoderms and trilobites
-Other	-Stylolites, stylobedding, stylocumulate -Superficial ooids are radial fibrous, from 0.05 to 0.3 mm. in diameter -Peloids average 0.2 mm. in diameter
No. of Thin-Sections Examined	-13
No. of Thin-Sections Point-Counted	-7

Figure 2.8. Selected features of the Peloidal Packstone/Grainstone (EPG) Lithofacies. Stratigraphic up is toward top of page in all photographs.

A. Photomicrograph of the Peloidal-Intraclastic Grainstone Subfacies showing both micrite and dolomicrite peloids. Thin-section has been stained with Alizarin Red S and potassium ferricyanide. Darker peloids are composed of calcite, while lighter peloids are dolomite. Pore-filling cement is blocky dolomite. Field of view is 6.5 mm in long dimension. Interstate 75 section. Sample I-79-6.2.

B. Polished slab of the Peloidal-Superficial Ooid Packstone/Grainstone Subfacies showing cross-stratification. Interstate 75 section. Sample I-77-2.0.

C. Outcrop of the Peloidal-Intraclastic Grainstone Subfacies. Knife is 9 cm in length. Interstate 75 section.

D. Photomicrograph of the Peloidal-Superficial Ooid Packstone/Grainstone Subfacies. Peloids and superficial ooids are the dominant allochems. Field of view is 6.5 mm in long dimension. Interstate 75 section. Sample I-78-0.5.

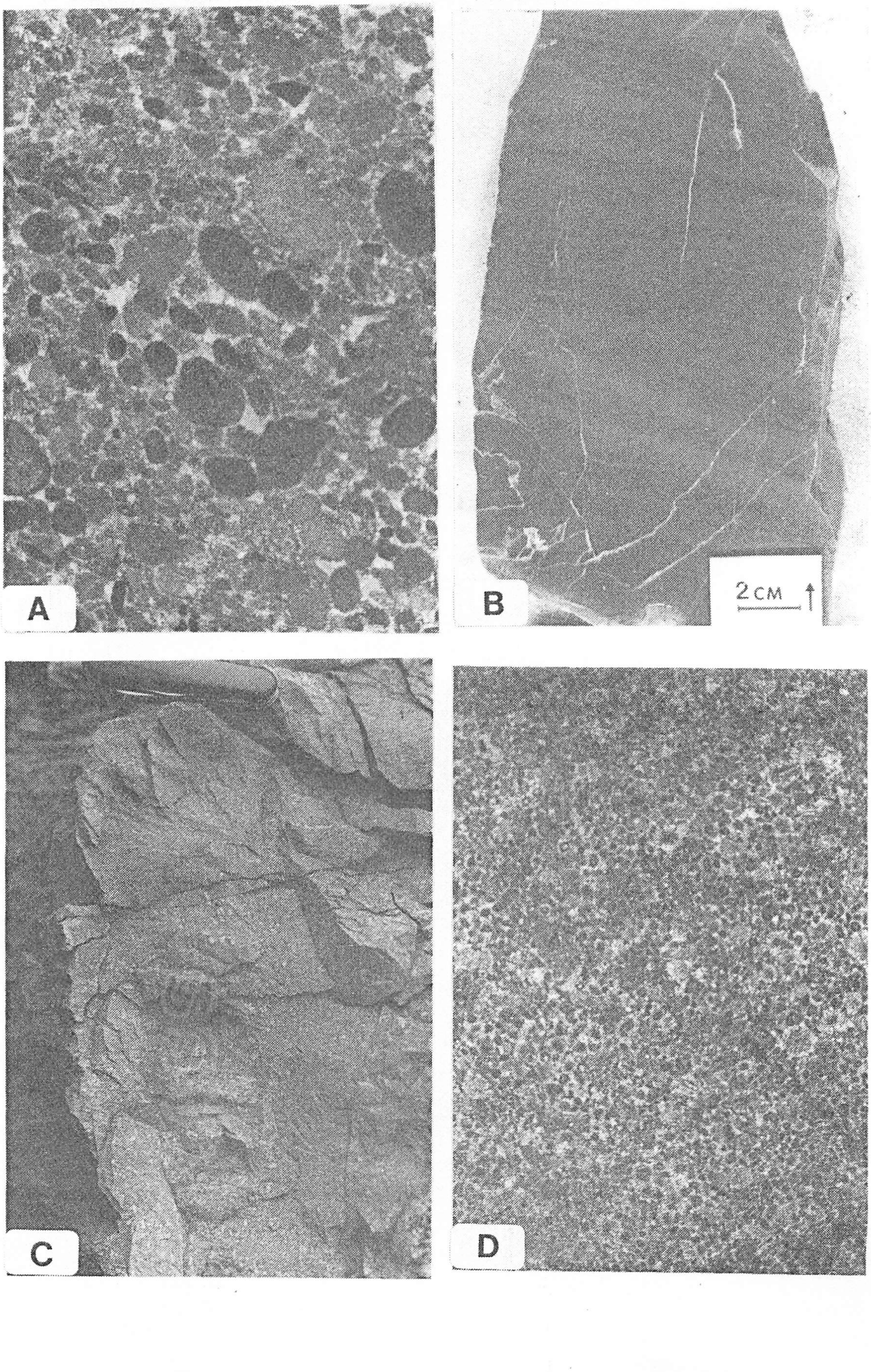
A
B
2 CM
C
D

is recognized through a thin stratigraphic interval in close association with cryptalgalaminates at the I-75 Section.

The Peloidal-Superficial Ooid Packstone/Grainstone Subfacies is much more abundant and is recognized from each Maynardville locality which has been examined. This Subfacies is characterized by the following grain types (in decreasing order of abundance): peloids >>> superficial ooids >> Girvanella sheaths > Girvanella tubules > Girvanella intraclasts. Abundant allochems tend to be very fine-grained, typically between 0.05 mm and 0.30 mm in diameter (Figure 2.8D). Other features of this Subfacies include fibrous and blocky calcite porefilling cement, cross-stratified bedforms (Figure 2.8B), thin argillaceous interlayers, burrows, and rare fossils.

Many allochems in the Peloidal Packstone/Grainstone Facies owe their origin to the activity of cyanobacteria. Collectively, these grains may account for 50% or more of the volume of a thin-section. Girvanella formed tubules, sheaths, peloids, oncoids, and intraclasts. There is little doubt that tubules and sheaths (intertwined tubules) are derived from Girvanella. In these particles Girvanella is well preserved as an unbranching, nonseptate tubule that is uniform in diameter (see Figure 2.9C). Tubules are 5 to 25 microns in diameter and may be several hundred microns in length. The tubule wall is composed of micrite a few microns thick.

The cyanobacterial origin of peloids and intraclasts may be tenuous if Girvanella is not identified. The amount of Girvanella in any one peloid or intraclast varies. Usually, only a few loose tubules are

Figure 2.9. Selected features of the Mudstone Interbedded with Shale (MWS) Lithofacies.

A. Outcrop of nodular to thin-bedded lime mudstone which is interbedded with partially dolomitized shale. Rock hammer for scale. Roaring Spring section.

B. Photomicrograph of *Girvanella* sheaths and peloids. Notice that many peloids appear to be cross-sectional and oblique cuts through individual tubules and small clusters of tubules. Field of view is 1.3 mm in long dimension. Interstate 75 section. Sample I-58-2.5.

C. Photomicrograph of well-preserved *Girvanella* tubules in lime mudstone. Field of view is 1.3 mm in long dimension. Interstate 75 section. Sample I-58-2.5.

D. Slab of the undersurface (?) of a mudstone bed showing disrupted, bioturbated fabric. Horizontal burrow may be *Planolites*. Interstate 75 section. Sample I-60-12.1.

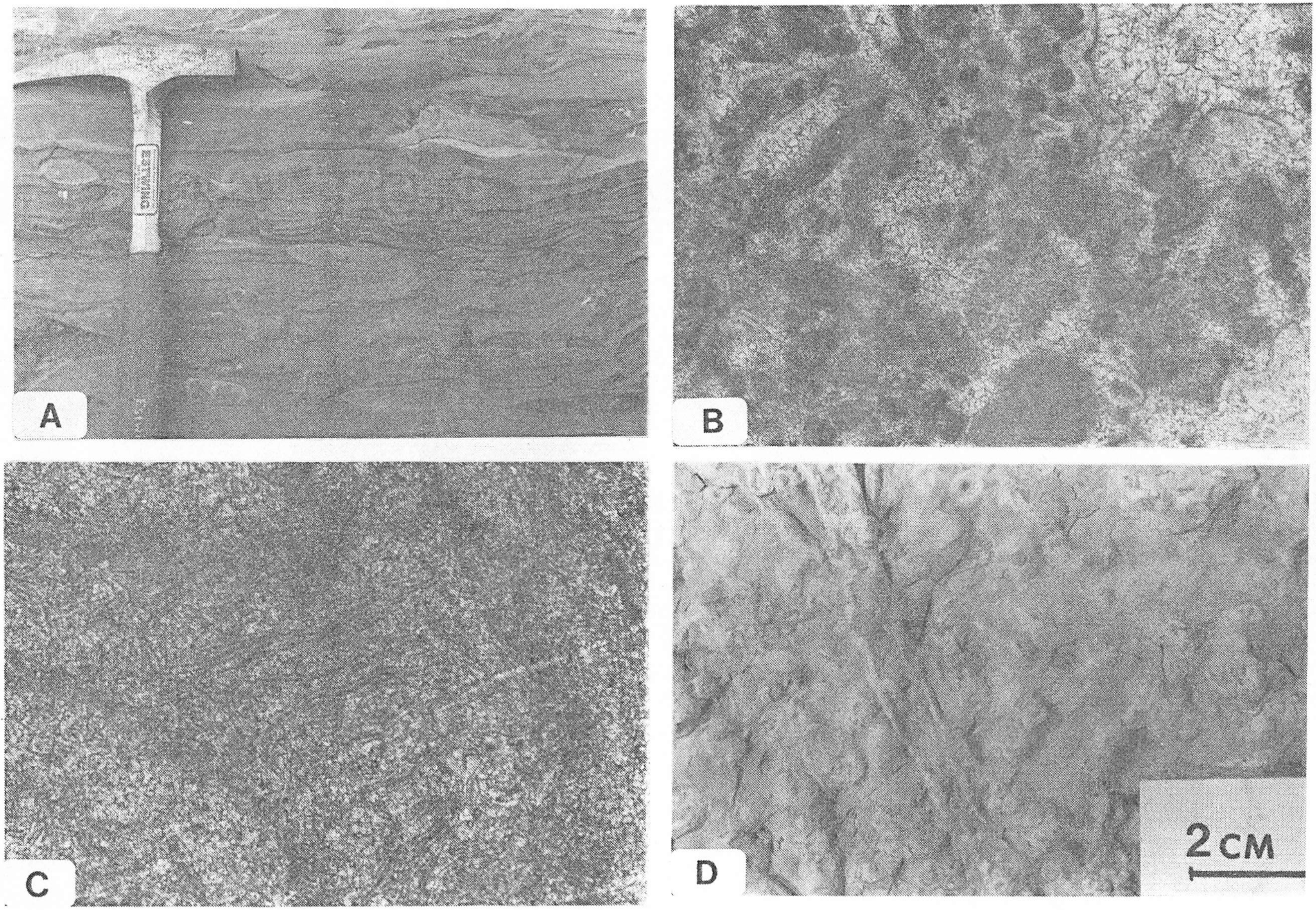
A
ESTWING
B
C
D
2 CM

surrounded by micrite and microspar. The sharpness of the transition from the tubule wall to the fine-grained matrix is variable. If this boundary is sharp, preservation is good, but if the boundary is gradational, preserved tubules are only vaguely recognized, or not recognized at all. Generally, the microstructure of Girvanella is obscured by micritization and/or micrite infilling of the tubules or by neomorphism of carbonate lime mud to micrite and microspar.

Interpretation

The precise environment of deposition of the Peloidal-Intraclastic Grainstone Subfacies is difficult to ascertain. Although deposition probably took place on a tidal flat, perhaps in or near tidal channels, additional data would be helpful in refining this interpretation. However, in central east Tennessee this Subfacies is not regionally extensive.

The dominant constituents of the Peloidal-Superficial Ooid Packstone/Grainstone Facies are peloids. Girvanella also contributed significantly to the original sediment. Mechanical fragmentation of subtidal Girvanella mats (see the Mudstone Facies) by high-energy events produced peloids and other subordinant grain types (tubules, sheaths, and intraclasts). These Girvanella peloids may be indistinguishable from other types of peloids such as fecal pellets, micritized grains, and recrystallized particles. However, based upon petrographic evidence, most peloids in the upper Conasauga Group appear to be derived from cyanobacteria, primarily Girvanella. The role of cyanobacteria as important sediment producers should not be underestimated. Throughout the Phanerozoic, physical breakdown of algae and cyanobacteria is regarded as a major sediment producing process (Wolfe, 1965; Aitken, 1966; Stockman and others, 1967; Ahr, 1971; Neuman and Land, 1975; Wray, 1977; Mullins and van Buren, 1979; Crevello and Schlager, 1980; Coniglio and James, 1985).

The peloidal carbonates described here are similar to subtidal sands of Shark Bay, the Persian Gulf, and the Great Bahama Bank (Purdy, 1963; Evans and others, 1973; Brown and Woods, 1974; Bathurst, 1975). These ancient carbonates resemble modern pellet sands in bed thickness, internal structure, constituent composition, and location (i.e., between higher energy shoals and lower energy tidal flats). The main difference involves the paucity of fecal pellets in the Maynardville.

Radial fibrous cortices occur on many peloids in the Peloidal Facies. This would suggest that where agitation was sufficient to entrain grains superficial ooids formed. Ooids which are less than 0.6 mm in diameter tend to have radial cortices (Heller and others, 1980). Larger ooids reveal a concentric or laminated fabric. This correlation has been noted by Medwedeff and Wilkinson (1983). As indicated by Heller and others (1980), smaller ooids were kept in suspension under shallow-water, moderate-energy conditions. These conditions permitted accretion of a radial cortex without grain abrasion. With increasing ooid size beyond the 0.6 millimeter threshold, bedload transport dominated. Superficial ooids in the Maynardville rarely exceed 0.3 mm in diameter.

This Facies was deposited as a subtidal sand sheet in water which was intermittently reworked by high-energy currents and/or storms. The occurrence of Girvanella peloids and intraclasts as well as tubules and sheaths support evidence for periodic high-energy events. Sets of planar tabular cross-strata, fine-grained and well-sorted peloids, and superficial cortices on peloids suggest grain reworking in moderately agitated water. Based on modern analogues, water depth was approximately 0-5 m. The occurrence of marine fibrous cement and rare burrows is consistent with this interpretation.

Mudstone Interbedded With Shale (MWS)

Description (Table 2.9)

The Mudstone Facies is present in the Nolichucky Shale and Maynardville Limestone (Figure 2.2). It is usually observed near the Nolichucky/Maynardville contact in close stratigraphic proximity to many of the lithofacies described in this study. Nodular- to thin- bedded lime mudstone alternates with laminated to thin-bedded shale (Figure 2.9A). Individual mudstone and shale layers range from <1 to 5 cm in thickness. The limestone-shale alternations form rock-units up to 4 m thick (Figure 2.3). On average, rock-unit thickness is 26 and 66 cm for the Nolichucky and Maynardville, respectively (Figure 2.3).

The Mudstone Facies is predominantly composed of lime mud (micrite/microspar) along with interbedded shale. Shale is partially to pervasively dolomitized; pervasive dolomitization occurs in the

Table 2.9. Characteristics of the MWS Lithofacies.

Features	Characteristics
Lithology (Folk, 1959; 1962)	-Fossil-bearing micrite interbedded with shale -Pelmicrite interbedded with shale -Biopelmicrite interbedded with shale
Color (Shale Only)	-Dark gray-green
Bed Thickness	-Laminated to thin-bedded -Discontinuous over 10's of cm.
Rock-Unit Thickness	-Very thin- to very thick-bedded
Sedimentary Texture and Structure	-Vertical and horizontal burrows -Nodular-bedded -Load casts, pseudonodules -Stylolite swarms -Faint lamination -Burrow mottled
Bed Contacts	
Upper	-Sharp
Lower	-Sharp
Fossils	-_Girvanella_, rare trilobites, echinoderms, inarticulate brachiopods, and sponge spicules
Other	-_Girvanella_ peloids in _Girvanella_ mudstone
No. of Thin-Sections Examined	-23
No. of Thin-Sections Point-Counted	-9

Maynardville. Other lesser abundant constituents include peloids, intraclasts, and skeletal material (Table 2.3). Occasionally, peloids and intraclasts form thin beds and lenses; these allochems resemble fragmented mudstone beds.

Petrography reveals an abundance of *Girvanella*-formed grains, such as peloids (Figure 2.9B) and intraclasts. In addition, *Girvanella* tubules are well preserved in many mudstone beds and nodules (Figure 2.9C). *Girvanella* must have played an important role in binding and perhaps in cementation of grains in this Facies. Shortly after death, intertwined calcified tubules would provide nucleating sites for micrite and other marine porefilling cements. Modern cyanobacteria similar to *Girvanella* produce a microcrystalline calcite wall structure during life. Precipitation of calcite cement in cyanobacterial tubules has been described from both modern and ancient shallow-water carbonate environments (Kobluk and Risk, 1977).

Original sedimentary layering is preserved in the mudstone unless the sediment was homogenized by bioturbation (Figure 2.9D). Generally, discrete vertical and horizontal burrows are observed and display interpenetrative tiering. Burrow walls show varying degrees of preservation; they are diffuse to sharp. Burrows are filled with skeletal debris, peloids, argillaceous material, and/or pore filling cement.

Interpretation

Nodular- to thin-bedded mudstone has been described from a number of different environmental settings. Often, this distinct bedding is attributed to differential compaction and pressure solution (see Logan and Semeniuk, 1976; Wanless, 1979). In the upper Conasauga Group, stylolitization is recognized as an important process. Low-amplitude stylolites and microstylolite seams are common. However, submarine lithification and subsequent erosion are depositional processes that also contribute to the overall appearance of this Facies. Lithification of subtidal cyanobacterial mats and later reworking during storm events would produce a bedding style similar to that of differential compaction and pressure solution (Bathurst, 1975; Allen, 1984).

The Mudstone Facies is interpretated as a quiet-water subtidal mud accumulation, below normal fairweather wave-base. Relatively slow, continuous sedimentation of lime mud is supported by the occurrence of interpenetrative tiering of burrows (Aigner, 1985; Wetzel and Aigner, 1986). Carbonate mud settled out marginal to the higher energy platform environments (e.g., Peloidal and Oncolitic Facies), where currents winnowed out much of the fine-grained sediment. The fine-grained mud was deposited on cyanobacterial mats. Girvanella and other filamentous cyanobacteria living within the mats promoted early lithification of lime mud. Seafloor lithification is also supported by the abundance of burrows with well-defined walls. This suggests that sediment was firm (Rhoads, 1970; Walker and Diehl, 1986). Periodic disturbance of lithified and semilithified crusts during storm events ripped up and transported Girvanella tubules, sheaths, peloids, and intraclasts to the carbonate platform as well as to the deeper water facies. Shale interlayers record the high-energy events, where numerous peloids, intraclasts, and skeletal debris are found.

Deposits similar to the Mudstone Facies are common in the geologic record (Wilson, 1975). Typically, they form on carbonate ramps as widespread mud blankets seaward of shoal-water complexes. Water depth varied from approximately 5 m to 15 m.

Oolitic Packstone/Grainstone (OPG)

Ooid packstone and grainstone beds range from a few centimeters to perhaps 10 or more meters in thickness. These ooid carbonates are common in the Nolichucky Shale (Figure 2.2) where they account for about 10% of the sequence. In the Maynardville Limestone this Lithofacies is rare (Figure 2.3) and thin, never exceeding 8 cm in thickness (Figure 2.3). Two types of oolitic packstone/grainstone are recognized in the upper Conasauga Group: thick lenticular buildups and thin sand sheets.

Description of Thick Lenticular Buildups (Table 2.10)

Lenticular ooid buildups or shoals are distinctive features of the Nolichucky Shale (Figure 2.10A). They occur as thick (up to 12 m) carbonate units that thin laterally and intergrade into adjacent shale. Thin ooid sheets are observed as lateral extensions of these carbonate buildups (Figure 2.11B). Several well-defined ooid shoals are recognized from the Interstate-75 and Roaring Spring sections, however,

Table 2.10. Characteristics of the OPG Lithofacies.

Features	Characteristics
Lithology (Folk, 1959; 1962)	-Poorly-washed oosparite -Oomicrite -Fossiliferous oomicrite -Poorly-washed fossiliferous oosparite
Bed Thickness	-Very thin- to very thick-bedded -Laterally continuous
Sedimentary Texture and Structure	-Bidirectional cross-stratification -Megaripples -Hardgrounds -Fine- to coarse-grained; well-sorted -Discontinuous mudstone interlayers
Bed Contacts	
Upper	-Sharp and planar to irregular
Lower	-Sharp and planar to scoured
Fossils	-Rare to abundant, echinoderms, trilobites, *Girvanella*, *Chancelloria*, and inarticulate brachiopods
Other	-Stylolites, stylobrecciation -Two varieties: (1) thin sand sheets and (2) thick lenticular buildups
No. of Thin-Sections Examined	-87
No. of Thin-Sections Point-Counted	-36

Figure 2.10. Selected features of the Oolitic Packstone/Grainstone (OPG) Lithofacies.

A. Outcrop of three distinct carbonate shoaling bodies. The lower two (#1 and #2) are oolitic. Cursory examination of the uppermost buildup (#3) reveals an abundance of trilobites and echinoderms; it most likely represents a fossiliferous shoal. The lower shoal is 6 m thick. Interstate 75 section.

B. Outcrop of bi-directional cross-beds. Rock hammer for scale. Interstate 75 section.

C. Outcrop of dolomitized lime mudstone which thickens within a trough. Mud-filled troughs are adjacent to megarippled bed surfaces on upper surface of oolite beds. Pencil is 9 cm long. Beech Grove section.

D. Photomicrograph of marine fibrous cement occluding original pore space. Field of view is 1.3 mm in long dimension. Photo taken under cross-polarized light. Interstate 75 section. Sample IOA 2.8.

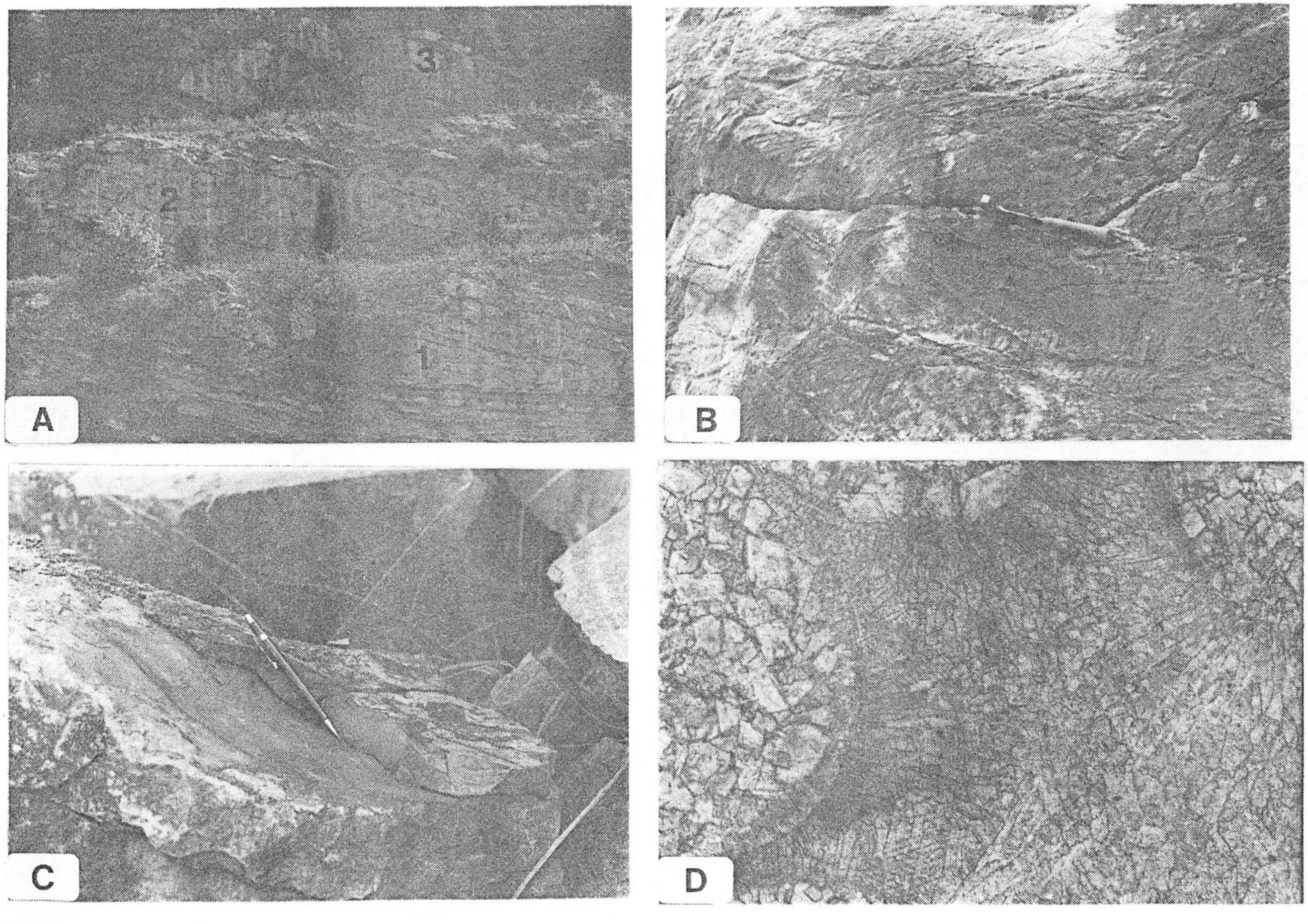
3
2
1
A
B
C
D

Figure 2.11. Additional features of the Oolitic Packstone/Grainstone (OPG) Lithofacies.

A. Outcrop of prominent hardground (at top of hammer) which is colonized by thrombolites. Mid-way up the sequence digitate stromatolites become apparent. These lithologies occur in stabilized oolite deposits at tops of ooid shoal buildups. Rock hammer is 25 cm in lenth. Interstate 75 section.

B. Outcrop of lower shoal (from Figure 2.10 A) showing thin ooid sheets as lateral extensions off of the buildup. Most thin beds observed from this part of the section are thin ooid sheets. Interstate 75 section.

C. Outcrop of ooid sand sheet. Internal structure, with the exception of discontinuous hardgrounds, is rare in these beds. Ruler is graduated in cm. Roaring Spring section.

D. Photomicrograph of Chancelloria (C). Chancelloria is characterized by its calcite walls and hollow centers, which are filled with micrite or void-filling cement. Field of view is 6.5 mm in long dimension. Interstate 75 section. Sample C-53.

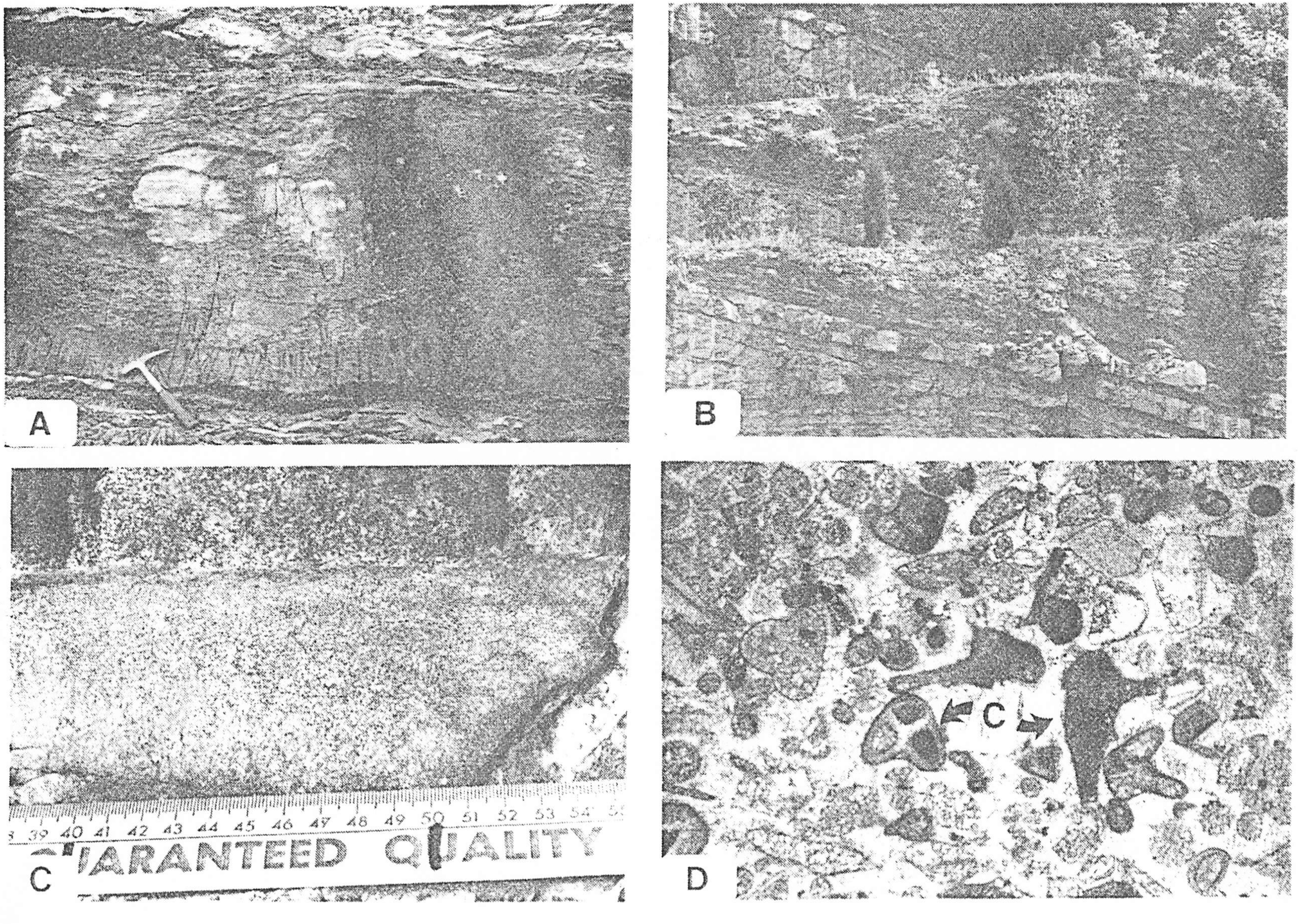
A
B
C
D
C

with improved lateral exposure, these features would probably be recognized elsewhere in central east Tennessee.

A 6 m thick ooid buildup has been examined in detail at the Interstate-75 Section (Weber and others, 1987; Foreman and others, 1988) (see lowermost carbonate shoal in Figure 2.10A). The ooid shoal is underlain by several meters of thinly interbedded shale and coarse-grained intraclastic and oolitic limestone. At the base of the shoal, laterally discontinuous intraclastic lobes grade upward into well-sorted, coarse-grained ooids. The lower 4.5 m thick interval is characterized by bidirectional cross-stratification (Figure 2.10B), shale and lime mudstone interlayers which thicken over troughs (Figure 2.10C), stylolites, and partial dolomitization. Hardgrounds increase in frequency toward the top of this interval. Ooids and fibrous cement account for 90% of the volume of the rock. In fact, all original pore space is filled by marine fibrous cement (Figure 2.10D). A prominent hardground marks the base of the upper part of the shoal, which extends up 1.5 m to the top of the deposit. Thrombolites colonized the hardground surface, and digitate stromatolites developed on top of the thrombolites (Figure 2.11A). Oncolitic packstone caps the upper shoal. Characteristics unique to this interval include: (1) the absence of cross-bedding, (2) burrowed and bioturbated lime mudstone, (3) micrite >> cement, and (4) abundant echinoderms. The shoal is overlain by shale and thin beds of intraclastic limestone.

Interpretation

Our knowledge of modern ooid shoals (i.e., Newell and Rigby, 1957; Purdy, 1963; Ball, 1967; Loreau and Purser, 1973; Hagan and Logan, 1974: Hine, 1977; Harris, 1979; Hine and others, 1981) reveals that the development of oolitic sand bodies is dependent on a number of factors (topographic complexity, physical processes, sea level history, early cementation, etc.). These interacting and complex factors form complicated facies mosaics. Nonetheless, several subenvironments recognized in modern ooid shoals can be discerned in Cambrian shoals. Modern shoals often show 4 interrelated subenvironments: (1) a preexisting topographic high on which shoal development was initiated, (2) an upcurrent area of mobile oolite sand, (3) a downcurrent area of stabilized oolite/skeletal sand which is crossed by (4) tidal channels and washover lobes.

Oolitic buildups within the Nolichucky Shale show broadly similar subenvironments to the modern. Shoal development initiated on a raised topographic surface (an intraclastic lobe) above fairweather wave base. Here, ooids formed and accumulated in an area of wave and current agitation (based on modern analogues, water depth was less than 5 m). Within the resultant mobile subenvironment, strong tidal currents produced large-scale cross-stratified oolite bedforms. Leeward of the mobile fringe belt, a stabilized sand flat was formed. Within this subenvironment, decreased agitation is reflected by an abundance of lime mud (micrite) and by the occurrence of oncoids. In addition, the abundance of radial ooids relative to monocrystalline and polycrystalline ooids suggests very shallow, yet quiet-water deposition (Chow and James, 1987). Tidal channels are not observed from the Nolichucky oolite at I-75.

Description of Thin Sand Sheets (Table 2.10)

Thin sand sheets range from 2 cm to 115 cm (average 19 cm) in thickness (Figure 2.3). Generally, sheet-like bedforms are laterally continuous over the scale of the outcrop (Figure 2.11B). Thin, laterally discontinuous bedforms (here included with thin ooid sheets), although rare, occur most commonly in the lower Nolichucky, stratigraphically below the thick lenticular ooid buildups. In the field ooid sand sheets exhibit scoured bases, intraclasts near the base, thin shale drapes, and megarippled upper bed surfaces. The absence of tabular cross-beds imparts a massive appearance to these rocks (Figure 2.11C). Sand sheets occur in close stratigraphic proximity to other carbonate and shale lithologies of the Nolichucky.

Sheet-like oolitic carbonates are composed mainly of ooids (0.25-1.25 mm in diameter), spherical to irregular intraclasts (mudstone, peloidal, or oolitic), and skeletal grains (Table 2.3). Skeletal constituents include echinoderms and trilobites with lesser abundant Girvanella, Chancelloria (Figure 2.11D), and inarticulate brachiopods. Girvanella tubules, sheaths, peloids, and intraclasts are locally abundant. Also, Girvanella is recognized in thin mudstone layers which occasionally drape the sand sheet.

Porefilling cement and fine-grained matrix (micrite) occur in subequal abundance (Table 2.3). Early cement phases include marine fibrous and syntaxial fibrics; blocky cement (ferroan and nonferroan) occlude remaining porosity during meteoric and burial diagenesis (see Foreman and others, 1988 for a more detailed assessment of porefilling history).

Interpretation

Thin sand sheets are interpreted as subtidal sand bodies that accumulated in the intrashelf basin, below normal wave-base. This interpretation might seem unconventional because oolite formation is indicative of rapid sedimentation in very shallow, turbulent water. However, in the Nolichucky Shale, weak current activity is substantiated by the presence of lime mud matrix and thin mudstone (*Girvanella* mat) interlayers, and by the absence of internal cross-bedding. In addition, the occurrence of corrosion surfaces, glauconite, and thin shale drapes above hardgrounds indicates periods of decreased sedimentation (Flugel, 1982). Sharp, scoured bases, abundant intraclasts, and megarippled upper bed surfaces suggest that high-energy events (storms) may have been responsible for large-scale movement of sand sheets. Hurricanes are recognized as the primary process for net sand movement in the Bahamas (Ball, 1967; Hine, 1977). Kozar (1986) derived a similar interpretation for the thin ooid sheets which he observed in the Maryville Limestone.

Fossiliferous Packstone/Grainstone (FPG)

Description (Table 2.11)

The fossiliferous Packstone and Grainstone Lithofacies is only recognized in the Nolichucky Shale (Figure 2.2). Very thin to very thick beds (Figure 2.3) of skeletal packstone (grainstone is rare) occur in close stratigraphic proximity to the Oolitic and Shale facies and to a lesser degree with other lithofacies of the Nolichucky. The skeletal beds form sheets or layers of limestone which are separated by shale partings, hardgrounds, and stylolite seams (Figure 2.12A). Internally, this Facies is massive, but large widely spaced intraclasts may be observed at the base of these units. Where intraclasts occur, grading is present. Bed contacts are typically sharp; bases are scoured. The skeletal limestones are medium- to coarse-grained. Skeletal grains make up from 25% to 50% of the rock (Table 2.3) and include trilobites and echinoderms, but sediments also contain inarticulate brachiopods, _Girvanella_, _Chancelloria_, and sponge spicules. Skeletal allochems may be loosely packed in mud-dominated packstone. In tightly packed rocks, line and sutured contacts dominate. Fibrous porefilling cement is abundant in some thin-sections, but porosity was not completely occluded by marine cement. Ferroan and nonferroan varieties of blocky cement fill remaining pore space.

Thick skeletal shoals similar to thick oolitic shoals in geometry are present at I-75 and Beech Grove (Figure 2.10A). Both stratigraphic sections were measured and described along a transect which did not

Table 2.11. Characteristics of the FPG Lithofacies.

Features	Characteristics
Lithology (Folk, 1959; 1962)	-Biomicrite -Biopelmicrite -Poorly-washed biopelsparite -Poorly-washed pelsparite
Bed Thickness	-Very thin- to very thick-bedded -Laterally continuous
Sedimentary Texture and Structure	-Hardgrounds -Corrosion surfaces -Rippled and megarippled tops -Burrows -Medium- to coarse-grained
Bed Contacts	
Upper	-Sharp and planar, also diffuse
Lower	-Sharp and scoured
Fossils	-Very abundant trilobites, echinoderms, and Chancelloria; also Girvanella, inarticulate brachiopods, sponge spicules, and molluscs
Other	-Intraclasts at base -Locally abundant glauconite -Ooids -Stylolites
No. of Thin-Sections Examined	-28
No. of Thin-Sections Point-Counted	-10

Figure 2.12. Selected features of fossil-dominated lithofacies (FPG and FPGWS).

A. Outcrop of the Fossiliferous Packstone/Grainstone (FPG) Lithofacies. This rock contains an abundance of trilobites, echinoderms, ooids, and intraclasts. Knife is 2 cm in width. Beech Grove section.

B. Polished slab of fining-upward sequence. Fossil debris fines upward into parallel-laminated calcareous shale. The transition from limestone to shale is gradational. Petrographic analysis reveals four distinct fining-upward sequences (arrows). A stylolite seam (S) is also present. Interstate 75 section. Sample I-69-14.5.

C. Photomicrograph of load structure. Field of view is 6.5 mm in long dimension. Interstate 75 section. Sample I-6-2.5.

D. Photomicrograph of pseudonodule. Field of view is 6.5 mm in long dimension. Interstate 75 section. Sample I-6-2.5.

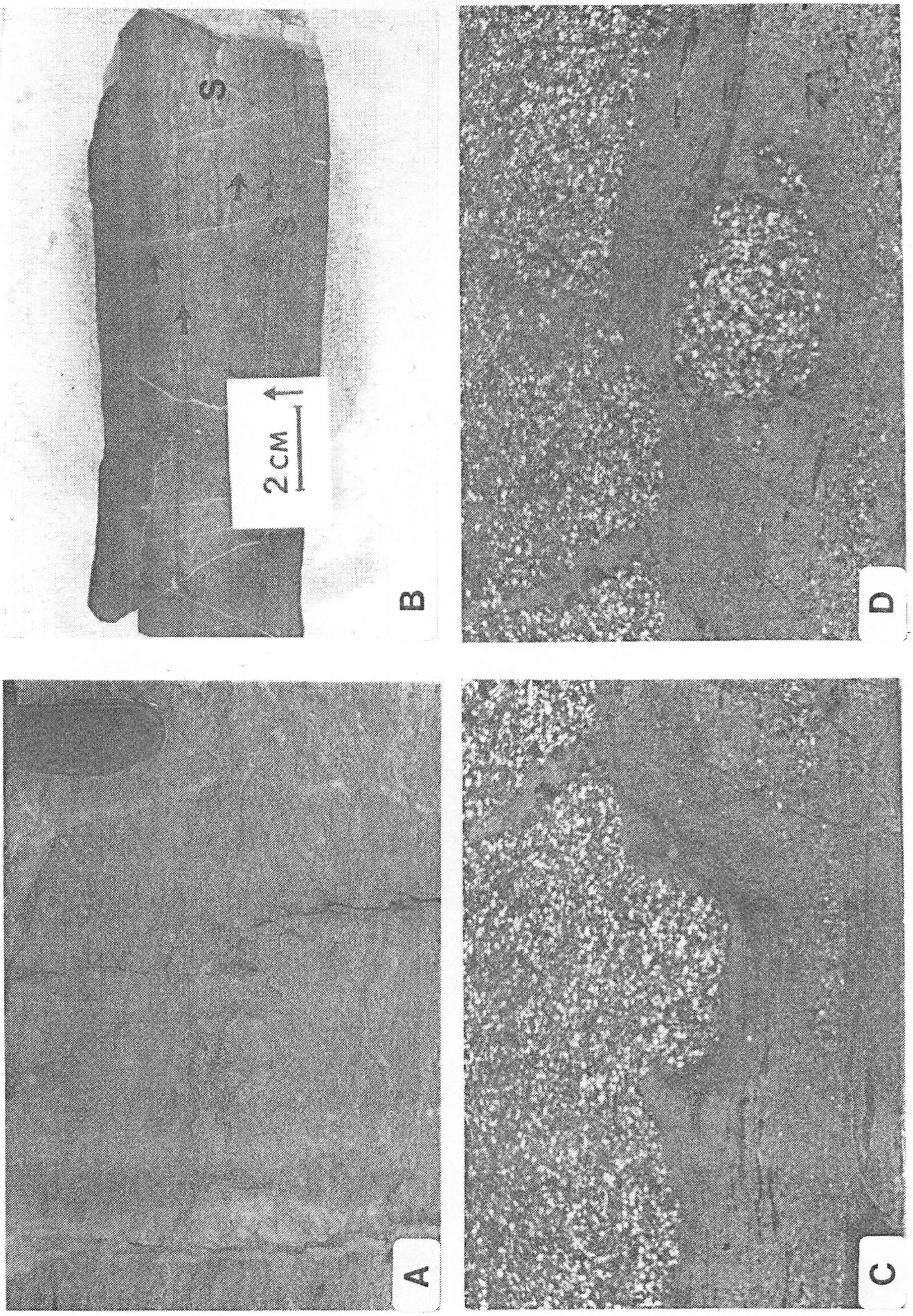
A
B
C
D
S
S
2 CM

intersect the skeletal-rich shoal-like buildups. At present, these fossil shoals have not been studied in detail; cursory examination revealed packed echinoderm and trilobite debris surrounded by coarsely crystalline cement, presumeably fibrous in habit.

Interpretation

Characteristic features of this facies (Table 2.11) and preferred stratigraphic position suggest an environmental interpretation which is similar to that for ooid sand sheets (see above). In this case however, nearby skeletal shoals supplied sediment for skeletal sand sheets.

The marine sand belt on the western edge of Florida Bay seems to be a reasonable modern analogue for skeletal sand sheets of the Nolichucky. Skeletal sand shoals are concentrated along shoreparallel belts (Ball, 1967). Similar facies have been described in the ancient (Anderson, 1972; Holloway, 1983). According to Ball (1967) and Aigner (1985) sand sheets are shed episodically from the shoals by storm events.

Fossiliferous Packstone/Grainstone Interbedded With Shale (FPGWS)

Description (Table 2.12)

This Facies is similar to the previously described Fossiliferous Packstone/Grainstone (FPG) Facies in two important ways. Both lithofacies are observed only in the middle and upper parts of the Nolichucky Shale as subordinant rock types (Figure 2.2), and they occupy similar stratigraphic horizons. Notably, the occurrence of FPGWS is

Table 2.12. Characteristics of the FPGWS Lithofacies.

Features	Characteristics
Lithology (Folk, 1959; 1962)	-Biopelmicrite interbedded with shale -Poorly-washed biopelsparite interbedded with shale -Poorly-washed biosparite interbedded with shale
Color (Shale Only)	-Dark gray-green
Bed Thickness	-Very thin- to thin-bedded -Discontinuous over 10's of cm.
Rock-Unit Thickness	-Medium- to very thick-bedded
Sedimentary Texture and Structure	-Basal lags -Fining upward sequences -Load structures and pseudonodules -Contorted bedding -Very fine- to medium-grained
Bed Contacts	
Upper	-Diffuse
Lower	-Sharp and irregular
Fossils	-Abundant trilobites and echinoderms; also, graptolites, *Chancelloria*, conodonts, and inarticulate brachiopods
Other	-Pyrite -Stylolites, stylolite seams
No. of Thin-Sections Examined	-12
No. of Thin-Sections Point-Counted	-7

dependent on the close stratigraphic proximity of FPG; the reverse relationship need not hold true.

Alternating limestone and shale comprise the FPGWS Facies. The limestone component is made up of thin skeletal layers of packstone and rare grainstone from <1 cm to 5 cm in thickness. Limestone beds display some degree of lateral persistence. Most beds average 1 cm to 2 cm in thickness, yet they may be laterally continuous for several meters. Dominant petrographic features include trilobite and echinoderm debris and peloids (Table 2.3). Interbedded with the thin carbonate layers is a structureless to faintly laminated green-gray shale, which ranges from <1 cm to 5 cm in thickness. Shale and lime packstone alternate to form thick rock-units which exceed 2.5 m in thickness (0.5 m is the mean) (Figure 2.3).

This Facies is further characterized by thin (up to 10 cm) fining-upward sequences (Figure 2.12B) that consist of coarse silt- to fine sand-sized skeletal debris at the base. Fragmented phosphate crusts, clay minerals, peloids, and glauconite are also incorporated into the sequence. Constituent grain types grade upward into finer size grades, until shale dominates. Parallel-laminated to wavy-laminated peloidal and fossiliferous silt-sized grains occur just beneath the shale dominated portion (Figure 2.12B). The lime packstone to shale transition represents continuous sedimentation, because hardgrounds, corrosion surfaces, and abrupt changes in grain size do not occur. Fining-upward sequences are underlain by sharp basal contacts. Little or no evidence of truncation (erosion) of underlying shale is observed.

The lower contacts are slightly undulose to planar. Sole structures such as tool marks and groove casts are not present.

Soft-sediment deformation is common (Figure 2.12C). Microload structures grade into well-formed pseudonodules (Figure 2.12D) through progressive bed loading of limestone on shale. In severe cases of differential compaction, contorted-bedding may be observed.

Interpretation

Hemipelagic sedimentation is proposed as the most likely process responsible for this Facies. Deposition took place below normal wave base. Several lines of evidence support this claim.

1. FPGWS is located in a position seaward of the Mudstone Facies.
2. FPGWS is interstratified with "deeper" water subwave-base basinal facies.
3. FPGWS contains an abundance of nonwinnowed shale.

The graded sequences occur in areas proximal to the sediment source. This is supported by the close stratigraphic association of FPGWS with skeletal shoals and sand sheets. The fining-upward layers probably result from high-energy conditions which suspended clay-, silt-, and fine sand-sized particles into dilute clouds (i.e., Reineck and Singh, 1972). Sediment clouds migrated to nearby areas. As the energy level decreased, clouds dissipated as coarser grains settled out, followed by finer size fractions. The parallel- to wavy-laminated interval is rare; this suggests that bottom hugging currents were only locally capable of sediment transport and reworking. Parallel laminations may also reflect suspension setting of particles.

Because this Facies does not occur often, definitive criteria which substantiate one depositional regime over another are lacking. For example, this Facies could be interpreted as a winnowed autochthonous shell bed resulting from storm scouring (i.e., Kreisa, 1981; Kreisa and Bambach, 1982). However, the paucity of skeletal debris in any shale bed thus far examined, the absence of scoured bases, and the lack of wave-formed sedimentary structures would tend to preclude this in situ model. In addition, allochthonous storm transport of sediment seems to be excluded because sole structures are absent, and bedforms suggestive of unidirectional currents are not recognized. Mass-sediment gravity transport seems unlikely as well. Depositional slopes necessary to initiate mass movement were not present. Also, the discontinuous nature of limestone beds distinguishes these deposits from the well-developed limestone-shale rhythmes of turbidite origin (e.g., see Shanmugam, 1978 for discussion).

Alternating carbonate and shale layers reveal evidence of soft-sediment deformation. Load structures, pseudonodules (after Skipper and Middleton, 1977), and microconvoluted bedding (after Dzulynski and Kotlarczyk, 1962) indicate very rapid sedimentation of coarser sediment on a hydroplastic mud layer leading to unequal loading (Reineck and Singh, 1980).

Laminated Peloidal Packstone/Grainstone (XPG)

Description (Table 2.13)

The laminated packstone and grainstone Facies is observed only in the Nolichucky Shale (Figure 2.2). These rocks are characterized by very thin- to very thick-bedded peloidal limestone with thin argillaceous and dolomitic partings. The limestone commonly forms continuous, parallel to wavy-parallel beds that average 24 cm in thickness (Figure 2.3), and rarely exceed 1-2 m. It is important to note that many beds, especially those thicker than 20-30 cm, are actually composite units and include the amalgamation of two or more depositional events. Where individual amalgamated layers are discerned by discrete bedding planes, basal contacts are scoured. Basal surfaces cut down into previously deposited sediment. These scours are filled by intraclastic, peloidal, and/or fossiliferous packstone and grainstone. Small scale scour/fill structures are termed gutter casts (i.e., Whitaker, 1973; Goldring and Aigner, 1982) (Figure 2.13A). In some instances the sediment is certainly allochthonous, whereas in other cases, intraclasts partially fill scours and are composed of the same lithology as that of the underlying strata. These clasts are locally reworked or autochthonous in nature. The undersides of several beds display bi-directional sole structures (e.g., groove casts and tool marks) (Figure 2.13B). Individual beds display fine to medium laminations (1-3 mm in thickness) that are composed of peloidal grainstone and lesser packstone. Quartz silt, opaque minerals,

Table 2.13. Characteristics of the XPG Lithofacies.

Features		Characteristics
Lithology (Folk, 1959; 1962)		-Fossiliferous pelsparite -Biopelsparite -Peloidal siltstone
Bed Thickness		-Very thin- to very thick-bedded
Sedimentary Structure		-Parallel laminations -Low-angle cross-lamininations -Amalgamated bedding -Microhummocky cross-stratification -Sole marks -Gutter casts -Burrows
Bed Contacts		
	Upper	-Sharp and scoured
	Lower	-Sharp and scoured
Fossils		-Common trilobites, echinoderms, inarticulate brachiopods, and *Girvanella*
Other		-Stylolites
No. of Thin-Sections Examined		-16
No. of Thin-Sections Point-Counted		-10

Figure 2.13. Selected features of the Laminated Peloidal Packstone/Grainstone (XPG) Lithofacies.

A. Outcrop of isolated gutter cast (GC). Knife is 9 cm in length. Stratigraphic up is toward the top of page in this sample. Roaring Spring section.

B. Outcrop of sole structures. Groove casts and tool marks are shown. Sole structures are not common features. This is probably a function of (1) the paucity of XPG beds and (2) the sparseness of good lateral exposure on the undersurfaces of beds. Width of field of view is approximately 1 m. Interstate 75 section.

C. Polished slab of horizontally laminated peloidal packstone. Beech Grove section. Sample BG-3-24.0.

D. Polished slab of low-angle cross-lamination within XPG. Interstate 75 section. Sample I-11-1.1.

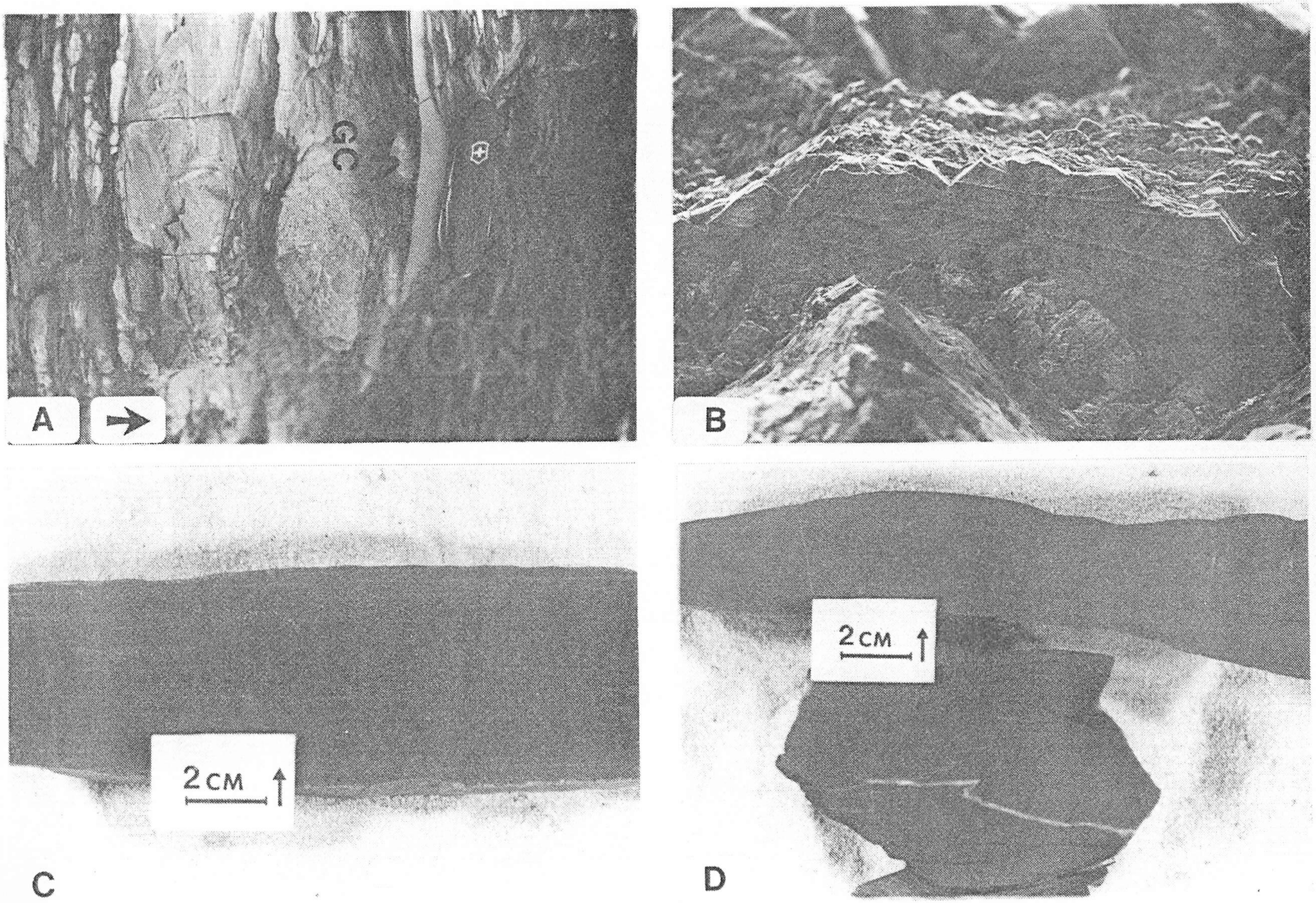
A
GC
B
2cm
C
2cm
D

trilobites, inarticulate brachiopods, echinoderms, and Girvanella are also present (See Table 2.3).

Bedform sequences in the Nolichucky of central east Tennessee vary considerably from those described by other workers from other areas or other units. Markello and Read (1981, Nolichucky of SW VA), Erwin (1981, Maryville of NE TN), and Kozar (1986, Maryville of Central E. TN) describe a complete progression of bedforms as follows:

> An ideal sequence exhibits a sharp, erosional base, followed by a graded intraclastic or skeletal layer. This is conformably overlain by parallel, then low-angle cross-lamination (microhummocky cross-stratification), and finally by wave ripples. The whole sequence is capped by argillaceous material.

In this study, a typical complete sequence commences with horizontal lamination on a sharp scoured base (Figure 2.13C), often followed by a thin interval of low-angle cross-lamination or microhummocky cross-lamination (Figure 2.13D), which is capped by a clay drape or thick shale. Caps display sharp erosional tops. Basal lags and wave ripples are rare.

Interpretation

Observations suggest that this Facies was deposited under conditions of low to high wave and current activity. Deposition occurred below normal wave base in deeper water on the basis of its stratigraphic position between the Mudstone and Shale Facies. Futhermore, sedimentary features characteristic of this Facies are strikingly similar to storm-dominated, modern and ancient, carbonate and siliciclastic shelves (Hayes, 1967; Reineck and Singh, 1972; Brenner and

Davies, 1973; Goldring and Bridges, 1973; Ager, 1974; Kelling and Mullin, 1975; DeRaaf and others, 1977; Brenchley and others, 1979; Kreisa, 1981; Morton, 1981; Nelson, 1982; Aigner, 1982 and 1985; Dott and Bourgeois, 1982; Einsele and Seilacher, 1982; Kreisa and Bambach, 1982). Clearly, our understanding of storm depositional systems has increased dramatically in recent years.

Sedimentary structures and bedform succession are particularly useful in reconstructing the depositional regime of this Facies. Basal erosion surfaces form as high-energy storm-generated waves and currents scour and suspend sediment. Partial truncation at the base of each successive carbonate layer produces sharp upper bed contacts. In this way the bedding sequence is formed of irregular amalgamated beds. In general, amalgamations are minor in vertical profile. This suggests that erosive currents were weak or short-lived. Based on the thickness of gutter casts, erosion rarely exceeded 6 cm. Above sharp basal contacts, parallel-laminated and low-angle (<10 degrees) cross-laminated (microhummocky) intervals formed during waning energy conditions (basal lags are uncommon in this Facies). Where both bedforms are recognized in the same bed, vertical transition is from parallel- to microhummocky-laminated. In addition, these bedforms grade laterally into one another. Their association may reflect changing hydrodynamic conditions. More importantly to this study, the associations of bedforms are recognized widely as products of storm deposition below fairweather wave base (Walker, 1985). Fine-grained argillaceous sediment usually caps the sequence. This upper unit formed after the storm event, as suspended clay-sized particles settled out. Wave ripple lamination is not recognized in this Facies. Wave ripples form as a traction lamination under the combined effects of unidirectional and ocscillatory currents (Harms and others, 1975). According to Brenchley (1985), wave ripples are observed frequently in proximal (nearshore) storm deposits. Further offshore, wave ripples decrease in abundance or may be absent. In addition, the paucity of basal lags and burrows, the presence of low-angle (versus high-angle) hummocky laminations, and the absence of a parallel-laminated horizon above the microhummocky interval suggest that deposition took place in deeper (offshore) water (Brenchley, 1985).

A definitive mechanism to explain the molding of silt- and sand-sized grains into microhummocky and parallel laminated bedforms still remains to be discovered. A number of models have been proposed (for discussion, see Walker, 1985); several are listed below:

1. Deposition from storm-generated density currents and concurrent reworking under oscillatory flow (Hamblin and Walker, 1979)
2. Storm-suspension of sediment in nearshore areas and hemipelagic redeposition offshore under the influence of wave-, tide-, or wind-driven currents (Reineck and Singh, 1972)
3. Sedimentation by high-energy oscillatory bottom-currents (Allen, 1984)
4. Autochthonous or "in situ" entrainment of sediment during storm events and suspension redeposition under the influence of weak oscillatory (wave) currents (Kreisa, 1981).

5. Combined unidirectional and oscillatory flows (Swift and others, 1983).

Laminated Peloidal Packstone/Grainstone Interbedded With Shale (XPGWS)

Description (Table 2.14)

Very thin- to thin-bedded peloidal packstone and grainstone is interbedded with thin (laminated) shale beds (Figure 2.14A and B). Individual limestone and shale layers are laterally discontinuous and range from <1 cm to 5 cm in thickness (Figure 2.3). Limestone layers are somewhat thicker than shale layers. This criterion is used to differentiate XPGWS from SWXPG in the field. Sedimentary structures and petrographic constituents differ between the two Facies, but these diagnostic features are usually microscopic in scale, and as a result are observed in polished slabs and thin-sections.

In the Nolichucky XPGWS accounts for approximately 20% of the total rock volume; XPGWS is rare in the Maynardville (Figure 2.2). Alternating thin limestone and shale form distinct lithological units that average 33 cm in thickness (Figure 2.3). Various features are recognized in limestone and include several types of lamination, pseudomudcracks, and soft-sediment deformation. Basal skeletal and intraclastic lags, micrograding, and burrows are less frequently observed. Peloids are the dominant petrographic constituent. Although some peloids may be fecal pellets, most are believed to be derived from subtidal _Girvanella_ mats. Clay minerals/micas and skeletal debris,

Table 2.14. Characteristics of the XPGWS Lithofacies.

Features	Characteristics
Lithology (Folk, 1959; 1962)	-Biopelsparite interbedded with shale -Biopelmicrite interbedded with shale
Color (Shale Only)	-Dark gray-green -Maroon
Bed Thickness	-Very thin- to thin-bedded -Discontinuous over 10's of cm.
Rock-Unit Thickness	-Very thin- to very thick-bedded
Sedimentary Texture and Structure	-Parallel laminations -Low-angle cross-laminations -Microhummocky cross-stratification -Loading, pseudonodules, and contorted-bedding -Very fine- to medium-grained -Pseudomudcracks -Size grading
Bed Contacts	
Upper	-Diffuse or sharp
Lower	-Sharp and scoured
Fossils	-Common; trilobites, echinoderms, *Girvanella*, *Chancelloria*, inarticulate brachiopods, sponge spicules
Other	-Basal lags -Silt-sized quartz interlayers -Stylolites
No. of Thin-Sections Examined	-38
No. of Thin-Sections Point-Counted	-8

Figure 2.14. Selected features of the Laminated Peloidal Packstone/Grainstone Interbedded with Shale (XPGWS) Lithofacies.

A. Outcrop of XPGWS. Field notebook is 17 cm tall. Interstate 75 section.

B. Polished slab of XPGWS showing fine-grained peloidal grainstone interbedded with thin shale. Internal laminae within limestone beds reveal parallel-, irregular-, and low-angle cross-laminations. Interstate 75 section. Sample I-74-0.3.

C. Outcrop of low-angle cross-lamination. Sets are truncated and exhibit erosional boundaries. Pencil is 15 cm in length. Beech Grove section.

D. Slab of the undersurface of a limestone bed which displays pseudomudcracks. Keys for scale. Beech Grove section.

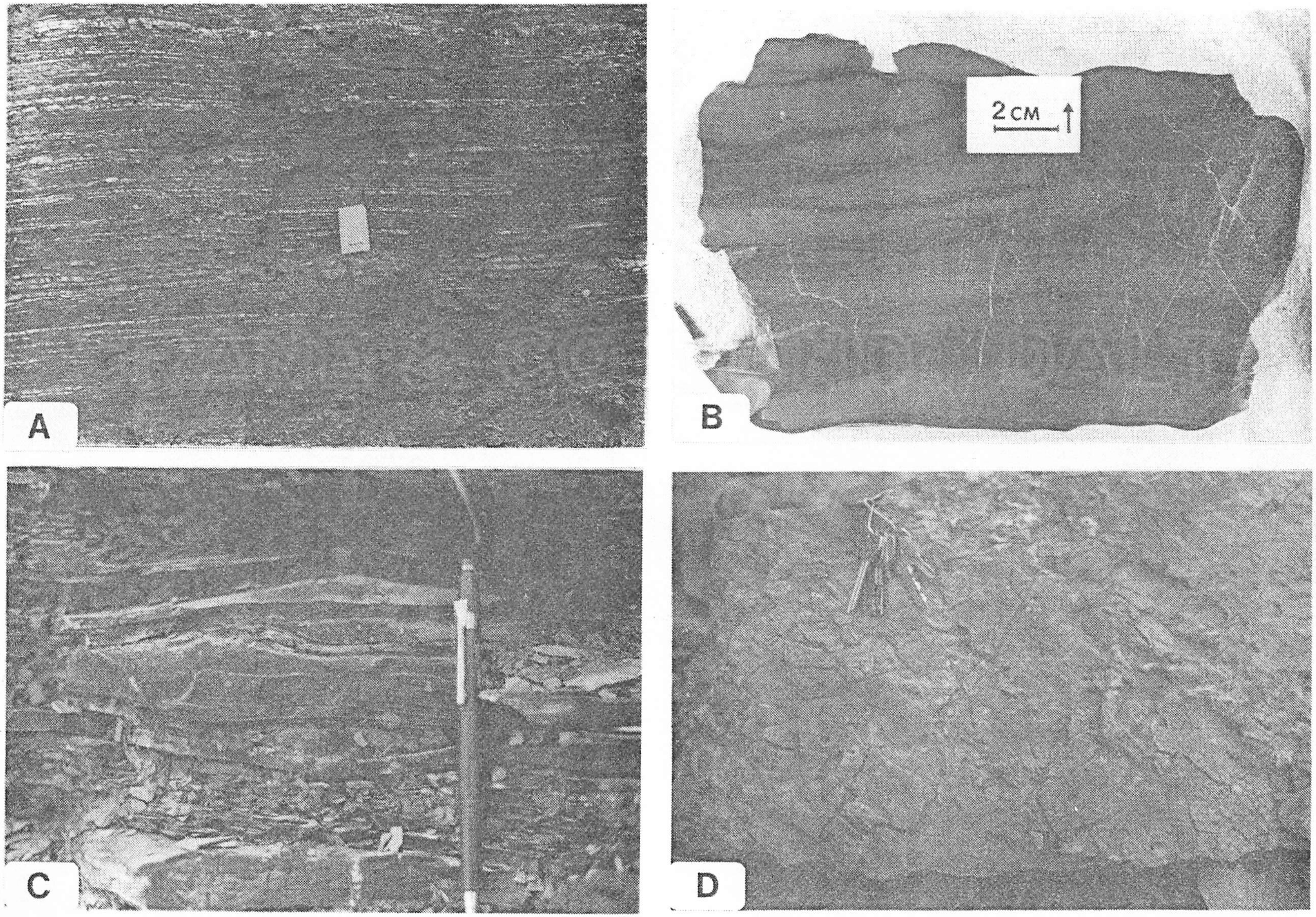
2 cm
A
B
C
D

primarily trilobites are other commonly observed petrographic features (Table 2.3). As expected, clay minerals are concentrated in shale beds, but in addition, fine-grained peloids, mica (biotite and muscovite), and quartz silt are locally abundant in shale. With exception of inarticulate brachiopods, skeletal allochems are rare in shale.

Limestone layers are made up of many laminations which are caused by compositional and/or grain size variations. In this Facies three types of stratification occur in abundance: (1) parallel lamination, (2) irregular lamination, and (3) low-angle (< 10 degrees) cross-lamination. Typically, low-angle cross-lamination sets are truncated and exhibit erosional boundaries (Figure 2.14C). This type of bedform resembles hummocky cross-stratification (HCS) after Harms and others, 1975), but in the Nolichucky HCS occurs on a smaller scale, and thus, is named microhummocky cross-stratification (Dott and Bourgeois, 1982). Wave ripple lamination, although uncommon in the Nolichucky of central east Tennessee, is an important feature in coeval rocks of southwestern Virginia (Markello and Read, 1981).

Graded or fining-upward sequences are characterized by sharp bases and gradational or diffuse tops. Evidence of scour is not as apparent here as in the XPG Facies; gutter casts and sole structures are rare. A basal layer of either medium-grained intraclasts or fine-grained skeletal debris fines upward into fine- to very fine-grained laminated peloidal grainstone. Limestone grades into shale (sharp tops are relatively rare).

Pseudomudcracks (Ksiazkiewicz, 1958) form polygonal patterns on the undersurfaces of many limestone beds of this Facies (Figure 2.14D). The vertical partings are several millimeters wide and up to 3 cm deep, and are filled with underlying and overlying sediment (shale). Vertical displacement of beds on either side of the parting cast produces microfaults, suggesting that limestone was lithified prior to movement.

Interpretation

Markello and Read (1981) provide evidence supporting a submarine origin for pseudomudcracks. In true mudcracks, mud layers are cracked and deflected upward along their periphery (i.e., Hardie and Ginsburg, 1977). In the Nolichucky, vertical fractures cut through limestone beds whereas the under- and overlying shale shows no evidence of cracks. In addition, internal laminations in limestone beds are not deflected or bowed. These structures probably reflect compaction and volume reduction of shale during dewatering (Markello and Read, 1981).

Much of the diagnostic environmental criteria of this Facies are found in the Peloidal Packstone/Grainstone (XPG) Facies. As a result, the environmental interpretation of both facies is broadly similar and details are not repeated here. However, three pertinent differences are recognized:

1. XPGWS reveals less evidence of scouring because sole structures, gutter casts, and amalgamated bedding are less common.
2. Burrows are less abundant in XPGWS.
3. Thin shale beds are abundant in XPGWS.

This Facies is interpreted as a storm deposit. Deposition occurred below fairweather wave-base in low to high current and wave activity (see under interpretation of XPG). The features above suggest that XPGWS was deposited in somewhat deeper water or during less intense but more frequent storms when compared to XPG. According to Brenchley (1985), distal storm deposits display less scouring (shallow erosion), fewer burrows, and thicker capping units.

Shale Interbedded With Laminated Peloidal Packstone/Grainstone (SWXPG)

Description (Table 2.15)

This Facies is up to 3 m thick (averages 40 cm) in the Nolichucky Shale and is practically nonexistent in the Maynardville Limestone (Figures 2.2 and 2.3). Shale is interbedded with planar-laminated to low-angle cross-laminated peloidal limestone lenses (Figure 2.15A). Shale beds are thin (<10 cm) and are compositionally identical to shale of the Shale Facies (see Shale Lithofacies description). Both Facies (S and SWXPG) occur in close stratigraphic proximity. Carbonate layers do not exceed 2 or 3 cm and are generally less than 0.5 cm in thickness, forming laterally discontinuous streaks that pinch and swell. The peloidal carbonates are further characterized by (1) sharp bases, (2) irregular, diffuse tops, (3) fining upward sequences, (4) thin, isolated skeletal lenses, and (5) fine to coarse silt-sized peloid grains.

Interpretation

This Facies is interpreted as a low-energy deposit which underwent deposition in "deeper" water. The basis for this interpretation is the

Table 2.15. Characteristics of the SWXPG Lithofacies.

Features	Characteristics
Lithology (Folk, 1959; 1962)	-Shale interbedded with (1) pelsparite, (2) pelmicrite, (3) biopelmicrite, (4) biomicrite
Color (Shale Only)	-Dark gray-green -Maroon
Bed Thickness	-Thinly laminated to thin-bedded
Rock-Unit Thickness	-Thin- to very thick-bedded
Sedimentary Texture and Structure	-Parallel lamination -Low-angle cross-lamination -Loading, pseudonodules, and contorted-bedding -Very fine- to medium-grained -Fining upward sequences
Bed Contacts	
Upper	-Diffuse and sharp
Lower	-Sharp and planar to irregular
Fossils	-Rare; echinoderms, trilobites, and inarticulate brachiopods
Other	-Very thin carbonate layers (<0.5 cm.) -Phosphate crusts
No. of Thin-Sections Examined	-29
No. of Thin-Sections Point-Counted	-9

Figure 2.15. Selected features of the shale-dominated lithofacies (SWXPG and S).

A. Outcrop of shale interbedded with laminated peloidal limestone (SWXPG). Notice the thin and discontinuous nature of limestone lenses. Rock hammer is 25 cm in length. Interstate 75 section.

B. Outcrop of Shale (S) Lithofacies. Field notebook is 17 cm tall. Interstate 75 section.

C. Photomicrograph of shale showing rare skeletal debris (trilobite). Light-colored particles are fine-grained dolomite rhombs. Field of view is 6.5 mm in long dimension. Joy 2 section. Sample J-2 819.5.

D. Photomicrograph of "ultra-thin" thin-section of shale which shows an abundance of very fine-grained peloids. Under cross-polarized light, peloids are difficult to distinguish from the dark shale groundmass. Field of view is 1.3 mm in long dimension. Interstate 75 section. Sample I-29-4.8.

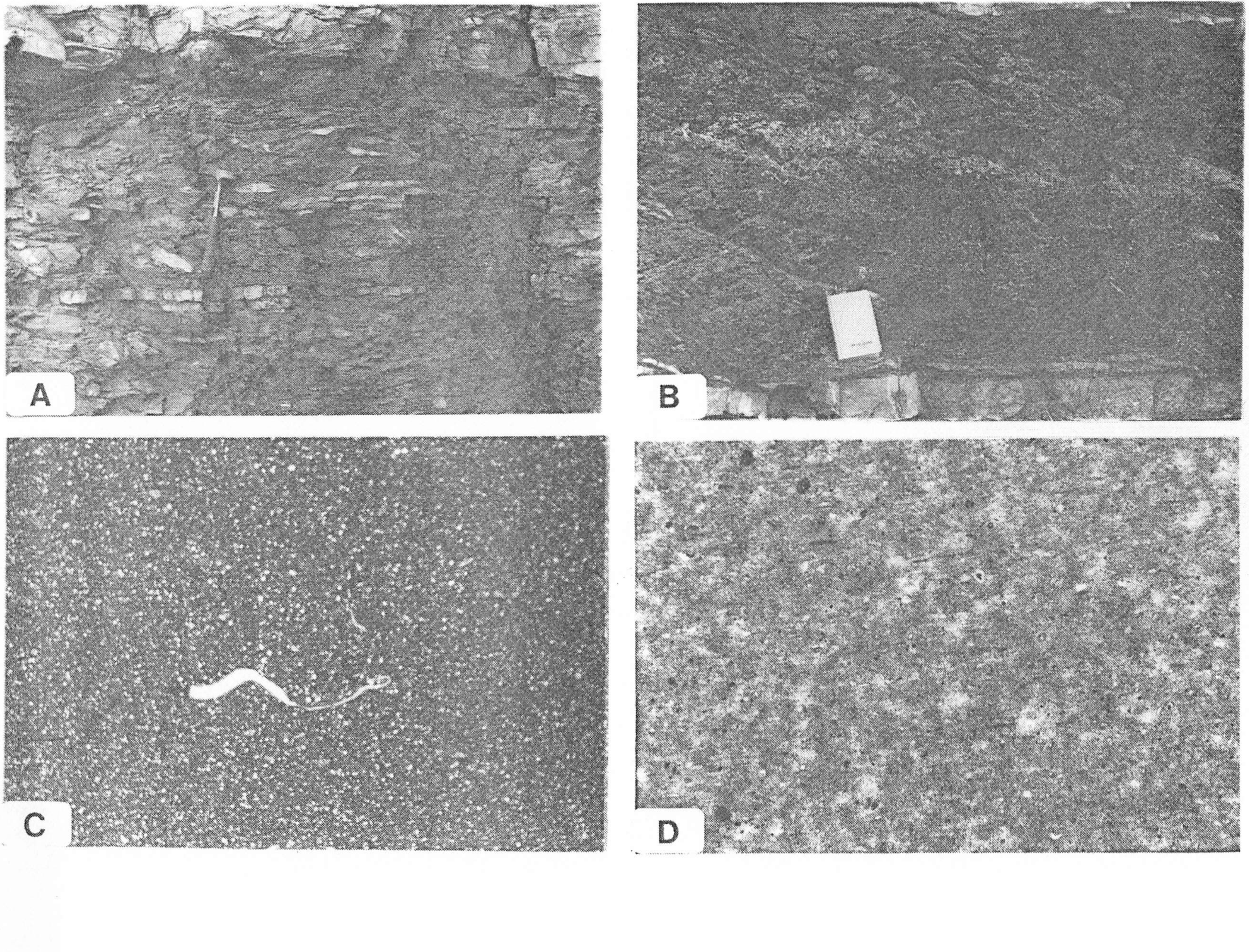
A
B
C
D

occurrence of thin planar- to cross-laminated silt-sized layers which grade upward into very fine-grained siliciclastic sediment (shale). The laminated and graded silt layers are referred to as "storm layers." During conditions of high wave-energy, sediment is eroded, suspended, and transported to the open sea. As the storm subsides, clouds of suspended sediment settle out forming planar laminations. Low-velocity bottom currents or wave oscillation may rework the sediment, transforming planar laminations into low-angle cross-laminations. Thus, carbonate silt lenses result from storm activity. Although not actually a storm deposit, these deposits represent distal products of storms. Similar types of deposits are recognized in the modern. Reineck and Singh (1972 and 1980) note that parallel to cross-laminated clay, silt, and fine sand are found as far as 45 km from the coast in the Gulf of Mexico and the North Sea at water depths of up to 40 m. In addition, DeRaaf and others (1977) recognized similar low-energy deposits from the Lower Carboniferous in Ireland.

Shale (S)

Description (Table 2.16)

Shale is very abundant in the Nolichucky (Figure 2.2) and accounts for approximately 40% to 60% of the total rock volume; these fine-grained siliciclastics are very rare in the Maynardville (Figure 2.2). Beds range from several centimeters to several meters in thickness (Figure 2.3). Distinct carbonate beds are absent (Figure 2.15B). The

Table 2.16. Characteristics of the S Lithofacies.

Features	Characteristics
Lithology	-Peloid-rich shale
Color (Shale Only)	-Dark gray-green -Maroon
Bed Thickness	-Very thin- to very thick-bedded -Laterally continuous
Sedimentary Texture and Structure	-Faint parallel lamination -Very fine-grained
Bed Contacts	
Upper	-Sharp; planar to scoured
Lower	-Sharp
Fossils	-Rare; echinoderms, trilobites, graptolites, and inarticulate brachiopods
Other	-Rare peloidal and fossiliferous lenses, <<1 cm. thick
No. of Thin-Sections Examined	-39
No. of Thin-Sections Point-Counted	-16

shale is gray-green and maroon, but weathers to gray, olive, brown, or black. It is fissile and calcareous, and occasionally reveals scattered trilobite, echinoderm, and inarticulate brachiopod debris (Figure 2.15C). Fossil debris, intraclasts, glauconite, and peloids are fine-grained. With exception of peloids, grain types occur as discrete and disseminated particles floating in shale. Peloids are notable features of this Facies and may account for as much as 50% to 60% of the rock (Figure 2.3). The precise abundance of peloids is difficult to establish because they exhibit diffuse or vague exterior boundaries with the surrounding clay and silt matrix (Figure 2.15D). Biotite and muscovite flakes, fine quartz and feldspar silt, and dolomite rhombs are also identified. X-ray diffraction data reveal a clay mineral suite which is dominated by a 10 Angstrom mixed-layered complex (illite-vermiculite and/or hydrated illite-chlorite), iron-chlorite, and kaolinite (See Appendix D).

Interpretation

The Shale Facies formed below normal wave-base in shallow water. A quiet water depositional setting is indicated by preserved parallel lamination and fine grain size. Although difficult to quantify, water depth is thought to have ranged from approximately 10 m to 50 m. Several lines of evidence are used to support this interpretation:

1. The Shale Facies is stratigraphically displaced from intertidal facies and lacks diagnostic features of extreme shallow water deposition or emergence.

2. Depositional slopes were very subtle. This is supported by the absence of turbidites, slump structures, and intraformational truncation surfaces.
3. Similar shale sequences are described from intrashelf basins of the Cambrian (Aitken, 1978; Markello and Read, 1981) and Mesozoic (Eliuk, 1978). These authors postulate comparable water depths.
4. Conformable contacts occur between shoaling carbonate sequences and thick shale.
5. Inferred water depth of interfingering facies is compatible to that of the Shale Facies.

On modern shelves most fine-grained sediment is introduced to the marine environment by deltaic depositional systems (Drake, 1976). Nearshore wind and tidal currents entrain fine-grained sediment into dilute clouds or nepheloid layers which move offshore into outer shelf and basinal areas. Settling of suspended particles takes place in quiet water (Swift, 1976; Leeder, 1982). This depositional process is known as suspension fallout or hemipelagic sedimentation (Tucker, 1981). The Shale Facies underwent deposition in a similar way. Most fine-grained siliciclastic particles were introduced into the basin by a river system that was located on the northern margin of the intrashelf basin (see Chapter 1). The delta was situated at least 200 km from central east Tennessee. According to Curray (1965), suspended terrigenous mud and silt would be deposited in near shore areas. However, widespread distribution of fine sediment is recognized a great distance from known land areas during Nolichucky time. This discrepency can be explained by numerous episodes of resuspension and redistribution of sediment during storm swells. Storm-generated surface and internal currents transport fine-grained sediment over wide geographic areas on modern shelves (Drake, 1976).

Very fine-grained peloids (<0.05 mm) are locally abundant in some shale thin-sections. Although the mode of occurrence of these peloids would suggest hemipelagic sedimentation, their genesis and source are not fully understood. The source of peloids may be threefold. Some may have been carried into the basin from the siliciclastic shelf to the north; however, most of the peloids probably underwent very local transport from nearby carbonate-forming environments or were transported in from the more distant carbonate peritidal environments to the east and southeast. The origin of fine-grained peloids is even more uncertain. Three possible origins are suggested:

1. Fecal pellets
2. Finely comminuted particles eroded from subtidal cyanobacterial mats
3. Calcite precipitation within and around clumps of bacteria (for further discussion, see Pratt, 1984; Chafetz, 1986).

Intraclastic Packstone/Grainstone (IPG)

Description

Limestone clast conglomerates in the Conasauga Group (Maryville Limestone and Nolichucky Shale) have been examined in detail by Weber and others (1985) and Kozar and others (1986). This work is summarized in Kozar (1986). The description and interpretation presented here for the Intraclastic Packstone/Grainstone Facies are abstracted from these previous works. For a more detailed discussion of this subject see Kozar (1986).

In the Nolichucky Shale, limestone clast conglomerate (IPG) beds range from 2 cm to 45 cm, but average only 9 cm in thickness (Figure 2.3). They account for about 10% of a stratigraphic section (Figure 2.2). Clasts are derived from nearby deeper water lithofacies. The diversity of intraclasts may be high in some beds, but in no case are very shallow water platform lithologies (e.g., cryptalgalaminates, stromatolites, or thrombolites) represented as clast types. The following intraclasts are recognized: mudstone, peloidal packstone, fossiliferous packstone, oolitic packstone, quartz silt, and shale. Individual clasts never exceed 50 cm in length and 10 cm in thickness. In outcrop most "large" clasts are from 5 cm to 10 cm in length and 0.5 cm to 2 cm thick.

Shale matrix conglomerates (Figure 2.16A), lime mud and coarse-grained matrix conglomerates (Figure 2.16B), and coarse-grained matrix conglomerates (Figure 2.16C) are the three types of intraclastic

Figure 2.16. Selected features of the Intraclastic Packstone/Grainstone (IPG) Lithofacies.

A. Shale matrix conglomerate. Interstate 75 section. Sample I-14-0.0.

B. Lime mud and coarse-grained matrix conglomerate. Note that clasts are normal to bedding. Interstate 75 section. Sample I-44-1.5.

C. Coarse-grained matrix conglomerate. Beech Grove section. Sample BG-Renalcid buildup (unit 6-3).

D. Slab of intraclasts which are projecting above the bed surface. Many of these clasts were "rafted" along the top of the debris flow. Knife is 9 cm in length. Beech Grove section.

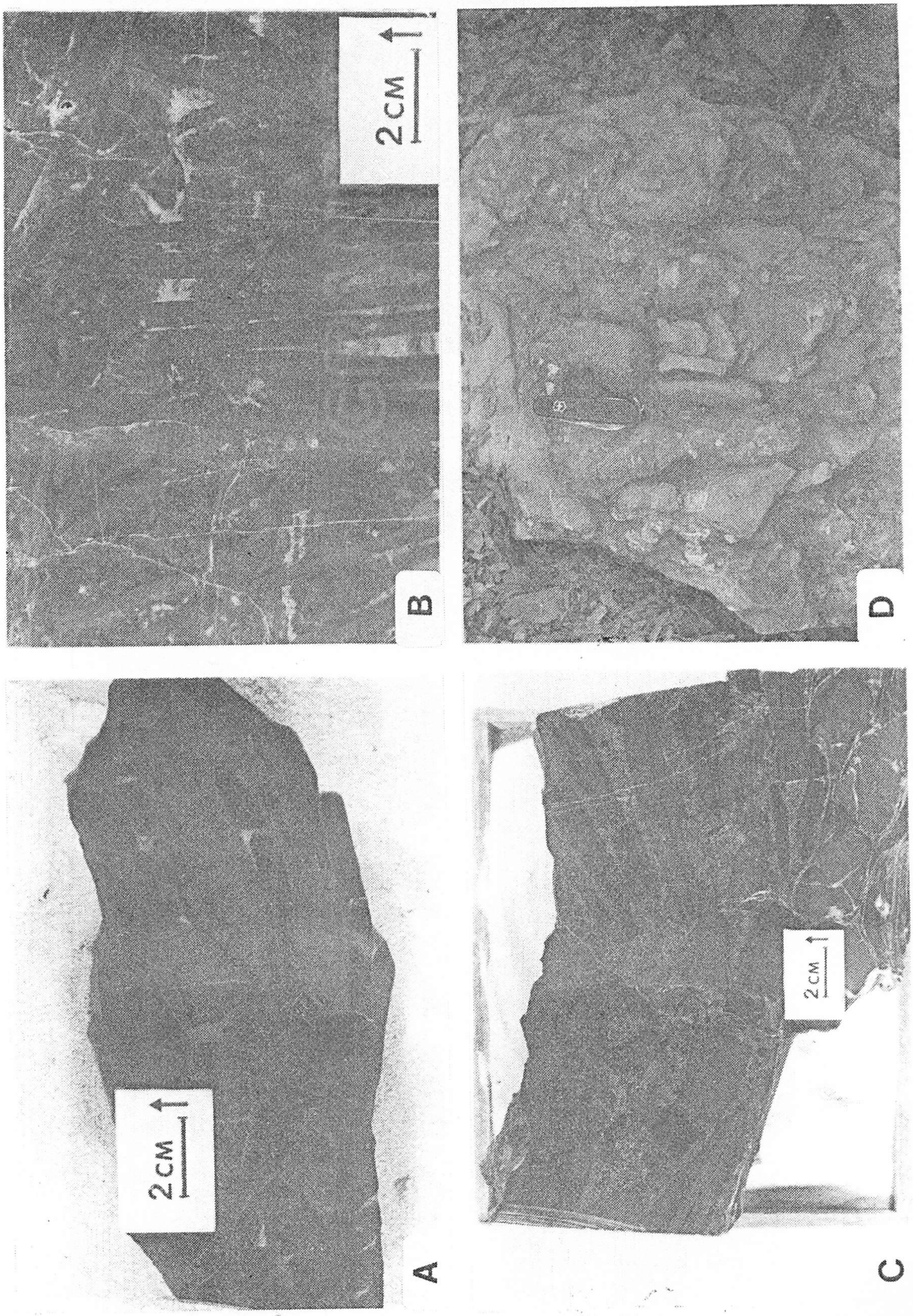
A
2CM
B
2CM
C
2CM
D

packstone/grainstone beds that occur in the Nolichucky Shale. Their characteristics are summarized in Tables 2.17, 2.18, and 2.19.

Interpretation

Limestone clast conglomerates are very distinctive and common features of Cambrian and Ordovician rocks. Most conglomeratic deposits formed from erosion and redeposition of partially consolidated sediment by storm processes in intertidal and shallow subtidal settings (e.g., Jones and Dixon, 1976; Markello and Read, 1981; Sepkoski, 1982; Demicco, 1983; Whisonant, 1987, Kopaska-Merkel, 1988). In the Nolichucky Shale an alternative explanation is proposed to explain the deposition of some conglomeratic beds. Mass-sediment gravity movement (debris flows) is also responsible for the genesis and transport of limestone clasts. Mass movement conglomeratic deposits in the Nolichucky differ from those described from similar aged rocks in the western United States and Canada (e.g., Cook and Mullins, 1983; Hiscott and James, 1985). Here, slump structures, rafted megablocks, and rotational/translational slides are absent.

Shale matrix conglomerates. These intraclastic beds are rare; they account for less than 1% of all conglomerate beds. Because they lack definitive evidence to support a single depositional mechanism, multiple origins are suspected. Small, rounded clasts (<1 cm to approximately 5 cm) probably were entrained during storms; larger clasts have an irregular shape, and were most likely deposited from subaqueous debris flows. It is important to note that some beds display only small

Table 2.17. Characteristics of shale matrix conglomerates.

Features	Characteristics
Associated Lithofacies	-Thick under- and overlying shale
Bed Thickness	-Very thin- to thin-bedded (2-8 cm)
Naure of Bedding Contact	-Sharp lower bedding surface -Irregular upper bedding surface
Bed Geometry	-Laterally discontinuous channels or lenses
Grading	-Absent
Sorting (Clasts)	-Poor; granule-pebble
Clast Orientation	-Random to subparallel
Matrix	-Shale
Clast Shape, Roundness	-Tabular, rounded, rare irregular varieties

Table 2.18. Characteristics of lime mud and coarse-grained matrix conglomerates.

Features	Characteristics
Associated Lithofacies	-Shale -Thin-bedded peloidal packstone
Bed Thickness	-Thin- to medium-bedded (3-15 cm)
Naure of Bedding Contact	-Planar lower bedding surface -Irregular to domal upper surface
Bed Geometry -Sheets	-Domal bedforms
Grading	-Rare to absent
Sorting (Clasts)	-Poor; granule-cobble
Clast Orientation	-Subparallel to random
Matrix	-Fine-grained lime mud -Coarse-grained skeletal and peloidal packstone
Clast Shape, Roundness	-Irregular, angular, tabular, and discoid
Other	-Rafted and projecting clasts -Mono- or polymictic clast associations

Table 2.19. Characteristics of coarse-grained matrix conglomerates.

Features	Characteristics
Associated Lithofacies	-Interbedded silty, peloidal limestone -Typically overlain by shale
Bed Thickness	-Thin- to thick-bedded (3-45 cm)
Naure of Bedding Contact	-Sharp planar to scoured bottom -Planar top
Bed Geometry	-Sheets -Low-relief channels -Thick channels
Grading	-Rare to absent
Sorting (Clasts)	-Moderate to poor; pebble-cobble
Clast Orientation	-Subparallel -Fanned
Matrix	-Well-washed skeletal and peloidal grainstone -Rare trapped lime mud
Clast Shape, Roundness	-Tabular to discoid, rounded edges
Other	-Hummocky cross-laminations -Planar laminations -Sole marks -Cement-filled shelter voids -Perched micrite -Dominantly monomictic

clasts. Thus, debris flows and clast entrainment during storms were probably mutually exclusive events.

Lime mud and coarse-grained matrix conglomerates. Fine-grained matrix support of intraclasts, coupled with random clast fabric suggests debris flow transport. About 25% of limestone clast conglomerates are of this type. The high proportion of matrix implies that buoyant strength of the flow results from the cohesive strength of the matrix. Frictional strength caused by grain-to-grain interaction in the matrix is not ruled out. Absence of grading, cement-filled shelter voids, and/or perched sediment precludes suspension settling of clasts. In addition, clasts tend to float on the top of these beds and project above the bed surface implying that they were "rafted" along by the flow (Figure 2.16D). Rafted clasts indicate rigid, plug flow (Hampton, 1972).

These debris flows moved over slopes which were less than 1 degree (Markello and Read, 1982). Also, this statement is supported by paleoenvironmental and palinspastic reconstructions in central east Tennessee. Flows moving over such low slopes require excess pore pressure for initiation of movement (Peirson, 1981). Excess pore pressure is caused by deposition on a semipermeable layer, overloading of the sediment, and liquefaction caused by storm, tidal, and/or wave activity (Nardin and others, 1979). In the Nolichucky sediment overloading and/or cyclic wave-loading initiated failure and mass-movement. These debris flows are similar to modern subaqueous debris flow deposits which traverse low slopes (Prior and Coleman, 1982).

Coarse-grained matrix conglomerates. Coarse matrix intraclastic beds are interbedded with storm-derived lithofacies. Their well-washed coarse skeletal and peloidal matrix suggests that sedimentation took place by erosion and redeposition during storm events. Storm-derived conglomerate deposits make up about 75% of all conglomeratic beds in the Nolichucky Shale. Other evidence which supports storm sedimentation includes "fanned" clast fabrics. The oscillatory component of storm waves reorients clasts. Also, lime mud caps represent suspension settling and infiltration of fine-grained sediment during the waning stages of storm activity. The absence of imbrication suggests that unidirectional currents did not play an important role in these deposits. Imbrication is common in current-generated accumulations (Whisonant, 1987).

Storm-generated currents (i.e., gradient currents) incised low-relief channels and transported intraclasts and coarse-grained matrix through the conduits. These channels closely resemble subtidal storm-surge channels, rip-channels, and progradational lobes (Seilacher, 1982; Markello and Read, 1982). Tractional bedload transport, directly related to high-energy conditions at the sediment-water interface, seems to be a likely mechanism to explain clast movement (Aigner, 1985). Although individual high-energy storm pulses created and filled channels or filled preexisting topographic lows with sediment, multiple events resulted in amalgamated channels or lobes. Episodic rather than continuous sedimentation is postulated for this Facies because of the widespread nature of amalgamated bedding geometry.

Summary of Depositional Environments

This Chapter focuses on the petrology and depositional environments of 14 lithotypes which are recognized in the Nolichucky/Maynardville sequence in central east Tennessee (Oak Ridge and Knoxville vicinity). Each lithotype reveals a unique suite of megascopic and microscopic features, which result from various depositional and diagenetic processes (Table 2.20). The particular combination of lithologic, sedimentologic, paleontologic, and early diagenetic components in the rock record was dictated by the local environmental setting.

Table 2.20. Summary of depositional environments.

Lithofacies (symbol)	Depositional Process and Paleoenvironmental Interpretation
CL	Cyanobacterial trapping, binding, and/or mineral precipitation of sediment; lower to upper intertidal, perhaps locally supratidal; low-energy tidal flat.
STROM	Cyanobacterial trapping, binding, and/or mineral precipitation of sediment; lower intertidal; low-energy tidal flat.
THROM	Bacterially induced; very shallow subtidal, 0-3 m; low- to moderate-energy.
NOPG	Oncoids bacterially induced; very shallow subtidal, 0-3 m, moderate-energy.
EPG	Peloids derived from _Girvanella_ mats; very shallow subtidal, 0-5 m; moderate- to high-energy.
MWS	_Girvanella_ mats; lime mud blankets or veneers; subtidal, 5-15 m; low-energy; open marine; subwave-base; hemipelagic deposition.
OPG (buildups)	Ooid-forming environment; very shallow subtidal, 0-5 m; moderate- to high-energy.
OPG (sheets)	Storm sand sheets; subtidal, 5-30+ m; low- to high-energy; subwave-base.
FPG	Storm sand sheets; subtidal, 5-30+ m; moderate- to high-energy; subwave-base.
FPGWS	Entrainment of silt- and sand-sized fossil debris into dilute "clouds"; subtidal, 5-30+ m; low- to moderate-energy; subwave-base; hemipelagic deposition.
XPG	Proximal storm reworked peloidal sands; subtidal, 5-30+ m; moderate- to high-energy; subwave-base.
XPGWS	Distal storm reworked peloidal sands; subtidal, 5-50 m; low- to moderate-energy; subwave-base.
SWXPG	"Storm layers"; subtidal, 5-50 m; low-energy; subwave-base; hemipelagic deposition and minor current reworking.
S	Hemipelagic settling of fine-grained siliciclastic particles; subtidal, 10-50 m; low-energy; subwave-base.
IPG	Storm reworking of lithified and semi-lithified sediment; ubiquitous; 0-50 m; shale matrix conglomerates deeper, coarse-grained matrix conglomerates shallower.

CHAPTER 3

USING MULTIPLE ANALYTICAL TECHNIQUES FOR THE RECOGNITION OF SEDIMENTARY CYCLES

Introduction

Cyclicity has aroused controversy within the geologic community for at least a century. Some geologists place considerable importance on stratigraphic cyclicity, perhaps overemphasizing the deterministic nature of past events. Others believe that cyclicity is rarely if ever observed in actual stratigraphic sections (for discussion see Duff and others, 1967; Schwarzacher, 1975). Several factors are responsible for this divergence of opinion: (1) the "term" cycle lacks a universally accepted definition, (2) subjective methods are commonly used to identify cyclicity, and (3) many powerful mathematical techniques cannot be used to confirm the presence of cycles.

A cycle refers to a series of events that occur in repeated order and lead back to some starting point: (e.g., ABCDEABCDE ... or ABCDEDCBABCDE ...) (Weller, 1964). Many geologists believe this definition is too restrictive. As a result, a preferred definition of a sedimentary cycle is as follows: a series of observations (rock types, bed thickness measurements, etc.) that occur in predictable pattern or follow certain order (Schwarzacher, 1975). This definition accounts for the variability or randomness which certainly exists in natural geologic systems. Assuming ABCDE contains random elements A and E, cyclicity is possible within the sequence: BCDAEBCDABCDBCDEA, etc.).

Numerous investigators have identified cycles within sedimentary rocks. Most previous studies have based the occurrence of cycles on (1) descriptive stratigraphic data, which typically lack statistical verification (Aitken, 1978; James, 1984; Aigner, 1985), (2) older, flawed versions of Markov chain analysis (Gingerich, 1969; Doveton, 1971; Lumsden, 1971; Tewari and Casshyap, 1983), or (3) computer-generated models not closely associated with actual stratigraphic data (Turcotte and Willemann, 1983; Read and others, 1986). The approach described here uses multiple analytical techniques to recognize cycles, but stratigraphic information serves as the data base.

A serious constraint of stratigraphic data is that many variables are based on a nominal or an ordinal scale of measurement. For example, rock types (lithologies) are classified into mutually exclusive categories. As a result, powerful techniques of parametric statistics cannot be conducted, but useful tests can be employed. A robust embedded Markov chain analysis, substitutability analysis, auto-association analysis, and runs test are proposed here for examining stratigraphic cyclicity. These statistical techniques are easily understood, require few assumptions, use nominal and ordinal data, detect subtle trends or cycles not normally observed by unaided processing, and employ computers for rapid processing of large data sets.

Discussion of Techniques

Markov Chain Analysis

During the past twenty years, Markov chain analysis has become a popular technique to identify cyclicity (Gingerich, 1969; Doveton, 1971; Hattori, 1976; Jones and Dixon, 1976; Tewari and Casshyap, 1983; and many others). Many stratigraphers and sedimentologists have not fully realized the problems involved with the application of Markov analysis. Recently, some investigations have noted potential sources of error (Hiscott, 1981; Carr, 1982; Powers and Easterling, 1982), and several lesser known but surmountable problems are discussed here. A statistically valid Markov model can be used to assess stratigraphic cyclicity.

Markov analysis is based on probability theory. The presence of a first-order Markovian process indicates that the occurrence of some lithology A is dependent only on the immediately preceding lithology A-1. Thus, lithology A will have a greater probability of overlying lithology A-1 than would be expected of an entirely random sequence of lithologies. In order to determine Markovian tendency, the stratigraphic position of each lithology must be recorded (Figure 3.1). This two-dimensional array is known as a transition frequency matrix, which may be structured in one of two ways. Equally spaced observation intervals result in a transition frequency matrix similar to Figure 3.1. In this case the transition probabilities are dependent on the observation interval (sample interval) and the thickness of each stratigraphic unit. This method poses a problem because successive

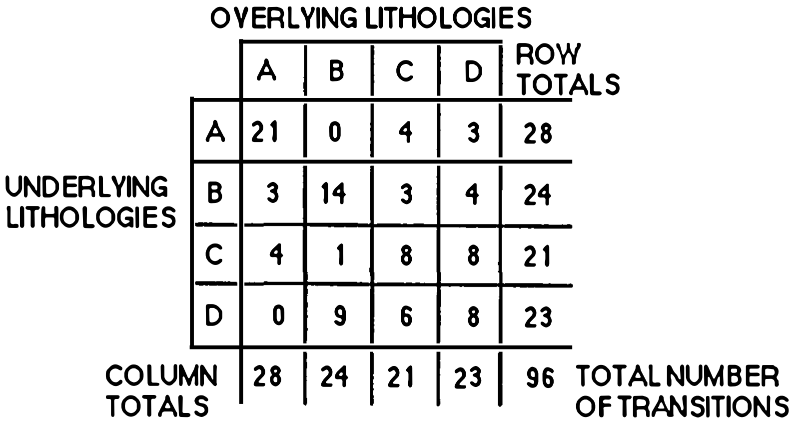

		OVERLYING LITHOLOGIES					
		A	B	C	D	ROW TOTALS	
UNDERLYING LITHOLOGIES	A	21	0	4	3	28	
	B	3	14	3	4	24	
	C	4	1	8	8	21	
	D	0	9	6	8	23	
COLUMN TOTALS		28	24	21	23	96	TOTAL NUMBER OF TRANSITIONS

Figure 3.1. Transition frequency matrix of a hypothetical stratigraphic column composed of four distinct lithologies (A-D). This 4 X 4 matrix exhibits 16 individual cells.

lithologies are usually not of equal thickness. An alternative, superior method involves recording each lithology without regard to some arbitrary sample interval. The transition from one lithology to an overlying, identical lithology is not permitted. A resulting transition frequency matrix contains a priori zeros along the main diagonal (Figure 3.2). Matrices structured in this way are examined for embedded Markov chains.

Several chi-square statistics are available to test transition frequency matrices for Markov properties (Powers and Easterling, 1982). Commonly, Pearson's chi-square statistic is used:

$$\text{Observed Chi-Square } (X^2) = \sum_{i=1}^{m} \sum_{j=1}^{m} (O_{ij}-E_{ij})^2/E_{ij},$$

where i=underlying lithology 1, 2, ..., m
j=overlying lithology 1, 2, ..., m
m=total number of lithologies

O_{ij} refers to the observed number of transitions from lithology i to lithology j. These values (O_{ij}) are obtained from the transition frequency matrix. For example; if in Figure 3.2, i=2 and j=3, then cell O_{23}=42. E_{ij} is the expected number of transitions from lithology i to j which should be observed if the lithologies are randomly distributed. The expected frequency (E_{ij}) is calculated for each cell as follows:

		OVERLYING LITHOLOGIES					
		A (j=1)	B (j=2)	C (j=3)	D (j=4)	ROW TOTALS	
UNDERLYING LITHOLOGIES	A (i=1)	0	22	15	19	56	
	B (i=2)	6	0	42	7	55	
	C (i=3)	7	33	0	20	60	
	D (i=4)	43	0	3	0	46	
	COLUMN TOTALS	56	55	60	46	217	TOTAL NUMBER OF TRANSITIONS (N)

Figure 3.2. Transition frequency matrix. Note the series of zeros along the main diagonal.

$$E_{ij}=n_j\ n_i/N,$$

where n_j=column total of j

n_i=row total of i

N =total number of transitions

The observed value of Pearson's chi-square statistic is compared to the actual chi-square distribution with $(m-1)^2$ degrees of freedom (Davis, 1986) and some level of significance. A chi-square distribution table is needed to determine the expected chi-square value. Thus, a succession of lithologies exhibits randomness if the observed chi-square value is less than the expected chi-square value at some chosen confidence level, commonly 95%. If the observed value is greater than the expected value, the lithologic sequence displays nonrandom, Markovian behavior.

If a transition frequency matrix exhibits nonrandomness, a difference matrix is computed to determine which lithologic transitions occur more (or less) frequently than expected. A difference matrix (Figure 3.3) results from the difference between the observed and expected frequency for each cell or transition ($O_{ij}-E_{ij}$ for each i, j). Each cell within the matrix contains either a positive or a negative number. Positive values reveal transitions that are more likely to occur.

OVERLYING LITHOLOGIES

		A	B	C	D
UNDERLYING LITHOLOGIES	A	0	+.12	-.01	-.05
	B	+.35	0	-.47	-.01
	C	+.03	-.08	0	-.03
	D	-.02	-.13	+.47	0

Figure 3.3. Difference matrix. It is standard convention to calculate values for each cell using the formula $O_{ij}-E_{ij}/n_i$.

There are two problems with the embedded Markov chain procedure described above. Because no vertical contacts between units of the same lithology are recorded, the observed transition frequency matrix will contain structural zeros along the main diagonal. According to Schwarzacher (1975), these diagonal zeros prevent the generation of a valid expected frequency matrix. The chi-square test becomes meaningless and order may be perceived in the stratigraphic section where no order actually exists.

Another problem involves the difference matrix. More than one cell may contain positive values, but only one positive cell value (one lithologic transition) may actually contribute to the nonrandomness of the system (Carr, 1982).

Failure to recognize these problems has led to false identification of order or cyclicity in the stratigraphic record. To eliminate these potential errors, a log-linear model of quasi-independence (Carr, 1982) should be used to test incomplete matrices (those containing structural or diagonal zeros). The presence of structural zeros does not disrupt the calculation of the expected frequency matrix. In addition, Brown (1974) described a procedure that isolates lithologic transitions which depart from randomness. At each iteration, a zero is substituted in the cell (transition) that causes greatest reduction in the chi-square statistic. The computer refits the remaining cells using the log-linear model and recalculates the chi-square statistic. This process is continued until the probability for chi-square of the observed frequency matrix exceeds some chosen level of significance. This procedure is included in the P2F BMDP computer program by Brown (1979).

Substitutability Analysis

Substitutability analysis has rarely been applied to stratigraphic data (Davis and Cocke, 1972; Doveton and Skipper, 1974; Allen, 1982). This is probably due to its obscure origin in speech therapy and image processing of satellite photographs (Rosenfeld and others, 1968). In geology, substitutability analysis is used to determine whether two or more lithologies characteristically substitute for one another in a stratigraphic sequence. For example, if two different lithologies are commonly underlain by a third lithology, the two overlying lithologies exhibit high substitutability. This type of substitution is called overlying substitutability (Figure 3.4). Underlying and mutual substitutability also occur (Figure 3.4).

A substitutability matrix is computed from a transition probability matrix, which in turn is derived from a transition frequency matrix. For a simple procedure see Davis (1986).

Substitutability matrices contain cells with values ranging from 0 to 1 and are symmetrical about the main diagonal (Figure 3.5). Because these matrices are symmetrical, conventional clustering methods are used to hierarchically classify lithologies exhibiting high substitutability. Although substitutability analysis does not invoke a formal statistical testing procedure, the computer produced dendograms retain all information of transition frequency matrices (Doveton and Skipper,

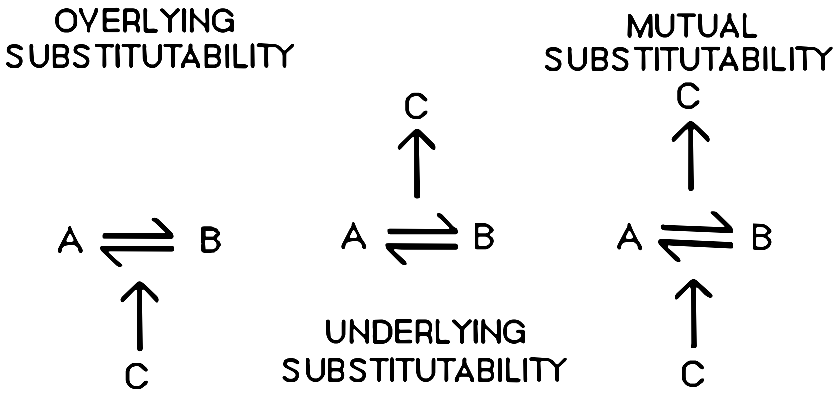

Figure 3.4. Lithologies A, B, and C are used to show the three types of substitutability. Horizontal arrows indicate high substitutability. Vertical arrows indicate relative stratigraphic position.

		OVERLYING LITHOLOGIES			
		A	B	C	D
UNDERLYING LITHOLOGIES	A	—	.27	.69	.12
	B	.27	—	.08	.99
	C	.69	.08	—	.22
	D	.12	.99	.22	—

Figure 3.5. An example of a substitutability matrix. High cell values (near 1.00) indicate high substitutability.

1974). However, it should be noted that dendogram linkages exhibit differing degrees of stability.

Auto-Association Analysis

Auto-association analysis is similar to the time-series technique known as autocorrelation. Both determine partial repetition in a sequence of data, but a major difference exists. Auto-association analyzes nonnumeric data. As a result, it is much less restrictive and can be applied to a sequence of lithologies (see Merriam and Sneath, 1967; Sackin and Merriam, 1969). Auto-association analysis was originally developed by Sackin and Sneath (1965) to compare amino acid chains.

Auto-association is a useful method for examining the repetitive nature of lithologic data (Davis, 1986). A hypothetical stratigraphic section consists of six lithologies which might be portrayed in ascending order as:

13456213141634562612345643456

Lithologies 3, 4, 5, and 6 commonly occur in order throughout the sequence. These lithologies represent the repetitive subset or cycle. The subset is moved one step at a time, past the complete set of lithologies (Figure 3.6). At each overlap position, the number of matches is recorded. The number of matches indicates the degree of similarity between the two sequence chains. A plot of match position

MATCH POSITION	OVERLAP POSITION	NUMBER OF COMPARISONS	NUMBER OF MATCHES
1	13456213141634562612345643456 3456	1	0
2	13456213... 3456	2	0
3	13456213... 3456	3	0
4	13456213... 3456	4	0
5	13456213... 3456	4	4
6	13456213... 3456	4	0

Figure 3.6. Auto-association analysis using hypothetical stratigraphic section and repetitive subset described in text.

versus the number of matches graphically displays regions of high and low association. Intervals of high association locate cycles within the stratigraphic section.

Runs Test

The runs test is a nonparametric statistical technique that examines sequential data for randomness (Davis, 1986). For example, the probability of obtaining 15 tails followed by 15 heads in 30 random coin tosses is very low. Likewise, the probability of regular alternation of heads and tails is also quite low. If the coin is unbiased, each toss is independent of the previous toss. The expected order of heads and tails should be between the two extremes.

A run is defined as an uninterrupted sequence of similar observations, succeeded and preceded by a different observation (Levin and Rubin, 1980). In order to conduct a runs test, each variable must be reduced to dichotomous observations (e.g., + and -, A and B, etc.). According to Davis (1986), runs tests are particularly applicable to many types of geologic data. For example, the unit thickness of repetitive lithologies can be compared throughout a stratigraphic section (Figure 3.7).

Cycles 1, 2, and 3 represent a run because the thickness of each cycle increases upward. On the other hand, decreasing unit thickness occurs from cycle 3 to 6 resulting in a downward run. Eventually, by observing each successive run, thickness data are reduced to a string of + (upward increasing thickness) and - (upward decreasing thickness)

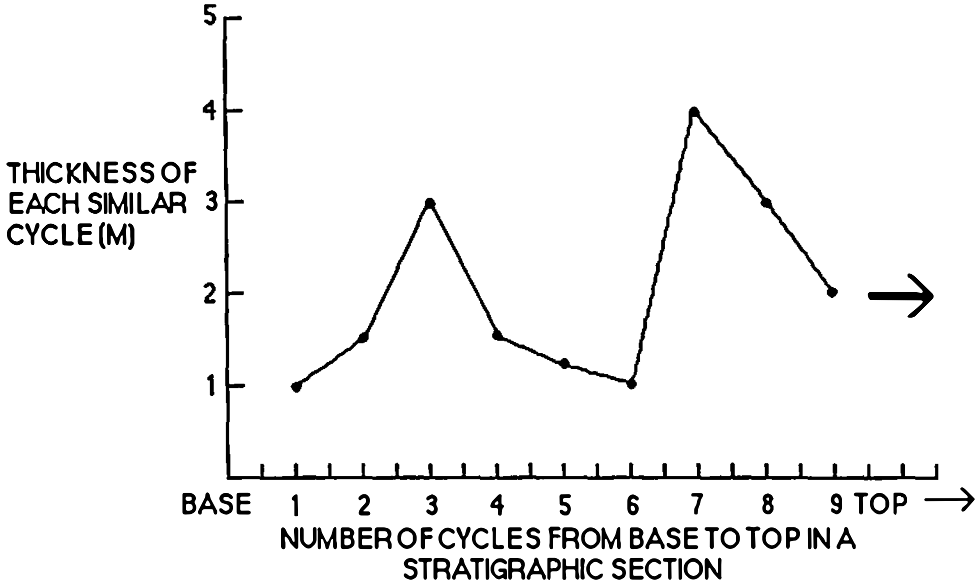

Figure 3.7. A plot showing the thickness of each similar cycle versus the number of cycles in a stratigraphic section.

signs. If a large data set exists, strings of + and - signs can be statistically tested (see Davis, 1986). It is important to note that runs tests cannot prove randomness, but are used to suggest that, at some level of confidence, a sequence is not random.

Integration of Techniques

Past studies have focused almost exclusively on Markov chain analysis to validate statistically the presence of cyclicity in stratigraphic sequences. As noted, many of the Markov chain analyses employed in earlier studies were flawed. These flaws are avoided by implementation of the log-linear Markov model. However, for Markov chain analyses to be valid, sample sizes must be sufficiently large to guarantee similarity between the sampling chi-square distribution (observed chi-square statistic) and the theoretical chi-square distribution (expected chi-square value). When expected frequencies are too small, the observed chi-square statistic will be overestimated. To avoid incorrect inferences from chi-square hypothesis tests, a general rule should be followed: no cell may have an expected frequency less than 1, and no more than 20% of the cells may have expected values less than 5 (Brown, 1985). According to Brown (1985), if this rule is not satisfied, the distribution of the chi-square statistic may differ widely from the theoretical chi-square distribution.

Although the log-linear Markov chain model is objective in nature and statistically valid, cyclic patterns are most apparent when lithologies are grouped into relatively few categories. Many stratigraphic sequences reveal 20 or more distinct lithologies (this is especially true for carbonate sequences). To satisfy the general rule of chi-square hypothesis testing, large numbers of lithologies must be reduced. Reduction often involves considerable subjectivity. The log-linear Markov technique is sensitive to minor changes in the structure of the original matrix. During this reduction process, variations in the procedure for grouping lithologies can cause significant changes to the nature of the Markov chain (Weber and others, 1986b). Thus, the presence or absence of cycles is dependent on the subjective criteria that are used to reduce the number of lithologies.

Substitutability analysis represents an objective approach to reduce the number of original lithologies systematically. Overlying substitutability (rather than mutual or underlying substitutability) is most sensible geologically for we are primarily interested in the temporal development of sequences. It is important to note that the reduction process by either subjective or objective means may over generalize stratigraphy to such an extent as to lead to geologically meaningless, though statistically valid, results.

Initially, overlying substitutability analysis is applied to a succession of lithologies (see Figure 3.8 for procedure). Next, embedded Markov chain analysis is conducted. If serial repetition of lithologies is revealed by Markov chain analysis, auto-association is carried out. Auto-association is used to locate cycles in the stratigraphic section. In addition, partial cycles (component cycles)

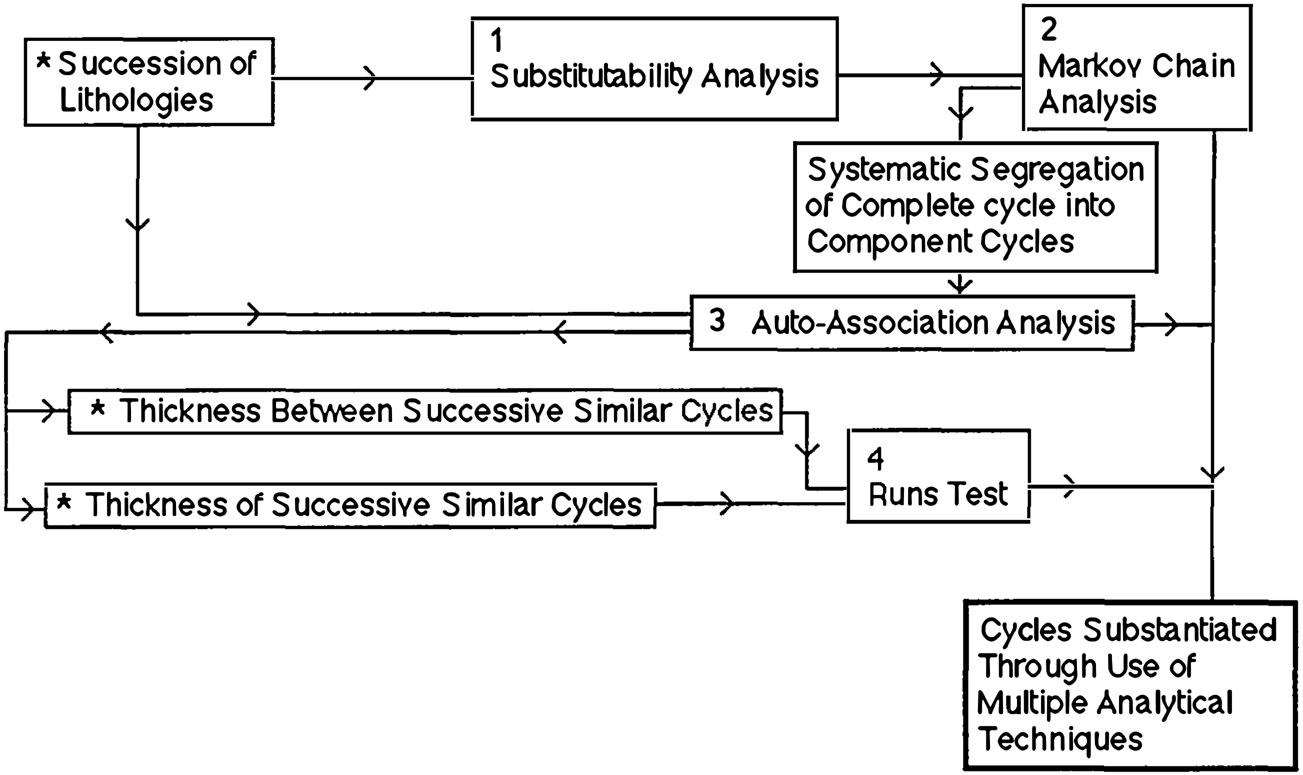

Figure 3.8. Flow diagram summarizing the procedure to test for presence of cycles. Numbers indicate order in which techniques are applied. Asterisk indicates initial data base.

can be identified within the sequence by applying auto-association to segregated parts of the complete cycle. For example, if A-B-C-D represents a complete cycle, partial cycles include: A-B, B-C, C-D, A-B-C, and B-C-D.

If the thickness of each lithologic unit is known, the thickness of each cycle (complete or partial) as well as the thickness between successive, similar cycles can be determined. An increase up section in the thickness of a particular cycle would suggest nonrandom process(es). Runs tests are used to determine the nonrandomness of cycles. The nonrandomness is expressed by the presence of too few or too many runs. Actual trends are determined by inspection.

Summary and Conclusions

Lithologic data (rock types) are classified into mutually exclusive categories of equal rank. As a result, many powerful mathematical techniques cannot be employed to detect stratigraphic cyclicity. Less powerful, but more statistically valid, techniques can be used in order to solve this problem. Substitutability analysis, embedded Markov chain analysis, auto-association analysis, and runs test are proposed to verify statistically the occurrence of cycles. Initially, overlying substitutability analysis is applied to a succession of lithologies. This technique reduces the number of original lithologies systematically. Next, embedded Markov chain analysis is conducted. Markov chain analysis is firmly established as a means to validate cyclicity within stratigraphic sequences. Although many older versions are flawed, the log-linear Markov model is objective in nature and statistically valid. If serial repetition of lithologies is revealed by Markov chain analysis, auto-association analysis is then carried out. Auto-association is used to locate cycles in the stratigraphic section. Finally, runs tests are applied to the thickness of each similar cycle (as well as between successive similar cycles) to determine the nonrandomness of the system.

An integrated approach of substitutability analysis, embedded Markov chain analysis, auto-association analysis, and runs tests has been applied to lithologic data (Weber and others, 1986a and see Chapter 4). This integration of analyses provides an independent test of cyclic trends and gives increased resolution to cycles in stratigraphic sequences. These methods eliminate the several sources of error in previously proposed techniques for recognizing cyclicity.

CHAPTER 4

CYCLICITY IN THE UPPER CAMBRIAN OF THE SOUTHERN APPALACHIANS: A TEST OF OBJECTIVE STATISTICAL TECHNIQUES

Introduction

It has been suggested that stratigraphic cyclicity is so widespread in the geologic record it may be considered a normal process (Wilson, 1975; Read and others, 1986). This theme is encountered often in the literature (Wanless and Weller, 1932; Rona, 1973; Dean and others, 1977; Hallam, 1977; Vail and others, 1977; Aitken, 1978; Crowell, 1978; Donovan and Jones, 1979; Saunders and others, 1979; Heckel, 1980; Clifton, 1981; Busch and Rollins, 1984; Driese and Dott, 1984; James, 1984; Heckel, 1986; Mack and James, 1986; Laferriere and others, 1987; Busch and West, 1987; etc.). Clearly, the importance of cyclicity cannot be underestimated. Through the identification of cycles, abundant and complex data are simplified into abbreviated trends. Not only can stratigraphic descriptions be reduced, but also cyclic patterns can be investigated further. For example, paleoenvironmental information is much more easily ascertained from a repetitive sequence than from some seemingly random arrangement of lithologies. Recently, the study of cyclicity has aroused a new wave of interest, and cycle models are being proposed from the repetitive nature of individual cycles (Read and others, 1986; Mack and James, 1986; Busch and West, 1987). Because such a premium is placed on the occurrence of cyclicity, care must be taken when identifying cyclic phenomena.

As indicated in the previous chapter, a preferred definition of a sedimentary cycle is as follows: a series of observations (rock types, bed thickness measurements, geochemical data, etc.) that occur in a predictable pattern or follow a certain order (c.f., American Geological Institute, Glossary of Geology). This definition accounts for the variability or randomness which exists in natural geologic systems.

Various types of cycles have been described in the geologic literature (first, second, and third order depositional sequences, as defined by Vail and others, 1977; grand cycles, following Aitken, 1978; cyclothems, after Wanless and Weller, 1932 and Moore, 1936). These cycles as well as numerous others can be placed into a hierarchy of genetic transgressive-regressive (i.e., deepening-shallowing relative to sea level) units (Busch, 1983; Busch and Rollins, 1984; Busch and West, 1987). The focus of this study is cyclothems (subsequently referred to as small scale cycles) which are simply cycles or rhythms of lithofacies. Busch and others (1985) have noted that cyclothemic patterns change laterally within the same genetic-stratigraphic unit (transgressive-regressive cycle) and thus are not laterally persistent among widely spaced localities. It is important to note that the lateral correlation or traceability of individual cyclothems over wide geographic areas is not of concern here; instead, the vertical and lateral extent of stratigraphic intervals containing identical, statistically valid cycles are of primary importance (that is "packages" of cyclothems are examined here).

The objectives of this Chapter are: (1) to examine the Late Cambrian Nolichucky Shale and Maynardville Limestone in east Tennessee for small scale cycles using a new approach (substitutability, embedded Markov chain, and modified autoassociation analyses) defined in the previous chapter, (2) to determine the significance of these cycles, if present and (3) to consider the implications of the techniques and examples given here for recognition of larger scale cyclicity in the geologic record.

Geologic Setting

Location/Stratigraphy

In eastern North America, Middle and Late Cambrian strata occur from Newfoundland to Alabama. These siliciclastic and carbonate rocks were deposited during the first major episode of Phanerozoic cratonic flooding along the North American continental margin. Coeval rocks of a similar depositional style occur in the western United States, Siberia, Australia, Asia, and elsewhere (Scotese and others, 1979).

Within the Valley and Ridge of east Tennessee, Middle and Upper Cambrian rocks crop out along a succession of southeastward dipping imbricate thrust sheets, which trend northeast to southwest (Figure 1.10). In the vicinity of Knoxville, formations of this age (excluding the Copper Ridge Dolostone) comprise the Conasauga Group

(Figure 1.11). From base to top the Conasauga Group includes: the Pumpkin Valley Shale, Rutledge Limestone, Rogersville Shale, Maryville Limestone, Nolichucky Shale, and Maynardville Limestone (Rodgers, 1953). In this study only the Upper Cambrian Nolichucky Shale and Maynardville Limestone are examined. The entire Group grades from dominantly dolostone in the east (northeastern Tennessee and southwestern Virginia), through intercalated carbonate and shale units in the Knoxville area to a sequence dominated by shale, west and southwest of Knoxville (see Figure 1.11). The Conasauga Group is underlain by the Lower Cambrian, predominantly siliciclastic Rome Formation largely of peritidal to marine shelf origin. Above the Conasauga Group are very shallow subtidal and peritidal carbonates of the Upper Cambrian Copper Ridge Dolostone, the lowermost formation of the Cambro-Ordovician Knox Group.

Eight stratigraphic intervals from five closely spaced localities have been examined for cyclicity (measured sections A-F excluding B of Figure 1.10). Five intervals were in the Nolichucky Shale, and three intervals were in the overlying Maynardville Limestone.

Lithology

Detailed stratigraphic analysis on a bed-by-bed scale within the Nolichucky Shale and Maynardville Limestone reveals a diverse assemblage of lithologies. However, only a small number of lithologies actually dominates this interval. Several rock types occur less frequently. These "rare" lithologies can be recategorized into geologically similar, but more commonly occurring lithologies. Reduction in the original number of lithologies is accomplished by substitutability analysis. Each of the eight continuous stratigraphic sequences (five within the Nolichucky and three in the Maynardville) was tested independently by substitutability analysis. As a result of this analysis, fourteen recurring lithologies are distinguished from this stratigraphic interval (Figure 4.1). The lithologic assemblage within the Nolichucky Shale differs significantly from that within the Maynardville Limestone (Figures 4.2 and 4.3). As a result, each formation was examined for cyclicity independently. This test procedure is necessary because lithologic homogeneity occurs only within each formation.

Little variation in the percent occurrence of any particular lithology exists from one locality to another (Figures 4.4 and 4.5). For example, in Figure 4.4 shale varies from 32% to 37%. Note that other lithologies vary to a greater extent, but considering that the geographic separation between any two localities ranges from 3 km to 60 km, these differences are minimal.

Within the Nolichucky Shale, ten commonly occurring lithologies are important (Figure 4.4). At any one locality from 7 to 9 lithologies may be present. Lithologies which are absent at one or more localities (e.g., FPG, FPGWS, EPG, SWXPG; refer to Figure 4.2 for meaning of lithologic abbreviations), generally are not major constituents at localities where they do occur. On the other hand, several lithologies occur at every locality (IPG, MWS, OPG, XPG, XPGWS, S; see Figure 4.2). Typically, these most frequently observed lithologies exhibit uniformity

Figure 4.1. Fourteen recurring lithologies within the upper Conasauga Group.

A=FPG, fossiliferous packstone/grainstone;
B=FPGWS, fossiliferous packstone/grainstone interbedded with shale;
C=MWS, mudstone interbedded with shale;
D=OPG, oolitic packstone/grainstone;
E=XPG, laminated peloidal packstone/grainstone;
F=XPGWS, laminated peloidal packstone/grainstone interbedded with shale;
G=EPG, peloidal packstone/grainstone;
H=IPG, intraclastic packstone/grainstone;
I=S, shale;
J=SWXPG, shale interbedded with laminated peloidal packstone/grainstone;
K=CL, cryptalgalaminate;
L=STROM, stromatolitic limestone;
M=THROM, thrombolitic limestone;
N=NOPG, oncolitic-oolitic packstone/grainstone

Scale bar=3 centimeters.

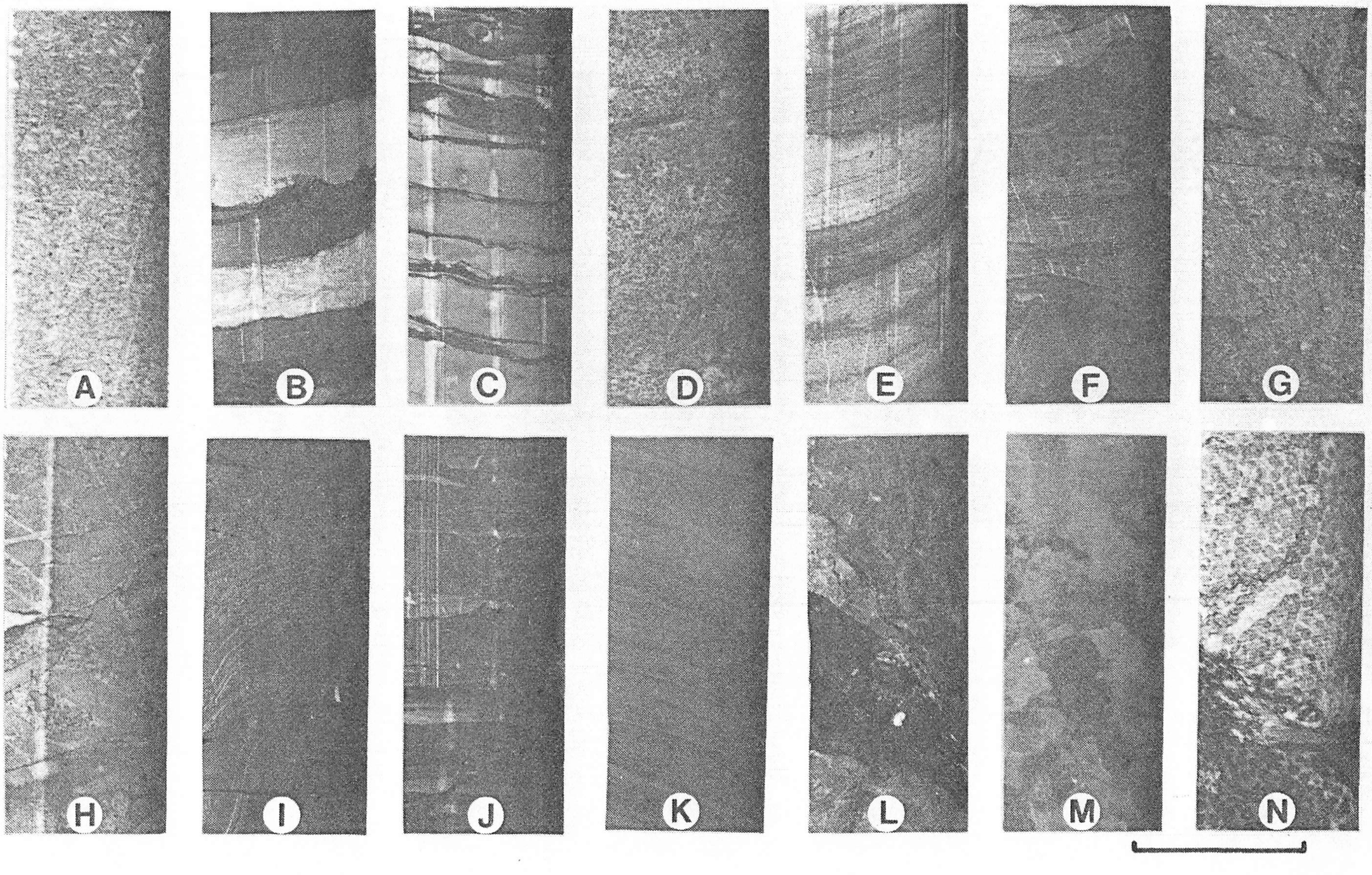
A
B
C
D
E
F
G
H
I
J
K
L
M
N

LITHOLOGY	CHARACTERISTICS	INTERPRETATION
FPG=Fossiliferous Pkst/Grnst Figure 4.6. A.	Thin- to medium-bedded (5-30 cm); glauconitic; locally graded; trilobites and echinoderms; rippled and megarippled tops; abundant intraclasts and hardgrounds	Subtidal; open marine subwave-base; storm sand sheets; high-energy
FPGWS=Fossiliferous Pkst/Grnst interbedded w/ Shale Figure 4.6. B.	Very thin- to thin-bedded (1-5 cm) limestone; separated by shale partings and thin interlayers, dolomite seams, and hardgrounds; trilobites and echinoderms; basal lags; fining-upward	Subtidal; open marine subwave-base; hemipelagic deposition; low-energy
MWS=Mudstone interbedded with Shale Figure 4.6. C.	Very thin- to thin-bedded (1-5 cm) limestone; shale interlayers (commonly dolomitized); contacts sharp; faintly laminated; vertical and horizontal burrows; stylolites common; rare echinoderms and trilobites	Subtidal; open marine subwave-base; hemipelagic deposition; low-energy
OPG=Oolitic Pkst/Grnst Figure 4.6. D.	Thin- to thick-bedded (5-50 cm); generally spherical particles; abundant fossils (echinoderms and trilobites); megarippled upper surfaces; discontinuous hardgrounds and shale drapes; sharp basal contacts	Subtidal; open marine subwave-base; storm reworked oolitic sand sheets; low/high-energy
XPG=Laminated peloidal Pkst/Grnst Figure 4.6. E.	Thin- to medium-bedded (5-30 cm); faint planar- and low-angle cross-laminations; bedding-plane traces; tool marks and groove casts; gutter casts	Subtidal; open marine subwave-base; storm reworked; high-energy
XPGWS=Laminated peloidal Pkst/Grnst interbedded with Shale Figure 4.6. F.	Very thin- to thin-bedded (1-5 cm) limestone; separated by shale interlayers; linsen-beds; microhummocky and planar laminations; burrows; fining-upward sequences; loading; microconvolutions; pseudonodules	Subtidal; suspension deposition and current reworking; low-energy
EPG=Peloidal Pkst/Grnst Figure 4.6. G.	Thin- to medium-bedded (5-30 cm); reworked and rounded pieces of consolidated calcareous mud; coincides with very small intraclasts; subrounded micritic particles; moderate-sorting; discontinuous hardgrounds	Subtidal; open marine subwave-base; storm reworked; high-energy
IPG=Intraclastic Pkst/Grnst Figure 4.6. H.	Thin- to thick-bedded (3-50 cm) reworking of other consolidated lithologies by bottom currents; internal structures absent; subparallel to random clast orientation; very poor sorting; clasts associated with fine- to coarse-grained matrix; clasts project above upper bedding surface; some clasts highly angular	Subtidal; open marine subwave-base; storm deposits; high-energy
S=Shale Figure 4.6. I.	Fine-grained silt and clay; megascopic fossils generally absent; lack sedimentary structures; color varies from dark gray-green to maroon	Subtidal; hemipelagic background deposition; low-energy
SWXPG=Shale interbedded w/ Laminated peloidal Pkst/Grnst Figure 4.6. J.	Predominantly shale with very thin- to thin-bedded (1-5 cm) laterally discontinuous peloid interlayers; Limestone: sharp, scoured bases and diffuse tops; loading; microconvolutions; pseudonodules	Subtidal; suspension deposition and current reworking; low-energy

Figure 4.2. Distinguishing features of the 10 most dominant lithologies recognized in the Nolichucky Shale.

LITHOLOGY	CHARACTERISTICS	INTERPRETATION
CL=Cryptalgal Laminites Figure 4.6. K.	Medium- to very thick-bedded (10 cm to > 1 m); irregular laminations; laminated dolostone; common mudcracks; microtepee structures; lacks fossils; frequent doming to low-relief LLH stromatolites	Lower to upper intertidal; perhaps supratidal
STROM=Stromatolites Figure 4.6. L.	Thick- to very thick-bedded (30 cm to > 1 m); laterally linked hemispheroids; laterally linked stacked hemispheroids less common; mottling; fenestral fabric	Lower intertidal; low-energy tidal flat
THROM=Thrombolites Figure 4.6. M.	Thick- to very thick-bedded (30 cm to > 1 m); unlaminated stromatolites with clotted or digitate fabric; Renalcis common; burrowed; flanked by fossiliferous, oolitic, and oncolitic pkst/grnst	Very shallow subtidal; above normal wave-base
NOPG=Oncolitic-oolitic Pkst/Grnst Figure 4.6. N.	Thick- to very thick-bedded (30 cm to > 1 m); ooids and oncoids commonly exceed 2 mm in diameter; occasional rippled surfaces	Very shallow subtidal; above normal wave-base; moderate-energy
XPGWS=Laminated peloidal Pkst/Grnst interbedded with Shale Figure 4.6. F.	Very thin- to thin-bedded (1-10 cm) limestone; separated by discontinuous shale drapes; scoured bases and tops; rare burrows; low-angle cross laminations	Subtidal; suspension deposition and current reworking; low-energy
EPG=Peloidal Pkst/Grnst Figure 4.6. G.	Thick- to very thick-bedded (30 cm to > 1 m); reworked cryptalgal laminite and mudstone peloids; intraclasts common; cross-stratified	Very shallow subtidal; above wave-base; moderate- to high-energy
IPG=Intraclastic Pkst/Grnst Figure 4.6. H.	Medium-bedded (10-30 cm); generally parallel clast orientation; coarse-grained matrix; little or no mudstone or shale in matrix	Subtidal; probably above normal wave-base; storm reworked; high-energy
S=Shale	Minor constituent	
SWXPG=Shale interbedded w/ Laminated peloidal Pkst/Grnst	Minor constituent	

Figure 4.3. Distinguishing features of the 9 most dominant lithologies recognized in the Maynardville Limestone.

Figure 4.4. Bar graph showing the distribution of the ten most common lithologies in the Nolichucky Shale at five different localities. Percent occurrence is standarized for each locality and is based on the number of transitions for any particular lithology divided by the total number of transitions at that locality. Each value is then normalized to 100%. For example, at the Joy #2 locality, OPG occurs 188 times out of 628 total transitions, thus 188/628 (100)=29.94%. The total number of lithologic transitions is much less for I-75 and BG. These sections only represent the upper ~90 meters of Nolichucky Shale. The lower portion is not exposed at these localities. These ten lithologies are the most common lithologies in the Nolichucky Shale (initially a number of other subordinant lithologies occurred, but during substitutability analysis less common lithologies were recategorized into geologically similar lithologies). At any one locality fewer than ten lithologies are observed. For example, at I-75 EPG and SWXPG are not observed. The absence of lithologies can be explained in one of two ways: (1) missing lithologies did not occur in the initial data base (marked by "Not Present") or (2) missing lithologies were present initially, but during substitutability analysis they were recategorized into a geologically similar lithology (e.g., at I-75 SWXPG substituted into S; it is marked by "Subst. to S").

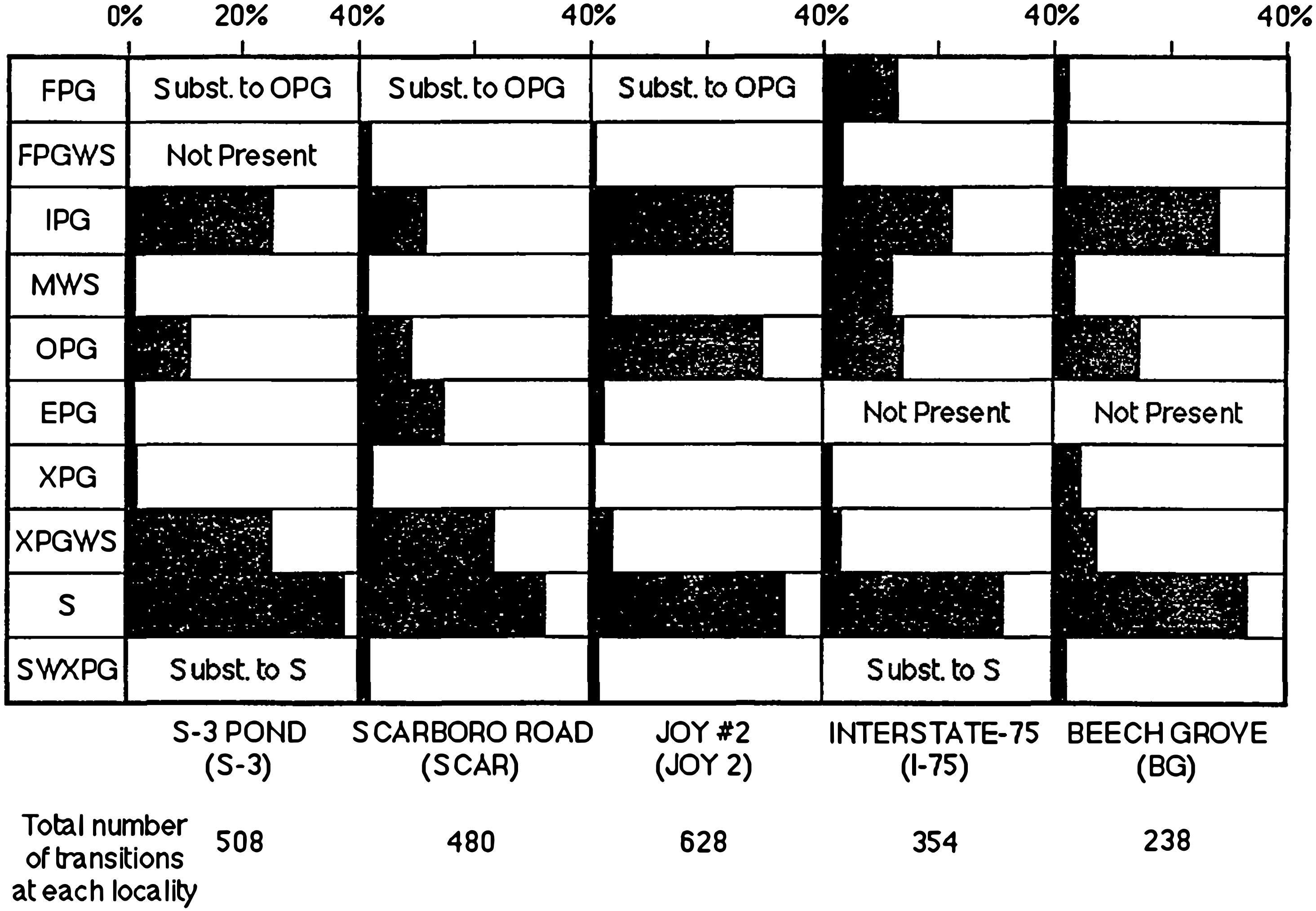

Figure 4.4 (continued)

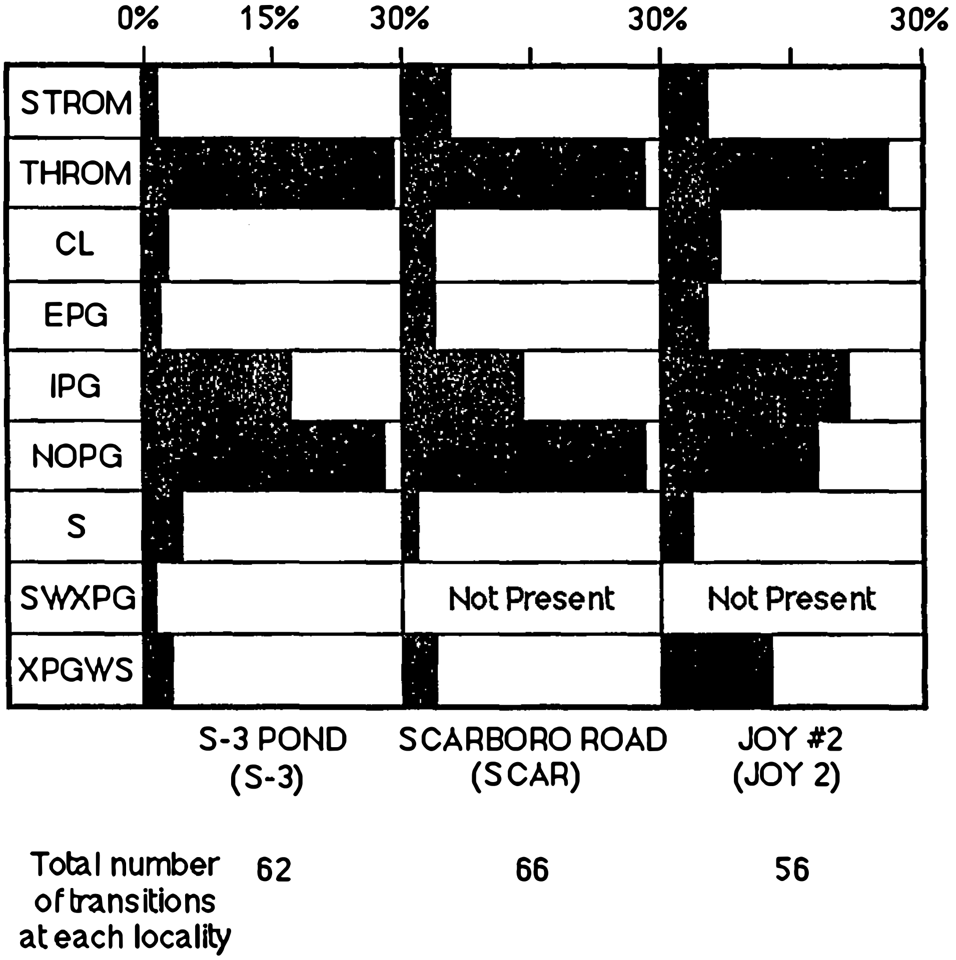

Figure 4.5. Bar graph showing the distribution of the nine most common lithologies in the Maynardville Formation at three different localities. Percent occurrence calculated as for Figure 4.4. Notice that the total number of lithologic transitions at each locality is small relative to those observed in Figure 4.4. Fewer transitions result because lithologies are much thicker. Prior to conducting embedded Markov chain analysis, transition frequency matrices for each locality were combined to increase the data base. This procedure reduced the number of sampling zeros within the matrix, making the Markov chain more statistically valid.

in percent occurrence from place to place. Lithologies within the Maynardville show a similar pattern (Figure 4.5). Lithologic assemblages within the Nolichucky Shale and Maynardville Limestone display little temporal or spatial variability. This suggests that the depositional regime during sedimentation of each of the formations was relatively constant. Thus, within the geographic area under investigation, significant environmental gradients were not present. However, it is important to note that a major lithologic change does take place across the Nolichucky-Maynardville boundary, which has led me to treat the two formations separately.

Depositional Environment

Prior to 1970, geologic investigations of the Nolichucky Shale and Maynardville Limestone in Tennessee and Virginia stressed generalized lithologic descriptions and paleontologic data (i.e., Hall and Amick, 1934; Butts, 1940; Rodgers and Kent, 1948; Raymond, 1959; Havryluk, 1963; and Derby, 1965). In recent years, several workers have inferred depositional models for upper Conasauga strata in the area (See Milici and others, 1973; Markello, 1979; and Markello and Read, 1981 and 1982). Milici and others (1973) conducted an examination of the Nolichucky Shale and Maynardville Formation exposed along U.S. Interstate 75 (locality B of this study) on Copper Ridge. They discerned several lithofacies: (1) stromatolitic bioherms, (2) thin, irregularly bedded algal limestones, (3) cobbly weathering limestones, (4) banded argillaceous limestones, (5) oolitic calcarenites, (6) intraclastic and oolitic washover beds, and (7) subaerially exposed limestones and dolostones. In general, strata from this locality were interpreted as "lagoonal" sediments, protected from oceanic currents and waves, bounded to the east by an extensive carbonate bank and to the west by siliciclastics.

Markello and Read (1981 and 1982) studied both the Nolichucky Shale and the Maynardville Limestone in Virginia. They defined three major depositional environments: an intrashelf basin (Nolichucky Shale), a carbonate ramp with subtle westward slopes (Maynardville Limestone), and a coeval peritidal carbonate platform to the east (Elbrook and/or Honaker Formations). Deposition in the intrashelf basin, as described by Markello and Read (1981), resulted in a complex interbedded assemblage of storm-generated calcareous shale, laminated calcareous siltstone, intraformational flat-pebble conglomerate, bioclastic limestone, and oolitic limestone. The carbonate ramp was characterized by below wave-base accumulations of fossil-rich "ribbon" carbonates, thin intraclastic limestone, and oolitic shoals.

In the vicinity of Knoxville, the Nolichucky Shale is characterized by dark gray-green to maroon shale, which is interbedded with carbonate mudstone, packstone, and grainstone (see Figure 4.2). Based upon environmentally sensitive criteria, this unit was deposited under storm-dominated subtidal marine conditions (Figures 4.2 and 4.6). Conversely, the Maynardville Limestone was deposited in very shallow subtidal, intertidal, and perhaps supratidal settings (Figure 4.6) and

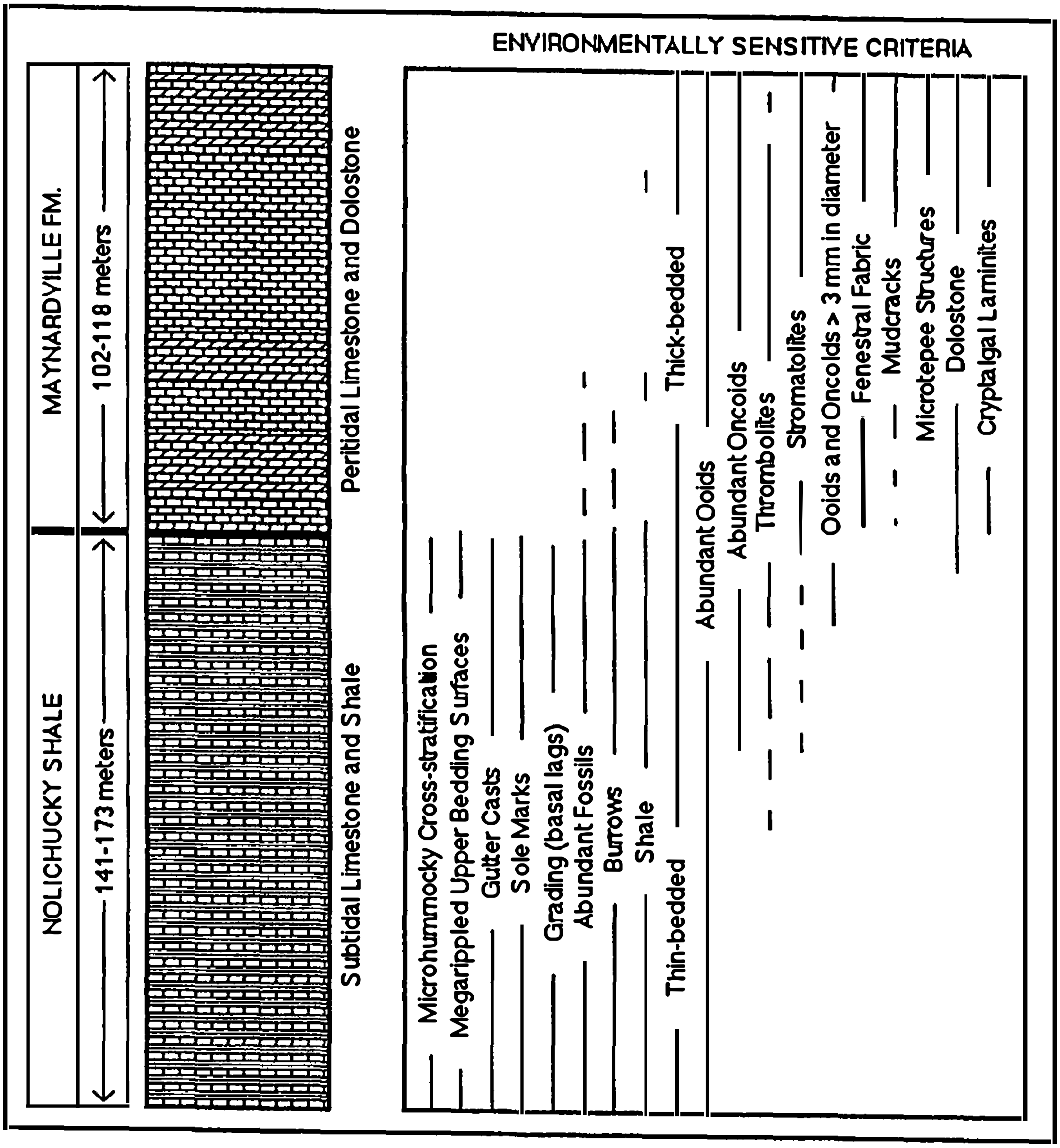

Figure 4.6. Generalized stratigraphic section of the Nolichucky Shale and Maynardville Limestone showing overall lithologic character and stratigraphic distribution of environmentally sensitive criteria.

is composed predominantly of algal (stromatolites, thrombolites, and cryptalgalaminates) and oncolitic/oolitic lithologies (see Figure 4.3).

Procedure

Overlying substitutability analysis, embedded Markov chain analysis, and modified autoassociation analysis were applied to the Nolichucky/Maynardville sequence in central east Tennessee. This quantitative approach takes place on three levels: (1) initial classification of lithologies, (2) categorizing lithologies, and (3) testing categorized lithologic data for cycles. The procedure for assessing stratigraphic cyclicity is described below using the Interstate-75 section (an identical procedure has been followed when testing other localities) because the most complex cyclic pattern emerges from analysis of this locality.

Classification of Lithologies

Lithologies must be defined in a rigorous and consistent fashion so that rock types remain mutually exclusive. Established rock classification schemes (e.g., Dunham, 1962) should be used. Inconsistent classification of rock units biases analysis of sequential data. The following must be avoided: (1) nonsystematic classification of dissimilar lithologies into one rock type, (2) indiscriminant assignment of a single lithology into several categories, and (3) generalization of a heterogeneous rock unit into a single lithology (i.e., fossiliferous packstone with mudstone lenses should be considered distinct from and thus independent of fossiliferous packstone with oolitic grainstone lenses).

During field examination every practical precaution was taken to objectively measure and consistently define each lithology. Each change in lithology as well as the thickness of each lithology was recorded in ascending stratigraphic order. At the I-75 locality, the upper 94 m of the Nolichucky Shale wwere examined; the lower 60 m were not exposed. Fifteen distinct lithologies were recognized (Figure 4.7). The stratigraphic position of each lithology was recorded into a transition frequency matrix (Figure 4.8). The transition from one lithology to an overlying, identical lithology was not permitted.

Categorizing Lithologies

Many stratigraphic sequences reveal numerous distinct lithologies. A large number of original lithologies must be reduced for two reasons: (1) cyclic patterns are most apparent when lithologies are grouped into relatively few categories, and (2) large matrices tend to invalidate Markov chain analysis (for discussion, see Weber and others, 1986). A standard method for reducing the number of lithologies is by subjectively combining them based on experience; however, the embedded Markov chain technique used here is sensitive to minor changes in the structure of the transition frequency matrix, and variation or inconsistency in the procedure for grouping lithologies can cause significant changes in the nature of the Markov chain. For this reason, an objective,

SYMBOL	NUMBER OF OCCURRENCES	LITHOLOGIES
A	2	THROM=Thrombolite
B	26	MWS=Mudstone interbedded with Shale
C	34	FPG=Fossiliferous Packstone/Grainstone
D	9	FPGWS=Fossiliferous Packstone/Grainstone interbedded with Shale
E	77	IPG=Intraclastic Packstone/Grainstone
F	8	M=Mudstone
G	4	XFPG=Laminated Peloidal Packstone/Grainstone interlayered with Fossiliferous Packstone/Grainstone lenses
H	14	MXPGWS=Mudstone with laminated Peloidal Packstone/Grainstone lenses interbedded with Shale
I	36	OPG=Oolitic Packstone/Grainstone
J	103	S=Shale
K	11	SWXPG=Shale interbedded with laminated Peloidal Packstone/Grainstone
L	12	UPG=Glauconitic Packstone/Grainstone with abundant Ooids and Fossils
M	5	XPG=Laminated Peloidal Packstone/Grainstone
N	17	FXPG=Fossiliferous Packstone/Grainstone interlayered with laminated Peloidal Packstone/Grainstone lenses
O	6	XPGWS=Laminated Peloidal Packstone/Grainstone interbedded with Shale

Figure 4.7. Lithologies observed at I-75 before grouping similar lithologies by use of substitutability analysis. Carbonate lithologies (except thrombolite) are after Dunham (1962) classification. Field classification of thrombolites follows Kennard and James (1987). Shale refers to fine-grained siliciclastic material predominantly of clay- and silt-sized particles.

Figure 4.8. A 15 X 15 transition frequency matrix which represents the upper 94 meters of the Late Cambrian Nolichucky Shale located along Interstate 75. This matrix exhibits 225 individual cells. Darkened cells along the main diagonal indicate structural zeros (identical lithologies cannot overlie one another). See Figure 4.7 for geologic meaning of abbreviated lithologic symbols. Asterisks (*) point out four column totals which do not sum to corresponding row totals. This row-column discrepancy exists because: (1) the lowermost lithology in the sequence differs from the uppermost lithology and (2) identical lithologies do not occur directly below and above a thin covered interval (see discussion of Driese and Dott, 1986). The covered or missing interval is 75 centimeters thick and occurs midway up the sequence.

OVERLYING LITHOLOGIES

UNDERLYING LITHOLOGIES

	A	B	C	D	E	F	G	H	I	J	K	L	M	N	O	row totals
A	■	0	0	0	0	0	0	0	0	1	0	0	0	1	0	2
B	0	■	0	0	26	0	0	0	0	0	0	0	0	0	0	26
C	0	0	■	2	1	1	0	0	2	21	3	2	0	1	1	34
D	0	0	1	■	3	0	0	0	0	4	1	0	0	1	0	10*
E	1	0	11	3	■	0	2	1	11	29	2	2	4	7	3	76*
F	0	0	2	1	0	■	0	2	1	1	0	1	0	0	0	8
G	0	0	1	0	2	0	■	1	0	0	0	0	0	0	0	4
H	0	1	1	0	1	2	0	■	1	7	0	0	0	1	0	14
I	0	0	0	2	0	0	1	1	■	27	4	1	0	0	0	36
J	1	21	13	1	26	3	1	9	18	■	1	4	1	4	0	103
K	0	2	1	0	0	2	0	0	1	1	■	2	0	2	0	11
L	0	0	3	0	1	0	0	0	0	7	0	■	0	0	0	11*
M	0	0	0	0	2	0	0	0	0	1	0	0	■	0	2	5
N	0	2	0	0	10	0	0	0	2	4	0	0	0	■	0	18*
O	0	0	1	0	5	0	0	0	0	0	0	0	0	0	■	6
column totals	2	26	34	9 *	77 *	8	4	14	36	103	11	12 *	5	17 *	6	364 total number of transitions

Figure 4.8 (continued)

iterative approach has been chosen to reduce the matrix size (number of lithologies) incrementally one lithology at a time. Overlying substitutability analysis is a classification procedure that uses computer clustering techniques to group lithologies on the basis of their context in a stratigraphic sequence. Two or more lithologies which exhibit high conditional probabilities of being underlain by similar lithologic assemblages are considered equivalent. More simply, if two different lithologies are commonly underlain by a third lithology, the two overlying lithologies exhibit high overlying substitutability. The two overlying lithologies are combined, thus reducing the total number of lithologies by one.

Substitutability analysis was applied to the I-75 data, and the results are given in Figures 4.9, 4.10, and 4.11. A transition frequency matrix (Figure 4.8) is used to generate a downward transition probability matrix (Figure 4.9). The downward probability matrix indicates the relative frequency with which one lithology is preceded by another lithology. Next, an overlying substitutability matrix (Figure 4.10) is computed from the probability matrix. Lithologic similarity is based on the tendency for lithologies to be preceded (underlain) by the same lithologies. A simple procedure is presented in Davis (1986) for constructing such matrices. The substitutability matrix (Figure 4.10) contains cells with values ranging from 0 to 1, and is symmetrical about the main diagonal. Because this matrix is symmetrical, conventional clustering methods can be used to hierarchically classify lithologies exhibiting high substitutability. Although

	A	B	C	D	E	F	G	H	I	J	K	L	M	N	O
A	0	.000	.000	.000	.000	.000	.000	.000	.000	.010	.000	.000	.000	.059	.000
B	.000	0	.000	.000	.338	.000	.000	.000	.000	.000	.000	.000	.000	.000	.000
C	.000	.000	0	.222	.013	.125	.000	.000	.056	.204	.273	.167	.000	.059	.167
D	.000	.000	.029	0	.039	.000	.000	.000	.000	.039	.091	.000	.000	.059	.000
E	.500	.000	.324	.333	0	.000	.500	.071	.306	.282	.182	.167	.800	.412	.500
F	.000	.000	.059	.111	.000	0	.000	.143	.028	.010	.000	.083	.000	.000	.000
G	.000	.000	.029	.000	.026	.000	0	.071	.000	.000	.000	.000	.000	.000	.000
H	.000	.038	.029	.000	.013	.250	.000	0	.028	.068	.000	.000	.000	.059	.000
I	.000	.000	.000	.222	.000	.000	.250	.071	0	.262	.364	.083	.000	.000	.000
J	.500	.808	.382	.111	.338	.375	.250	.643	.500	0	.091	.333	.200	.235	.000
K	.000	.077	.029	.000	.000	.250	.000	.000	.028	.010	0	.167	.000	.118	.000
L	.000	.000	.088	.000	.013	.000	.000	.000	.000	.068	.000	0	.000	.000	.000
M	.000	.000	.000	.000	.026	.000	.000	.000	.000	.010	.000	.000	0	.000	.333
N	.000	.077	.000	.000	.130	.000	.000	.000	.056	.039	.000	.000	.000	0	.000
O	.000	.000	.029	.000	.065	.000	.000	.000	.000	.000	.000	.000	.000	.000	0

Figure 4.9. Downward transition probability matrix. This matrix is computed by dividing each cell of the transition frequency (Figure 4.8) by its corresponding column total. For geologic meaning of character symbols see Figure 4.7.

	A	B	C	D	E	F	G	H	I	J	K	L	M	N	O
A	1	.700	.967	.649	.475	.500	.866	.754	.960	.443	.381	.775	.858	.910	.567
B	.700	1	.741	.227	.691	.766	.404	.950	.850	.017	.178	.757	.240	.490	.000
C	.967	.741	1	.628	.518	.558	.815	.807	.958	.436	.369	.811	.789	.887	.504
D	.649	.227	.628	1	.166	.270	.843	.391	.602	.912	.824	.712	.723	.725	.675
E	.475	.691	.518	.166	1	.493	.274	.655	.594	.050	.149	.500	.163	.329	.035
F	.500	.766	.558	.270	.493	1	.289	.679	.662	.100	.254	.775	.172	.524	.063
G	.866	.404	.815	.843	.274	.289	1	.522	.278	.749	.660	.671	.891	.860	.655
H	.754	.950	.807	.391	.655	.679	.522	1	.873	.133	.287	.797	.336	.535	.085
I	.960	.850	.958	.602	.594	.662	.278	.873	1	.383	.387	.864	.705	.844	.439
J	.443	.017	.436	.912	.050	.100	.749	.133	.383	1	.903	.513	.608	.602	.636
K	.381	.178	.369	.824	.149	.254	.660	.287	.387	.903	1	.590	.392	.463	.432
L	.775	.757	.811	.712	.500	.775	.671	.797	.864	.513	.590	1	.532	.770	.391
M	.858	.240	.789	.723	.163	.172	.891	.336	.705	.608	.392	.532	1	.908	.778
N	.910	.490	.887	.725	.329	.524	.860	.535	.844	.602	.463	.770	.908	1	.689
O	.567	.000	.504	.675	.035	.063	.655	.085	.439	.636	.432	.391	.778	.689	1

Note: This matrix is computed from the downward probability matrix using the following equation:

$$OS_{ab} = \frac{\sum_{i=1}^{m} P_{ai}\, P_{bi}}{\sqrt{\sum_{i=1}^{m} P_{ai}^{2} \sum_{i=1}^{m} P_{bi}^{2}}}$$

where,

OS_{ab} = overlying substitutability of states a and b,
P_{ai} = transition probability to the ith state, given state a,
P_{bi} = transition probability to the ith state, given state b,
m = number of states in the system.
For geologic meaning of character symbols, see Figure 4.7.

Figure 4.10. Overlying substitutability matrix.

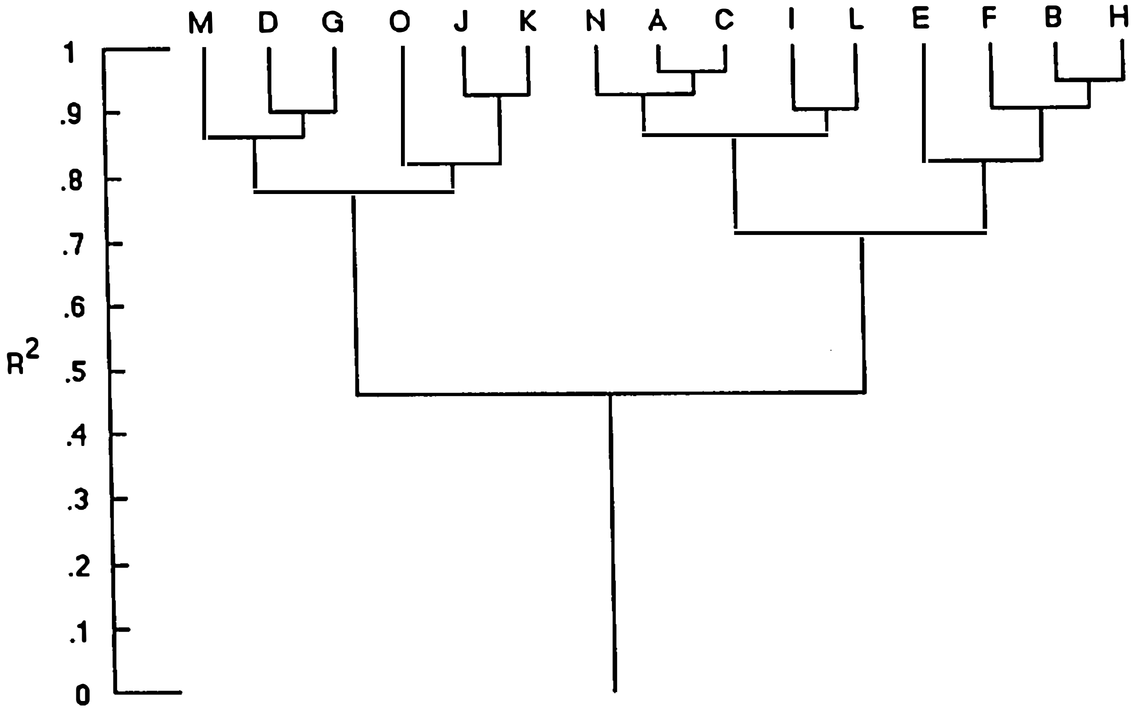

Figure 4.11. Overlying substitutability dendogram (for geologic meaning of character symbols see Figure 4.7); R^2=the squared multiple correlation, which is the sum of squares between all clusters divided by the corrected total sum of squares. Lithologies correlated at a high value of R^2 are more likely to substitute for each other in the sequence and can therefore be combined into a single category. These pairings are combined successively until the resultant matrix reaches a more manageable size.

substitutability analysis does not invoke a formal statistical testing procedure, the computer produced dendograms retain all information of transition frequency matrices (Doveton and Skipper, 1974).

Hierarchical clustering of the overlying substitutability matrix reveals a dendogram (Figure 4.11). This graph is used to reduce incrementally the size of the transition frequency matrix. From Figure 4.11, it is observed that lithologies A and C are the first to cluster. This indicates high interchangeability within the stratigraphic sequence. Subsequently, both lithologies are combined into one composite lithology. As a result of this process, the transition frequency matrix is reduced from 15 to 14 lithologies. This procedure is continued.

Testing For Cyclicity

Two compatible techniques are employed for testing sequential lithologic data for cyclicity. Initially, first-order embedded Markov chain analysis is conducted. If serial repetition of lithologies is revealed by Markov chain analysis, modified autoassociation analysis is then carried out to locate cycles in the stratigraphic section.

Although embedded Markov chain analysis is useful, it does have some limitations which have not always been appreciated by geologists. First-order embedded Markov chain analysis only indicates Markovian tendency between some lithology $\underline{t}$ and its immediate predecessor $\underline{t-1}$. Within a stratigraphic sequence the application of Markov chain analysis may reveal one or more statistically valid lithologic transitions. If, for example, two lithologic pairs occur and can be stacked, a longer term cycle will result (two lithologic transitions say t underlain by t-1 and t-1 underlain by t-2 are typically represented as t-2 overlain by t-1, which is overlain by t). This simplistic approach is usually followed. However, a problem occurs because according to first-order Markov chain theory, t-2 has no affect on the occurrence of t. Thus, the cycle t-2 to t-1 to t may not actually occur in the stratigraphic sequence. A procedure is needed to test stratigraphic columns to determine if longer order chains can be recognized. Markov chains classified by higher order and greater dependence could be used to examine longer term chains, but restructuring of first-order transition frequency matrices to higher order matrices is tedious especially if several stratigraphic sequences are examined. To circumvent the problem of recognizing higher order chains, I propose the use of modified autoassociation analysis as an empirical way of assessing cyclicity.

An iterative approach is used to analyze Upper Cambrian stratigraphic sections for cycles as the number of lithologies are reduced. Again, I-75 data are presented. After each one step (one lithology) reduction in the transition frequency matrix, embedded Markov chain analysis was conducted. Initially, as the size of the matrix decreases, the complexity of the Markov chain increases. This results because the first few clustered lithologic pairs are highly significant. Distortion increases as successive levels of clusters are averaged together. As a result, Markovian tendency diminishes rapidly, most trends break down in one or two iterations (Figure 4.12). The same general pattern is observed for each stratigraphic interval which was tested.

At I-75 the 8 X 8 (i.e., using 8 lithologies) transition frequency matrix (Figure 4.13) reveals the best developed Markov chain. Lithologic transitions which depart from randomness are selectively identified by the computer and are shown in Figure 4.14. Those transitions which occur more often than expected are graphically displayed in Figure 4.15. The most significant serial repetition of lithologies (cycle) is chosen. This cycle is further examined through modified autoassociation analysis (Figure 4.16), which indicates the stratigraphic position and range of each cycle. Also, by knowing the thickness of each individual cycle in the stratigraphic sequence, a mean thickness value is calculated for each type of cycle. Through this approach the significance of cyclicity can be determined.

Results

An integrated approach of overlying substitutability analysis, embedded Markov chain analysis, and modified autoassociation analysis was applied separately to each of five stratigraphic intervals in the Nolichucky Shale and to one composite section, representing three nearby localities in the Maynardville Limestone (the original, unmanipulated transition frequency matrices, downward transition probability matrices, substitutability matrices, etc. are on file at the Department of Geological Sciences). Lithologic units in the Maynardville are much

MATRIX SIZE	SUBSTITUTED LITHOLOGIES (Number of occurrences of lithologies are in parentheses)
14 X 14	THROM (2) → FPG (34)
13 X 13	MWS (26) ← MXPGWS (14)
12 X 12	FXPG (17) → FPG (34) [THROM (2)]
11 X 11	S (103) ← SWXPG (11)
10 X 10	FPGWS (9) ← XFPG (4)
9 X 9	OPG (36) ← UPG (12)
8 X 8	M (8) → MWS (26) [MXPGWS (14)]
7 X 7	FPGWS (9) [XFPG (4)] ← XPG (5)
6 X 6	FPG (34) [FXPG (17), THROM (2)] ← OPG (36) [UPG (12)]
5 X 5	S (103) [SWXPG (11)] ← XPGWS (6)

ITERATION WAS TERMINATED

COMPLEXITY OF MARKOV CHAIN

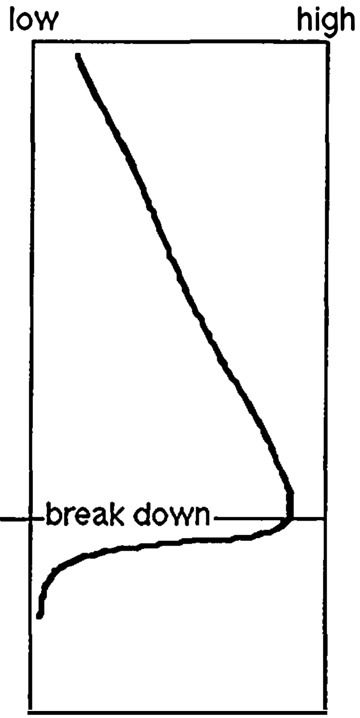

Figure 4.12. Iterative approach used to identify most complex Markov chain. By the eighth cluster (7 X 7 matrix) successive levels of clusters had been averaged sufficiently to cause enough distortion to break down the Markov chain.

OVERLYING LITHOLOGIES

UNDERLYING LITHOLOGIES

	C(N, A)	D(G)	E	B(H, F)	I(L)	J(K)	O	M	row totals
C(N, A)	▨	2	11	3	6	29	1	0	52
D(G)	3	▨	5	1	0	5	0	0	14
E	19	5	▨	1	13	31	3	4	76
B(H, F)	4	1	27	▨	3	8	0	0	43
I(L)	3	3	1	1	▨	38	0	0	46
J(K)	21	2	26	37	25	▨	0	1	112
O	1	0	5	0	0	0	▨	0	6
M	0	0	2	0	0	1	2	▨	5
column totals	51	13	77	43	47	112	6	5	354 total number of transitions

Figure 4.13. An 8 X 8 transition frequency matrix for I-75 outcrop of Nolichucky. This matrix is derived from the original 15 X 15 matrix. Reduction of matrix size was accomplished by applying overlying substitutability analysis. Symbols are used to abbreviate full lithologic names, for interpretation see Figure 4.7.

Step no.	Transition type	Observed frequency	Expected frequency	(Obs. freq./ N) X 100	Chi Square	Probability (80% conf.)	Remarks
1	O ↑ M	2	0.03	0.56	152.57	0.0000	?
2	E ↑ B(H,F)	27	3.11	7.63	116.55	0.0000	*
3	B(H,F) ↑ J(K)	37	3.69	10.45	77.08	0.0002	*
4	J(K) ↑ I(L)	38	5.77	10.73	55.53	0.0257	*
5	E ↑ O	5	0.26	1.41	44.67	0.1523	*
6	D(G) ↑ I(L)	3	0.36	0.85	36.01	0.4211	?

Figure 4.14. Computer-generated table showing results of Markov chain analysis for I-75 outcrop of Nolichucky. Symbols are used to abbreviate full lithologic names, for interpretation see Figure 4.7. Under remarks column: *=likely transitions; ?=geologically weak transitions because of their low total number of occurrences relative to the total number of transitions. The total number of transitions (N)=354.

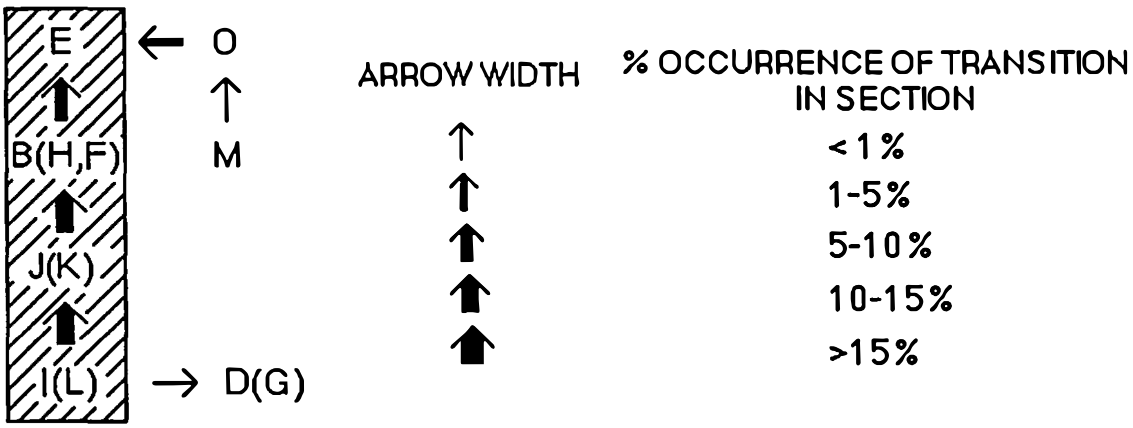

Figure 4.15. Graphical display of lithologic transitions which are observed more often than expected in the Nolichucky outcrop at I-75. Note that arrow widths indicate the normalized percent occurrence of a lithologic transition with respect to all transitions in a stratigraphic section [(observed frequency / total number of transitions) X 100]. Shaded area highlights the most significant serial repetition.

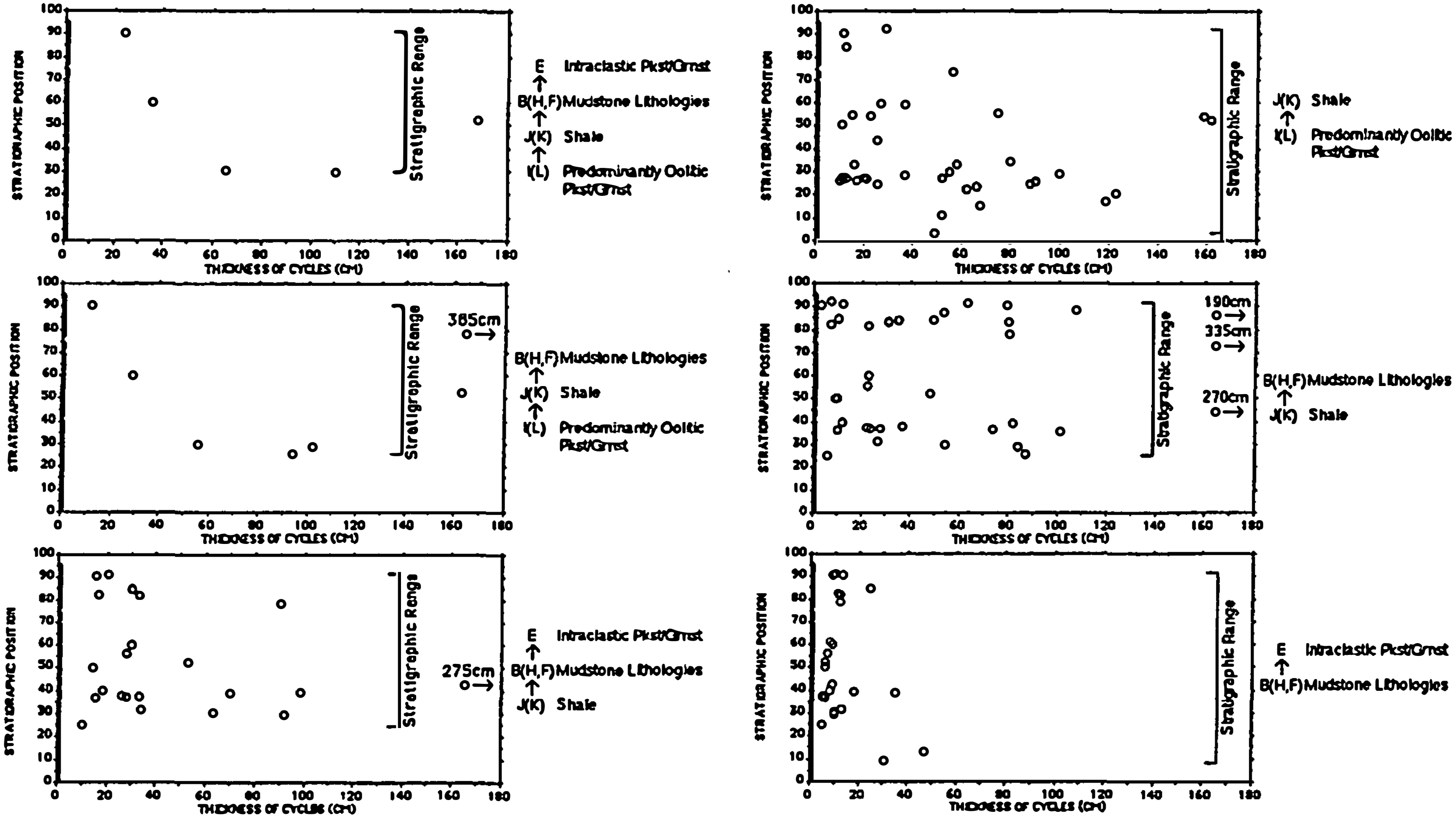

Figure 4.16. Modified autoassociation analysis showing the stratigraphic position and range of cycles for Nolichucky Shale at I-75 outcrop. X-Y plots show the complete cycle and each partial cycle. Each point which falls along the Y-axis represents a failed match of the pertinent cycle at that stratigraphic position. Stratigraphic position is in meters.

thicker, so data from the Joy 2, Scarboro Road, and S-3 Pond cores were combined to increase the total number of lithologic transitions. This enables a more valid test of Markov chain analysis to be conducted.

The results for the I-75 locality have been previously summarized. Those for the other four localities analyzed are shown in Figures 4.17 and 4.18 (transition frequency matrices used to generate cycles and a graphical display of pertinent cycles are presented here; computer generated tables showing statistical details and autoassociation diagrams are available from the Department of Geological Sciences).

The vertical and lateral extent of stratigraphic intervals of identical, statistically valid cycles at all localities is shown in Figure 4.19. Important observations relative to that figure are as follows:

1. "NC" refers to stratigraphic intervals where cyclicity does not occur.
2. No cycles are observed in the Nolichucky Shale at Beech Grove or in the Maynardville Limestone at Scarboro Road.
3. The Maynardville portion of the Joy 2 section is divided into two columns because two distinct cycles that occur there have overlapping stratigraphic ranges.
4. The I-75 section is divided into six columns. The complete cycle (most widely spaced dot pattern) is represented along with each of the five partial cycles (more tightly packed dot patterns).

Figure 4.17. Transition frequency matrices that reveal the most complex Markov chain. Nolichucky Shale localities include Beech Grove (a), Joy 2 (b), Scarboro Road (c), and S-3 Pond (d). The composite section (e) reflects lithologic transitions in the Maynardville Limestone (combined data from Joy 2, Scarboro Road, and S-3 Pond localities). Lithologic abbreviations are keyed to Figures 4.1, 4.2, and 4.3. Lithologies which occur less often are not displayed in parentheses following the dominant lithologic type as in Figure 4.13. Only the dominant lithologies are presented here.

OVERLYING LITHOLOGIES

UNDERLYING LITHOLOGIES

a	MWS	FPGWS	IPG	OPG	S	SWXPG	FPG	XPG	XPGWS	
MWS		0	8	1	0	0	0	0	0	9
FPGWS	0		4	0	1	0	0	0	0	5
IPG	0	3		7	40	2	1	4	11	68
OPG	0	0	1		26	1	2	3	2	35
S	6	2	39	22		2	2	4	3	80
SWXPG	1	0	4	1	0		0	0	0	6
FPG	0	0	2	2	1	1		0	0	6
XPG	0	0	0	0	8	0	1		2	11
XPGWS	2	0	10	3	3	0	0	0		18
	9	5	68	36	79	6	6	11	18	238

OVERLYING LITHOLOGIES

UNDERLYING LITHOLOGIES

b	FPGWS	OPG	EPG	IPG	MWS	XPG	S	SWXPG	XPGWS	
FPGWS		0	0	0	1	0	2	0	0	3
OPG	1		1	64	4	3	108	0	7	188
EPG	0	3		0	2	0	7	2	1	15
IPG	0	55	1		3	0	86	4	5	154
MWS	1	4	10	6		0	1	0	0	22
XPG	0	2	0	0	0		1	0	0	3
S	1	114	3	76	6	0		3	9	212
SWXPG	0	1	0	3	4	0	1		0	9
XPGWS	0	9	0	5	2	0	6	0		22
	3	188	15	154	22	3	212	9	22	628

UNDERLYING LITHOLOGIES

c	IPG	EPG	MWS	OPG	S	XPG	SWXPG	FPGWS	XPGWS	
IPG		1	0	6	37	2	2	0	7	55
EPG	0		0	3	55	5	1	4	6	74
MWS	3	3		0	0	0	0	0	0	6
OPG	4	1	1		30	4	0	1	4	45
S	17	31	2	9		0	4	4	88	155
XPG	1	3	0	2	3		0	0	3	12
SWXPG	1	3	0	2	1	0		0	3	10
FPGWS	0	1	3	1	0	1	0		3	9
XPGWS	29	31	1	22	28	0	3	0		114
	55	74	7	45	154	12	10	9	114	480

UNDERLYING LITHOLOGIES

d	EPG	MWS	IPG	OPG	S	XPG	XPGWS	
EPG		0	0	0	4	0	1	5
MWS	0		0	1	0	0	3	4
IPG	1	0		12	97	4	11	125
OPG	0	0	4		42	2	6	54
S	2	0	63	18		1	104	188
XPG	0	0	3	0	4		0	7
XPGWS	2	4	55	23	41	0		125
	5	4	125	54	188	7	125	508

UNDERLYING LITHOLOGIES

e	STROM	THROM	CL	EPG	IPG	NOPG	S	SWXPG	XPGWS	
STROM		6	1	0	0	2	0	0	0	9
THROM	3		2	3	15	33	1	0	0	57
CL	0	3		0	0	6	0	0	0	9
EPG	2	1	0		0	6	0	0	0	9
IPG	0	7	0	1		8	2	0	11	29
NOPG	3	36	7	5	0		1	0	0	52
S	0	1	0	0	3	0		0	1	5
SWXPG	0	1	0	0	0	0	0		0	1
XPGWS	0	0	0	0	12	0	1	0		13
	8	55	10	9	30	55	5	0	12	184

Figure 4.17 (continued)

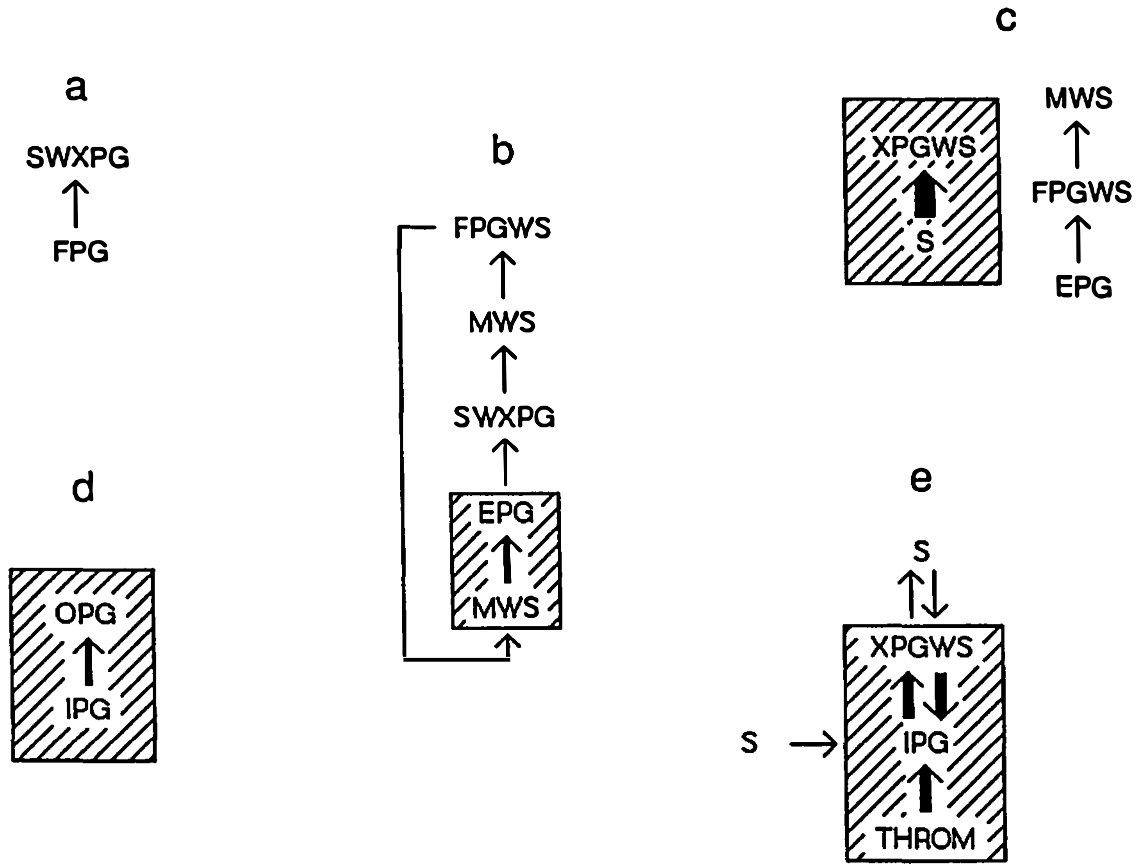

Figure 4.18. Graphic display of cycles as determined from embedded Markov chain analysis of transition frequency matrices in Figure 4.17. Only those lithologic transitions which are observed more often than expected are displayed. Geologically significant cycles, if present, are emphasized by diagonal pattern. Letters a, b, c, and d correspond to Nolichucky sections at Beech Grove, Joy 2, Scarboro Road, and S-3 Pond, respectively. Cycles observed in the Maynardville are shown (e). Arrow widths are calculated as in Figure 4.15.

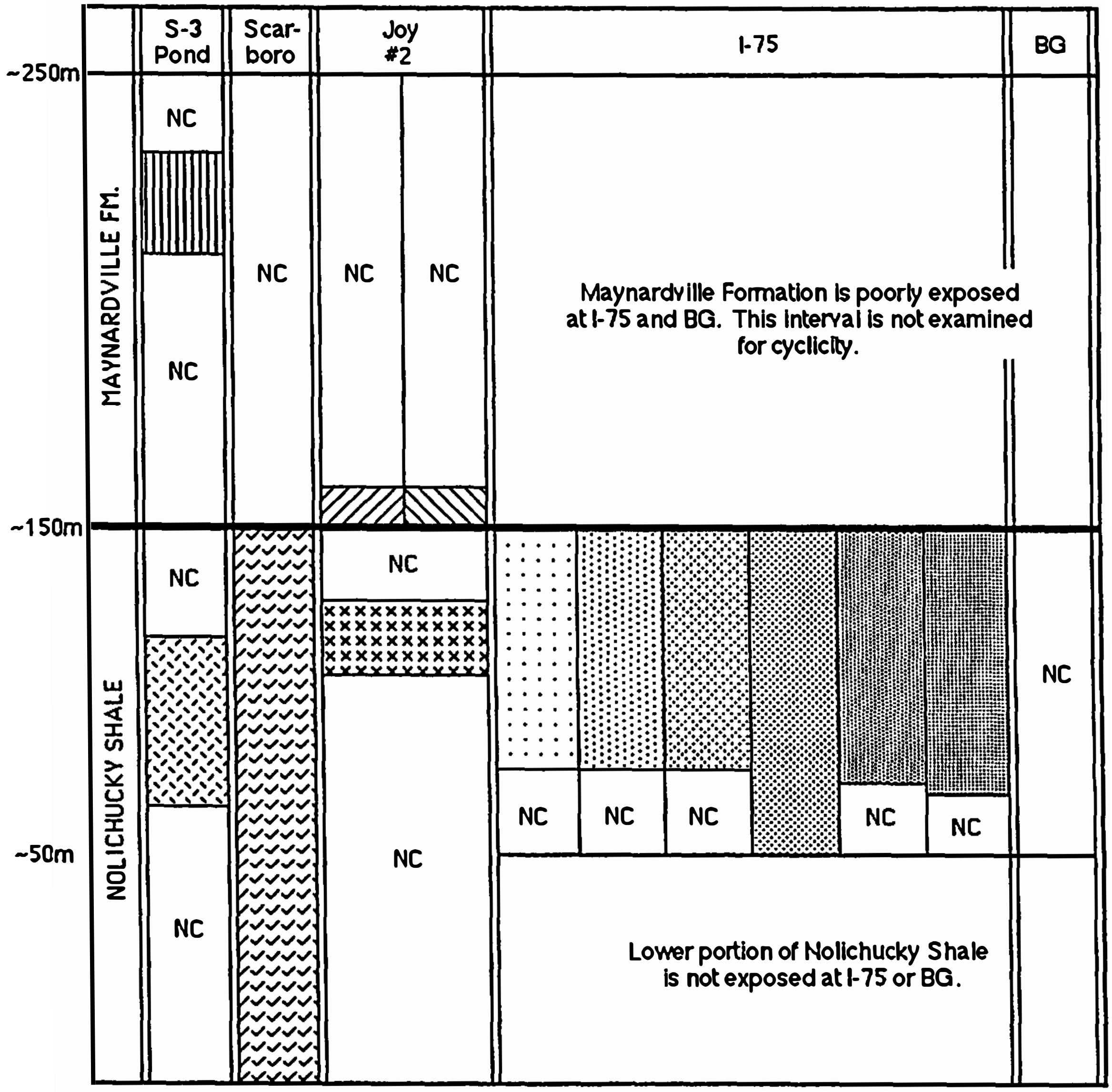

Figure 4.19. The vertical and lateral extent of stratigraphic intervals of identical, statistically valid cycles. Five localities have been examined for cyclicity (BG=Beech Grove road cut; I-75=Interstate 75 road cut; Joy 2=Joy 2 core; Scarboro=Scarboro Road core; S-3 Pond=S-3 Pond core). NC=no cyclicity discovered in this interval. Patterns for cycle types are defined in Figure 4.20.

Figure 4.20 lists pertinent characteristics of each type of cycle displayed in Figure 4.19. Examination of Figure 4.20 reveals that twelve distinct cycles are recognized in the Nolichucky/Maynardville sequence (only four complete cycles are observed). Cycles are comprised only of seven different lithologies. Other lithologies are present in the initial database (see Figures 4.2 and 4.3), but they are not cyclic in occurrence (e.g., cryptalgal laminites are an important lithologic constituent within the Maynardville Limestone, but they do not overlie or underlie any particular lithology with sufficient repetition to be identified as cyclic).

A useful parameter for assessing the "importance" of the various cycles is the percent of the total stratigraphic section which is composed of each cycle. Only three partial cycles at I-75 and the complete cycle at Scarboro Road account for more than 10% of the total thickness of their respective stratigraphic sections (see asterisks in right column of Figure 4.20). Three of these cycles appear to be variations on a similar theme; shale overlain by mudstone or fine-grained pellet lithologies, which underlie intraclastic grainstones. In other words, shale which lacks storm beds grades up into muddy limestone with faint lamination (low energy storm reworking) and then into storm intraclastic beds reworked from hardgrounds. Cycle tops do not exhibit vadose features or other evidence of emergence. Occasionally, this cycle is floored by storm reworked ooid grainstones.

Evidence for cyclicity in the Nolichucky/Maynardville sequence is very weak. Most types of cycles are "simple" (characterized by two

Figure 4.20. Characteristics of each cycle shown in Figure 4.19. Percent of stratigraphic section composed of each cycle is calculated by: [(number of cycles X average thickness of that cycle) / total thickness of stratigraphic section] X 100.

FORMATION NAME	LOCALITY [TKN. OF SECTION]	PATTERN WHICH REPRESENTS CYCLE (C=complete cycle; P=partial cycle)	TYPE OF CYCLE	NO. OF CYCLES	AVE. TKN. OF EACH CYCLE (CM)	% OF STRAT. SECTION COMPOSED OF EACH CYCLE
Nolichucky Shale	Beech Grove (BG) [86.21 m.]	NO GEOLOGICALLY SIGNIFICANT CYCLES OBSERVED				
	Interstate 75 (I-75) [94.28 m.]	░ C	↑ IPG MWS S OPG	5	85	4.51
		▒ P	↑ MWS S OPG	7	119	8.84
		▒ P	↑ IPG MWS S	23	49	* 11.95
		▓ P	↑ S OPG	38	50	* 20.15
		▥ P	↑ MWS S	37	60	* 23.55
		▦ P	↑ IPG MWS	27	13	3.72
	Joy #2 [172.54 m.]	⊠ C	↑ EPG MWS	10	46	2.67
	Scarboro [144.46 m.]	⋁ C	↑ XPGWS S	88	81	* 50.39
	S-3 Pond [146.83 m.]	⁙ C	↑ OPG IPG	12	56	4.58
Maynardville Formation	Composite Section from: Joy #2, Scarboro, and S-3 Pond [399.27 m.]	□ C	↑↓ XPGWS IPG THROM	0	0	0.00
		▥ P	↑ IPG THROM	15	107	4.02
		▨ P	↑ XPGWS IPG	11	75	1.38
		▧ P	↑ IPG XPGWS	12	74	1.47

Figure 4.20 (continued)

lithologies) and are not continuous through a stratigraphic section. More complex cycles (involving three or more lithologies) are revealed only in the Nolichucky Shale at I-75, but the complete (4 part) cycle occurs only five times. This number should be greater if there was a strong cyclic control to the development of the sequence.

Although substitutability analysis and embedded Markov chain analysis indicate that the complete cycle within the Maynardville Limestone is statistically valid, autocorrelation analysis shows that the complete cycle does not actually occur and thus is not geologically meaningful. Three partial cycles occur in the Maynardville composite section. Each represents 4% or less of the complete stratigraphic column (see Figure 4.20). Thus, the Maynardville Limestone in the sections studied here exhibits poorly developed cyclicity. Because the Maynardville represents very shallow subtidal, intertidal, and supratidal environments where minor changes in sea level would affect lithologic distribution, cyclicity should be more apparent. Conversely, the Nolichucky which shows greater cyclicity was deposited predominantly under shallow to intermediate depth subtidal conditions.

Problems Involved in Analysis of Cyclicity

Numerous investigators have identified cycles within sedimentary rocks. Many previous studies have based the occurrence of cycles on (1) descriptive stratigraphic data, which typically lack statistical verification (e.g., Aitken, 1978; Bush and Fischer, 1981; Aigner, 1985),

(2) older, flawed versions of Markov chain analysis (Gingerich, 1969; Anderson and Goodman, 1957), or (3) computer-generated models not associated closely with actual stratigraphic data (Turcotte and Willemann, 1983). The approach described here uses several analytical techniques to model cycles, but stratigraphic information serves as the data base.

A serious constraint of stratigraphic data is that many variables are based on a nominal or an ordinal scale of measurement. For example, rock types (lithologies) are classified into mutually exclusive categories. As a result, powerful techniques of parametric statistics cannot be used; I have demonstrated here that useful tests may still be employed. These techniques require few assumptions, use nominal and ordinal data, detect subtle trends or cycles not observed normally by unaided processing, and employ computers for rapid processing of large data sets.

The integrated approach proposed here is superior to many other techniques which have been applied to assess stratigraphic cyclicity; nonetheless, this method is not without potential drawbacks as noted below.

1. Classification of lithologies involves some degree of subjectivity. Care must be taken to objectively define mutually exclusive lithologies. Bias can be reduced through use of rock classification schemes such as that of Dunham (1962).
2. The chi-square statistic is used to test transition frequency matrices for Markov properties (Powers and Easterling, 1982).

Thus, the sample size (the total number of transitions for each matrix) must be sufficiently large to guarantee similarity between the sampling chi-square distribution (observed chi-square statistic) and the theoretical chi-square distribution (expected chi-square value). When expected frequencies are too small, the observed chi-square statistic will be overestimated. To avoid incorrect inferences from chi-square hypothesis tests, a general rule should be followed: no cell may have an expected frequency less than 1, and no more than 20% of the cells may have expected values less than 5 (Brown, 1985). According to Brown (1985), if this rule is not satisfied, the distribution of the chi-square statistic may differ from the theoretical chi-square distribution. Several matrices from the Nolichucky/Maynardville data presented here do not meet these requirements. However, the number of transitions measured is sufficiently large to obtain statistically reliable estimates of the transition probabilities. Several matrices have been tested for Markov chains after increasing the sample size. Data were added proportionately to each cell of the matrix. This procedure did not alter results significantly.

3. In order to obtain a valid Markov chain, probabilities associated with the transitions between lithologies must not change substantially through time (Harbaugh and Bonham-Carter, 1970). This concept is known as stationarity. If, for example,

a thick stratigraphic interval could be divided into smaller subintervals, transition frequency matrices constructed from each subinterval should be approximately equal to each other (should exhibit similar transition probabilities). If stationarity is not maintained, each subinterval should be reexamined separately for cycles. Unfortunately, many times subintervals do not exhibit a sufficiently large number of transitions (see #2 above) unless the stratigraphic sequence is exceptionally thick and/or reveals numerous transitions. Stationarity is broadly maintained within the Nolichucky Shale and within the Maynardville Formation, at least on a large scale. Because significant depositional and diagenetic environmental gradients were not present in each formation, lithologies should exhibit similar transition probabilities within each formation. However, several cycles occur only in selected portions of the complete stratigraphic interval. This suggests that stationarity does not exist at a finer-scale. For stationarity to be maintained in the strictest sense, cycles would have to recur (i.e., ABCABC...) throughout the stratigraphic interval being investigated. Clearly, few if any stratigraphic sequences would display stationarity at this scale.

4. The first-order, discrete-lithology, discrete-time embedded Markov chain is considered in this study. This model was selected because it is geologically reasonable and is

structurally simple. It seems ideally suited to the complexity of natural environments, yet it is robust enough to maintain validity even when "confronted with" rare events. Other higher-order Markov models may be equally appropriate.

Conclusions

The following conclusions are drawn from this investigation:

1. First order Markovian cyclicity is very rare in the shallow subtidal, intertidal, and supratidal Maynardville Formation.
2. No small-scale cycles are observed in the Nolichucky Shale at the Beech Grove locality or in the Maynardville Limestone in the Scarboro Road core.
3. The subtidal limestone and shale lithologies within the Nolichucky Shale exhibit the most well-developed cycles. However, the majority of these cycles are "simple," involving no more than two lithologies.
4. The absence of well-developed cycles within the Nolichucky/Maynardville sequence is probably attributed to local variability in the occurrence and distribution of lithologies in response to the storm-dominated paleoenvironmental setting (see Chapter 2).
5. The Markov method (approach employed here) for stratigraphic analysis of small-scale cycles in the Late Cambrian of east Tennessee reveals that local processes were probably of prime

importance in producing the simple cycles discerned because some coeval parts of the sequence show cyclicity at one locality but not at another, and some intervals at a given locality show no cyclicity at all.

The results suggest that at the scale of this analysis local control of lithologic repetition is more important than larger scale controls such as geoidal, tectonic, or glacioeustatic. Although these large scale processes doubtless occur, and must have effect on sedimentation, their record in the rocks may be almost totally masked by the response to very localized events. Thus, I would recommend greater caution in the interpretation of the causes of cyclicity, and in the testing of theoretical models constructed from assumptions about sea level changes, subsidence, and sedimentation rates. Although such models are important steps in the search for order in the stratigraphic record, establishment of the model must be followed by objective testing using real, detailed stratigraphic data. The study by Goldhammer and others (1987) is just such a test which seems to validate one model of how short-term cyclicity may be produced. The results presented here suggest, however, that the rather regular and predictable cyclicity demonstrated by Goldhammer and others (1987) may be well recorded only in some environmental settings while absent in others.

CHAPTER 5

ENVIRONMENTAL SYNTHESIS AND MODEL FOR THE UPPER CONASAUGA NOLICHUCKY SHALE AND MAYNARDVILLE LIMESTONE SEQUENCE

Introduction

Middle and Late Cambrian time is recorded in much of continental North America and elsewhere by the widespread occurrence of carbonate and fine-grained siliciclastic rocks. Typically, these rocks were deposited in tropical, cratonic or epeiric seas. During the Late Cambrian in central east Tennessee and surrounding areas, deposition occurred within an epeiric sea (see Chapter 1). Epeiric seas are rare today; the best modern analogues include the Persian Gulf, Shark Bay, Florida Bay and the Bahamas region, and the North Sea. However, these areas are not nearly as extensive as were most ancient epeiric seas. Also, ancient epeiric seas were, in general, more uniformly shallow, except where they were rarely differentiated into localized deeper intracratonic sub-basins. The Nolichucky Shale was deposited within such an intracratonic sub-basin.

The interbedded package of limestone, dolostone, and shale, which comprises the Nolichucky Shale and Maynardville Limestone in central east Tennessee, was deposited in the transition between an intracratonic basin and a shallow-water carbonate platform. This transition shows no marked change in regional paleoslope. In particular, a well-defined shelf-slope break indicated by shoreparallel reefal and sand bank accumulations is absent. It has been suggested by Shaw (1964), Irwin (1965), Ahr (1973), and Wilson (1975) that in the absence of a shelf-slope break the transition from very shallow- to deeper-water can be referred to as a ramp, and that in such a situation depositional facies patterns tend to be distributed in bands which are roughly parallel to the strandline. Wave and current activity increases as the shoreline is approached (Ahr, 1973), and carbonate grainstone deposits grade offshore into progressively deeper-water, lower-energy carbonates, which finally pass into more basinal argillaceous limestone and shale (Shaw, 1964; Irwin, 1965). Generally, it is assumed that a relatively uniform and gently sloping seafloor topography favors widespread distribution of facies with monotonous wedge-shaped geometries which thicken seaward. Excluding shelf margin environments such as reefs or oolitic sand banks, which occur as shore parallel accumulations, carbonate shelf facies patterns are more complex. According to these other workers, areal distribution of facies on a shelf reveal rapid changes in sediment type laterally forming a mosaic pattern of facies distinctly different from ramp patterns (Laporte, 1967).

The main objective of this Chapter is to discuss the vertical and lateral association of lithofacies and to generate a paleoenvironmental and paleobathymetric model based on the temporal and spatial distribution of facies in the Nolichucky and Maynardville. These reconstructions dispel the notion that ramp-like paleobathymetric profiles (i.e., those profiles not characterized by well-developed shelf marginal reefs or laterally extensive carbonate sand banks) result in broad laterally continuous facies belts parallel or nearly parallel to the strand. Instead, environmental patterns on this Cambrian ramp were much more irregular and mosaic-like than predicted by the ramp depositional model of earlier workers.

Stratigraphic Setting

During early Late Cambrian time deposition took place along the eastern margin of North America and was dominated by a broad carbonate rim predominantly composed of very shallow peritidal facies (Bird and Dewey, 1970). Adjacent to the carbonate platform were subtidal carbonates and siliciclastics which graded further toward the craton (northwest direction) into nearshore siliciclastic environments. Southeast of the platform was a subsiding marine basin. According to Hatcher (1978), an island-arc complex was separated from the eastern margin of the North American craton by a back-arc basin. During deposition of the Nolichucky and Maynardville formations, eastern Tennessee was located in a climatic zone that was approximately 20 degrees south latitude (Scotese and others, 1979) (Figure 5.1).

Distribution of Lithofacies

Results of the analysis of cyclicity (Chapter 4) strongly suggest that lithofacies of the Nolichucky and Maynardville formations are not

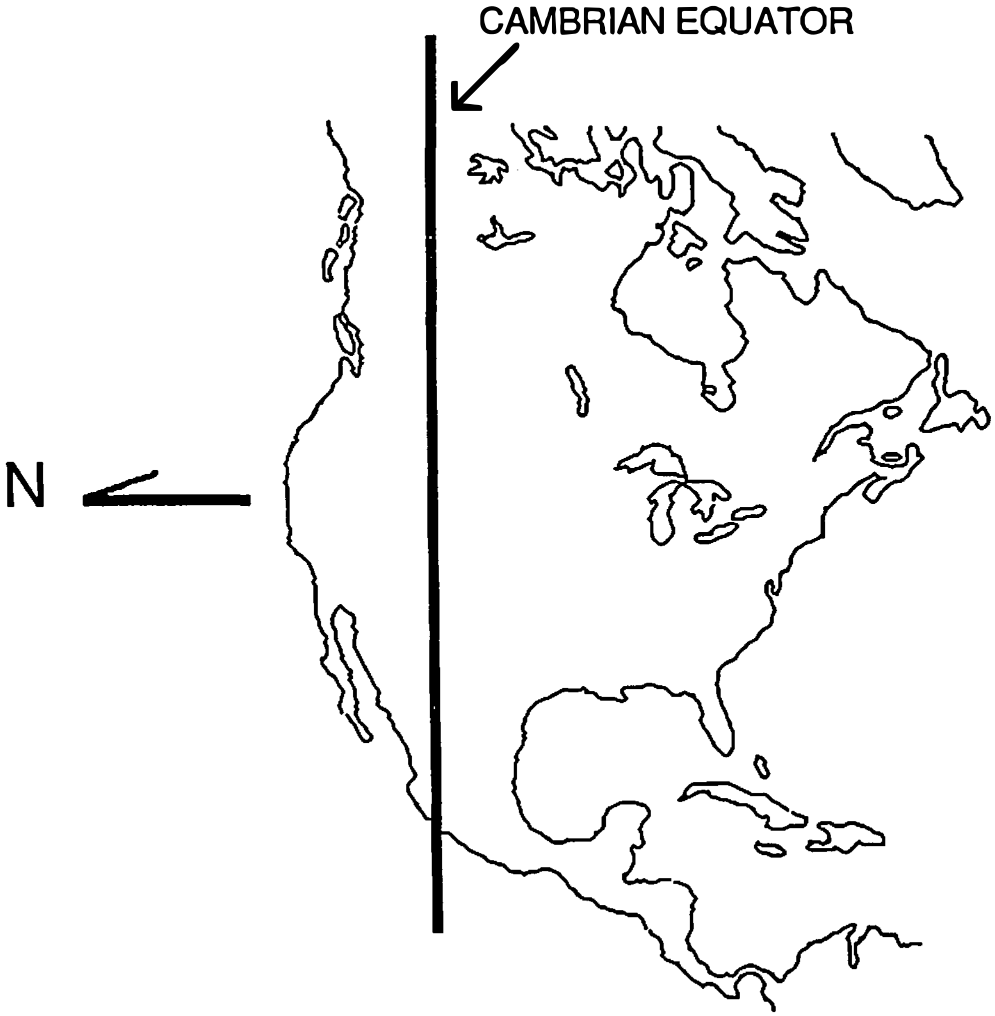

Figure 5.1. North America showing the location of the equator during Middle and Late Cambrian time (after Scotese and others, 1979).

stacked in any predictable arrangement. Also, they indicate that local processes were of prime importance in producing the rare, simple cycles which are observed. Because coeval parts of the sequence show cyclicity at one locality but not at another and because some localities reveal no cyclicity at all, it is not possible to trace stratigraphic intervals of cyclicity laterally. The lack of correlation is further elucidated through a more traditional graphic approach. Figure 5.2 displays stratigraphic columns for each exposed locality and drill core which has been examined as a part of this study. The variability in lithofacies pattern and distribution exists even though geographic separation between any two stratigraphic columns ranges from several hundred meters to 55 km (see Figures 1.12 and 5.3). Clearly, correlative progradational sequences, which are common in the Maryville Limestone (see Erwin, 1981; Simmons, 1984; Kozar, 1986), are conspicuously absent within the Nolichucky Shale and Maynardville Limestone. Thus, local environmental factors (rather than eustatic sea level changes, tectonic events, or regional changes in sediment production/subsidence) apparently controlled the temporal and spatial distribution of lithofacies.

Origin of Sedimentary Features and Structures

The Nolichucky Shale was deposited within a storm-dominated paleoenvironmental setting. Evidence supporting this interpretation comes from the sedimentary structures described in Chapter 2 and includes:

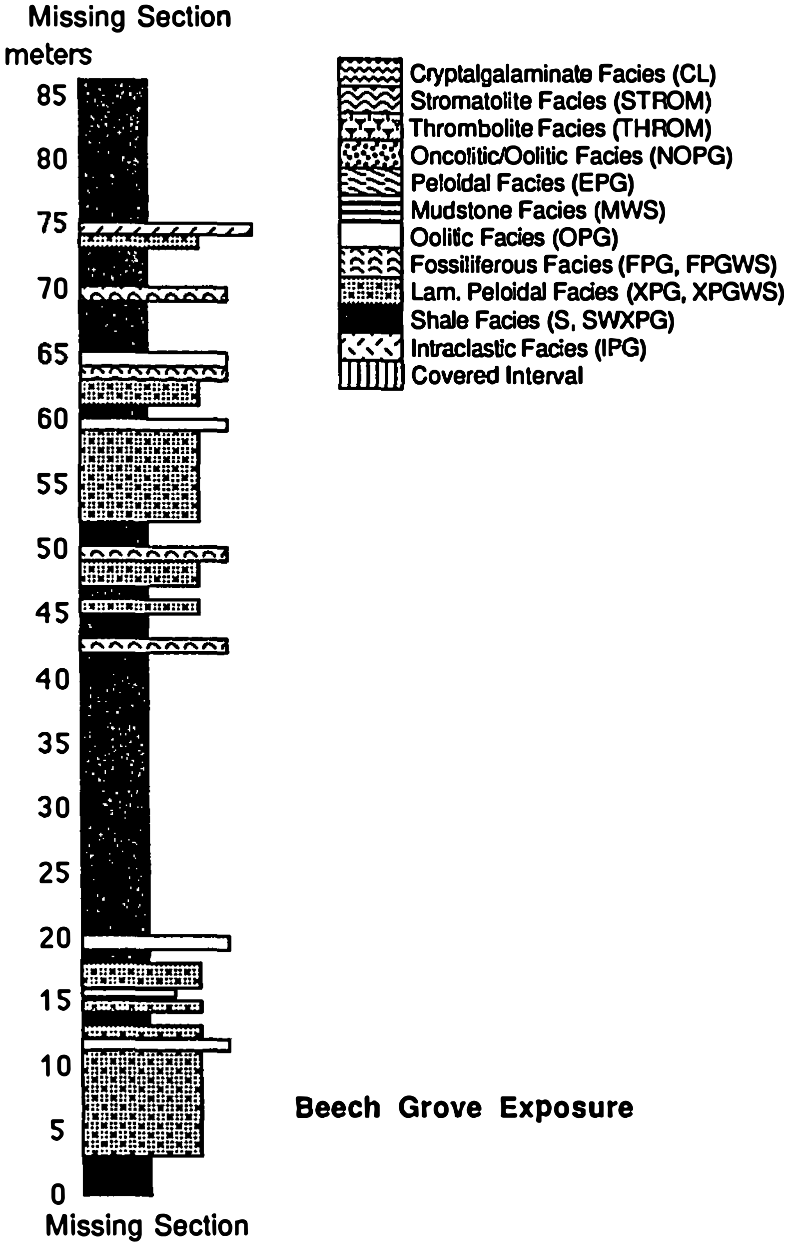

Figure 5.2. Columnar section of the Nolichucky Shale. In this figure, each stratigraphic column was derived from analysis of each 1 meter increment of the complete column. Within each 1 meter thick interval, the dominant lithofacies was identified and recorded. As a result of this approach, the actual variability of lithofacies is greater than that depicted here.

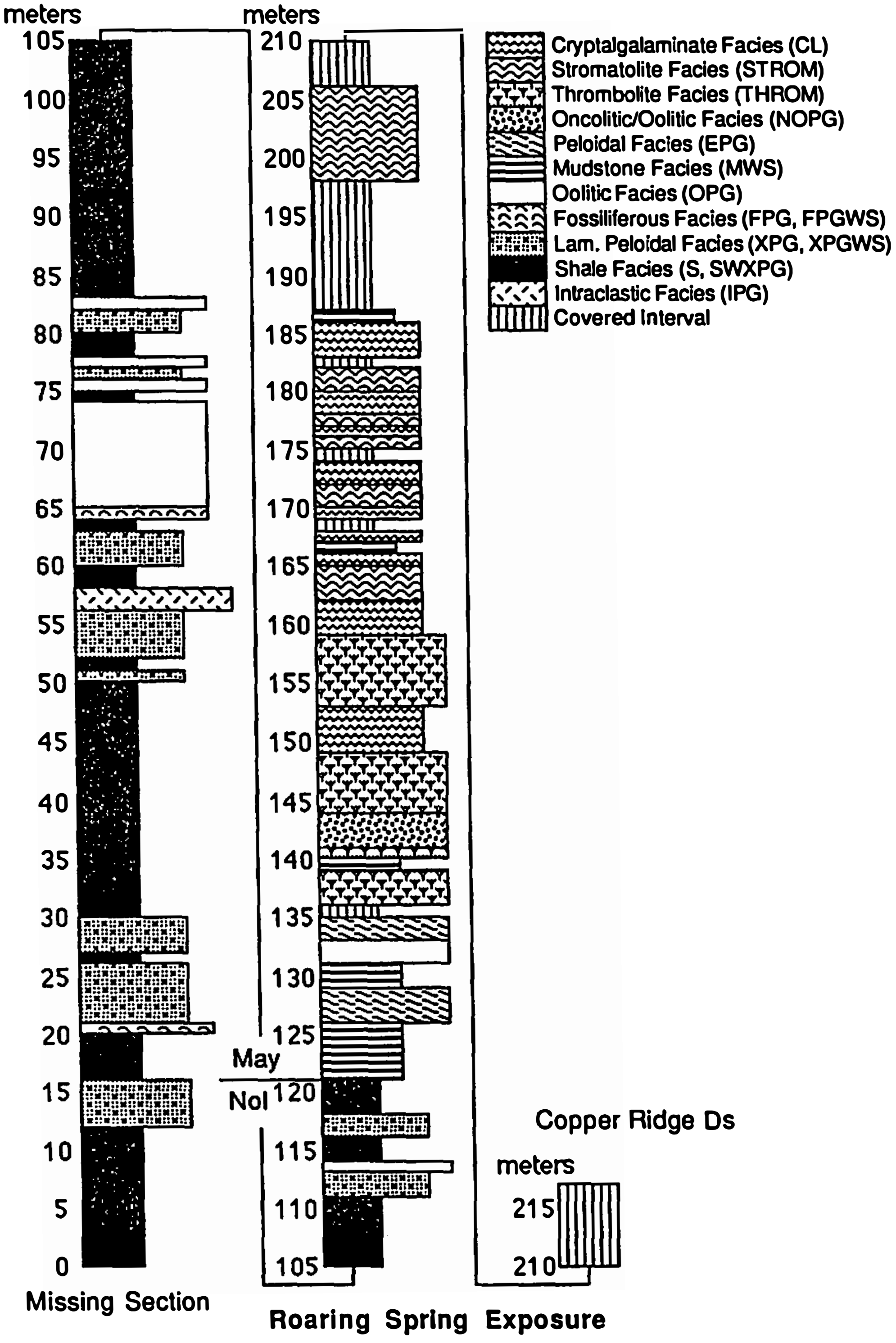

Figure 5.2 (continued). Columnar section of the Nolichucky Shale and Maynardville Limestone.

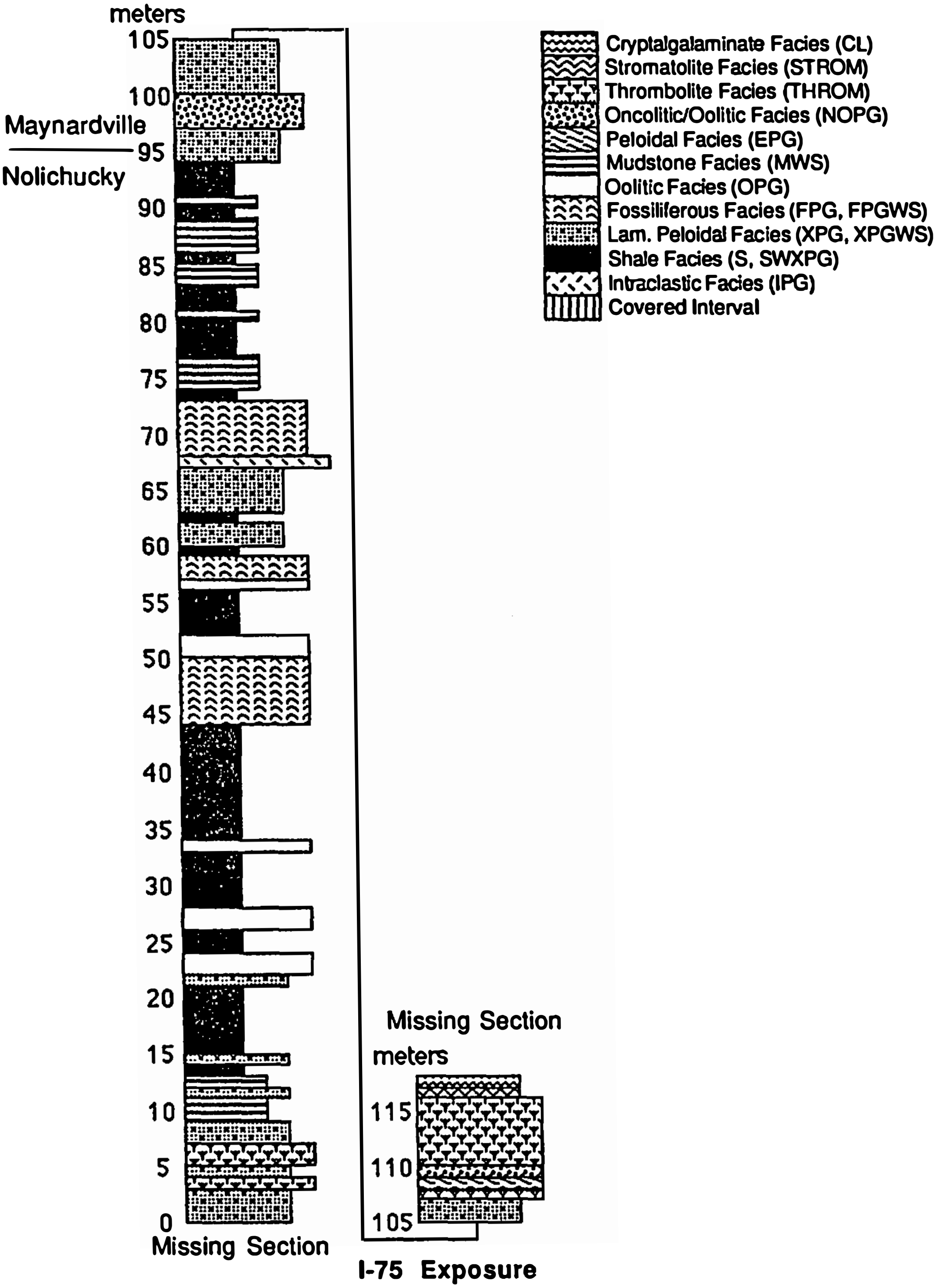

Figure 5.2 (continued). Columnar section of the Nolichucky Shale and Maynardville Limestone.

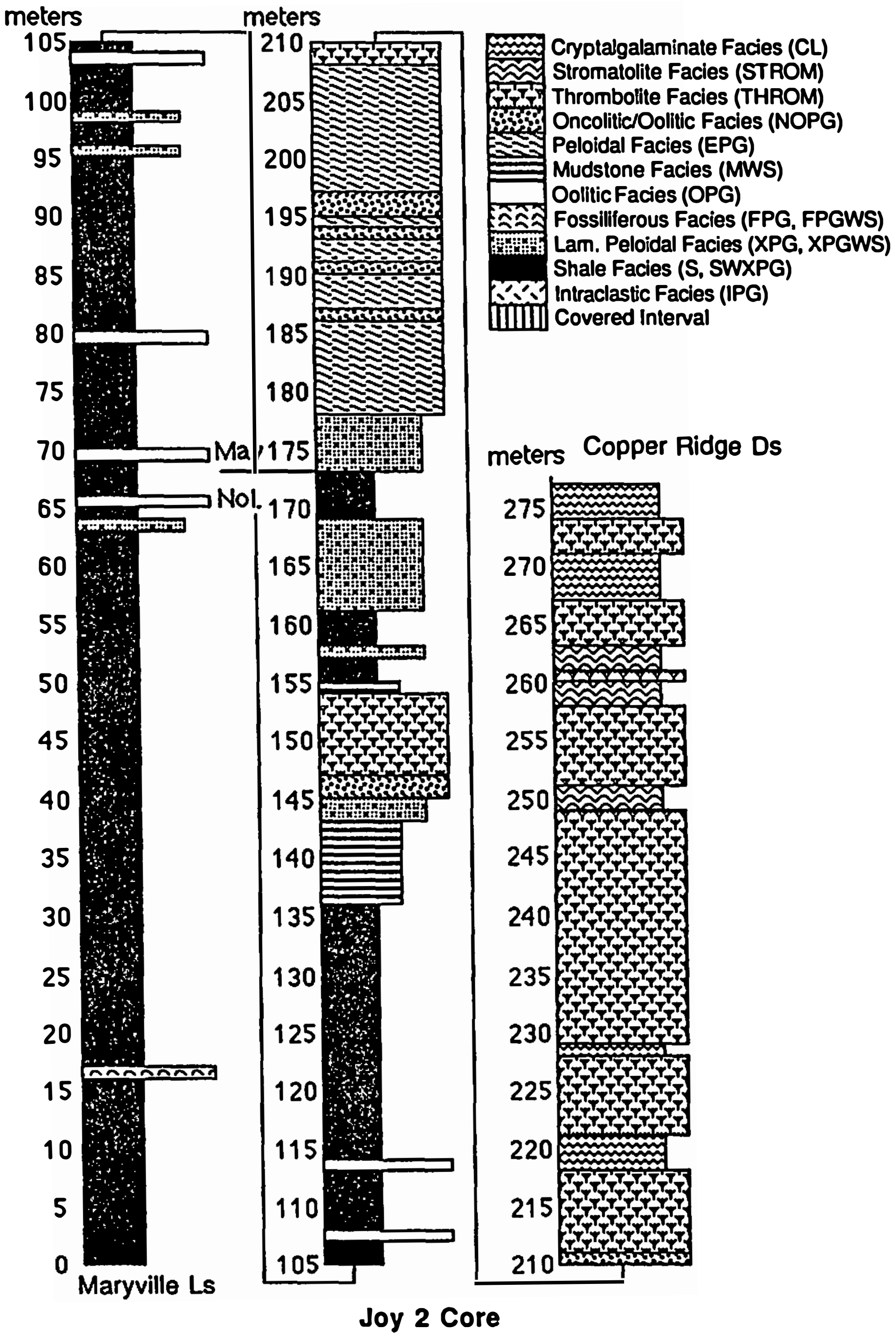

Figure 5.2 (continued). Columnar section of the Nolichucky Shale and Maynardville Limestone.

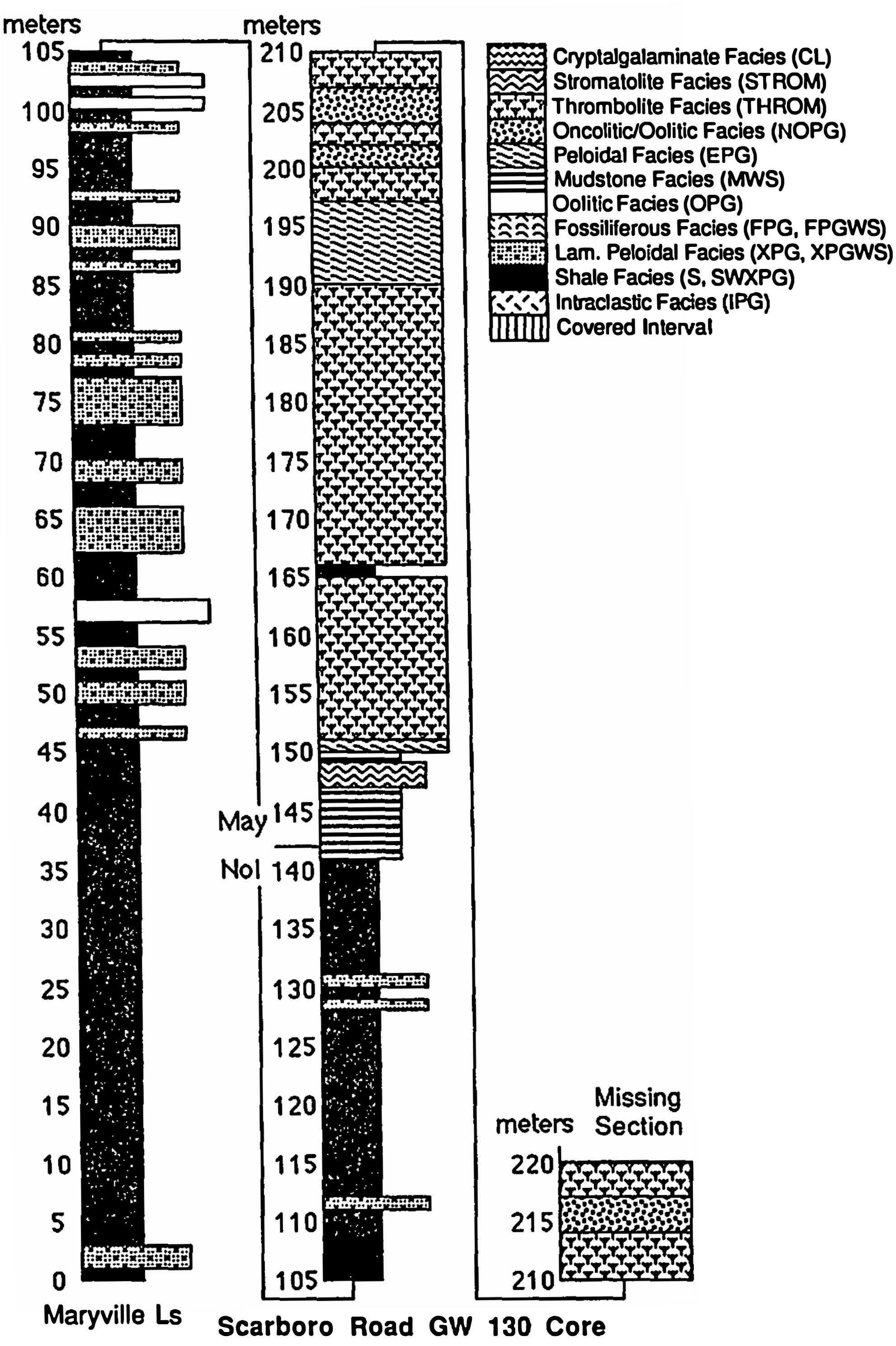

Figure 5.2 (continued). Columnar section of the Nolichucky Shale and Maynardville Limestone.

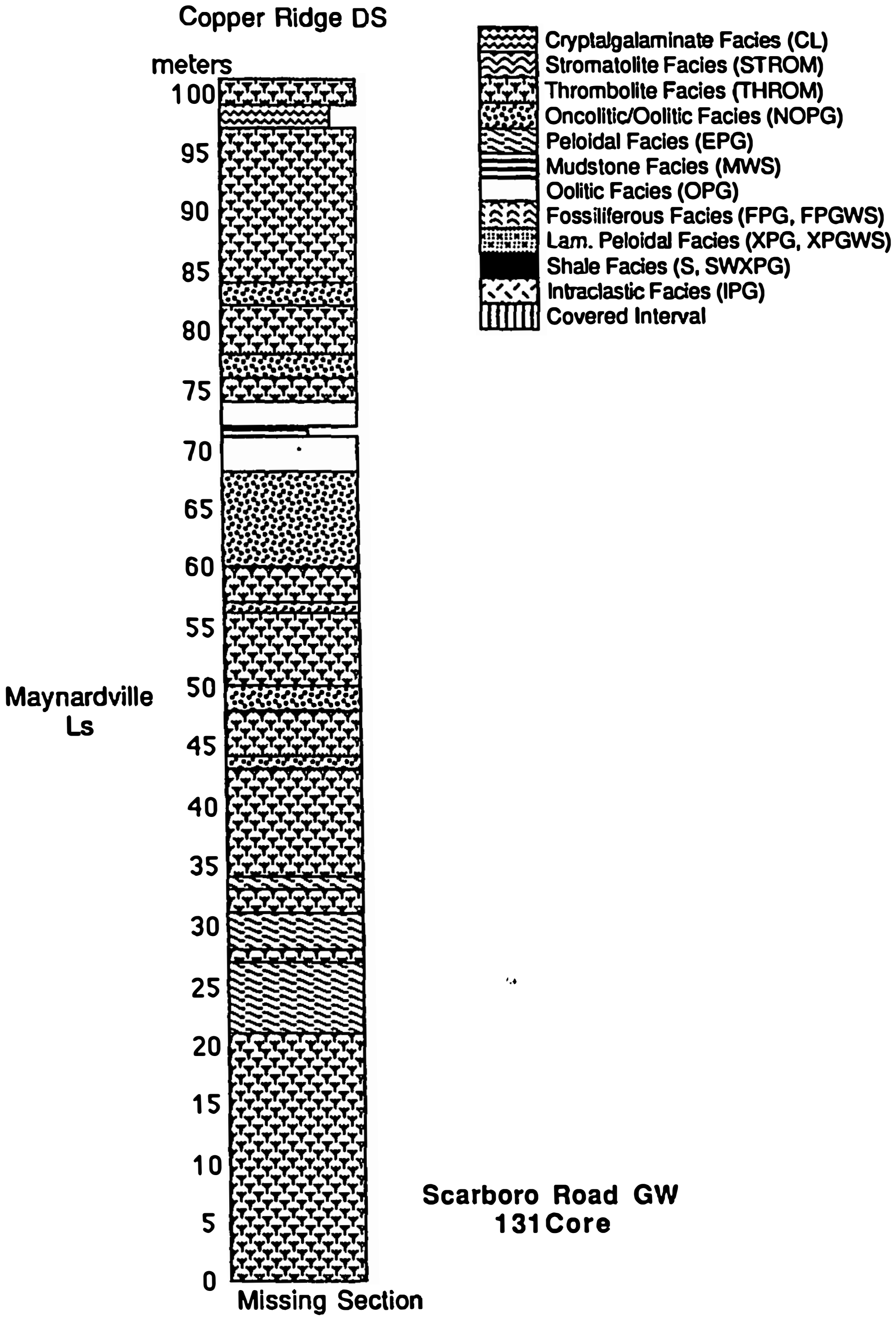

Figure 5.2 (continued). Columnar section of the Maynardville Limestone.

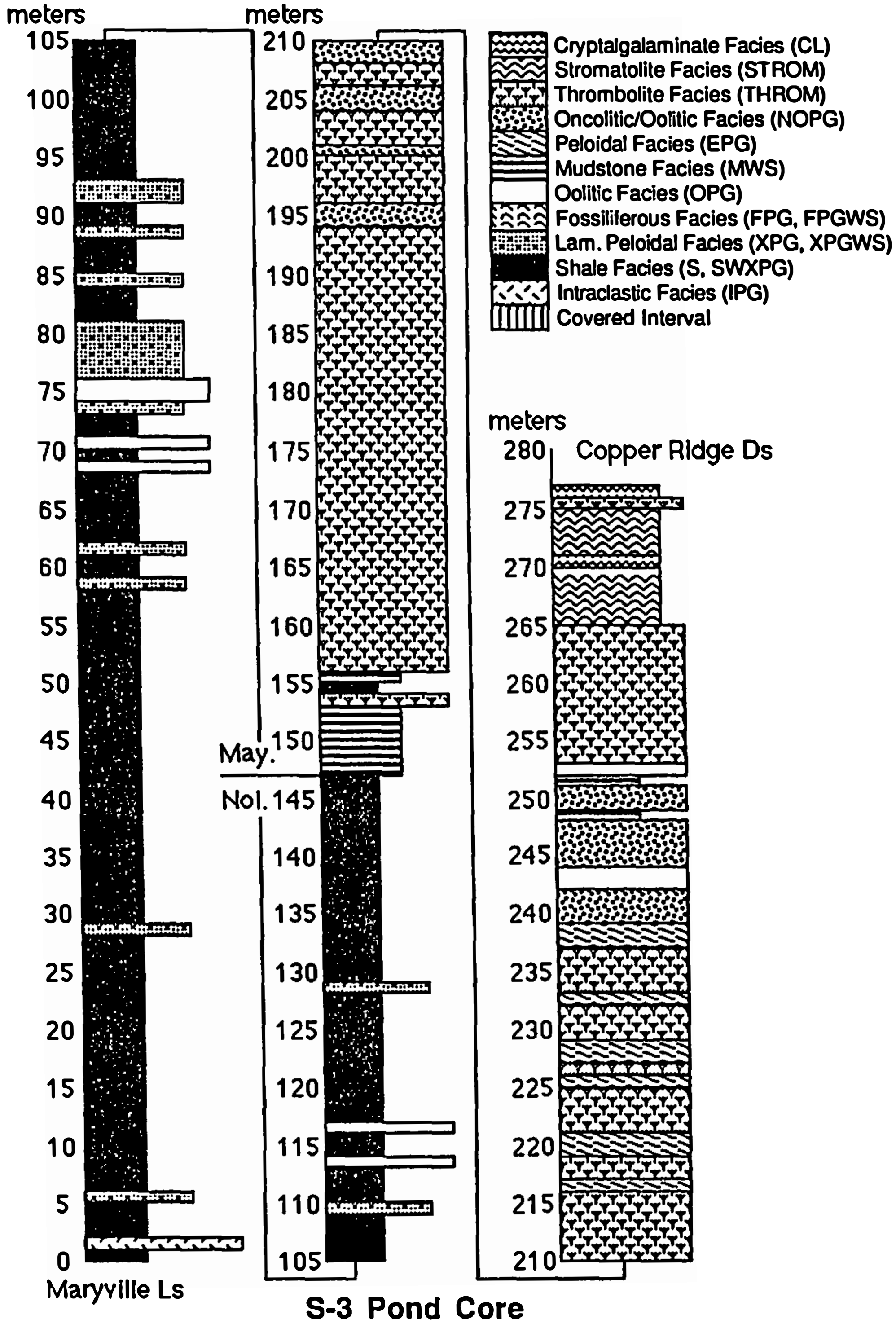

Figure 5.2 (continued). Columnar section of the Nolichucky Shale and Maynardville Limestone.

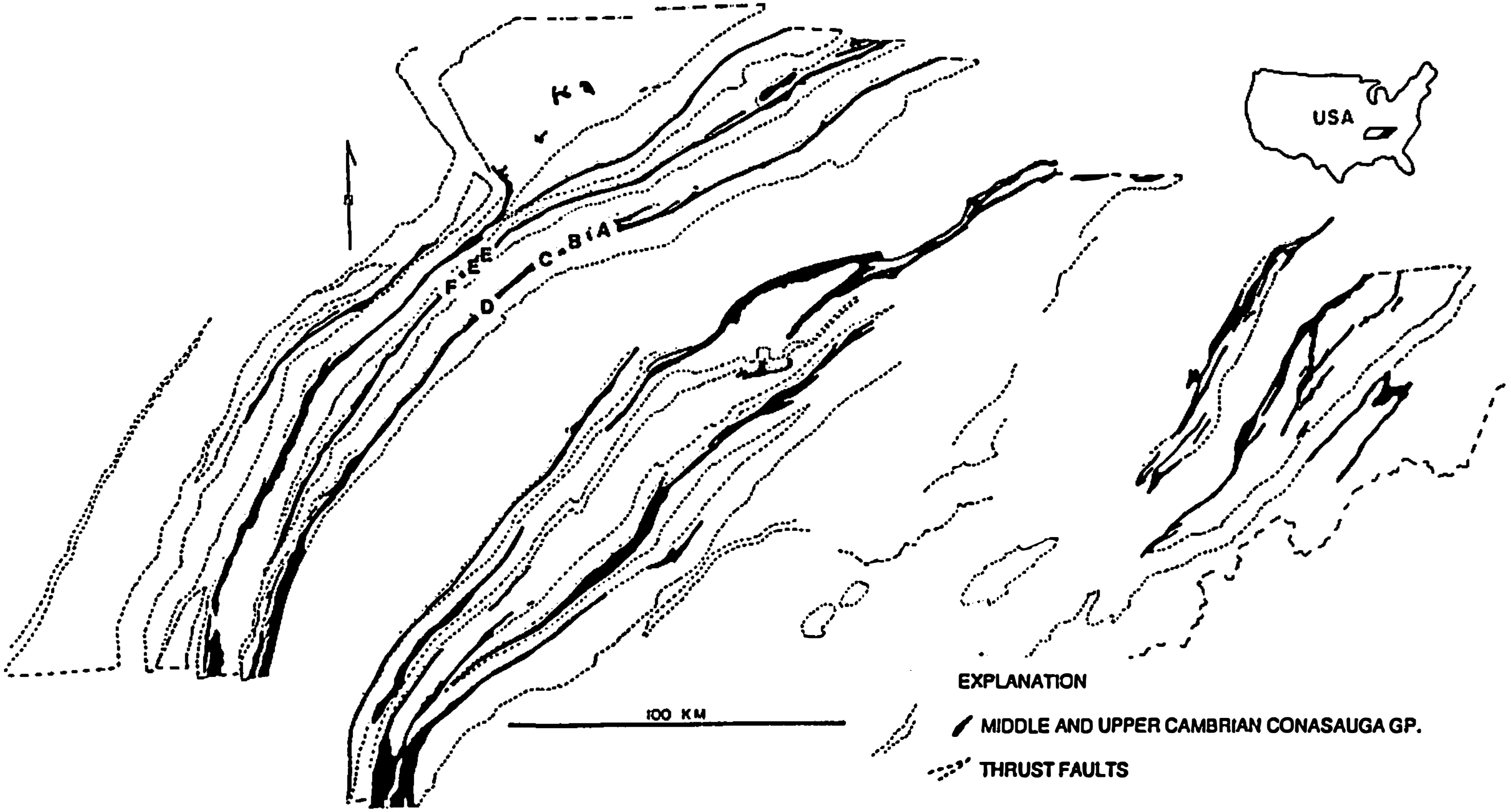

Figure 5.3. Palinspastic base map (after Roeder and Witherspoon, 1978) showing localities (A=Beech Grove, B=Roaring Spring, C=Interstate 75, D=Joy 2, E=Scarboro Road GW 130, E'=Scarboro Road GW131, and F=S-3 Pond)..

1. Microhummocky cross-stratification
2. Basal lags
3. Fining-upward sequences
4. Diffuse bed tops
5. Load structures
6. Shale drapes and lenses in thick grainstone units
7. Microconvoluted bedding
8. Amalgamated bedding
9. Sole marks
10. Gutter casts
11. Thin-bedded carbonate sand sheets as lateral extensions of thick lenticular buildups

Conversely, the Maynardville Limestone is similar in most cases to ancient tidally influenced deposits studied by Laporte (1967), Walker (1973), and many others. This interpretation is justified for the following origins for features common in the Maynardville.

1. Mudcracks form on subaerial exposure as wet sediments desiccate.
2. Sediment laminae of planar and domal stromatolites are trapped during episodic suspension transport.
3. Ooids, oncoids, and patch "reefs" (thrombolites) form in environments characterized by some degree of continuous turbulence.
4. Evaporites are not observed, suggesting sediments were not exposed for prolonged periods.

5. Transition from intertidal facies (cryptalgalaminates and stromatolites) to subtidal lithofacies (thrombolites, and oolitic and oncolitic lithologies) indicate horizontal changes in degree of exposure and therefore topographic relief (i.e., Figure 5.2 and Walther's Law).

Although any individual characteristic could be explained by nontidal mechanisms, an origin in the tidal regime provides the most parsimonious explanation for the suite of sedimentary features. No doubt storm events transported much sediment onto the tidal flat (e.g., Dott, 1974) and wind-generated waves must have also reworked sediment. These forces are associated with tidal environments. However, beaches and storm ridges, features diagnostic of wave and storm action on shores not strongly affected by tides (see Wright, 1984), are not observed in the Maynardville.

Depositional Model

The paleoenvironmental reconstructions proposed here are derived primarily from information found in Chapters 2 and 4, and the temporal and spatial distribution of lithofacies as revealed from the columnar sections in this Chapter. In central east Tennessee the Nolichucky/Maynardville sequence is subdivided into a slightly "deeper" intracratonic basin and a shallow intracratonic basin (Nolichucky Shale) (Figure 5.4), and a peritidal platform (Maynardville Limestone) (Figure 5.5). The lower 50 to 75 m of the Nolichucky Shale was deposited

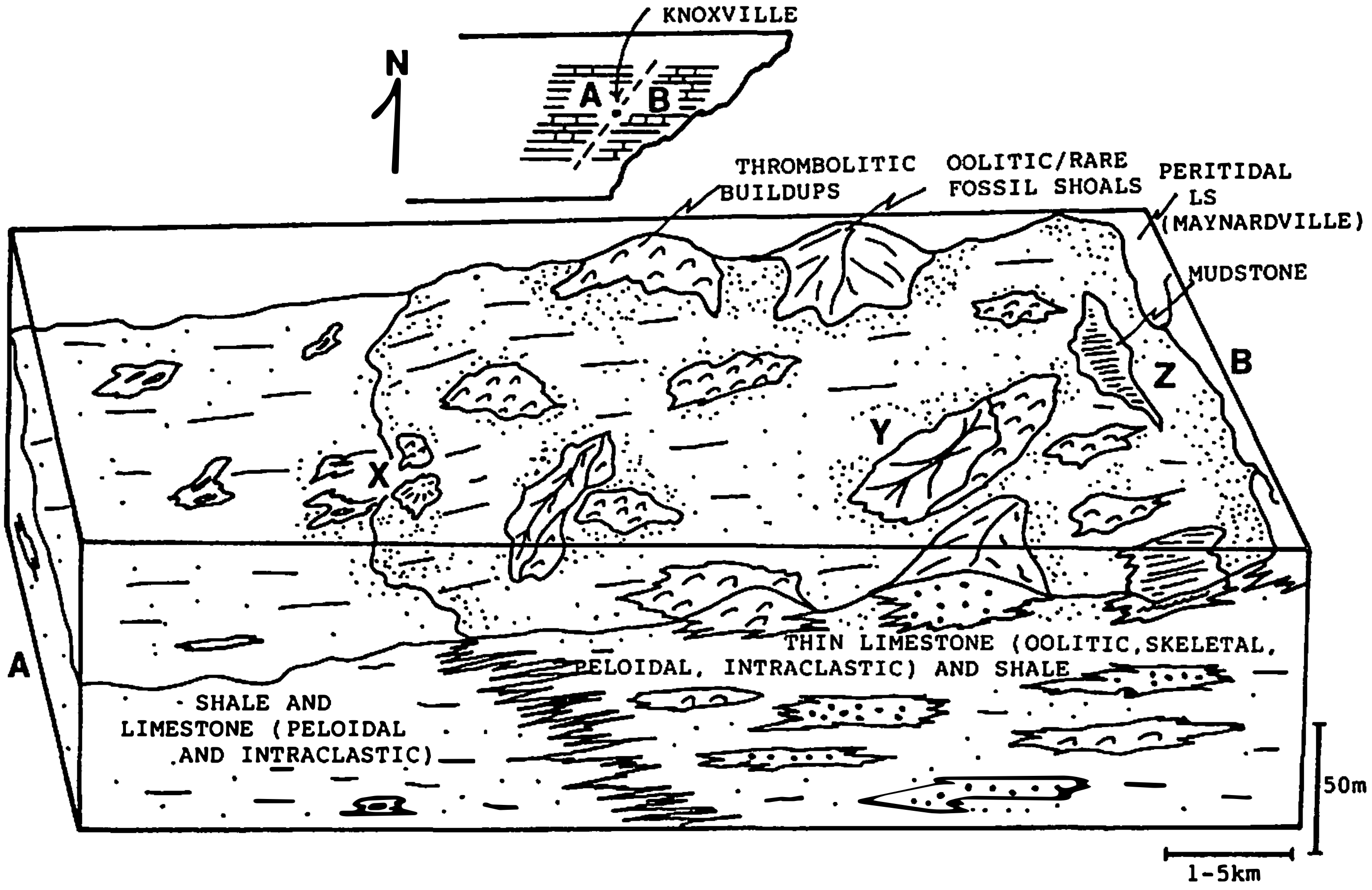

Figure 5.4. Generalized block diagram showing major lithofacies patterns and environments of the Nolichucky Shale. Note that the left portion of the reconstruction shows the "deeper" intracratonic basin; to the right (east) is the shallow intracratonic basin. Areas X, Y, and Z are shown in more detail in the block diagrams of Figures 5.6, 5.7, and 5.8.

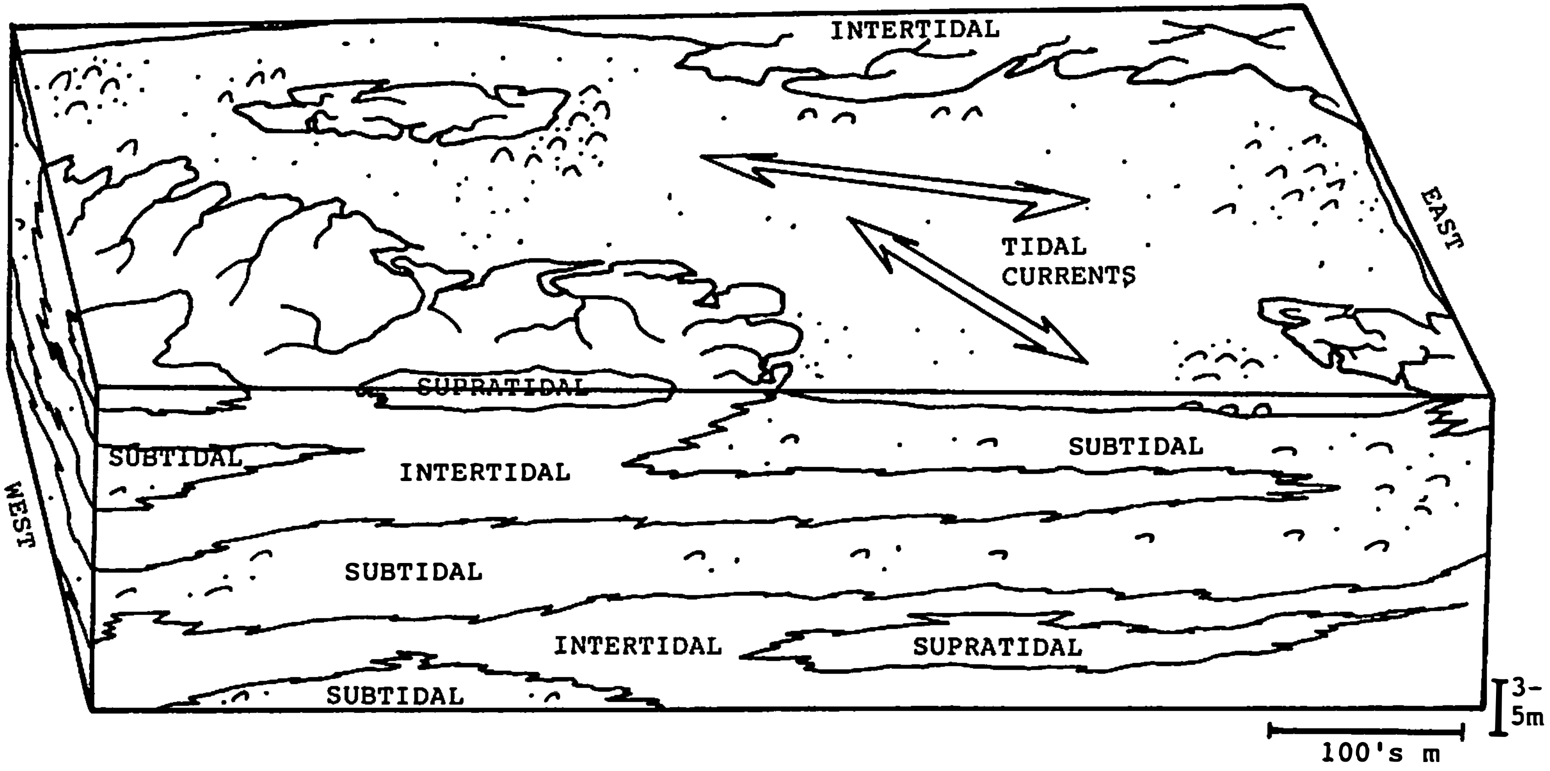

Figure 5.5. Three-dimensional reconstruction of the Maynardville Limestone. Broad low-relief islands (intertidal), local patch "reefs" (thrombolites) (subtidal), and oncolitic, oolitic, and peloidal (subtidal) limestone with a stratigraphic record of laterally discontinuous subtidal, intertidal, and rare supratidal deposits.

in water that was probably on the order of 30 to 50 m deep. Where the lower portion of the Nolichucky is exposed, it is characterized by shale and thin (< 5 cm) limestone interlayers (Figure 5.6). Limestone is primarily peloidal and intraclastic. Oscillatory currents associated with overhead-passing storm waves were barely able to rework the sediment into lenticular limestone interlayers, and the bases of these layers are commonly nonerosional. Carbonate layers are planar to low-angle cross-laminated, and fine upward, reflecting deposition from combined traction (bedload) and suspension fallout.

Above the lower portion of the Nolichucky Shale, an overall balance between sediment production/supply and relative sea level rise was maintained. Water depth ranged from a meter or less along shoal crests to 30+ m in adjacent subtidal areas. The shallow intracratonic basin was affected by storm and fairweather wave activity. Oolitic, fossiliferous, and thrombolitic shoals were deposited and accreted vertically in water depths above fairweather wave-base (Figure 5.7). As sea level was approached, carbonate production was diminished greatly or was terminated, and shoal development ceased. Continued subsidence and subsequent storm-generated sedimentation eventually buried these buildups.

Movement of unconsolidated or nonstabilized portions of the shoals resulted in migrating oolitic, skeletal, and intraclastic sand sheets of varying hydraulic regimes in association with storm waves and currents. Other facies of this basin display an abundance of features characteristic of storm-dominated settings (e.g., gutter casts, microhummocky

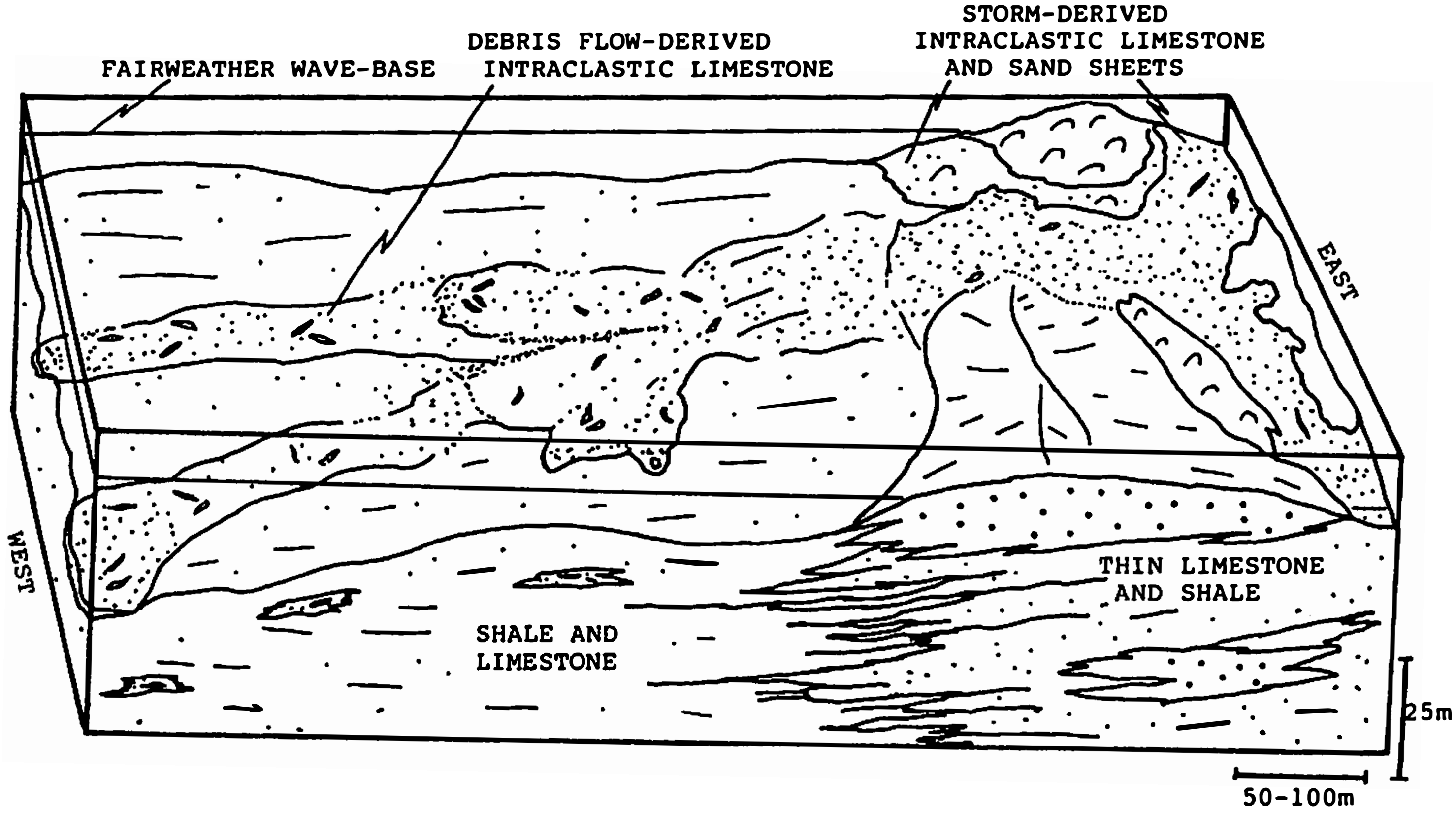

Figure 5.6. Detailed block diagram showing area "X" of Figure 5.4.

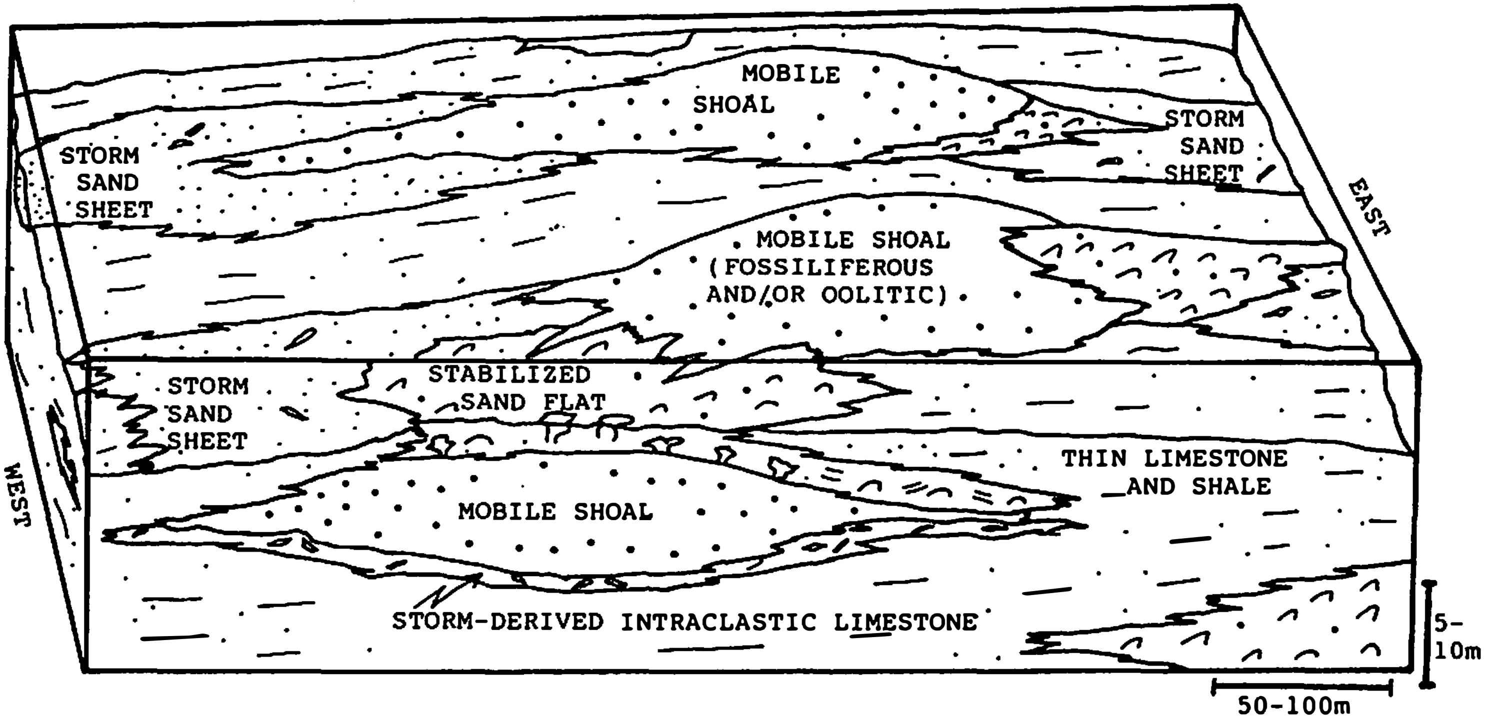

Figure 5.7. Detailed block diagram showing area "Y" of Figure 5.4.

cross-stratification, amalgamated beds, etc.) Also, thick accumulation of lime mudstone associated with subtidal cyanobacterial mats were deposited peripheral to a prograding peritidal carbonate platform (Figure 5.8).

In central east Tennessee the Maynardville Limestone was deposited in very shallow water (< 5 m) to locally emergent conditions. This interpretation differs significantly from the subtidal setting proposed by Markello and Read (1982) for the Maynardville in southwestern Virginia. They indicate that deposition took place further downslope, well below fairweather wave-base. In this study, the Maynardville is primarily composed of the Thrombolitic Lithofacies (see Figure 5.2).

The Maynardville Limestone represents small tidal flats that accreted vertically and moved laterally (Figure 5.5). Sediment production occurred in open water subtidal areas which were adjacent to tidal flats. Tides, storms, and fairweather waves transported sediment to nearby low-relief intertidal banks and to supratidal islands. In the Nolichucky, however, the majority of carbonate production occurred in and around shoals and within cyanobacterial mats. Storms were effective in moving carbonate sediment off the shoals and mats into adjacent subtidal areas. In addition, intense storms probably transported sediment from the peritidal carbonate platform (Maynardville) to the subtidal intracratonic basin (Nolichucky).

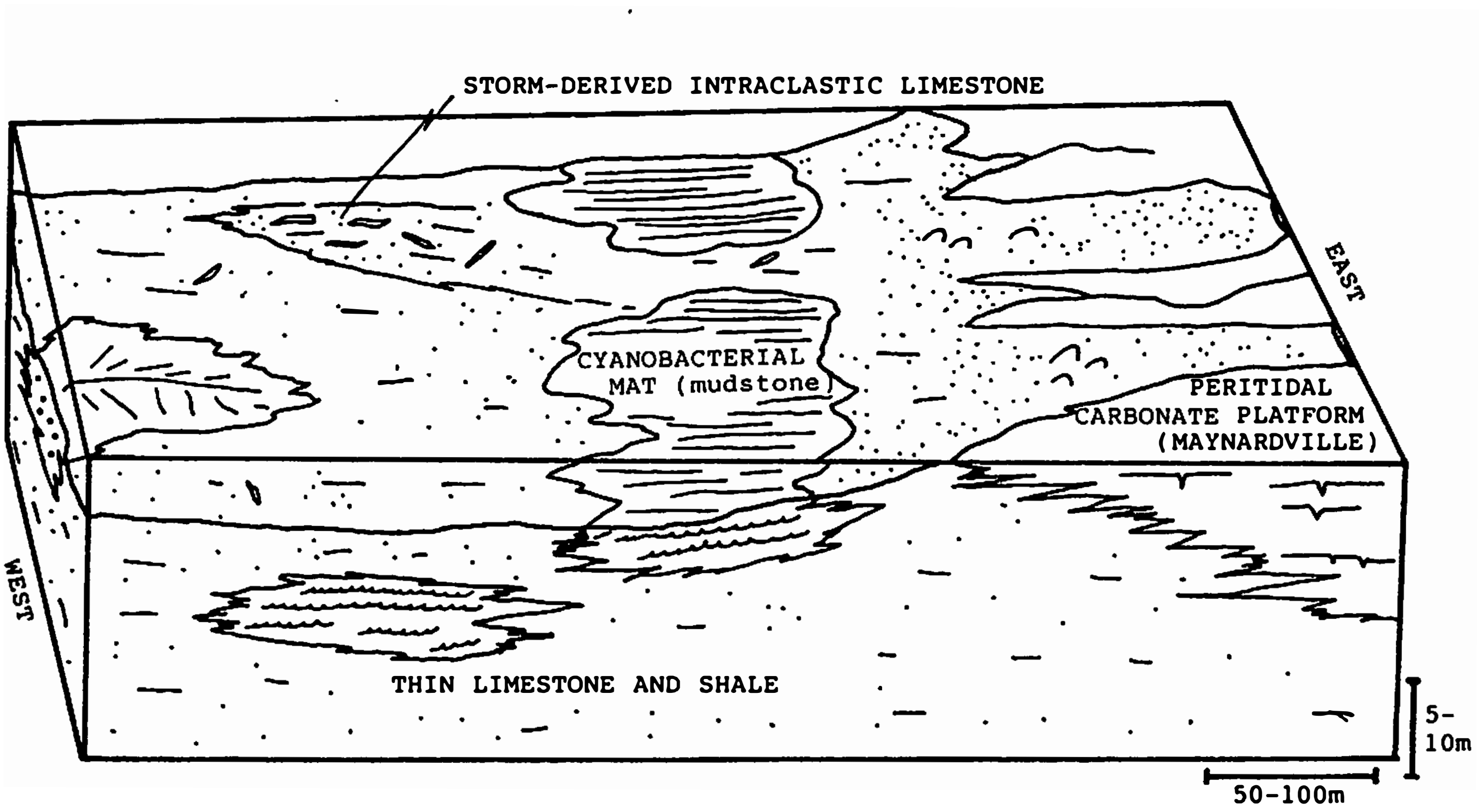

Figure 5.8. Detailed block diagram showing area "Z" of Figure 5.4.

CHAPTER 6

SUMMARY AND CONCLUSIONS

1. Within the Valley and Ridge of the southern Appalachians, Middle and Late Cambrian rocks crop out along a succession of southeastward dipping imbricate thrust sheets, which trend northeast-southwest. In the vicinity of Knoxville and Oak Ridge (central east Tennessee), Middle and Upper Cambrian formations (excluding the Copper Ridge Dolostone) comprise the Conasauga Group. From base to top the Conasauga Group includes: the Pumpkin Valley Shale, Rutledge Limestone, Rogersville Shale, Maryville Limestone, Nolichucky Shale, and Maynardville Limestone. The Conasauga Group grades from dominantly dolostone in the east (northeastern Tennessee and southwestern Virginia), through intercalated carbonate and shale units in the Knoxville and Oak Ridge area to a sequence dominated by shale, west and southwest of central east Tennessee (see Chapter 1).

2. Three complete trilobite zones are present in the upper Conasauga sequence. <u>Cedaria</u> and <u>Crepicephalus</u> Zones occur throughout much of the Nolichucky Shale, whereas the base of the overlying <u>Aphelaspis</u> Zone occurs in the upper portion of the Nolichucky Shale, and that zone continues through the Maynardville (see Chapter 1).

3. Conodonts are present in the Nolichucky Shale. The most abundant protoconodont is <u>Prooneotodus tenuis</u>. <u>Furnishina furnishi</u> is

the most dominant paraconodont. These forms are, however, long ranging and thus have little biostratigraphic significance (see Chapter 1).

4. The interbedded package of limestone, dolostone, and shale that makes up the Nolichucky Shale and Maynardville Limestone in central east Tennessee was deposited in the transition between an intracratonic basin (intrashelf basin, after Markello and Read, 1981 and 1982) and a shallow-water carbonate platform. The transition shows no marked change in regional paleoslope (see Chapters 1 and 5).

5. By early Late Cambrian (Nolichucky time), deltaic sediments (predominantly shale) were being shed into the basin (near present-day Lexington, Kentucky). The delta drained parts of northern Kentucky, Ohio, and perhaps southern Canada. At this time limestone was the dominant depositional product along the southern and eastern portion of the intracratonic basin. Between the areas dominated by shale and limestone is a zone of mixing where fine-grained siliciclastics and carbonates occur in subequal abundance. Central east Tennessee is located in the zone of mixed carbonate-siliciclastic deposition (see Chapter 1).

6. During deposition of the Maynardville Limestone in central east Tennessee, the intracratonic basin was cut off from the clastic source, and thus, became greatly constricted in size as limestone filled the basin. By late Maynardville time, the intracratonic basin shoaled to sea level (see Chapters 1 and 5).

7. Throughout much of east Tennessee, the Nolichucky Shale has been subdivided into a lower and upper shale. Between the shale

intervals is a regionally traceable unit known as the Bradley Creek Limestone Member. In the Knoxville and Oak Ridge vicinity this Member is not usually present (see Chapters 1 and 5).

8. The Maynardville is divided into two regionally persistent members: the Low Hollow Limestone Member and the Chances Branch Dolostone Member. Although this subdivision may be possible and appropriate in some areas of east Tennessee, in the Knoxville and Oak Ridge vicinity, placement of the contact between these members is extremely subjective and is not used in this investigation. The Chances Branch Member is characterized by an increase in the abundance of dolostone and fine-grained carbonate lithologies (stromatolites and cryptalgalaminates). Although an increase in dolostone is noted up-section, this increase is gradual and varies significantly from one nearby locality to another (see Chapters 1 and 5).

9. Fourteen major lithofacies are identified in the upper Conasauga Group. The assemblage of facies within the Nolichucky Shale differs significantly from that within the Maynardville Limestone. The Nolichucky contains an abundance of thick shale and thinly bedded shale and limestone lithologies, whereas the Maynardville is composed of very thick-bedded carbonate, predominantly limestone (see Chapter 2).

10. The Nolichucky Shale was deposited primarily in a subtidal setting. Water depth ranged from 5 to 50 m except along crests of shoals (oolitic, fossiliferous, and thrombolitic), where local emergence may have occurred (see Chapter 2).

11. The Maynardville consists primarily of thick-bedded oncolitic/oolitic grainstone, thrombolites, stromatolites, and cryptalgalaminates. In central east Tennessee the Maynardville was deposited above wave-base in very shallow water, less than 5 m deep. According to the model presented by Markello and Read (1982), in southwestern Virginia the Maynardville Limestone was deposited downslope from peritidal facies (Elbrook and/or Honaker Dolostone) in a subtidal setting. They indicate that deposition took place well below fairweather wave-base (see Chapters 2 and 5).

12. Overlying substitutability analysis, embedded Markov chain analysis, and modified autoassociation analysis applied to upper Conasauga Group lithologic data show that cyclicity is rare in the peritidal Maynardville Limestone. Subtidal limestone and shale facies within the Nolichucky Shale exhibit the most well-developed cycles. However, the majority of these cycles are "simple," involving no more than two lithologies (lithofacies). The absence of well-developed cycles within the Nolichucky/Maynardville sequence is attributed to local variability in the occurrence and distribution of lithologies (lithofacies). Local processes (i.e., storms and tides) were probably of prime importance in producing the simple cycles discerned (see Chapter 4).

13. In central east Tennessee the Nolichucky/Maynardville sequence is subdivided into a slightly "deeper" intracratonic basin (30-50 m, lower Nolichucky) and a shallow intracratonic basin (5-30 m, upper

Nolichucky), and a peritidal platform (0-5 m, Maynardville Limestone) (see Chapters 5 and 2).

14. The Nolichucky Shale was deposited in a storm-dominated paleoenvironmental setting. The majority of carbonate production occurred in and around shoals and within cyanobacterial mats. Storms were effective in moving carbonate sediment off the shoals and mats into adjacent subtidal areas. In addition, intense storms probably transported sediment from the peritidal carbonate platform (Maynardville) to the subtidal intracratonic basin (Nolichucky) (see Chapter 5).

15. The Maynardville Limestone represents small tidal flats that accreted vertically and migrated laterally. Sediment production occurred in open water subtidal areas which were adjacent to tidal flats. Tides, storms, and fairweather waves transported sediment to nearby low-relief intertidal banks and perhaps also down-ramp to the Nolichucky environments (see Chapter 5).

16. Paleoenvironmental reconstruction indicates that the distribution of facies along the Nolichucky/Maynardville bathymetric profile was much more irregular and mosaic-like than predicted by the depositional model of earlier workers (see Chapter 5).

LIST OF REFERENCES

LIST OF REFERENCES

Ager, D.V., 1974, Storm deposits in the Jurassic of the Moroccan High Atlas: Paleogeography, Paleoclimatology, Paleoecology, v. 15, p. 83-93.

Ahr, W.M., 1971, Paleoenvironment, algal structures, and fossil algae in the upper Cambrian of central Texas: Journal of Sedimentary Petrology, v. 41, p. 205-216.

Ahr, W.M., 1973, The carbonate ramp: an alternative to the shelf model: Transactions of the Geological Society of the Gulf Coast Association, 23rd Annual Convention, p. 221-225.

Aigner, T., 1982, Calcareous tempestites: strom-dominated stratification in Upper Muschelkalk limestones (Middle Trias, SW-Germany), in Einsele, G. and Seilacher, A., eds., Cyclic and Event Stratification: Springer-Verlag, New York, p. 180-198.

Aigner, T., 1985, Storm Depositional Systems: Berlin, Springer Verlag, 174 p.

Aitken, J.D., 1966, Middle Cambrian to Middle Ordovician cyclic sedimentation, southern Rocky Mountains of Alberta: Bulletin of Canadian Petroleum Geology, v. 14, p. 405-441.

Aitken, J.D., 1967, Classification and environmental significance of cryptalgal limestones and dolomites, with illustrations from the Cambrian and Ordovician of southwest Alberta: Journal of Sedimentary Petrology, v. 37, p. 1163-1178.

Aitken, J.D., 1978, Revised models for depositional grand cycles, Cambrian of the southern Rocky Mountains: Bulletin of Canadian Petroleum Geology, v. 26, p. 515-542.

Alberstadt, L.P. and Reesman, A.L., 1978, Significance of authigenic K-feldspar in Cambrian-Ordovician carbonate rocks of the Proto-Atlantic shelf in North America: additional comments regarding the southeastern United States (discussion): Journal of Sedimentary Petrology, v. 48, p. 679-683.

Allen, J.R.L., 1984, Sedimentary Structures: Their Character and Physical Basis: Elsevier, Amsterdam, 663 p.

Allen, P.A., 1982, Cyclicity of Devonian fluvial sedimentation, Cunningsburgh Peninsula, SE Shetland: Geological Society of London Quarterly Journal, v. 139, pt. 1, p. 49-58.

Ammermann, M.L. and Keller, G.R., 1979, Delineation of Rome trough in eastern Kentucky by gravity and deep drilling data: American Association of Petroleum Geologists Bulletin, v. 63, p. 341-353.

An, T., 1981, Recent progress in Cambrian and Ordovician conodont biostratigraphy of China, in Teichert, C., Liu, L., and Chen, P., (eds.), Paleontology in China, 1979: Geological Society of America Special Paper 187, p. 209-225.

An, T., 1982, Study of the Cambrian conodonts from North and Northeast China: University of Tsukuba, Science Reports of the Institute of Geoscience, Section B, v. 3, p. 113-159.

Anderson, E.J., 1972, Sedimentary structure assemblages in transgressive and regressive calcarenites: 24th International Geological Congress, Montreal, Section 6, p. 369-378.

Anderson, T.W., and Goodman, L.A., 1957, Statistical inference about Markov chains: Annals of Mathematical Statistics, v. 28, p. 89-110.

Ball, M.M., 1967, Carbonate sand bodies of Florida and the Bahamas: Journal of Sedimentary Petrology, v. 37, p. 556-591.

Bathurst, R.G.C., 1975, Carbonate Sediments and Their Diagenesis: Developments in Sedimentology 12: Elsevier, Amsterdam, 658 p.

Bauld, J., 1981, Occurrence of benthic microbial mats in saline lakes: Hydrobiologia, v. 81, p. 87-111.

Bearce, D.N. and McKinney, F.K., 1977, Archeocyathids in east Alabama: Significance to the geologic interpretation of the Coosa deformed belt: Geology, v. 5, p. 467-470.

Bearce, D.N., 1977, Stratigraphic problems of the eastern Coosa Valley, in Bearce, D.N. (ed.), Cambrian and Devonian Stratigraphic Problems of Eastern Alabama: Alabama Geological Society Guidebook, 15th Annual Field Trip, p. 37-53.

Beardsley, R.W. and Cable, M.S., 1983, Overview of the evolution of the Appalachian Basin: Northeastern Geology, v. 5, p. 137-145.

Bell, G., 1978, Paleontology of the Conasauga Formation in Jefferson County, in Kidd, J.T. and Shannon, S.W., (eds.), Stratigraphy and Structure of the Birmingham Area, Jefferson County, Alabama: Alabama Geological Society Guidebook, 16th Annual Field Trip, p. 87-92.

Bird, J.M. and Dewey, J.F., 1970, Lithosphere plate continental margin tectonics and the evolution of the Appalachian Orogen, Geological Society America Bulletin, v. 81, p. 1031-1060.

Brasier, M.D., 1980, Microfossils: George Allen and Unwin, London, 193 p.

Brenchley, P.J., 1985, Storm influenced sandstone beds: Modern Geology, v.9, p. 369-396.

Brenchley, P.J., Newall, G., Stanistreet, I.G., 1979, A storm surge origin for sandstone beds in an epicontinental platform sequence, Ordovician, Norway: Sedimentary Geology, v. 22, p. 185-217.

Brenner, R.L. and Davies, D.K., 1973, Storm generated coquinoid sandstone: genesis of high energy marine sediments from the Upper Jurassic of Wyoming and Montana: Geological Society of America Bulletin, v. 84, p. 1685-1697.

Bridge, J., 1956, Stratigraphy of the Mascot-Jefferson City zinc district, Tennessee: U.S. Geological Survey Professional Paper 277, 76 p.

Brown, M.B., 1974, Identification of sources of significance in two-way contingency tables: Applied Statistics, v. 23, p. 405-413.

Brown, M.B., 1979, Two-way frequency tables, empty cells, and departures from independence, in Dixon, W.J., and Brown, M.B., eds., BMDP Statistical Software Manual: Los Angeles, University of California Press, p. 278-296.

Brown, M.B., 1985, Two-way and multiway frequency tables: measures of association and the log-linear model (complete and incomplete tables), in Dixon, W.J., ed., BMDP statistical software manual: Los Angeles, University of California Press, p. 143-206.

Brown, R.G. and Woods, P.J., 1974, Sedimentation and tidal-flat development, Nilemah Embayment, Shark Bay, Western Australia, in Logan, B.W. and others, Evolution and Diagenesis of Quaternary Carbonate Sequences, Shark Bay, Western Australia: American Association of Petroleum Geologists Memoir 22, p. 316-340.

Burne, R.V. and Moore, L.S., 1987, Microbialites: Organosedimentary deposits of benthic microbial communities: Palaios, v. 2, p. 241-254.

Busch, R.M., 1983, Sea level correlation of punctuated aggradational cycles (PACs) of the Manlius Formation, central New York: Northeastern Geology, v. 5, p. 82-91.

Busch, R.M., and Rollins, H.B., 1984, Correlation of Carboniferous strata using a hierarchy of transgressive-regressive units: Geology, v. 12, p. 471-474.

Busch, R.M., and West, R.R., 1987, Hierarchal genetic stratigraphy: A framework for paleoceanography: Paleoceanography, v. 2, p. 141-164.

Busch, R.M., West, R.R., Barrett, F.J., and Barrett, T.R., 1985, Cyclothems versus a hierarchy of transgressive-regressive units, in Watney, W.L., Kaesler, R.L., and Newell, K.D., eds., Recent interpretations of late Paleozoic cyclothems: Society of Economic Paleontologists and Mineralogists, Mid-Continent Section, Proceeding of Third Annual Meeting and Field Conference, October 11-13, 1985, Lawrence, Kansas.

Buschbach, T.C., 1964, Cambrian and Ordovician strata of northeastern Illinois: Illinois Geological Survey, Report Investigation 218, 90 p.

Buschbach, T.C., 1970, Cambrian and Ordovician strata of north-central Illinois, in 34th Annual Tri-State Field Conference Guidebook: Northern Illinois University, Dekalb, p. 27-30.

Bush, J.H., and Fischer, H.J., 1981, Stratigraphic and depositional summary of middle and upper Cambrian strata in northeastern Washington, northern Idaho, and northwestern Montana, in Taylor, M.E., ed., Short Papers for the Second International Symposium on the Cambrian System, U.S.Geological Survey Open-File Report 81-743, p. 67-70.

Butts, C., 1926, Paleozoic rocks, in Adams, G.I., Butts, C., Stephenson, L.W., and Cooke, W.J., (eds.), Geology of Alabama: Alabama Geological Survey Special Report 14, p. 1-229.

Butts, C., 1940, Geology of the Appalachian valley in Virginia: Virginia Geological Survey Bulletin 52, 568 p.

Butts, C., 1941, Geology of the Appalachian valley in Virginia: Virginia Geological Survey Bulletin 52, part 2, 271 p.

Calvert, W.L., 1962, Sub-Trenton rocks from Lee County, Virginia to Fayette County, Ohio: Ohio Geological Survey Report Investigation 45, 57 p.

Carr, T.R., 1982, Log-linear models, Markov chains and cyclic sedimentation: Journal of Sedimentary Petrology, v. 52, p. 905-912.

Chafetz, H.S., 1986, Marine peloids: a product of bacterially induced precipitation of calcite: Journal of Sedimentary Petrology, v. 56, p. 812-817.

Chayes, F., 1956, Petrographic Modal Analysis: Allen and Urwin, London, 193 p.

Chow, N. and James, N.P., 1987a, Cambrian grand cycles: A northern Appalachian perspective: Geological Society of America Bulletin, v. 98, p. 418-429.

Chow, N. and James, N.P., 1987b, Facies-specific, calcitic and bimineralic ooids from Middle and Upper Cambrian platform carbonates, western Newfoundland, Canada: Journal of Sedimentary Petrology, v. 57, p. 907-921.

Clendening, J.A., 1978, Cambrian acritarchs from eastern Tennessee and western Virginia, U.S.A. (abs.): Palynology, v. 2, p. 216.

Clifton, H.E., 1981, Progradational sequences in Miocene shoreline deposits, southeastern Caliente Range, California: Journal of Sedimentary Petrology, v. 51, p. 165-184.

Colton, G.W., 1970, The Appalachian basin; its depositional sequences and their geological relationships, in Fisher, G.W., and others, (eds.), Studies of Appalachian Geology; Central and Southern: John Wiley, New York, p. 5-43.

Coniglio, M. and James, N.P., 1985, Calcified algae as sediment contributors to early Paleozoic limestones: evidence from deep-water sediments of the Cow Head Group, western Newfoundland: Journal of Sedimentary Petrology, v. 55, p. 746-754.

Cook, H.E. and Mullins, H.T., 1983, Basin margin, in Scholle, P.A., Bebout, D.G., and Moore, C.H., eds., Carbonate Depositional Evnironments: American Association of Petroleum Geologists Memoir 33, 708 p.

Cook, H.E. and Taylor, M.E., 1977, Comparison of continental slope and shelf environments in the upper Cambrian and lowest Ordovician of Nevada, in Cook, H.E. and Enos, P., (eds.), Deep-Water Carbonate Environments: Society of Economic Paleontologists and Mineralogists Special Publication 25, p. 51-81.

Cook, T.D. and Bally, A.W., 1975, Stratigraphic Atlas of North and Central America: Princeton University Press, 272 p.

Crevello, P.D. and Schlager, W., 1980, Carbonate debris sheets and turbidites, Exuma Sound, Bahamas: Journal of Sedimentary Petrology, v. 50, p. 1121-1148.

Crowell, J.C., 1978, Gondwana glaciation, cyclothems, continental positioning, and climate changes: American Journal of Science, v. 278, p. 1345-1372.

Curray, J.R., 1965, Late Quarternary history, continental shelves of the United States, in Wright, H.E. and Frey, D.G., eds., The Quaternary of the United States, Princeton University Press, New Jersey, p. 723-735.

Davies, G.R., 1970, Algal-laminated sediments, Gladstone Embayment, Shark Bay, Western Australia, in Logan, B.W., and others, Carbonate Sedimentation and Environments, Shark Bay, Western Australia: American Association of Petroleum Geologists Memoir 13, p. 169-205.

Davis, J.C. and Cocke, I.M., 1972, Interpretation of complex succession by substitutability analysis, in Merriam, D.F. (ed.), Mathematical Models of Sedimentary Processes: Plenum, New York, 271 p.

Davis, J.C., 1986, Statistics and Data Analysis in Geology (second edition): New York, John Wiley and Sons, 646 p.

Dean, W.E., Gardiner, J.V., Jansa, L.F., Cepek, P., and Seibold, E., 1977, Cyclic sedimentation along the continental margin of northwest Africa, in Lancelot, Y., Siebold, E., and others, eds., Initial Reports of the Deep Sea Drilling Project, v. XLI: Washington, D.C., U.S. Government Printing Office, p. 965-989.

Demicco, R.V., 1983, Wavy and lenticular-bedded carbonate ribbon rocks of the upper Cambrian Conococheague Limestone, central Appalachians: Journal of Sedimentary Petrology, v. 53, p. 1121--1132.

Demicco, R.V., 1985, Platform and off-platform carbonates of the upper Cambrian of western Maryland, U.S.A.: Sedimentology, v. 32, p. 1-22.

Denison, R.E., Lidiak, E.G., Bickford, M.E., and Kisvarsanyi, E.B., 1984, Geology and geochronology of Precambrian rocks in the Central Interior Region of the United States: U.S. Geological Survey Professional Paper 1241-C, p. C14-C17.

DeRaaf, J.F.M., Boersma, J.R., and van Gelder, A., 1977, Wave-generated structures and sequences from a shallow marine succession, Lower Carboniferous, County Cork, Ireland: Sedimentology, v. 24, p. 451-483.

Derby, J.R., 1965, Paleontology and stratigraphy of the Nolichucky Formation in southeast Virginia and northeast Tennessee: unpublished Ph.D. dissertation, Virginia Polytechnic Institute and State University, Blacksburg, 465 p.

Dickson, J.A., 1966, Carbonate identification and genesis as revealed by staining: Journal of Sedimentary Petrology, v. 36, p. 491-505.

Donovan, D.T., and Jones, E.J.W., 1979, Causes of world-wide changes in sea level: Journal of the Geological Society of London, v. 136, p. 187-192.

Dott, R.H., 1974, Cambrian tropical storm waves in Wisconsin: Geology, v. 2, p. 243-246.

Dott, R.H. and Bourgeois, J., 1982, Hummocky stratification: significance and its variable bedding sequence: Geological Society of America Bulletin, v. 93, p. 663-680.

Doveton, J.H., 1971, An application of Markov chain analysis to the Ayrshire coal measures succession: Scottish Journal of Geology, v. 7, no. 1, p. 11-27.

Doveton, J.H., and Skipper, K., 1974, Markov chain and substitutability analysis of a turbidite succession, Cloridorme Formation (Middle Ordovician), Gasp_, Qu_b_c: Canadian Journal of Earth Science, v. 11, p. 472-488.

Downie, C., 1984, Acritarchs in British stratigraphy: Geological Society of London Special Report 17, 26 p.

Drake, D.E., 1976, Suspended sediment transport and mud deposition on continental shelves, in Stanley, D.J. and Swift, D.J.P., eds., Marine Sediment Transport and Environmental Management: Wiley, New York, p. 127-158.

Driese, S.G., and Dott, R.H., 1984, Model for sandstone-carbonate "cyclothems" based on upper Member of Morgan Formation (Middle Pennsylvanian) of northern Utah and Colorado: American Association of Petroleum Geologists Bulletin, v. 68, p. 574-597.

Driese, S.G. and Dott, R.H., 1986, Model for sandstone-carbonate "cyclothems" based on upper Member of Morgan Formation (Middle Pennsylvanian) of northern Utah and Colorado: Reply: American Association of Petroleum Geologists Bulletin, v. 70, p. 206.

Duff, P. McL.D., Hallam, A., and Walton, E.K., 1967, Cyclic Sedimentation: Amsterdam, Elsevier, 280 p.

Dunham, R.J., 1962, Classification of carbonate rocks according to depositional texture, in Ham, W.E., ed., Classification of carbonate rocks: American Association of Petroleum Geologists Memoir 1, p. 108-121.

Dzulynski, S. and Kotlarczyk, J., 1962, On load casted ripples: Annals of the Geological Society of Pologne, v. 32, p. 148-159.

Einsele, G. and Seilacher, A., eds., 1982, Cyclic and Event Stratification: Springer-Verlag, Berlin, 536 p.

Eliuk, L.S., 1978, The Abenaki Formation, Nova Scotia Shelf, Canada-a depositional and diagenetic model for a Mesozoic carbonate platform: Bulletin of Canadian Petroleum Geology, v. 26, p. 424-514.

Erwin, P.N., 1981, Stratigraphy, depositional environments, and dolomitization of the Maryville and upper Honaker Formations (Cambrian), Tennessee and Virginia: unpublished M.S. thesis, Duke University, 232 p.

Evans, G., Murray, J.W., Biggs, H.E.J., Bate, R., and Bush, P.R., 1973, The oceanography, ecology, sedimentology, and geomorphology of parts of the Trucial Coast barrier island complex, Persian Gulf, in Purser, B.H., ed., The Persian Gulf: Holocene Carbonate Sedimentation and Diagenesis in a Shallow Epicontinental Sea: Springer-Verlag, New York, p. 233-277.

Flugel, E., 1982, Microfacies Analysis of Limestone: Springer-Verlag, New York, 633 p.

Foreman, J.L., Weber, L.J., and Walker, K.R., 1988, Diagenetic patterns in a Late Cambrian oolite shoal, Nolichucky Formation, east Tennessee: Southeastern Sectional Meeting of the Geological Society of America, Columbia, South Carolina.

Freeman, L.B., 1953, Regional subsurface stratigraphy of the Cambrian and Ordovician in Kentucky and vicinity: Kentucky Geological Survey, Series 9, Bulletin 12, 352 p.

Friedman, G.M., 1980, Dolomite is an evaporite mineral: evidence from the rock record and from sea marginal ponds of the Red Sea, in Zenger, D.H., Dunham, J.B., and Ethington, R.L., eds., Concepts and Models of Dolomitization: Society of Economic Paleontologists and Mineralogists Special Publication No. 28, p. 69-80.

Friedman, G.M. and Radke, B., 1979, Evidence for sabkha overprint and conditions of intermittent emergence in Cambrian-Ordovician carbonates of northeastern North America and Queensland, Australia: Northeastern Geology, v. 1, p. 18-42.

Gebelein, C.D., 1976, Open marine subtidal and intertidal stromatolites (Florida, The Bahamas and Bermuda), in Walter, M.R., ed., Stromatolites: Elsevier, New York, p. 381-388.

Gilbert, O.E., 1981, Paleozoic evolution of the Valley and Ridge thrust belt in Alabama: unpublished Ph.D. dissertation, University of Tennessee, Knoxville, 295 p.

Gingerich, P.D., 1969, Markov analysis of cyclic alluvial sediments: Journal of Sedimentary Petrology, v. 39, p. 330-332.

Ginsburg, R.N., 1960, Ancient analogues of Recent stromatolites: 21st International Geological Congress Report, Part 22, p. 26-35.

Ginsburg, R.N., Isham, L.B., Bein, S.J., and Kuperburg, J., 1954, Laminated algal sediments of South Florida and their recognition in the fossil record: unpublished report No. 54-21, Coral Gables, Florida, Marine Laboratory, University of Miami, 337 p.

Goldhammer, R.K., Dunn, P.A., and Hardie, L.A., 1987, High frequency glacio-eustatic sea level oscillations with Milankovitch characteristics recorded in Middle Triassic platform carbonates in N. Italy: American Journal of Science (in press).

Goldring, R. and Aigner, T., 1982, Scour and fill: the significance of event separation, in Einsele, G. and Seilacher, A., eds., Cyclic and Event Stratification: Springer-Verlag, Berlin, p. 355-362.

Goldring, R. and Bridges, P., 1973, Sublittoral shelf sandstones: Journal of Sedimentary Petrology, v. 43, p. 736-747.

Haase, C.S., Walls, E.C., and Farmer, C.D., 1985, Stratigraphic and structural data for the Conasauga Group and Rome Formation on the Copper Creek fault block near Oak Ridge, Tennessee: Preliminary results from test borehole ORNL-Joy 2: Oak Ridge, Tennessee, Oak Ridge National Laboratory ORNL/TM-9159.

Hagan, G.M. and Logan, B.W., 1974, Development of carbonate banks and hypersaline basins, Shark Bay, Western Australia, in Logan, B.W. and others, Evolution and Diagenesis of Quaternary Carbonate Sequences, Shark Bay, Western Australia: American Association of Petroleum Geologists Memoir 22, p. 61-139.

Hall, G.M. and Amick, H.C., 1934, The section on the west side of Clinch Mountain, Tennessee: Tennessee Academy of Science Journal, v. 9, p. 157-168 and 195-220.

Hallam, A., 1977, Secular changes in marine inundation of USSR and North America through the Phanerozoic: Nature, v. 269, p. 769-772.

Hamblin, A.P. and Walker, R.G., 1979, Storm-dominated shallow marine deposits: the Fernie-Kootenay (Jurassic) transition, southern Rocky Mountains: Canadian Journal of Earth Science, v. 16, p. 1673-1690.

Hampton, M.A., 1972, The role of subaqueous debris flow in generating turbidity currents: Journal of Sedimentary Petrology, v. 42, p. 775-793.

Harbaugh, J.W., and Bonham-Carter, G., 1970, Computer Simulation in Geology: New York, John Wiley and Sons, Inc., 575 p.

Hardeman, W.D., Miller, R.A., and Swingle, G.D., 1966, Geologic map of Tennessee, east sheet: Tennessee Division of Geology, State Geologic Map, sheet 1 of 4.

Hardie, L.A., ed., 1977, Sedimentation on the Modern Carbonate Tidal Flats of Northwest Andros Island, Bahamas: Johns Hopkins University Studies in Geology, no. 22, 202 p.

Hardie, L.A. and Ginsburg, R.N., 1977, Layering: the origin and environmental significance of lamination and thin bedding, in Hardie, L.A., ed., Sedimentation on the Modern Carbonate Tidal Flats of Northwest Andros Island, Bahamas: Johns Hopkins University Studies of Geology, v. 22, p. 50-123.

Harms, J.C., Southard, J.B., Spearing, D.R., and Walker, R.G., 1975, Depositional environments as interpreted from primary sedimentary structures and stratification sequences: Society of Economic Paleontologists and Mineralogists Short Course No. 2, 161 p.

Harris, L.D., 1964, Facies relations of exposed Rome Formation and Conasauga Group of northeastern Tennessee with equivalent rocks in the subsurface of Kentucky and Virginia: U.S. Geological Survey Profession Paper 501-B, p. B25-B29.

Harris, L.D., 1965, Geologic map of the Tazewell quadrangle, Claiborne County, Tennessee: U.S. Geological Survey Map GQ-465.

Harris, L.D., 1969, Kingsport Formation and Mascot Dolomite (Lower Ordovician) of east Tennessee: Tennessee Division of Geology, Report of Investigations, no. 23, p. 1-39.

Harris, L.D., 1973, Dolomitization model for upper Cambrian and lower Ordovician carbonate rocks in the eastern United States: U.S. Geological Survey Journal of Research, v. 1, p. 63-78.

Harris, L.D. and Mixon, R.B., 1970, Geologic map of the Howard Quarter quadrangle, northeastern Tennessee: U.S. Geological Survey Geological Quadrangle Map GQ-842.

Harris, P.M., 1979, Facies anatomy of a Bahamian ooid shoal: Sedimenta VII, The Comparative Sedimentology Laboratory, The University of Miami, 163 p.

Hasson, K.O. and Haase, C.S., 1988, Lithofacies and paleogeography of the Conasauga Group (Middle and Late Cambrian) in the Valley and Ridge Province of east Tennessee: Geological Society of America Bulletin, v. 100, p. 234-246.

Hatcher, R.D., 1978, Tectonics of the western Piedmont and Blue Ridge, southern Appalachians: rewiew and speculation: American Journal of Science, v. 278, p. 276-304.

Hattori, I., 1976, Entropy in Markov chain and discrimination of cyclic patterns in lithologic succession: Journal of Mathematical Geology, v. 8, no. 4, p. 477-497.

Havryluk, Thor, 1963, The geology and petrographic study of the Bean Station area, Grainger and Hawkins Counties Tennessee: unpublished M.S. thesis, University of Tennessee, Knoxville, 49 p.

Hayes, M.O., 1967, Hurricanes as geological agents-case studies of Hurricanes Carla, 1961 and Cindy, 1963: Bureau of Economic Geology, Texas Report of Investigations 61, 56 p.

Heckel, P.H., 1980, Paleogeography of eustatic model for deposition of midcontinent upper Pennsylvanian cyclothems, in Fouch, T.D., and Magathan, E.R., eds., Paleozoic paleogeography of the west-central United States: Rocky Mountain Section of the Society of Economic Paleontologists and Mineralogists, p. 197-217.

Heckel, P.H., 1986, Sea-level curve for Pennsylvanian eustatic marine transgressive-regressive depositional cycles along midcontinent outcrop belt, North America: Geology, v. 14, p. 330-334.

Heller, P.L., Komar, P.D., and Pevear, D.R., 1980, Transport processes in ooid genesis: Journal of Sedimentary Petrology, v. 50, p. 943-952.

Helton, Walter, L., 1967, Lithostratigraphy of the Conasauga Group between Rogersville and Kingsport, Tennessee: unpublished Ph.D. dissertation, University of Tennessee, Knoxville, 94 p.

Hine, A.C., 1977, Lily Bank, Bahamas: History of an active oolite sand shoal: Journal of Sedimentary Petrology, v. 47, p. 1554-1581.

Hine, A.C., Wilber, R.J., and Neuman, A.C., 1981, Carbonate sand bodies along contrasting shallow bank margins facing open seaways in northern Bahamas: American Association of Petroleum Geologists Bulletin, v. 65, p. 261-290.

Hiscott, R.N., 1981, Chi-square tests for Markov chain analysis: Journal of Mathematical Geology, v. 13, no. 1, p. 69-80.

Hiscott, R.N. and James, N.P., 1985, Carbonate debris flows, Cow Head Group, Western Newfoundland: Journal of Sedimentary Petrology, v. 55, p. 735-745.

Hoffman, P., 1976, Environmental diversity of middle Precambrian stromatolites, in Walter, M.R., ed., Stromatolites, Developments in Sedimentology, Elsevier, New York, p. 599-613.

Holloway, S., 1983, The shell-detrital calcirudites of the Forest Marble Formation (Bathonian) of southwest England: Proceedings of the Geological Association, v. 94, p. 259-266.

Howe, J.R. and Thompson, T.L., 1984, Tectonics, sedimentation, and hydrocarbon potential of the Reelfoot rift: Oil and Gas Journal, v. 12, p. 179-190.

Howell, B.F. and Mason, J.F., 1938, Correlation of Middle Cambrian faunas of North America: Journal of Paleontology, v. 12, p. 295-297.

Hubert, J.F., Sucheki, R.K., and Callahan, R.K.M., 1977, The Cow Head Breccia: sedimentology of the Cambro-Ordovician continental margin, Newfoundland, in Cook, H.E. and Enos, P., (eds.), Deep-Water Carbonate Environments: Society of Economic Paleontologists and Mineralogists Special Publication 25, p. 125-154.

Ingram, R.L., 1954, Terminology for the thickness of stratification and parting units in sedimentary rocks: Geological Society of America Bulletin, v.65, p. 937-938.

Irwin, M.L., 1965, General theory of epeiric clear water sedimentation: American Association of Petroleum Geologists Bulletin, v. 49, p. 445-459.

James, N.P., 1979, Shallowing-upward sequences in carbonates, in Walker, R.G., ed., Facies Models: first edition, Geoscience Canada Reprint Series 1, p. 109-121.

James, N.P., 1984, Shallowing-upward sequences in carbonates, in Walker, R.G., ed., Facies models (second edition), Geoscience Canada Reprint Series 1, p. 213-228.

James, N.P. and Kobluk, D.R., 1978, Lower Cambrian patch reefs and associated sediments; southern Labrador, Canada: Sedimentology, v. 25, p. 1-35.

Janssens, A., 1973, Stratigraphy of the Cambrian and lower Ordovician rocks in Ohio: Ohio Geological Survey Bulletin 64, 197 p.

Jones, B. and Dixon, O.A., 1976, Storm deposits in the Read Bay Formation (upper Silurian), Somerset Island, Arctic Canada (An application of Markov chain analysis): Journal of Sedimentary Petrology, v. 46, no. 2, p. 393-401.

Keith, B.D. and Friedman, G.M., 1977, A slope-basin-plain model, Taconic sequence, New York and Vermont: Journal of Sedimentary Petrology, v. 47, p. 1220-1241.

Keller, G.R. and others, 1975, Possible Precambrian rifting in the southeast United States (abs.): American Geophysical Union Transactions, v. 56, p. 602.

Kelling, G. and Mullin, P.R., 1975, Graded limestones and limestone-quartzite couplets: possible storm-deposits from the Moroccan Carboniferous: Sedimentary Geology, v. 13, p. 161-190.

Kendall, C.G.St.C. and Skipwith, P.A., d'E., 1968, Recent algal mats of a Persian Gulf lagoon: Journal of Sedimentary Petrology, v. 38, p. 1040-1058.

Kennard, J.M., and James, N.P., 1987, Thrombolites and stromatolites: Two distinct types of microbial structures: Palaios, v. 1, p. 492-503.

Kepper, J.C., 1972, Paleoenvironmental patterns in Middle to lower Upper Cambrian interval in eastern Great Basin: American Association of Petroleum Geologists Bulletin, v. 56, p. 503-527.

Kepper, J.C., 1981, Sedimentology of a Middle Cambrian outer shelf margin with evidence for syndepositional faulting, eastern California and western Nevada: Journal of Sedimentary Petrology, v. 51, p. 807-822.

Kidd, J.T. and Neathery, T.L., 1976, Correlation between Cambrian rocks of the southern Appalachian geosyncline and the interior low plateaus: Geology, v. 4, p. 767-769.

Kinsman, D.J. and Park, R.K., 1976, Algal belt and coastal sabkha evolution, Trucial Coast, Persian Gulf, in Walter, M.R., ed., Stromatolites: Elsevier, New York, p. 421-433.

Kobluk, D.R. and Risk, M.J., 1977, Micritization and carbonate-grain binding by endolithic algae: American Association of Petroleum Geologists Bulletin, v. 61, p. 1069-1082.

Kopaska-Merkel, D.C., 1988, Depositional environments and stratigraphy of a Cambrian mixed carbonate/terrigenous platform deposit: West-central Utah, U.S.A.: Carbonates and Evaporites, v. 2, p. 137-147.

Kozar, M.G., 1986, The stratigraphy, petrology, and depositional environments of the Maryville Limestone (Middle Cambrian) in the vicinity of Powell and Oak Ridge, Tennessee: unpublished M.S. thesis, University of Tennessee, Knoxville, 242 p.

Kozar, M.G., Weber, L.J., and Walker, K.R., 1986, Transport mechanisms and genesis of limestone clast conglomerates with examples from the Cambrian of east Tennessee (abs.): American Association of Petroleum Geologists, v. 70, p. 609.

Kreisa, R.D., 1981, Storm-generated sedimentary structures in the subtidal marine facies with examples from the Middle and Upper Ordovician of southwest Virginia: Journal of Sedimentary Petrology, v. 51, p. 823-848.

Kreisa, R.D. and Bambach, R.K., 1982, The role of storm processes in generating shell beds in Paleozoic shelf environments, in Einsele, G. and Seilacher, A., eds., Cyclic and Event Stratification: Springer-Verlag, New York, p. 200-207.

Krumbein, W.E., 1983, Stromatolites-the challenge of a term in space and time: Precambrian Research, v. 20, p. 493-531.

Ksiazkiewicz, M., 1958, Submarine slumping in the Carpathian flysch: Annals of the Geological Society of Pologne, v. 28, p. 123-150.

Laferriere, A.P., Hattin, D.E., and Archer, A.W., 1987, Effects of climate, tectonics, and sea-level changes on rhythmic bedding patterns in the Niobrara Formation (Upper Cretaceous), U.S. Western Interior: Geology v. 15, p. 233-236.

Laporte, L.F., 1967, Carbonate deposition near mean sea-level and resultant facies mosaics: Manlius Formation (Lower Devonian) of New York State: American Association of Petroleum Geologists Bulletin, v. 51, p. 73-101.

Laporte, L.F., 1971, Paleozoic carbonate facies of the central Appalachian shelf: Journal of Sedimentary Petrology, v. 41, p. 724-740.

Leeder, M.R., 1982, Sedimentology: Process and Product: George Allen and Unwin, London, 344 p.

Levin, R.I. and Rubin, D.S., 1980, Applied Elementary Statistics: Prentice-Hall, Inc., Englewood Cliffs, New Jersey, 579 p.

Lochman-Balk, C. and Wilson, J.L., 1958, Cambrian biostratigraphy in North America: Journal of Paleontology, v. 32, p. 312-350.

Lochman-Balk, C., 1971, The Cambrian of the craton of the United States, in Holland, C.T. (ed.), The Cambrian of the New World: Wiley Interscience, New York, p. 79-167.

Logan, B.W., Hoffman, P., and Gebelein, C.D., 1974, Algal mats, cryptalgal fabrics, and structures, Hamelin Pool, Western Australia, in Logan, B.W., and others, Evolution and Diagenesis of Quaternary Carbonate Sequences, Shark Bay, Western Australia: American Association of Petroleum Geologists Memoir 22, p. 140-194.

Logan, B.W., Rezak, R., and Ginsburg, R.N., 1964, Classification and environmental significance of algal stromatolites: Journal of Geology, v. 72, p. 68-83.

Logan, B.W. and Semeniuk, V., 1976, Dynamic metamorphism, processes and products in Devonian carbonate rocks, Canning Basin, Western Australia: Geologic Society of Australia, Special Publication No. 6, 138 p.

Lohmann, K.C., 1976, Lower Dresbachian (Upper Cambrian) platform-to-basin transition in eastern Newada and western Utah: an evaluation through lithologic cycle correlation: Brigham Young University Geology Studies 23, p. 111-122.

Loreau, J.P. and Purser, B.H., 1973, Distribution and ultrastructure of Holocene ooids in the Persian Gulf: Springer-Verlag, New York, p. 279-328.

Lumsden, D.N., 1971, Markov chain analysis of carbonate rocks: Applications, limitations, and implications as exemplified by the Pennsylvanian System in southern Nevada: Geological Society of American Bulletin, v. 82, no. 2, p. 447-462.

Mack, G.H., 1980, Stratigraphy and depositional environments of the Chilhowee Group (Cambrian) in Georgia and Alabama: American Journal of Science, v. 280, p. 487-517.

Mack, G.H., and James, W.C., 1986, Cyclic sedimentation in the mixed siliciclastic-carbonate Abo-Hueco transitional zone (Lower Permian), southwestern New Mexico: Journal of Sedimentary Petrology, v. 56, p. 635-647.

Markello, J.R. and Read, J.F., 1982, Upper Cambrian intrashelf basin, Nolichucky Formation, southwest Virginia Appalachians: American Association of Petroleum Geologists Bulletin, v. 66, p. 860-878.

Markello, J.R., 1979, Carbonate ramp to deeper shale shelf transitions of an upper Cambrian (Dresbachian) shelf embayment, Nolichucky Formation, southwest Virginia: unpublished M.S. thesis, Virginia Polytechnic Institute and State University, Blacksburg, 162 p.

Markello, J.R., and Read, J.F., 1981, Carbonate ramp-to-deeper shale shelf transitions of an upper Cambrian intrashelf basin, Nolichucky Formation, southwest Virginia Appalachians: Sedimentology, v. 28, p. 573-597.

Markello, J.R., Tillman, C.G., and Read, J.F., 1979, Lithofacies and biostratigraphy of Cambrian and Ordovician platform and basin facies carbonates and clastics, southwestern Virginia, in Glover, L. and Read, J.F., (eds.), Guides to Field Trips 1-3: Geological Society America Field Trip Guides, Southeastern Section, Blacksburg, VA, p. 42-87.

Mathews, R.K., 1984, Dynamic Stratigraphy: Prentice-Hall, New Jersey, 2nd edition, 489 p.

McCalley, H., 1897, Report on the valley regions of Alabama, part 2, on the Coosa Valley region: Alabama Geological Survey, 862 p.

McConnell, R., 1967, Lithostratigraphy and petrography of the upper Cambrian Maynardville Formation within the Copper Creek Fault belt of east Tennessee: M.S. Thesis, Unviersity of Tennessee, Knoxville, 92 p.

McIlreath, I.A., 1977, Accumulation of a Middle Cambrian deep-water limestone debris apron adjacent to a vertical escarpment, southern Rocky Mountains, Canada, in Cook, H.E. and Enos, P., (eds.), Deep-Water Carbonate Environments: Society of Economic Paleontologists and Mineralogists Special Publication 25, p. 113-124.

McKinney, F.K., 1977, Archaeocyatha of the Shady Formation, Sleeping Giants, Talladega County, Alabama, in Bearce, D.N., (ed.), Cambrian and Devonian Stratigraphic Problems of Eastern Alabama: Alabama Geological Society Guidebook, 15th Annual Field Trip, p. 16-19.

McLaughlin, R.E., 1973, Observations on the biostratigraphy and stratigraphy of Knox County, Tennessee and vicinity: Tennessee Division of Geology Bulletin, no. 70, p. 25-62.

Medwedeff, D.A. and Wilkinson, B.H., 1983, Cortical fabrics in calcite and aragonite ooids, in Peryt, T.M., ed., Coated Grains: Springer-Verlag, Berlin, p. 109-115.

Merriam, D.F., and Sneath, P.H.A., 1967, Comparison of cyclic rock sequences using cross-association, in Teichert, C., and Yochelson, E., eds., Essays in Paleontology and Stratigraphy, R.C. Moore Commemorative Volume: Kansas University Special Publication 2, p. 521-538.

Milici, R.C., 1973, The stratigraphy of Knox County, Tennessee: Tennessee Division of Geology Bulletin, no. 70, p. 9-24.

Milici, R.C., Brent, W.B., and Walker, K.R., 1973, Depositional environments in upper Conasauga lagoon-fill sequences along I-75 at Copper Ridge, Knox County, Tennessee: Tennessee Division of Geology Bulletin, no. 70, p. 138-143.

Miller, J.F., 1984, Cambrian and earliest Ordovician conodont evolution, biofacies, and provincialism: Geological Society of America Special Paper 196, p. 43-68.

Miller, R.H., Sundberg, F.A., Harma, R.H., and Wright, J., 1981, Late Cambrian stratigraphy and conodonts of southern Nevada: Alcheringa, v. 5, p. 183-196.

Moore, R.C., 1936, Stratigraphic classification of the Pennsylvanian rocks of Kansas: Kansas Geological Survey Bulletin, v. 22, p. 1-256.

Morton, R.A., 1981, Formation of storm deposits by wind-forced currents in the Gulf of Mexico and the North Sea, in Nio, S.D., Schuttenheim, R.T.E. and van Wiering, T.C.E., eds., Holocene Marine Sedimentation in the North Sea Basin: International Association of Sedimentologists Special Publication 5, p. 385-396.

Mullins, H.T. and van Buren, H.M., 1979, Modern modified carbonate grain flow deposits: Journal of Sedimentary Petrology, v. 49, p. 747-752.

Nardin, T.R., Hein, F.J., Gorsline, D.S., and Edwards, B.D., 1979, A review of mass movement processes, sediment and acoustic characteristics, and contrasts in slope and base-of-slope systems versus canyon-fan-basin floor systems, in Doyle, L.J. and Pilkey, O.H., eds., Geology of Continental Slopes: Society of Economic Paleontologists and Mineralogists, Special Publication 27, p. 61-73.

Nelson, C.H., 1982, Modern shallow-water graded sand layers from storm surges, Bering Shelf: a mimic of Bouma sequences and turbidite systems: Journal of Sedimentary Petrology, v. 52, p. 537-545.

Neuman, A.C. and Land, L., 1975, Lime mud deposition and calcareous algae in the Bight of Abaco, Bahamas: A budget: Journal of Sedimentary Petrology, v. 45, p. 763-786.

Newell, N.D. and Rigby, J.K., 1957, Geological studies of the Great Bahama Bank, in Regional Aspects of Carbonate Deposition: Society of Economic Paleontologists and Mineralogists Special Publication No. 5, p. 15-72.

Oder, C.R.L. and Bumgarner, J.V., 1961, Stromatolitic bioherms in the Maynardville (upper Cambrian) limestone, Tennessee: Geological Society of America Bulletin, v. 72, p. 1021-1028.

Palmer, A.R., 1962, Glyptagnostus and associated trilobites in the United States: U.S. Geological Survey Professional Paper 374 F, 45 p.

Palmer, A.R., 1971, The Cambrian of the Appalachians and eastern New England regions, eastern United States, in Holland, C.H., (ed.), The Cambrian of the New World: New York, Wiley Interscience, p. 169-217.

Peirson, T.C., 1981, Dominant particle support mechanisms in debris flows at Mt. Thomas, New Zealand and implications from flow mobility: Sedimentology, v. 28, p. 49-60.

Pfeil, R.W. and Read, J.F., 1980, Cambrian carbonate platform margin facies, Shady Dolomite, southwestern Virginia, U.S.A.: Journal of Sedimentary Petrology, v. 50, p. 91-116.

Playford, P.E. and Cockbain, A.E., 1976, Modern algal stromatolites at Hamblin Pool, a hypersaline barred basin in Shark Bay, Western Australia, in Walter, M.R., ed., Stromatolites, Developments in Sedimentology, Elsevier, New York, p. 389-413.

Powers, D.W., and Easterling, R.G., 1982, Improved methodology for using embedded Markov chains to describe cyclical sediments: Journal of Sedimentary Petrology, v. 52, p. 913-923.

Pratt, B.R., 1984, Epiphyton and Renalcis-Diagenetic microfossils from calcification of coccoid blue-green algae: Journal of Sedimentary Petrology, v. 54, p. 948-971.

Pratt, B.R. and James, N.P., 1982, Cryptalgal-metazoan bioherms of early Ordovician age in St. George Group, western Newfoundland: Sedimentology, v. 29, p. 499-542.

Prior, D.B. and Coleman, J.M., 1982, Active slides and flows in unconsolidated marine sediments on the slopes of the Mississippi Delta, in Saxov, S. and Nieuwenhuis, J.K., eds., Marine Slides and Other Mass Movements: Plenum Press, New York, p. 21-49.

Purdy, E.G., 1963, Recent calcium carbonate facies of the Great Bahama Bank: Sedimentary Facies: Journal of Geology, v. 71, p. 472-497.

Purser, B.H. and Evans, G., 1973, Regional sedimentation along the Trucial Coast, SE Persian Gulf, in Purser, B.H., ed., The Persian Gulf: Holocene Carbonate Sedimentation and Diagenesis in a Shallow Epicontinental Sea: Springer-Verlag, New York, p. 211-231.

Rasetti, F., 1965, Upper Cambrian trilobite faunas of northeastern Tennessee: Smithsonian Miscellaneous Collection, v. 148, no. 3, 127 p.

Raymond, R.H., 1959, Paleontology of a portion of the Nolichucky Shale and Maynardville Limestone (Cambrian) of the Powell quadrangle, Tennessee: unpublished M.S. thesis, University of Tennessee, Knoxville, 58 p.

Read, J.F., 1982, Carbonate platforms of passive (extensional) continental margins: types, characteristics, and evolution: Tectonophysics, v. 81, p. 195-212.

Read, J.F., Grotzinger, J.P., Bova, J.A., and Koerschner, W.F., 1986, Models for generation of carbonate cycles: Geology v. 14, p. 107-110.

Rees, M.N., 1986, A fault-controlled trough through a carbonate platform: The Middle Cambrian House Range embayment: Geological Society of America Bulletin, v. 97, p. 1054-1069.

Rees, M.N., Brady, M.J., and Rowell, A.J., 1976, Depositional envoronments of the upper Cambrian Johns Wash Limestone (House Range, Utah): Journal of Sedimentary Petrology, v. 46, p. 38-47.

Reineck, H.E. and Singh, I.B., 1972, Genesis of laminated sand and graded rhythmites in storm-sand layers of shelf mud: Sedimentology, v. 18, p. 123-128.

Reineck, H.E. and Singh, I.B., 1980, Depositional Sedimentary Environments with Reference to Terrigenous Clastics: Springer-Verlag, New York, 549 p.

Reinhardt, J., 1977, Cambrian off-shelf sedimentation, central Appalachians, in Cook, H.E. and Enos, P. (eds.), Deep-Water Carbonate Environments: Society of Economic Paleontologists and Mineralogists Special Publication 25, p. 125-154.

Resser, C.E., 1938, Cambrian System (restricted) of the southern Appalachians: Geological Society of America Special Paper 15, 139 p.

Rhoads, D.C., 1970, Mass properties, stability, and ecology of marine muds related to burrowing activity, in Crimes, T.P. and Harper, J.C., eds., Trace Fossils: Geological Journal Special Issue (SEPM), p. 87-111.

Rodgers, J. and Kent, D.F., 1948, Stratigraphic section at Lee Valley, Hawkins County, Tennessee: Tennessee Division of Geology Bulletin, v. 55, 47 p.

Rodgers, J., 1953, Geologic map of east Tennessee with explanatory text: Tennessee Division of Geology Bulletin, v. 58, 168 p.

Rodgers, J., 1968, The eastern edge of the North American continent during the Cambrian and Early Ordovician, in Zen, E.A., and others, (eds.), Studies of Appalachian Geology: Northern and Maritime: New York, John Wiley, p. 141-150.

Roeder, D.H., and Witherspoon, W.D., 1978, Palinspastic map of east Tennessee: American Journal of Science, v. 278, p. 543-550.

Rona, P.A., 1973, Worldwide unconformities in marine sediments related to eustatic changes of sea level: Nature and Physical Science, v. 244, p. 25-26.

Rosenfeld, A., Huang, H.K., and Schneider, V.H., 1968, An application of cluster detection to text and picture processing: University of Maryland Computer Science Center, Technical Report 68-68, 64 p.

Ross, R.J., 1975, Early Paleozoic trilobites, sedimentary facies, lithospheric plates, and ocean currents, in Martinsson, A., (ed.), Evolution and Morphology of the Trilobita, Trilobitoidea and Merestomata: Fossils Strata, v. 4, p. 307-329.

Sackin, M.J. and Sneath, P.H.A., 1965, Amino acid sequences in proteins: a computer study: Biochemical Journal, v. 96, p. 70P-71P.

Sackin, M.J., and Merriam, D.F., 1969, Auto-association, a new geological tool: Journal of Mathematical Geology v. 1, p. 7-16.

Samman, N.F., 1975, Sedimentation and stratigraphy of the Rome Formation in Tennessee: unpublished Ph.D. dissertation, University of Tennessee, Knoxville, 337 p.

Saunders, W.B., Ramsbottom, W.H.C., and Monger, W.L., 1979, Mesothemic cyclicity in the mid-Carboniferous of the Ozark shelf region?: Geology v. 7, p. 293-296.

Schwarzacher, W., 1975, Sedimentation models and quantitative stratigraphy: Amsterdam, Elsevier, 382 p.

Scotese, C.R., Bambach, R.K., Barton, C., van der Voo, R., and Ziegler, A.M., 1979, Paleozoic base maps: Journal of Geology, v. 87, p. 217-277.

Seilacher, A., 1982, Distinctive features of sandy tempestites, in Einsele, G. and Seilacher, A., eds., Cyclic and Event Stratification: Springer-Verlag, New York, p. 333-349.

Sepkoski, J.J., 1982, Flat-pebble conglomerates, storm deposits, and the Cambrian bottom fauna, in Einsele, G. and Seilacher, A., eds., Cyclic and Event Stratification: Springer-Verlag, New York, 536 p.

Shanmugam, G., 1978, The stratigraphy, sedimentology, and tectonics of the Middle Ordovician Sevier Shale basin in east Tennessee: unpublished Ph.D. dissertation, Unviersity of Tennessee, 222 p.

Shanmugam, G. and Walker, K.R., 1980, Sedimentation, subsidence, and evolution of foredeep basin in the Middle Ordovician: American Journal of Science, v. 280, p. 479-496.

Shaw, A.B., 1964, Time in Stratigraphy: McGraw-Hill, New York, 365 p.

Shinn, E.A., 1969, Submarine lithification of Holocene carbonate sediments in the Persian Gulf: Sedimentology, v. 12, p. 109-144.

Shinn, E.A., 1983, Tidal flat, in Scholle, P.A., Bebout, D.G. and Moore, C.H., eds., Carbonate Depositional Environments: American Association of Petroleum Geologists Memoir 33, p. 171-211.

Silberman, J.D., 1972, Proceedings of technical sessions, Kentucky oil and gas association, 34th and 35th Annual Meeting 1970-1971: Kentucky Geological Survey, Series X, Special Publication 21, p. 35-46.

Simmons, W.A., 1984, Stratigraphy and depositional environments of the Middle Cambrian Maryville Limestone (Conasauga Group) near Thorn Hill Tennessee: unpublished M.S. thesis, University of Tennessee, 275 p.

Skipper, K. and Middleton, G.V., 1975, The sedimentary structures and depositional mechanics of certain Ordovician turbidites, Cloridorme Formation, Gaspe Pennisula, Quebec: Canadian Journal of Earth Sciences, v. 12, p. 1934-1952.

Sloss, L.L., 1963, Sequences in the cratonic interior of North America: Geological Society of America Bulletin, v. 74, p. 93-114.

Stockman, K.W., Ginsburg, R.N., and Shinn, E.A., 1967, The production of lime mud by algae in south Florida: Journal of Sedimentary petrology, v. 37, p. 633-648.

Swift, D.J.P., 1976, Continental shelf sedimentation, in Stanley, D.J. and Swift, D.J.P., eds., Marine Sediment Transport and Environmental Management: Wiley, New York, p. 311-350.

Swift, D.J.P., Figueiredo, A.G., Freeland, G.L., and Oertel, G.F., 1983, Hummocky cross-stratification and megaripples: A geological double standard?: Journal of Sedimentary Petrology, v. 53, p. 1295-1317.

Tappan, H., 1980, The Paleobiology of the Plant Protists: W.H. Freeman and Company, San Francisco, 1028 p.

Tarkoy, P.J., 1967, Lithostratigraphy and Petrology of the Upper Cambrian Maynardville Formation within the Hunter Valley Fault belt of east Tennessee: unpublished M.S. thesis, University of Tennessee, Knoxville, 99 p.

Tarkoy, P.J., 1970, Upper Cambrian Maynardville Formation within the Clinchport fault belt of east Tennessee: Transactions of the Illinois State Academy of Science, v. 63, p. 305-318.

Taylor, M.E. and Cook, H.E., 1976, Continental shelf and slope facies in the upper Cambrian and lowest Ordovician of Nevada, in Robinson, R.A. and Rowell, A.J., (eds.), Cambrian Paleontology and Environments of Western North America, A Symposium: Brigham Young University Geology Studies, v. 23, part 2, p. 181-214.

Tewari, R.C. and Casshyap, S.M., 1983, Cyclicity in Early Permian fluviatile Gondwana coal measures: An example from Giridih and Saharjuri Basins, Bihar, India: Sedimentary Geology, v. 35,- p. 297-312.

Tucker, M.E., 1981, Sedimentary Petrology: Wiley and Sons, New York, 252 p.

Turcotte, D.L., and Willemann, J.H., 1983, Synthetic cyclic stratigraphy: Earth and Planetary Science Letters, v. 63, p. 89-96.

Vail, P.R., Mitchum, R.M., and Thompson, S., 1977, Seismic stratigraphy and global changes in sea level, part 4: Global cycles of relative changes of sea level: American Association of Petroleum Geologists Memoir 26, p. 83-98.

Walker, K.R., 1973, Stratigraphy and environmental sedimentology of Middle Ordovician Black River Group in the type area--New York State: Bulletin of the New York State Museum of Science Services 419, 43 p.

Walker, K.R. and Diehl, W.W., 1986, The effects of synsedimentary substrate modification on the composition of paleocommunitites: Paleoecologic succession revisted: Palaios, v. 1, p. 65-74.

Walker, K.R., Shanmugam, G., and Ruppel, S.C., 1983, A model for carbonate to terrigenous clastic sequences: Geological Society of America Bulletin, v. 94, p. 700-712.

Walker, K.R. and Simmons, W.A., 1985, The Middle Cambrian Conasauga Group in the Thorn Hill section: an intracraton platform/basin complex, in Walker, K.R., ed., The Geologic History of the Thorn Hill Paleozoic Section (Cambrian-Mississippian), eastern Tennessee: University of Tennessee Studies in Geology 10, p. 14-25.

Walker, R.G., 1985, Geologic evidence for storm transportation and deposition on ancient shelves, in Tillman, R.W., Swift, D.J.P., and Walker, R.G., eds., Shelf Sands and Sandstone Reservoirs: Society of Economic Paleontologists and Mineralogists Short Course Notes, No. 13, p. 243-302.

Wanless, Jr. H.R., 1979, Limestone response to stress: pressure solution and dolomitization: Journal of Sedimentary Petrology, v. 49, p. 437-462.

Wanless, H.R., and Weller, J.M., 1932, Correlation and extent of Pennsylvanian cyclothems: Geological Society of America Bulletin, v. 43, p. 1003-1016.

Webb, E.J., 1969. Geologic history of the Cambrian System in the Appalachian basin: Kentucky Geological Survey Special Publication, Series 10, no. 18, p. 7-15.

Webb, E.J., 1980, Cambrian sedimentation and structural evolution of the Rome Trough in Kentucky: unpublished Ph.D. dissertation, University of Cincinnati, 98 p.

Weber, L.J., 1985, Stratigraphy and depositional environments of the lower Knox Group (Copper Ridge Dolomite and Chepultepec Dolomite) along U.S. Route 25E., in Walker, K.R., ed., The Geologic History of the Thorn Hill Paleozoic Section (Cambrian-Mississippian), Eastern Tennessee: University of Tennessee Studies in Geology 10, Tennessee, p. 32-42.

Weber, L.J., Foreman, J.L., Walker, K.R., and Cantrell, D.L., 1987, Comparative sedimentology and petrology of Cambrian, Ordovician, and Modern ooid shoal deposits (abs.): Geological Society of America Abstracts with Program, v. 19, p. 884.

Weber, L.J., Kozar, M.G., and Walker, K.R., 1985, Microstratigraphy of Cambrian algal buildups (abstract): Geological Society of America Abstracts with Program, v. 17, p. 746.

Weber, L.J., Walker, K.R., and McKinney, M.L., 1986a, Discernment of cyclicity in carbonate-shale sequences using multiple analytical techniques (abs.): Geol. Soc. Amer. Abs. w. Prog., v. 18, no. 6.

Weber, L.J., Walker, K.R., and McKinney, M.L., 1986b, Using multiple analytical techniques for the recognition of sedimentary cycles: The Compass, v. 64, p. 13-22.

Weber, L.J., Walker, K.R., McKinney, M., Kozar, M., and Haase, S., 1986, An improved method for determining cyclic sedimentation: Application of substitutability and Markov chain analysis to the Late Cambrian of East Tennessee (abs.): Society of Economic Paleontologists and Mineralogists Midyear Meeting Abstracts with Program, v.3, p. 114-115.

Weller, J.M., 1964, Development of the concept and interpretation of cyclic sedimentation: Kansas Geol. Surv. Bull., v. 169, no. 2, p. 607-621.

Wentworth, C.K., 1922, A scale of grade and class terms for clastic sediments: Journal of Geology, v. 30, p. 377-392.

Wetzel, A. and Aigner, T., 1986, Stratigraphic completeness: Tiered trace fossils provide a measuring stick: Geology, v. 14, p. 234-237.

Whisonant, R.C., 1987, Paleocurrent and petrographic analysis of imbricate intraclasts in shallow-marine carbonates, Upper Cambrian, southwestern Virginia: Journal of Sedimentary Petrology, v. 57, p. 983-994.

Wilson, J.L., 1975, Carbonate facies in geologic history: Berlin, Springer-Verlag, 471 p.

Wolfe, K.H., 1965, Gradational sedimentary products of calcareous algae: Sedimentology v. 5, p. 1-37.

Woodward, H.P., 1929, The age and nomenclature of the Rome (Watauga) Formation of the Appalachian Valley: Journal of Geology, v. 37, p. 592-602.

Wray, J.L., 1977, Calcareous Algae: Elsevier, New York, 180 p.

Wright, V.P., 1984, Peritidal carbonate facies: a review: Geology Journal, v. 19, p. 309-325.

APPENDICES

APPENDIX A

STANDARD MEASUREMENT CONVENTIONS

STANDARD MEASUREMENT CONVENTIONS

Bed thickness terminology used in the text and in measured sections follows Ingram (1954). Grain size is based loosely on the Wentworth (1922) size classification.

Bed Thickness

Very thick-bedded	>100.0 cm.
Thick-bedded	30.0-100.0 cm.
Medium-bedded	10.0-30.0 cm.
Thin-bedded	3.0-10.0 cm.
Very thin-bedded	1.0-3.0 cm.
Laminated	0.3-1.0 cm.
Thinly laminated	<0.3 cm.

Grain Size

Coarse-grained	grains visible to the unaided eye and readily identifiable (>1.0 mm.)
Medium-grained	grains visible with hand lens and readily identifiable (~0.25-1.0 mm.)
Fine-grained	grains visible with hand lens, but not readily identifiable (~0.10-0.25 mm.)
Very fine-grained	grains not visible with hand lens (~<0.10 mm.)

APPENDIX B

DESCRIPTION OF STRATIGRAPHIC SECTIONS

NOTE:

1. Field descriptions are recorded in ascending order from oldest to youngest.

2. Unit thickness (Unit tkn.) and cumulative thickness (Cum. tkn.) are given in meters.

3. Terminology of samples

    a. Each sample is prefixed with an alpha-numeric or combined alpha-numeric-numeric code to indicate locality. For example:

        BG=Beech Grove Section
        RS=Roaring Spring Section
        I-75=Interstate 75 Section
        A=Interstate 75 Section
        B=Interstate 75 Section
        C=Interstate 75 Section
        IOA=Interstate 75 Section
        J-2=Joy 2 Core Section
        SCAR=Scarboro Road Core Section
        S-3=S-3 Pond Core Section

    b. Thin-sectioned samples are underlined.

    c. Following each sample number, a reference number is affixed. The reference number shows where each sample was collected with respect to the Nolichucky/Maynardville contact (mbM=meters below base of Maynardville Limestone; maN=meters above top of Nolichucky Shale).

4. Thin-sections cited here and elsewhere within this dissertation are part of a permanent collection which resides at the Department of Geological Sciences*, University of Tennessee, Knoxville, TN 37996-1410.

    * Thin-sections which were made from the Joy 2 subsurface drill core are housed at ORNL.

BEECH GROVE SECTION AND SAMPLES

Nearly 87 m of exposed Nolichucky Shale crop out along the northeastern side of State Route 33 (Maynardville Highway) just north of the small community known as Beech Grove. More specifically, the section is located 8.3 km north of Halls, TN and 1.7 km south of the Knox-Union County line. The lower portion of the Nolichucky Shale is highly weathered and is not exposed. Field descriptions begin at the base of a more-or-less complete road cut exposure.

UNIT	TKN. (m.)	CUM. TKN. (m.)	DESCRIPTION
			UNEXPOSED NOLICHUCKY SHALE
1-1	8.7	8.7	NOLICHUCKY SHALE. Shale and limestone, shale: brown, weathering red to tan-brown; very fine to fine grained; laminated. Visible mica flakes. Fissile. Chippy weathering. Abiotic. Iron and/or manganese staining. Calcareous. Limestone (mudstone to packstone): medium gray, weathering light gray; very fine to coarse grained; planar and cross laminated to thin bedded, regular and uneven. Echinoderms, trilobites, and Chancelloria (?). Partially dolomitized. Argillaceous. Gradational lower contact. Thin shale drapes cut carbonate laminae. Shale dominates at base, limestone increases up unit. Load casts at base of limestone which overlie shale. Samples: BG-0, 90.5 mbM; BG-1-3.1, 89.1 mbM; BG-1-4.8, 88.5 mbM; BG-1-17.1, 84.8 mbM; BG-1-25.2, 82.3 mbM.
1-2	0.9	9.6	Shale and limestone (shale description similar to 1-1), limestone (packstone to grainstone): medium gray, weathering light gray; medium to coarse grained; planar and cross laminated to medium bedded, regular and uneven. Sharp lower contact. First occurrence of intraclastic limestone. Burrows common, 3-5 millimeters in diameter, perpendular to bedding, simple straight tubes. Intraclastic limestone: random orientation, laminated and cross laminated clast

			lithology, many clasts resemble under lying beds, mean clast size is 2 centimeters, maximum clast size is 5.1 centimeters, clasts elongate with rounded to sharp edges, flat lower bedding surface, clasts project above irregular upper surface.
2-1	1.9	11.5	Limestone (mudstone to grainstone), light gray, weathering light to dark gray, brown where dolomitized; very fine to coarse grained; laminated to thin bedded, irregular and uneven. Gradational lower contact. Thin shale partings. Low amplitude stylolite seams. Near base of unit, laminated mudstones grade laterally into fossiliferous grainstones. Grains include peloids, ooids, trilobites, and intraclasts. Partial dolomitization. Well sorted, dolomitized, laterally discontinuous (lenticular) oolitic grainstone fills depressions on underlying mudstone to grainstone. Textural inversion in oolitic lenses where undulating thin shale drapes cut through the oolite. Intraclastic grainstone dominates upper part of unit. Contacts between various lithologies are sharp. Intraclastic limestone: random orientation, laminated and cross laminated clast lithology, mean clast size 1 to 3 centimeters long, 0.6 to 1.3 centimeters thick, clasts elongate with rounded to sharp edges. Sample: BG-2-5.7, 78 .7 mbM.
3-1	4.9	16.4	Limestone and shale, limestone (mudstone to peloidal packstone): medium gray, weathering light gray; very fine to medium grained; laminated to thin bedded, regular to irregular and uneven. Shale: medium to light gray to brown, weathering tan-gray to brown; very fine grained; laminated, regular and uneven. Abiotic. Sharp lower contact. Partially dolomitized. Lower 0.3 meters of unit exhibit gray, mottled shales and contain 1 to 5 millimeter limestone (laminate mudstone) nodules. Above 0.3 meters shales abruptly become brown, less

			calcareous and fossiliferous, and contain no limestone nodules. Samples: BG-3-6.2, 78.5 mbM; BG-3-2.5, 77.7 mbM; BG-3-5.0, 77.0 mbM.
3-2	7.8	24.2	Shale and limestone (shale description similar to 3-1), limestone (packstone to grainstone), medium gray, weathering light gray; medium to coarse grained; medium to thick bedded, regular and uneven. Gradational lower contact. Oolitic packstone and grainstone 0.2 to 0.6 meters thick separated by shale and nodular limestone intervals 0.3 to 1.2 meters thick. Oolitic beds pinch and swell and are laterally continuous over observed exposure. Thinner limestone beds are fossiliferous peloidal packstones. Laterally discontinuous, lenticular, calcareous siltstones. Limestone nodules in shale: micritic, elongate, flattened, approximately 5 centimeters long and 1 to 2 centimeters thick. Intraclastic packstone/grainstone near top of unit. Samples: BG-3-24.0, 71.2 mbM; BG-3-28.8, 69.7 mbM; BG-3-35.5, 67.7 mbM; BG-3-35.7, 67.6; BG-3-41.0, 66.0 mbM.
3-3	4.3	28.5	Shale and limestone (shale description similar to 3-1), limestone medium to dark gray, weathering light gray; very fine to coarse grained; laminated to medium bedded, regular and uneven. Echinoderms. Gradational lower contact. This unit differs from 3-2 in that: (1) shales are more calcareous with locally abundant limestone (mudstone) nodules and (2) limestone interbeds are commonly mudstone. Thickest limestone interbeds are oolitic grainstones. As in unit 3-2, intraclastic grainstones increase toward the top of the unit. Some thin bedded echinoderm-rich packstone. Sample: BG-3-55.5, 61.6 mbM.
3-4	9.9	38.4	Shale, dark gray to brown, weathering tan-gray to brown; very fine grained; laminated, regular and even. Abiotic. Gradational lower contact. Rare thin

			bedded intraclastic limestones (grainstone) which exhibit clasts projecting into overlying shales. Uppermost 5.5 meters is partially covered. Samples: BG-3-56.0, 61.4 mbM; BG-3-66.2, 58.3 mbM; BG-3-69.2, 57.4 mbM; BG-3-70.0, 57.2 mbM.
4-1	5.3	43.7	Limestone and shale, limestone (mudstone to packstone): medium gray, weathering light gray; very fine to coarse grained; laminated to medium bedded, irregular and uneven. Shale (2 types): green-brown and gray-black, weathering brown and light gray; very fine to medium grained; laminated, regular and uneven. Small inarticulate brachiopod valves and disarticulated trilobite carapaces. Gradational lower contact. Shale drapes between limestone beds. Intraclastic limestone (packstone): random orientation, largest clasts 0.2 meters wide and 0.1 meters long. Intraclastic beds increase up unit, shale beds decrease to discontinuous partings and drapes. Calcareous siltstone and silty fossiliferous wackestone and packstone, no grading observed. Above 2.4 meters mottled limestone dominates. Mottled limestone: discontinuous limestone beds cut by thin shale partings, silt, or sand lenses, which may be partially to pervasively dolomitized. Gently undulating stylolite seams. Upper surfaces of lime stone beds may represent rippled bedforms. From 2.4 to 5.3 meters above the base, several cycles exist: thin limestone interbedded with shale grade upward into thin mottled limestones which are capped by 0.1 to 0.2 meter thick intraclastic fossiliferous, oolitic, glauconitic, packstone/grainstone. Two types of shale thicken and thin laterally, but overall thickness of shale remains the same. Typical sequence: thin brown shale overlies limestone which in turn is overlain by black shale; limestone caps the sequence. Dark shale appears more calcareous, both varieties contain limestone (mudstone) nodules. Limestone nodules (mudstone): very common in shales, rare fossils,

			distributed as discrete 3-D flattened masses parallel to bedding, and over and underlying shale conform exterior irregularities around nodules. Samples: BG-4-0.5, 51.5 mbM; BG-4-1.5, 51.2 mbM; BG-4-4.2, 50.4 mbM; BG-4-4.3, 50.3 mbM; BG-4-8.0, 49.2 mbM; BG-4-9.7, 48.7 mbM; BG-4-17.5, 46.3 mbM.
4-2	5.3	49.0	Shale and limestone, shale: predominantly gray, weathering light gray; very fine grained; laminated. Abiotic. Limestone (mudstone to packstone): medium gray, weathering light gray; very fine to coarse grained; laminated to thick bedded. Trilobites. Gradational lower contact. Shale contains abundant limestone (mudstone) nodules. Samples: BG-4-18.4, 46.0 mbM; BG-4-25.5, 43.9 mbM; BG-4-31.5, 42.1 mbM.
5-1	6.2	55.2	Limestone (wackestone to grainstone; occasional mudstone), medium to dark gray, weathering light gray; fine to coarse grained; predominantly medium to thick bedded, irregular and uneven. Whole inarticulate brachiopods, trilobites, ostracodes (?), and echinoderms. Sharp lower contact. Mottled limestones: carbonates occur with continuous to discontinuous sandy, silty, perhaps dolomitized partings. Partings: tan to brown, weathering brown; fine to medium grained; laminated to cross laminated, discontinuous on local scale. Allochemical constituents in limestone beds vary considerably over short lateral distance. Coarsening upward cycle from 5.4 to 6.2 meters: mottled limestone (wackestone) interbedded with gray and brown shale are overlain by oolitic, glauconitic, fossiliferous grainstone. Samples: BG-5-0.0, 41.1 mbM; BG-5-3.5, 40.0 mbM; BG-5-4.8, 39.6 mbM; BG-5-5.7, 39.3 mbM; BG-5-7.2, 38.9 mbM; BG-5-12.4, 37.3 mbM; BG-5-17.3, 35.8 mbM.
5-2	4.8	60.0	Limestone and shale (limestone and shale description similar to 5-1). Sharp basal contact. Several 1 to 3 meter coarsening

			upward cycles: interbedded limestones and shales which are capped by oolitic, glauconitic, fossiliferous packstone/grainstone and discontinuous (lenticular) silty beds. Samples: BG-5-22.5, 34.2 mbM; BG-5-36.0, 30.1 mbM.
6-1	4.9	64.9	Shale and limestone, shale: dark gray, weathering light gray; very fine to medium grained; laminated. Rare fossils, inarticulate brachiopods and trilobites. Limestone (mudstone to grainstone): medium to dark gray, weathering light gray; fine to coarse grained; laminated to thin bedded, irregular and uneven. Sharp basal contact. 3 types of limestone beds: (1) mudstone to packstone nodules, (2) trilobite packstone, and (3) intraclastic packstone to grainstone. Limestone nodules: discrete 3-D bodies, flattened, overlying shale drapes conform to nodules, sparsely fossiliferous. Typical upward coarsening cycle: (1) shale, (2) nodular limestones (mudstone) in shale, (3) limestone (mudstone) bed 0.13 to 0.25 centimeters thick which is laterally continuous over several meters (base of limestone sequence is irregular), (4) intraclastic packstone/grainstone, (5) trilobite packstone (capping rock), and (6) oolitic grainstone (capping rock) (upper surface is irregular); within these cycles the base of limestone intervals show: pseudo-mudcracks exhibiting shaley/silty material injected into cracks and vertical, simple burrows. Intraclastic beds are underlain by nodular limestones showing pseudo-mudcracks; clast diversity: trilobite packstone, laminated pelletal clasts, non-laminated mudstones, and cross laminated clasts. Deformation features common: (1) load casts on base of limestones which overlie shale and (2) shale drapes which conform to shape of limestone nodules. Samples: BG-6-0.5, 29.9 mbM; BG-6-2.0, 29.5 mbM; BG-6-3.1, 29.1 mbM; BG-6-7.5, 27.8 mbM; BG-6-10.1, 27.0 mbM; BG-6-12.5, 26.3 mbM; BG-6-15.7, 25.3 mbM.

6-2	6.0	70.9	Shale (description similar to 6-1). Gradational basal contact. Thin limestone (mudstone to packstone) beds occur. 0.8 meter thick intraclastic limestone bed occurs 3.1 meters above the base. Clasts project above upper irregular surface. Clasts exhibit random to subparallel orientation with respect to bedding. Partially dolomitized. Samples: BG-6-23.7, 22.8 mbM; BG-6-27.4, 21.7 mbM; BG-6-28.2, 21.5 mbM.
6-3	0.5	71.4	Limestone (boundstone and mudstone to grainstone), medium gray, weathering light gray, brown where dolomitized; fine to coarse grained; thick bedded, irregular and uneven. Trilobites, algae, and echinoderms. Sharp basal contact. Unit is lensoidal. Normal fault with 0.5 meter displacement. Upper portion of unit consists of in situ growth of algae (*Renalcis* and *Girvanella*). Upper surface is mound-shaped.
6-4	15.4	86.8	Limestone and shale (limestone and shale descriptions similar to 6-1). Sharp basal contact. Above the algal limestone and extending for 2.4 meters, shales are interbedded with 3 types of carbonates: mudstone, trilobite packstone/wackestone, and intraclastic packstone. Throughout the remainder of unit 6-4 occur pseudo-mudcracks, intraclastic packstones, and channels (?). Normal fault with 0.6 meters of displacement occurs 4.0 meters above the base. Samples: BG-6-40.5, 17.7 mbM; BG-6-50.6, 14.6 mbM; BG-6-56.8, 12.7 mbM; BG-6-65.2, 10.2 mbM; BG-6-86.9, 3.6 mbM.
6-5	3.2	90.0	Covered interval.

Partially Exposed MAYNARDVILLE LIMESTONE

ROARING SPRING SECTION AND SAMPLES

This section was measured along the east side of Hill Road at Roaring Spring. The lower part of the Nolichucky Shale is not exposed here, however, measurements began 2.1 kilometers south of Hill Cemetery at the first, well exposed oolitic grainstone. At this locality the Nolichucky Shale is 121 meters thick while the Maynardville Limestone is estimated to be at least 96 meters in thickness.

UNIT	TKN. (m.)	CUM. TKN. (m.)	DESCRIPTION
			UNEXPOSED NOLICHUCKY SHALE
1	12.0	12.0	NOLICHUCKY SHALE. Shale and limestone, thin to thick shale interbedded with pelletal?, oolitic, and intraclastic limestone. Shale: dark gray green; very fine grained; laminated. Limestone (packstone and grainstone): fine to coarse grained; very thin to medium bedded, planar and low angle cross lamination.
2	4.0	16.0	Limestone and shale, pelletal? limestone interbedded with thin shale. Limestone (packstone): fine grained; very thin to thin bedded, low angle cross lamination. Rare intraclastic beds. Shale: dark gray green; very fine grained; faintly laminated.
3	4.0	20.0	Shale and limestone, thin to thick shale interbedded with oolitic limestone. Shale: dark gray green, weathering light gray; very fine grained; faintly laminated. Limestone (packstone and grainstone): fine to coarse grained;

			very thin to medium bedded, planar and low angle cross lamination. Stylolites? Loading. Pseudonodules.
4	1.0	21.0	Limestone (packstone and grainstone): medium to coarse grained; thick bedded. Fossiliferous, trilobites and echinoderms. Stylolites.
5	5.0	26.0	Limestone and shale, pelletal? intraclastic, and oolitic limestone interbedded with thin shale. Limestone (packstone and grainstone): fine to coarse grained; very thin to thick bedded, planar and low angle cross lamination. Loading. Pseudonodules. Pseudomudcracks. Sole marks. Shale: dark gray green; very fine grained.
6	1.0	27.0	Shale and limestone, thin to thick shale interbedded with pelletal? limestone. Shale: light to dark green gray; very fine grained; faintly laminated. Limestone (packstone and grainstone): fine grained; very thin to thin bedded.
7	3.0	30.0	Limestone and shale, pelletal? and intraclastic limestone interbedded with thin shale. Limestone (packstone and grainstone): fine to coarse grained; very thin to thick bedded, low angle cross lamination. Limestone clast conglomerates show monomictic clast associations, variable clast sizes (< 9 centimeters in long dimension), and clasts projecting into overlying shale. Rarely oolitic. Gutter casts.
8	20.0	20.0	Shale and limestone, thin to very thick shale interbedded with rare pelletal?, oolitic, and intraclastic limestone. Shale: dark green brown, weathering light brown; very fine grained; faintly laminated. Limestone (packstone and grainstone): fine to coarse grained; very thin to medium bedded, planar and low angle cross lamination.
9	1.0	51.0	Limestone and shale, pelletal? limestone interbedded with thin shale. Limestone

			(packstone and grainstone): fine grained; very thin to thin bedded, planar and low angle cross lamination. Loading. Pseudonodules. Intraclastic.
10	1.0	52.0	Shale: gray green; very fine grained; faintly laminated; otherwise nondescript.
11	4.0	56.0	Limestone and shale, pelletal? and intraclastic limestone interbedded with shale. Limestone (packstone and grainstone): fine to coarse grained; thin to thick bedded, planar and low angle cross lamination.
12	2.0	58.0	Limestone and shale, intraclastic and oolitic limestone interbedded with thin shale. Limestone (packstone and grainstone): medium to coarse grained; thin to thick bedded. Limestone clast conglomerates show subparallel to random clast orientation, polymictic clast associations, a wide variety of clast sizes, and clasts projecting into overlying lithologies. Shale: dark green brown to gray; very fine grained; faintly laminated. Perhaps some trilobite debris.
13	2.0	60.0	Shale and limestone, thin to thick shale interbedded with intraclastic and oolitic limestone. Shale: dark gray green; very fine grained; faintly laminated. Limestone (packstone and grainstone): medium to coarse grained; thin to medium bedded.
14	3.0	63.0	Limestone and shale, pelletal? limestone interbedded with thin shale. Limestone (packstone and grainstone): fine grained; very thin to medium bedded, planar and low angle laminations. Intraclastic. Oolitic, ooids may exceed 2 millimeters in diameter. Shale: dark gray green; very fine grained. Sample: RS1, 59.0 mbM.
15	1.0	64.0	Shale and limestone, thin and thick shale interbedded with fossiliferous limestone. Shale: dark gray green; very fine grained; faintly laminated. Limestone (packstone and grainstone): medium to

			coarse grained; very thin to medium bedded. Trilobites. Echinoderms.
16	1.0	65.0	Limestone (packstone and grainstone): medium to coarse grained; medium to thick bedded. Fossiliferous, trilobites and echinoderms. Oolitic. Stylolites.
17	9.0	74.0	Limestone (packstone and grainstone): coarse grained; thick to very thick bedded. Oolitic, ooids exceed 2 millimeters in diameter. Fossiliferous, trilobites and echinoderms. Oolitic shoal. Abundant marine fibrous cement. Differential packing of allochems. Intraclastic. Samples: RS2, 52.5 mbM; RS3, 49.4 mbM.
18	1.0	75.0	Shale and limestone, thin to thick shale interbedded with intraclastic and oolitic limestone. Shale: dark gray green; very fine grained. Limestone (packstone and grainstone): medium to coarse grained; thin to medium bedded.
19	1.0	76.0	Limestone and shale, oolitic, intraclastic, and pelletal? limestone interbedded with thin shale. Limestone (packstone and grainstone): fine to coarse grained; very thin to medium bedded, planar and low angle cross lamination. Shale: dark gray; very fine grained.
20	1.0	77.0	Limestone and shale, pelletal? and oolitic limestone interbedded with shale. Limestone (packstone and grainstone): fine to coarse grained; very fine to medium bedded. *Renalcis*?
21	1.0	78.0	Limestone (packstone and grainstone): coarse grained; thick bedded. Oolitic. Stylolitic.
22	2.0	80.0	Shale: dark gray green; very fine grained; faintly laminated.
23	2.0	82.0	Limestone and shale, pelletal? limestone interbedded with thin shale. Limestone (packstone and grainstone): fine grained; thin bedded, planar and low

			angle cross lamination. Intraclastic. Oolitic. Shale: dark gray green; very fine grained.
24	1.0	83.0	Limestone (packstone and grainstone): coarse grained; thick bedded. Oolitic. Coarse ooids range in size from 1 to 2 millimeters.
25	28.0	111.0	Shale and limestone, thick shale interbedded with rare intraclastic, oolitic, and pelletal? limestone. Shale: dark gray green; very fine grained; faintly laminated. Limestone (packstone and grainstone): fine to coarse grained; very thin to thin bedded, planar and low angle cross lamination. Sole marks. Pseudonodules. Loading. Gutter casts. Intraclastic and oolitic lenses. Samples: RS4, 36.6 mbM; RS5, 30.2 mbM; RS6, 24.1 mbM; RS7, 14.1 mbM.
26	2.0	113.0	Limestone and shale, pelletal? limestone interbedded with thin shale. Limestone (packstone and grainstone): fine grained; thin bedded, planar and low angle cross lamination. Oolitic. Intraclastic. Shale: dark gray green; very fine grained; faintly laminated.
27	1.0	114.0	Limestone and shale, oolitic and pelletal? limestone interbedded with thin shale. Limestone (packstone and grainstone): fine to medium grained; thin to medium bedded.
28	2.0	116.0	Shale and limestone, thin to thick shale interbedded with oolitic, intraclastic, and pelletal? limestone. Shale: dark gray green; very fine grained; faintly laminated. Limestone (packstone and grainstone): fine to coarse grained; very thin to thick bedded, planar and low angle cross lamination. Stylolites. Loading. Pseudonodules. Gutter casts.
29	2.0	118.0	Limestone and shale, pelletal? limestone interbedded with thin to thick shale. Limestone (packstone and grainstone): fine to coarse grained; very thin to

			medium bedded. Loading. Pseudonodules. Gutter casts. Shale: dark gray green, very fine grained; faintly laminated. Sample: RS8, 4.1 mbM.
30	3.0	121.0	Shale and limestone, thin to thick shale interbedded with rare pelletal? and intraclastic limestone. Shale: dark gray green; very fine grained; faintly laminated. Limestone (packstone and grainstone): fine to coarse grained; thin to medium bedded. Limestone clasts in shale. Sample: RS9, 1.7 mbM.
31	5.0	126.0	<u>MAYNARDVILLE LIMESTONE</u>. Limestone and shale, nodular and bedded lime mudstone interbedded with very thin discontinuous shale drapes. Limestone (mudstone and packstone to grainstone): fine grained; thin to medium bedded. Rare limestone clast conglomerates. Fossiliferous, trilobites and echinoderms. Peloidal. Oolitic. Burrows. Petroliferous.
32	3.0	129.0	Limestone and shale, peloidal limestone and lime mudstone interbedded with thin shale drapes. Limestone (mudstone and packstone): fine to medium grained, thin to very thick bedded. Burrows. Superficial ooids? Algal peloids and intraclasts? Dolomitization
33	2.0	131.0	Limestone and shale, lime mudstone interbedded with thin shale drapes. Limestone (mudstone and packstone to grainstone): fine to medium grained; thin to thick bedded, cross stratified. Burrows. Superficial ooids? Peloids.
34	2.0	133.0	Limestone (mudstone and packstone to grainstone): fine to coarse grained; thin to thick bedded, cross stratified? Rare burrowed lime mudstone interbedded with thin shale drapes. Oolitic, some ooids may exceed 2 millimeters in diameter. Superficial ooids? Dolomitization.
35	2.0	135.0	Limestone (packstone and grainstone): fine to medium grained; very thick bedded. Superficial ooids? algal peloids?

			Renalcis? Stylolites. Some dolomitization. Upper part covered. Sample: RS11, 13.3 maN.
36	1.0	136.0	Covered interval.
37	3.0	139.0	Limestone (boundstone and mudstone to grainstone): fine to coarse grained; very thick bedded. Thrombolite with algal peloidal, oolitic, oncolitic, and mudstone filling interalgal areas. *Renalcis*? Stylolites.
38	1.0	140.0	Limestone and shale, lime mudstone interbedded with thin shale drapes. Limestone (mudstone): fine grained; thick bedded. Burrowed. Rare fossils, trilobites and echinoderms. Thrombolitic at base and top.
39	1.0	141.0	Limestone (boundstone and mudstone to grainstone): fine to coarse grained; thick bedded. Thrombolite. Fossil debris and ooids fill interalgal regions. Clotted fabric. Stylolites. Dolomitization (partial).
40	3.0	144.0	Limestone (boundstone and packstone to grainstone): fine to coarse grained; thick bedded. Thrombolitic at base and top of unit, otherwise oncolitic. Oncoids exceed 1 centimeter in diameter. Stylolites. Oolitic?
41	5.0	149.0	Limestone (boundstone and mudstone to grainstone): fine to coarse grained; very thick bedded. Thrombolite. Partial dolomitization. Interalgal areas primarily filled with mudstone and oolitic packstone and wackestone. Stylolites. Samples: RS12, 23.9 maN; RS13, 25.1 maN; RS14, 27.8 maN.
42	4.0	153.0	Limestone (boundstone and packstone to grainstone): medium grained; very thick bedded. Cryptalgal laminites. Ultra thin wavy laminations. Microtepee structures? Sample: RS15, 31.5 maN.

43	6.0	159.0	Limestone and dolostone (boundstone): fine to medium grained; very thick bedded. Thrombolitic. Fenestral fabric? Sample: RS16, 36.1 maN.
44.	3.0	162.0	Dolostone and limestone (boundstone and packstone to grainstone): fine to medium grained; medium to thick bedded. Cryptalgal laminite. Rare shale interbeds. Laterally discontinuous mudstone lenses. Mudcracks?
45	3.0	165.0	Dolostone and limestone (boundstone): fine grained; thick bedded. Stromatolites intergrade with lesser abundant cryptalgal laminites. Irregular wavy lamination grade laterally into laterally linked hemisperoids.
46	1.0	166.0	Dolostone (boundstone and packstone to grainstone): fine to medium grained; thick bedded. Cryptalgal laminites intergrade with lesser abundant stromatolites.
47	1.0	167.0	Limestone and shale, lime mudstone interbedded with thin shale drapes. Limestone (mudstone): fine grained; thin bedded. Algal peloids. Rare fossil debris?
48	1.0	168.0	Limestone and dolostone (boundstone and packstone to grainstone): fine grained; thick bedded. Cryptalgal laminites.
49	1.0	169.0	Covered interval.
50	1.0	170.0	Limestone and dolostone (boundstone and packstone to grainstone): fine grained; thick bedded. Cryptalgal laminites.
51	2.0	172.0	Dolostone (boundstone and grainstone): fine to medium grained; very thick bedded. Stromatolites and cryptalgal laminites. Fenestral fabric. Sample: RS17, 50.6 maN.
52	2.0	174.0	Dolostone and limestone (boundstone and packstone to grainstone): fine to medium grained; medium to thick bedded.

			Cryptalgal laminites. Rare dolomitized mudstone.
53	1.0	175.0	Covered interval.
54	1.0	176.0	Limestone (boundstone and packstone to grainstone): fine grained; thick bedded. Covered at base. Stromatolitic above.
55	1.0	177.0	Limestone (boundstone and packstone to grainstone): fine grained; thick bedded. Cryptalgal laminites. Stromatolites. Wavy ultra thin laminations grade laterally into laterally linked hemispheroids.
56	1.0	178.0	Limestone (boundstone and packstone to grainstone): fine to medium grained; thick bedded. Stromatolitic. Rare cryptalgal laminites. Stylolitic.
57	2.0	180.0	Dolostone and limestone (boundstone and packstone to grainstone): fine grained; thick bedded. Cryptalgal laminites and stromatolites.
58	2.0	182.0	Dolostone (boundstone and packstone to grainstone): fine grained; very thick bedded. Stromatolitic. Covered at top.
59	1.0	183.0	Covered interval.
60	3.0	186.0	Dolostone and limestone (boundstone and packstone to grainstone): fine grained; very thick bedded. Cryptalgal laminites. Covered interval at top. Sample: RS18, 64.2 maN.
61	1.0	187.0	Limestone (boundstone and mudstone to grainstone): fine grained; thick bedded. Cryptalgal laminites at base overlain by mudstone. Algal peloids?
62	11.0	198.0	Covered interval.
63	8.0	206.0	Dolostone and limestone (boundstone and packstone to grainstone): fine grained; thick to very thick bedded. Stromatolitic. Laterally linked hemispheroids and domal stromatolites.

			Fenestral fabric. Microtepee structures. Sample: RS19, 83.8 maN.
64	11.0	217.0	Covered Interval.
			COPPER RIDGE DOLOSTONE.

INTERSTATE 75 SECTION AND SAMPLES

The I-75 section described here is located on the northeastern side of Interstate 75 approximately 2 km north of the Emory Road interchange. Nearly 100 m of Nolichucky Shale and 25 m of Maynardville Limestone are exposed continuously along the lowermost bench, at road level. The lower part of the Nolichucky Shale is highly weathered, and thus is not exposed. Field measurements and descriptions begin at the base of the well-exposed section at the lowermost observed oolitic grainstone.

UNIT	TKN. (m.)	CUM. TKN. (m.)	DESCRIPTION
			UNEXPOSED NOLICHUCKY SHALE
1	6.6	6.6	NOLICHUCKY SHALE. Shale and limestone (nodular and undulatory bedded limestone in shale), shale: green-brown and medium gray, weathering brown and light gray; very fine to fine grained. Mottled (bioturbated?). Shale intervals 0.3 to 15.3 centimeters thick. Inarticulate brachiopods. Partially dolomitized. Intraclasts are randomly oriented in shale 2.1 meters above base. Limestone (mudstone to packstone): medium gray, weathering light gray; fine to coarse grained; planar and cross laminated to medium bedded, irregular and even to uneven. Oolitic. Lenticular beds, limestone "channels" in shale trend from N 35°E to N 55°E. Vertical and horizontal burrows. Load casts. Groove casts. Gutter casts. Fossiliferous. Limestone clast conglomerates exhibit fanned clasts, subparallel to random clast orientation, abrupt change from polymictic to monomictic over short lateral distances. Samples: I-1-0.0, 100.2 mbM;

			I-1-0.3, 100.1 mbM; I-1-7.4, 97.9 mbM; I-1-8.0, 97.8 mbM; I-1-11.6, 96.7 mbM; I-1-15.5, 95.5 mbM; I-1-17.0, 95.0 mbM.
2	0.4	7.0	Limestone (packstone), medium to dark gray, weathering light gray; coarse grained; thick bedded, irregular and uneven. Limestone clast conglomerate at base. Oolitic-well sorted, shale and mudstone drapes. Thin, discontinuous shale drapes. Vuggy porosity. Fossiliferous-trilobites and echinoderms. Laminated and hemispheroidal organosedimentary structures near top, hemispheroids 6.1 centimeters tall. Samples: I-2-0.5, 93.4 mbM; I-2-1.0, 93.3 mbM; I-2-2.1, 93.0 mbM.
3	1.3	8.3	Mottled Limestone (boundstone and mudstone to grainstone), medium to light gray, weathering light gray; fine to coarse grained; thick bedded. Shale pervasively dolomitized-dolomitized areas impart a mottled appearance to the unit. Irregular vugs. Planar laminated and cross laminated organosedimentary structures. Laterally linked hemispheroids toward top. Oolitic. Fossiliferous-trilobites. Stylolites. Domal upper surface. Intraclastic. Fluid injection structures? Samples: I-3-0.8, 93. 0 mbM; I-3-1.0, 92.9 mbM; I-3-4.2, 91.9 mbM.
4	1.7	10.0	Limestone and shale (undulatory bedded limestone), Limestone (predominantly mudstone and wackestone): medium to dark gray, weathering light gray; very fine to medium grained; laminated and cross laminated to thin bedded, irregular and uneven. Lenticular beds. Vertical and horizontal burrows. Fossiliferous-trilobites and inarticulate brachiopods. Load casts. Shale: olive green and dark gray, weathering green brown to light gray; very fine grained; laminated. Partings usually continuous and are 0.3 to 0.6 centimeters thick. Sample: I-4-0.9, 91.6 mbM.

5	1.6	11.6	Mottled limestone (boundstone and mudstone to packstone), medium gray, weathering light gray to pale tan yellow; very fine to coarse grained; thick bedded, irregular and uneven. Lower 15 centimeters intraclastic-polymictic, maximum clast size 0.4 meters long; 0.06 meters thick, average size 0.09 meters long; 0.03 meters thick, random to subparallel clast orientation. Load casts. Above 15 centimeters-mottled fabric (limestone interbedded with discontinous dolostone partings). Vertical fract ures cut algal bodies and are filled with shale which has been partially to pervasively dolomitized. Upper surface of unit traces outline of algal "heads". Within algal bodies-fossiliferous and oolitic. Algal laminations near top. Samples: I-5-0.0, 90,2 mbM; I-5-2.8, 89.3 mbM.
6	1.6	13.2	Limestone and Shale (undulatory limestone in part nodular bedded limestone), limestone (mudstone to wackestone): medium gray, weathering medium to light gray; fine to medium grained; planar laminated and cross laminated to thin bedded, irregular and uneven. Lenticular. Fossiliferous-trilobites. Slump structure? Vertical burrows. Shale: dark gray, weathering light to dark gray; very fine grained; laminated. Continuous to discontinuous shale partings. Sample: I-6-2.5, 87.8 mbM.
7	0.2	13.4	Limestone and shale (undulatory bedded limestone), limestone (mudstone to wackestone): medium to dark gray, weathering light gray; fine to medium grained; planar laminated and cross laminated to thin bedded, irregular and uneven. Resembles unit 6 except contains less shale. Very thin and discontinuous shale partings. Fossiliferous. Sample: I-7-0.0, 87.0 mbM.
8	0.5	13.9	Limestone (mudstone to grainstone), medium gray, weathering light gray to brown; fine to coarse grained; fine to medium

			bedded, irregular and uneven. Coarsening upward sequence. Ooids well sorted and partially dolomitized. Rare shale partings. Laterally, beds difficult to trace because of lenticular nature. Samples: I-8-1.0, 87.5 mbM; I-8-4.0, 86.5 mbM.
9	0.9	14.8	Limestone and shale (undulatory bedded limestone), limestone (mudstone to packstone/grainstone): light to medium gray, weathering light gray to tan brown; very fine to coarse grained; planar and cross laminated to thin bedded, irregular and uneven. Most beds lenticular. Coarsening upward sequence. Upper 25 centimeters oolitic. Shale partings in upper portion of oolite. Sample: I-9-2.8, 85.4 mbM.
10	0.3	15.1	Shale, brown, weathering brown to gray brown; very fine to fine grained. Mottled. Abiotic. Iron stained. Calcareous. Laminated. Sample: I-10-0.8, 85.2 mbM
11	0.9	16.0	Shale and limestone (nodular to undulatory bedded limestone), shale: dark gray and green brown (at top), weathering gray brown to green brown; very fine grained. Structureless. Abiotic. Iron staining. Lacks carbonate interbeds. Limestone (mudstone to grainstone): light gray to medium gray, weathering light gray to tan; very fine to medium grained; planar and cross laminated to thin bedded, irregular and uneven. Lensoidal, thin beds laterally discontinuous over 1 meter or less. Vertical and horizontal burrows, 0.3 centimeters in diameter. Samples: I-11-0.8, 84.9 mbM; I-11-1.1, 84.8 mbM.
12	0.5	16.5	Limestone and Shale (undulatory bedded limestone), limestone (mudstone to grainstone): light gray, weathering light gray to tan; fine to coarse grained; planar and cross laminated to thin bedded, irregular to uneven. Discontinuous shale partings cut limestone beds, shale partings weather gray-green. Dolomitized intervals. Secondary vugs

			1-2 millimeters in diameter. Intraclastic at base. Fossils-trilobites and *Chancelloria*? Coarse grained at base, fining toward top. Sample: *I-12-0.5*, 8 4.0 mbM.
13	0.2	16.7	Shale and Limestone (nodular and undulatory bedded limestone), Shale: green brown, weathering light to dark brown; very fine grained; laminated. Abiotic. Discontinuous limestone beds. Limestone (mudstone to packstone): medium gray, weathering light gray; fine to medium grained; planar and cross laminated, irregular and uneven. Fossils-trilobites and *Chancelloria*?
14	0.3	17.0	Limestone (packstone/grainstone), light gray where dolomitized tan, weathering light gray to tan; coarse grained; thin to medium bedded, irregular and uneven. Stylolites. Limestone clast conglomerate exhibits polymictic clasts, random clast orientation, clasts from 6.1 to 9.2 centimeters long by 1.5 centimeters thick, fanned clasts, and clasts which project into overlying shale. Unit is lenticular. Sample: *I-14-0.0*, 53.5 mbM.
15	1.9	18.9	Shale and limestone (nodular and undulatory bedded limestone), Shale: medium to dark gray, weathering light gray, very fine grained. Rare limestone nodules. Abiotic. Structureless. Color banding. Limestone (mudstone and wackestone): medium gray, weathering light gray; fine to medium grained; planar and cross laminated to thin bedded, irregular and uneven. Fossiliferous-echinoderms, trilobites, *Chancelloria*? Lense shaped beds with scoured bases, irregular top. Pseudomudcracks on lower surface. Groove casts and tool marks on sole of thin limestone beds 48 centimeters from top of unit. Sole marks only observed on bases of laminated to cross laminated fine to medium grained limestone. Rare vertical burrows. Thin shale beds, laminations, and partings. Samples: *I-15-2.6*, 82.4 mbM; *I-15-3.8*, 82.0 mbM.

16	0.4	19.3	Limestone (predominantly packstone/grainstone), medium to dark gray, weathering light gray to brown; fine to coarse grained; thin to medium bedded, irregular and uneven. Fossiliferous. Intraclastic. Oolitic. Shale drapes cut ooid beds. Intraclasts (polymictic clast types) within oolitic portion. Thin limestone beds separated by dolomitized shale and stylolite seams within the lower 9.2 centimeters. Upper 30.5 centimeters is oolitic. Lense shaped beds pinch out over lateral distances o f 10's of meters. Sample: I-16-0.4, 81.2 mbM.
17	2.5	21.8	Shale and limestone (undulatory bedded limestone), shale: green brown (proximal to limestone beds) otherwise dark gray, weathering green brown to gray to white; very fine grained; laminated. Rare fossils (inarticulate brachipods) in gray shale. Contact between 2 varieties of shale is sharp. Maroon shale rare. Vertical burrows. Limestone (packstone/grainstone): light to medium gray, weathering pale yellow to red brown; medium to coarse grained; thin bedded, irregular and uneven. Beds discontinuous over several meters. Load casts. Sole marks? Intraclastic, bioclastic, oolitic, and pelletal. Samples: I-17-6.4, 78.9 mbM; I-17-7.3, 78.7 mbM.
18	0.2	22.0	Limestone and shale (undulatory bedded limestone), limestone (mudstone to packstone/grainstone): medium gray, weathering red brown to pale yellow to gray; fine to coarse grained; thin bedded, irregular and uneven. Beds lenticular, pinching out over centimeters to meters. Load casts. Burrows, usually vertical. Groove casts? Clasts at top of unit project into overlying shales. Shale: green, weathering pale green; very fine grained; laminated. Discontinuous drapes.
19	0.4	22.4	Limestone and shale (undulatory bedded limestone; nodular bedded intervals

			predominate within lower 2/3 of unit), limestone (mudstone to packstone/grainstone): medium gray, weathering light gray, brown where dolomitized; fine to coarse grained; planar and cross laminated to thin bedded, irregular and uneven. Vertical and horizontal burrows. Pseudomudcracks at base of thin limestone beds. Mudstone at base grading upward into wackestone, then fossiliferous packstone, and finally near the top, intraclastic packstone. Limestone clast conglomerate exhibit clasts which project into overlying shales, monomictic clast associations, laminated and cross laminated clasts. Most beds discontinuous over scale of outcrop (several meters). Shale: green and medium to dark gray, weathering green brown and light gray; very fine grained; laminated.
20	1.2	23.6	Shale: green brown, dark gray, and maroon, weathering pale brown, light gray, and maroon; very fine grained; laminated. No limestone interbeds.
21	3.2	26.8	Shale and limestone (undulatory bedded limestone), shale: dark gray, weathering light gray; very fined grained; laminated. Limestone (mudstone to packstone/grainstone): light to medium gray, weathering light brown; fine to coarse grained; planar and cross laminated to thin bedded, irregular and uneven. Lenticular limestone clast conglomerate beds pinch out over short lateral distances resulting in different intraclastic lithologies from what initially appears to be the same bed. Stylolite s. Iron staining. Dolomitization. Secondary vugs. Pseudomudcracks. Lithologies observed from the lower 27.5 centimeters of the unit include packed intraclastic grainstone, isolated clasts in grainstone matrix, and brecciated intraclasts with chaotic orientation. Isolated clasts in grainstone matrix is most abundant and a typical sequence includes from base to top: randomly oriented coarse pebble

			clast lag overlain by subparallel clasts which are sparsely packed, which is overlain by tightly packed clasts in shale matrix. Samples: I-21-0.0, 76.6 mbM; I-21-0.6, 76.4 mbM; I-21-2.2, 75.9 mbM; I-21-4.1, 75.3 mbM; I-21-8.2, 72.9 mbM.
22	0.7	27.5	Limestone (packstone/grainstone), light to medium gray, weathering light gray to red brown where dolomitized; coarse grained; thin to thick bedded. Low amplitude stylolite seams. Shale drapes, partially dolomitized. Lower 24.4 centimeters is oolitic and intraclastic, but predominantly intraclastic. Remainder of unit is oolitic. Oolitic shoal exposed on bench above road cut. Samples: I-22-0.0, 73.4 mbM; I-22-1.8, 72.9 mbM. Lower oolite shoal (first bench above road cut). Numbers corres pond to meters above base of shoal: IOA 0.0; IOA 0.3; IOA 0.9; IOA 1.0; IOA 1.5; IOA 1.8; IOA 2.6; IOA 2.8; IOA 3.75; IOA 3.9; IOA 4.5; IOA 4.9; IOA 5.1; IOA 5.3; IOA 5.4; IOA 5.75; IOA 5.9.
23	0.3	27.8	Shale (and one limestone interbed), shale: dark gray and green brown, weathering brown to gray white; very fine grained. Abiotic. Structureless. Rare burrows. Limestone (packstone/grainstone): medium gray, weathering light gray; coarse grained; thin bedded. Polymictic limestone clast conglomerate bed 12.2 centimeters above base. Irregular and uneven. Sample: I-23-0.4, 72.6 mbM.
24	1.0	28.8	Limestone (mudstone to grainstone), medium gray, weathering light gray to red brown; coarse grained; laminated to thin bedded, irregular and uneven. Rare interbeds of shale, partially dolomitized. Stylolitic. Fossil debris-trilobites and echinoderms. Oncolitic? Burrowed. Intraclastic at base grading upward into cross-stratified oolite. Ooids are 1 to 2.5 millimeters in diameter, commonly dolomitized. Discontinuous mudstone fills troughs in

			oolite. Oolitic shoal exposed on bench above road cut. Samples: I-24-2.2, 71.7 mbM; I-24-2.4, 71.7 mbM.
25	1.7	30.5	Shale with occasional limestone interbeds, shale: brown gray and dark gray, weathering red brown and medium gray; very fine grained. Abiotic. Structureless. Limestone (mudstone to grainstone): medium gray, weathering light gray; fine to coarse grained; planar laminated to thin bedded, irregular and uneven. Burrows. Intraclastic, polymictic clast association. Fossiliferous. Oolitic. Samples: I-25-0.6, 71.2 mbM; I-25-3.9, 70.2 mbM.
26	3.1	33.6	Limestone (packstone and grainstone), medium gray, weathering light gray to brown; coarse grained; thin to thick bedded, irregular and uneven. Intraclasts, rare. Bioclasts, partially dolomitized. Ooids, partially dolomitized, hardgrounds, differential packing observed when comparing spar rich horizons to spar poor horizons, skeletal material (debris) randomly oriented in ooid matrix, bedding surfaces not rippled, no cross-stratification, and lateral decrease in grain size. Limestone beds are lense shaped, laterally shales thicken at expense of limestone beds. Discontinous thin shale partings to interbedded shale up to 15.3 centimeters thick. Fractures filled with sparry calcite cement. Irregular and low amplitude stylolite seams. Samples: I-26-8.2, 67.2 mbM; I-26-core, 67.2 mbM; I-26-flank, 67.2 mbM.
27	0.7	34.3	Shale and limestone (nodular bedded limestone), shale: dark gray, weathering light gray; very fine grained. Structureless. Abiotic. Limestone (mudstone and wackestone): medium gray, weathering light gray, fine grained; laminated and thin bedded. Burrowed. Fossiliferous, trilobites. Nodules, several centimeters long and several

			centimeters wide and 1.5 centimeters thick (on average).
28	0.5	34.8	Limestone (packstone and grainstone), light to medium gray, weathering light tan gray to red brown; coarse grained; thin to medium bedded, irregular and uneven. Fosssiliferous, sparse intraclasts in bioclastic matrix. Oolitic. Thin shale interbeds and partings. Intraclasts more common toward top of unit. Sample: I-28-1.6, 65.4 mbM.
29	2.7	37.5	Shale and limestone (nodular bedded limestone), shale: dark gray and green brown, weathering light gray and brown; very fine grained; laminated. In part mottled. Green shale adjacent to limestone beds. Limestone (mudstone to grainstone): medium gray, weathering light gray; fine to coarse grained; thin to medium bedded, irregular and uneven. Burrows-vertical, straight, simple, and 1-2 centimeters in diameter. Pseudomudcracks. Intraclastic. Fossiliferous. Limestone nodules-elongate, 15.3 centimeters long, fine grained, mudstone, burrowed, and some contain significant proportion of siliciclastic material. Samples: I-29-4.8, 63.9 mbM; I-29-5.7, 63.7 mbM; I-29-6.9, 63.3 mbM.
30	0.6	38.1	Limestone (packstone to grainstone), light to medium gray, weathering light gray to tan brown; coarse grained; medium to thick bedded, irregular and uneven. Fining upward sequence-intraclastic packstone at base with fossiliferous and oolitic matrix, top becomes predominantly fossiliferous and oolitic. Very thin irregular, discontinuous shale partings which are commonly dolomitized. Fracture/fills. Stylolites. Fossiliferous-trilobites, echinoderms, and inarticulate brachiopods.
31	0.6	38.7	Limestone (packstone to grainstone), light to medium gray, weathering light gray to tan brown; coarse grained; medium to thick bedded, irregular and uneven.

			Fining upward sequence-intraclastic packstone at base with fossiliferous and oolitic matrix, top becomes predominantly fossiliferous and oolitic. Discontinuous to continuous shale partings up to 12.2 centimeters thick which are commonly dolomitized. Fracture/fills. Stylolites. Fossiliferous-trilobites, echinoderms, and inarticulate brachiopods. Hardgrounds. Shale: dark gray and green brown, weathering light gray and brown; very fine grained; laminated. Abiotic. Sample: I-31-1.3, 61.7 mbM.
32	1.6	40.3	Shale and limestone (nodular and undulatory bedded limestone), shale: dark gray, weathering light gray and green brown to white; very fine grained; structureless to laminated. Iron stained. Limestone (mudstone to grainstone): medium gray, weathering light gray; very fine to coarse grained; planar and cross laminated to thin bedded, irregular and uneven. Lenses typically intraclastic and pinch out over several meters. Limestone lenses and nodules-planar to cross laminated, mudstone, burrowed mudstone, nodules are very fine grained, and lenses are fine to coarse grained. Intraclastic beds-clasts 12.2 X 1.5 centimeters, random to fanned orientation, packstone to grainstone matrix. Thin discontinuous, burrowed mudstone may occur at base of intraclastic lense. Samples: I-32-1.9, 60.9 mbM; I-32-2.0, 60.9 mbM.
33	0.4	40.7	Limestone (packstone to grainstone), medium gray, weathering light gray; medium to coarse grained; thin bedded, irregular and uneven. Intraclasts-12.2 centimeters long X 12.2 centimeters wide X 1.5 centimeters thick, polymictic. Fossiliferous-inarticulate brachiopods and trilobites. Oolitic. Hardgrounds. Stylolites. Dolomitization. Thin discontinuous shale partings.
34	3.5	44.2	Shale and limestone (nodular and undulatory bedded limestone), shale: dark

			gray, weathering light gray to white; very fine grained; structureless. Abiotic. Pyrite. Limestone (mudstone to grainstone): medium gray, weatering light gray; very fine to coarse grained; planar and cross laminated to thick bedded, irregular and uneven. Nodules-typically mudstone in composition, very fine to fine grained, and peloidal. Discontinuous to continuous bedded limestone. Intraclastic beds rare. Slump structure? near top. Oolitic. Fossiliferous. Stylolitic. Abundant hardgrounds. Samples: I-34-2.5, 58.7 mbM; I-34-10.6, 56.3 mbM.
35	0.6	44.8	Limestone (mudstone to grainstone), medium gray, weathering light gray to brown; coarse grained; thin to medium bedded, irregular and uneven. Partially dolomitized. Intraclastic beds-clast diversity increases toward top of unit, largest clasts near base (clast size decreases upward), clasts project into overlying shales, oolitic and fossiliferous matrix within intraclastic limestone increases in grain size up unit. Low amplitude stylolite seams. Shale partings and interbeds toward the top of unit. Sample: I-35-1.0, 55.7 mbM.
36	2.8	47.6	Shale and limestone (undulatory and nodular bedded limestone), shale: dark gray and green brown, weathering light gray to white and pale green brown; very fine grained; laminated to structureless to mottled. Iron stained. Rare inarticulate brachiopods and trilobites. Limestone (mudstone to packstone): medium gray, weathering light gray; very fine to coarse grained; planar and cross laminated to thin bedded, irregular and uneven. Nodules and thin lenses increase up unit. Fossiliferous-trilobites. Samples: I-36-2.9, 54.5 mbM; I-36-7.1, 53.2 mbM.
37	0.6	48.2	Limestone (wackestone to grainstone), medium gray, weathering medium to light gray; fine to coarse grained; thin

			bedded, irregular and even to uneven. Intraclastic beds-polymictic, larger at base decreasing in size up unit, random clast orientation, subrounded to subangular, and thin laminated wackestone/packstone partings. Thin, partially dolomitized shale partings. Stylolites. Vuggy porosity. Fossils and ooids as matrix within intraclastic beds, matrix grain size increases up unit.
38	0.6	48.8	Shale and limestone (undulatory and nodular bedded limestone), shale; medium to dark gray, weathering white to red brown; very fine grained; mottled. Limestone (mudstone to grainstone): medium gray, weathering light gray; very fine to coarse grained; laminated to thin bedded. Fossiliferous. Intraclasts-small, polymictic. Lenticular limestone beds in lower 1/3 give way to nodules in upper part of unit.
39	0.9	49.7	Limestone and shale (lower 30.5 centimeters undulatory bedded limestone, rest of unit is limestone interbedded with thin, discontinuous shale drapes), limestone (mudstone to grainstone): medium gray, weathering light gray to brown; fine to coarse grained; thin bedded, irregular and uneven. Intraclasts-coarsest at base, clasts sparser and smaller up unit. Fossils-increase in grain size upward (near top fossils several mm. in length), trilobites, echinoderms, and inarticulate brachiopods. Samples: I-39-1.5, 50.9 mbM; C39, 51.2 mbM.
40	0.5	50.2	Shale and limestone (nodular bedded limestone), shale: medium to dark gray, weathering light to medium gray; very fine grained; laminated to structureless. Abiotic. Iron stained. Limestone (mudstone, in part packstone): medium gray, weathering light gray; very fine to medium grained; planar and cross laminated to thin bedded, irregular and uneven. Thin nodules and lensoidal beds which are discontinuous over 10's of centimeters. Burrowed. Peloidal.

41	2.2	52.4	Limestone and shale (undulatory bedded limestone), limestone (packstone to grainstone): medium gray, weathering light gray to tan brown where dolomitized; medium to coarse grained; planar and cross laminated to thin bedded, irregular and uneven. Thin shale partings. Stylolites. Fossiliferous-trilobites and echinoderms. Vertical spar filled fractures. Intraclastic beds-clasts project into overlying beds. Sample: I-41-4.1, 48.7 mbM.
42	0.2	52.6	Shale, dark gray and olive green, weathering light gray to brown; very fine grained; laminated. Fossiliferous-trilobites and inarticulate brachiopods. Burrows. Sample: I-42-0.3, 47.7 mbM.
43	2.0	54.6	Limestone (packstone to grainstone), medium gray, weathering light gray to patchy brown; coarse grained; thin to medium bedded, irregular and uneven. Pseudomudcracks at base. Occasional thin shale drapes and rare interbeds up to 3.1 centimeters thick. Discontinuous bedded. Stylolites. Spar filled fractures. Samples: I-43-0.5, 47.4 mbM; I-43-6.4, 45.4 mbM; C43-0, 46.5 mbM; C43-1, 46.0 mbM.
44	0.6	55.2	Shale and limestone (undulatory and nodular bedded limestone), shale: dark gray and olive green, weathering light gray to pale green; very fine grained; structureless to mottled. Color banding. Thickest shale interval is 9.2 centimeters. Limestone (packstone to grainstone): light to dark gray, weathering light gray to brown; fine to coarse grained; laminated to thin bedded, irregular and uneven. Lensoid shaped beds. Intraclastic-clasts project into overlying shale, average clast size is 6.1 X 6.1 X 1.5 centimeters. Fossiliferous-trilobites. Iron stained. Burrowed. Samples: I-44-1.5, 45.1 mbM; C44, 44.0 mbM.

45	1.0	56.2	Limestone (packstone to grainstone), dark gray, weathering dark gray to black; coarse grained; thin to thick bedded, irregular and uneven. Rare thin continuus to discontinuous shale partings usually dolomitized. Fossiliferous. Oolitic. Intraclastic. Low amplitude stylolite seams. Sample: I-45-3.2, 44.0 mbM.
46	0.5	56.7	Shale and limestone (nodular and undulatory bedded limestone), shale: dark gray, weathering medium to light gray to white; very fine grained; structureless to mottled. Trilobite fossil zones. Iron stained. Pyrite. Limestone (mudstone to packstone): medium to dark gray, weathering light gray; fine to coarse grained; planar and cross laminated to thin bedded, irregular and uneven. Mudstone grades laterally into packstone. Nodules-mudstone, burrowed mudstone. Fossiliferous. Intraclastic. Sample: I-46-1.0, 43.7 mbM.
47	0.7	57.4	Limestone (packstone to grainstone), medium gray, weathering light gray; medium to coarse grained; laminated to medium bedded, irregular and uneven. Occasional dolomitized shale partings. Stylolitic. Coarsening upward sequence. Spar cement fracture filling.
48	1.3	58.7	Shale and limestone (nodular bedded and rare undulatory bedded limestone), shale: dark gray, weathering light gray; very fine grained; structureless. Abiotic. Iron stained. Limestone (mudstone to packstone): medium gray, weathering light gray; fine to medium grained; planar and cross laminated to thin bedded, irregular and uneven. Lensoidal beds. Sole structures-exclusively from laminated and cross laminated packstone/grainstone intervals. Tool marks/groove casts trend: N 22°E, N 19°E, N 25°E, N 1°E, N 0°E, and N 4°W. Outcrop attitude: N 65°E, 23°SE. Sample: I-48-3.7, 41.7 mbM.

49	0.9	59.6	Limestone and shale (nodular bedded limestone), limestone (packstone to grainstone): medium to dark gray, weathering light to medium gray to brown where dolomitized; coarse grained; laminated to thick bedded, irregular and uneven. Lense shaped beds. Fossiliferous. Oolitic, upper 36.6 centimeters. Allochems partially dolomitized. Shale drapes. Rare intraclasts. Shale: dark gray and olive green, weathering light gray and brown; very fine grained; laminated. Abiotic. Thickest shale in terval is 3.1 centimeter thick. Vertical fractures filled with calcite cement. Sample: I-49-1.1, 41.2 mbM.
50	0.8	60.4	Limestone and shale (undulatory to nodular bedded limestone), limestone (mudstone to grainstone): dark gray, weathering light gray; very fine to coarse grained; laminated to thin bedded, irregular and uneven. Vertical burrows. Fossiliferous-trilobites. Intraclastic-thickest beds, clasts project into overlying shales, lensoidal beds, some clasts up to 9.2 centimeter long. Shale: dark gray, weathering light gray; very fine grained; structureless. Abiotic. Burrows in calcareous shale. Color banded. Iron stained. Samples: I-50-0.5, 40.4 mbM; I-50-1.2, 40.2 mbM.
51	0.7	61.1	Limestone (packstone and grainstone), medium gray, weathering light gray to dark gray, brown where dolomitized; coarse grained; thick bedded, irregular and uneven. Secondary vugs. Lower 15.3 centimeters is intraclastic. Upper 58.0 centimeters-intraclastic, oolitic, fossiliferous, and glauconitic/phosphatic. Sample: I-51-0.5, 39.6 mbM.
52	0.6	61.7	Limestone and shale (undulatory to nodular bedded limestone), limestone (mudstone to grainstone): dark gray, weathering light gray; very fine to coarse grained; laminated to thin bedded, irregular and uneven. Vertical burrows. Fossiliferous-trilobites. Intraclastic.

			Shale: dark gray, weathering light gray; very fine grained; structureless. Abiotic. Burrows. Iron stained.
53	1.7	63.4	Limestone (packstone and grainstone), medium to dark gray, weathering light to medium gray, brown where dolomitized; medium to coarse grained; thick bedded, regular and uneven. Oolitic. Fossiliferous-some trilobites several mm. long. Rare intraclasts. Dolomitized shale partings. Vertical fracture/fills. Stylolites-low to high amplitude, amplitude ~1.5 centimeters. Vuggy porosity. Sample: I-53-1.7, 38.0 mbM.
54	0.3	63.7	Limestone (packstone to grainstone), medium gray, weathering light gray; medium to coarse grained; thin bedded, irregular and uneven. Oolitic. Thin discontinuous shale drapes. Lower 3.1 centimeters-dark gray shale. Unit 54 is an oolitic cap to unit 53.
55	3.1	66.8	Limestone and shale (nodular and undulatory bedded limestone), limestone (mudstone to grainstone): medium to dark gray, weathering light gray to red brown where iron stained; very fine to coarse grained; planar and cross laminated to medium bedded, irregular and uneven. Pseudomudcracks. Intraclastic beds-thickest beds, clasts project, fanned clasts, lenticular bedded, covered with oolitic cap which gives the bed an overall uniform thickness. Fossiliferous-trilobites and graptolites (*Dendroidea*). Oolitic. Sole marks-groove casts trend N 49° E, N 24° E. Burrowed. Secondary Vugs. Shale: dark gray, weathering gray to white; very fine grained; laminated. Typically 0.9 centimeters thick or less. Abiotic. Samples: I-55-0.2, 36.4 mbM; I-55-0.8, 36.3 mbM; I-55-10.1, 33.4 mbM.
56	1.2	68.0	Limestone and shale (undulatory and nodular bedded limestone), limestone (mudstone to grainstone): medium to dark gray, weathering light gray to red brown

			where iron stained; very fine to coarse grained; planar and cross laminated to medium bedded, irregular and uneven. Intraclastic beds-thickest beds, clasts project, fanned clasts, lenticular bedded, intraclats in shale matrix. Fossiliferous-trilobites, graptolites (*Dendroidea* in calc. shales and argill. lmsts.). Oolitic. Burrowed. Shale: dark gray, weathering gray to white; very fine grained; laminated. Abiotic. Similar to unit 55 except basal 30.5 centimeters is somewhat more shale rich. Sample: *I-56-1.2*, 33.0 mbM.
57	1.0	69.0	Limestone and shale (undulatory bedded limestone), limestone (mudstone to grainstone): medium gray, weathering gray, brown where dolomitized; fine to coarse grained; laminated to thin bedded, irregular and uneven. Fossiliferous-graptolites. Intraclasts-monomictic clasts float in calcareous shale matrix, some clasts normal to bedding. Burrowing. Pseudomudcracks-dolomitized shale and micrite occur where clasts pulled apart. Thin discontinuous shale partings. Shale: medium to dark gray, weathering gray to brown, fine grained; laminated. Dolomitized. Beds rarely exceed 3.1 centimeters in thickness. Fossiliferous-trilobites. Peloidal. Sample: *I-57-1.6*, 31.7 mbM.
58	3.0	72.0	Limestone and shale (undulatory and mottled bedded limestone), limestone (mudstone to grainstone): medium to dark gray, weathering gray to red brown; fine to coarse grained; laminated to thin bedded, irregular and uneven. Intraclastic beds, matrix dolomitized, thickest beds. Lenticular beds. Pseudomudcracks filled with dolomitized shale. Vugs. Shale: green to gray, weathering green gray; very fine to medium grained; laminated. Shale intervals 0.3 to 3.1 centimeters thick. Graptolitic. Shales are more calcareous when compared to previous units containing shale.

			Mottled. Samples: I-58-2.5, 30.4 mbM; A1-1, 28.2 mbM.
59	0.3	72.3	Limestone (packstone), medium to dark gray, weathering gray to black to red brown; coarse grained; laminated to thin bedded, irregular and uneven. Low amplitude stylolite seams. Thin shale drapes near top-1.8 centimeter thick but laterally thicken and thin. Intraclastic-random to subparallel orientation. Vuggy. Samples: I-59-0.4, 27.8 mbM; A2-1, 28.2 mbM.
60	4.0	76.3	Limestone and shale (undulatory and nodular bedded limestone), limestone (mudstone to grainstone): medium to dark gray, weathering gray to red brown; fine to coarse grained; laminated to thin bedded, irregular and uneven. Intraclastic beds, matrix dolomitized, thickest beds. Lenticular beds. Petroliferous. Fossiliferous-trilobites very abundant near top of unit. Vugs. Shale: green to gray, weathering green gray; very fine to medium grained; laminated. Samples: I-60-3.0, 27.0 mbM; I-60-12.1, 24.2 mbM; I-60-12.6, 24.1 mbM; A2-2, 27.7 mbM; A3-1, 27.1 mbM; A4-0, 26.7 mbM; A4-1, 26.5 mbM; A5-1, 25.8 mbM; A6-1, 24.7 mbM; A6-2, 24.5 mbM; C-60, 28.0 mbM.
61	1.3	77.6	Limestone and shale (mottled and undulatory bedded limestone), limestone (wackestone to packstone): gray, weathering gray to brown; medium to coarse grained; laminated to thin bedded, irregular and uneven. Fossiliferous-trilobites. Intraclastic-monomictic. Pseudomudcracks. Shale: dark gray, weathering light gray; very fine grained; laminated. Thin partings. Dolomitized. Samples: I-61-0.5, 23.7 mbM; I-61-2.0, 23.3 mbM; A7-1, 23.2 mbM; A8-1, 22.9 mbM.
62	0.8	78.4	Limestone and shale (mottled and undulatory bedded limestone), limestone (wackestone to packstone): gray, weathering gray to brown; medium to coarse

			grained; laminated to thin bedded, irregular and uneven. Pseudomudcracks. Fossiliferous-trilobites. Intraclastic-monomictic. Vugs. Shale: dark gray and green brown, weathering light gray and brown; very fine grained; laminated. Thin partings and continuous beds up to 6.1 centimeters thick. Dolomitized. Samples: I-62-1.2, 22.2 mbM; I-62-1.3, 22.2 mbM; A9-T, 21.8 mbM.
63	3.9	82.3	Limestone and shale (undulatory and nodular bedded limestone), limestone (mudstone to grainstone): dark gray, weathering medium gray to light gray; fine to coarse grained; laminated to thin bedded, irregular and uneven. Burrows. Fosssiliferous-trilobites. Intraclastic. Vuggy. Dolomitization. Pseudomudcracks (pull-a-parts in cross section). Iron stained. Mudstone nodules common toward top. Shale: dark gray and olive green, weathering light gray and green brown; very fine to fine grained; laminated. Shale intervals from 6.1 to 36.6 centimeters thick. Samples: I-63-2.0, 21.2 mbM; I-63-8.9, 19.1 mbM; A10-1, 21.6 mbM; A11-0, 20.1 mbM; A11-1, 19.6 mbM; A12-1, 19.0 mbM; A13-1, 18.1 mbM.
64	0.3	82.5	Limestone (packstone to grainstone), dark gray, weathering gray to brown; coarse grained; medium bedded, irregular and uneven. Intraclastic-polymictic, subparallel orientation, largest clasts 15.3 X 3.1 centimeters, average clasts 1.5 X 0.6 centimeters, clasts project into overlying shales. Stylolites. Hardgrounds. Rare shale drapes near base. Sample: I-64-0.7, 17.7 mbM.
65	2.6	85.2	Shale and limestone (undulatory and nodular bedded limestone), shale: dark gray to green gray, weathering green gray, brown where dolomitized; very fine to fine grained; laminated. Fossiliferous-graptolites, trilobites. Mottled. Pelleted. Limestone (mudstone to grainstone): medium gray, weathering light gray; fine to coarse grained;

			planar and cross laminated to medium bedded, irregular and uneven. Intraclastic. Fossiliferous-trilobites. Limestone nodules-rounded to elongate, mudstone to grainstone, fossiliferous-trilobites. Samples: I-65-2.9, 16.8 mbM; I-65-5.7, 16.0 mbM; A14-1, 16.9 mbM.
66	2.2	87.4	Limestone and shale (undulatory and nodular bedded limestone), limestone (mudstone to grainstone): medium gray, weathering medium gray; fine to coarse grained; planar and cross laminated to medium bedded, irregular and uneven. Intraclastic. Fossiliferous-trilobites. Shale: dark gray to green gray, weathering green gray, brown where dolomitized; very fine to fine grained; laminated. Fossiliferous-graptolites, trilobites. Mottled. Pelleted. Sample: I-66-5.6, 13.3 mbM.
67	0.3	88.4	Shale, dark gray, weathering light to dark gray; very fine grained; structureless. Mottled. Abiotic. Samples: I-67-0.5, 12.6 mbM; A18, 12.2 mbM; B1, 11.9 mbM.
68	2.5	90.9	Limestone and shale (undulatory bedded limestone), limestone (mudstone to grainstone): medium gray, weathering medium gray; fine to coarse grained; planar and cross laminated to medium bedded, irregular and uneven. Pseudomudcracks. Vuggy. Intraclastic. Fossiliferous-trilobites. Shale: dark gray to green gray, weathering green gray, brown where dolomitized; very fine to fine grained; laminated. Fossiliferous-graptolites, trilobites. Mottled. Pelleted. Very thin, irregular and usually discontinous partings. Samples: I-68-2.2, 11.1 mbM; I-68-7.4, 9.5 mbM; B2, 11.4 mbM; B3, 9.9 mbM.
69	4.4	95.3	Limestone and shale (undulatory bedded limestone), limestone (mudstone to grainstone): medium gray, weathering medium gray; fine to coarse grained; planar and cross laminated to thin

			bedded, irregular and uneven. Pseudomudcracks. Calcite filled fractures. Vuggy. Intraclastic-stylobrecciated. Iron stained. Oolitic. Fossiliferous-trilobites. Shale: dark gray to green gray, weathering green gray, brown where dolomitized; very fine to fine grained; laminated. Fossiliferous-graptolites, trilobites. Mottled. Pelleted. Very thin, irregular and usually discontinous partings. Resembles unit 68 except shale more abundant in lower 1.5 meters. Samples: I-69-4.9, 7.8 mbM; I-69-9.5, 6.4 mbM; I-69-14.5, 4.9 mbM; B5, 8.6 mbM; B6, 7.9 mbM; B7, 7.0 mbM; B9, 5.6 mbM; B10-A, 5.0 mbM.
70	0.5	95.8	Shale, dark gray, tinted green gray, weathered dark green gray; very fine grained; laminated. Mottled. Abiotic.
71	2.6	98.4	Limestone and shale (undulatory and nodular bedded limestone), limestone (mudstone to grainstone): medium gray, weathering light gray; fine to coarse grained; laminated to thin bedded, irregular and uneven. Commonly argillaceous. Thin continuous to discontinuous shale partings. Intraclasts in shale and argillaceous limestone matrix. Pseudomudcracks. Lenticular bedded. Samples: I-71-2.8, 3.5 mbM; I-71-7.6, 2.1 mbM; B10-B, 2.3 mbM.
72	0.4	98.8	Limestone (wackestone to grainstone), medium gray, weathering light gray; medium to coarse grained; laminated to thin bedded, irregular and uneven. Vuggy. Stylolites predominant near top of unit. Coarsening upward cycle. Oolitic-partially dolomitized. Fossiliferous. Thin shale drapes. Samples: I-72-1.2, 1.4 mbM; B12, 1.4 mbM.
73	1.4	100.2	Shale and limestone (nodular and rarely undulatory bedded limestone), shale: green gray, weathering green gray; very fine grained; structureless. Abiotic. Limestone (mudstone to packstone): medium gray, weathering light gray; fine to

			medium grained; laminated to thin bedded, irregular and uneven. Laterally continuous over several meters. Chaotic clast orientation. Argillaceous. Elongate nodules are randomly oriented. Intraclastic-some angular clasts, random orientation. Pseudomudcracks (pull-aparts). Samples: I-73-3.1, 0.5 mbM; B13, 0.5 mbM; B14, 0.4 mbM.
74	3.8	104.0	MAYNARDVILLE LIMESTONE. Limestone and shale (ribbon to mottled bedded limestone), limestone (mudstone to packstone): medium gray, weathering light gray; fine to coarse grained; planar and cross laminated to medium bedded, irregular and uneven. Burrowed. Intraclastic-especially at base of unit. Oolitic. Iron stained. Fossiliferous-trilobites. rare vugs. Shale: green brown, weathering brown; very fine grained; laminated. Shale intervals usually less than 3.1 centimeters thick. Dolomitization. Argillaceous. Samples: I-74-0.3, 0.1 maN; I-74-9.8, 3.1 maN; B15, 1.3 maN; B17, 1.8 maN.
75	2.2	106.2	Limestone and shale (ribbon to mottled bedded limestone), limestone (mudstone to packstone): medium gray, weathering light gray; fine to coarse grained; planar and cross laminated to medium bedded, irregular and uneven. Stylolitic. Burrowed. Intraclastic. Oolitic. Iron stained. Fossiliferous. Rock colored black adjacent to fractures, petroliferous. Rare vugs. Shale: green brown, weathering brown; very fine grained; laminated. Shale intervals usually less than 3.1 centimeters thick. Dolomitization. Argillaceous. Sample: I-75-0.0, 3.8 maN.
76	7.6	113.8	Limestone and shale (ribbon to mottled bedded limestone), limestone (mudstone to packstone): dark gray to black, weathering light gray to pale brown; fine to coarse grained; planar and cross laminated to medium bedded, irregular and uneven. Stylolitic. Burrowed.

			Intraclastic. Oolitic. Iron stained. Fossiliferous. Rock colored black adjacent to fractures, petroliferous. Rare vugs. Cross stratified grainstone near to top of the unit. Shale: green brown, weathering brown; very fine grained; laminated. Shale intervals usually less than 3.1 centimeters thick and very discontinuous. Dolomitization. Argillaceous. Samples: I-76-5.0, 7.5 maN; I-76-11.4, 9.5 maN; I-76-24.6, 13.5 maN.
77	1.5	115.3	Limestone (grainstone), light gray, weathering light gray; fine to medium grained; thick bedded, irregular and uneven. Cross stratified-planar tabular cross sets with bent toe sets. Peloidal or oolitic. Vuggy. Attitude of outcrop-N 70°E, 12°SE. Paleocurrent trend-N 20°E. Possible herring bone cross beds. Sample: I-77-2.0, 14.2 maN.
78	2.7	118.0	Limestone and argillaceous limestone (mottled to ribbon bedded limestone), Limestone (mudstone to packstone): light to medium gray, weathering light gray; very fine to coarse grained; thick bedded. Stylolites. Vuggy. Lower 0.9 meters-oolitic, fossiliferous. Rest of unit-resembles unit 76, interbedded limestone and argillaceous limestone. Sample: I-78-0.5, 15.3 maN.
79	3.0	121.0	Lower 52 centimeters similar to unit 78. Upper 248 centimeters-limestone and argillaceous limestone (mottled to ribbon bedded limestone), limestone (packstone to grainstone): light gray, weathering light gray; very fine to coarse grained; thick bedded. Cross stratification most apparent in upper 1/2 of unit. Discontinuously bedded. Stylolites. Petroliferous. Upper 1.2 meters intraclastic-small clasts, cross stratified nature of clasts, average size 2-4 mm. in diameter, slightly elongate, polymictic. Coarsening upward cycle. Vuggy. Samples: I-79-0.0, 17.8 maN; I-79-6.2, 19.7 maN.

80	1.5	122.5	Limestone (mudstone to packstone to boundstone), medium gray, weathering light gray; very fine to coarse grained; medium to thick bedded. Stylolitic. Algal laminations-ultra thin laminations, wavy, laminations thicken along highs. Intraclastic. Laminated and cross laminated, scoured base. Dolostone partings. Samples: I-80-1.3, 21.2 maN; I-80-4.9, 22.3 maN.
81	2.3	124.8	Limestone (mudstone to wackestone to boundstone), medium to dark gray, weathering light gray; fine to medium grained; discontinuous to thick bedded. Stylolites, high amplitude. Dolostone partings. Mottled appearance. Vuggy porosity. Peloidal. Fossiliferous-trilobites. Upper part of unit finely laminated. Abundant spar filled vugs, pseudomorphs after evaporites? Samples: I-81-1.4, 22.7 maN; I-81-5.9, 24.1 maN.
82	0.4	125.2	Limestone (mudstone to packstone to boundstone), light and medium gray, weathering light gray; very fine to coarse grained; medium to thick bedded. Stylolitic. Algal laminations-ultra thin laminations, wavy, laminations thicken along highs. Laminated and cross laminated. Dolostone partings. Samples: I-82-0.3, 24.7 maN; I-82-0.5, 24.8 maN.
			UNEXPOSED MAYNARDVILLE LIMESTONE

JOY 2 SECTION

The Joy 2 subsurface drill core is located 1.0 km east of the Anderson-Roane County line and is approximately 5 km southeast of the ORNL main plant site. The bore hole is collared on the crest of Copper Ridge, just south of Bearden Creek. A complete Nolichucky and Maynardville section is represented.

UNIT	TKN. (m.)	CUM. TKN. (m.)	DESCRIPTION
			MARYVILLE LIMESTONE.
1	16.0	16.0	NOLICHUCKY SHALE. Shale and limestone, thin to thick bedded shale interbedded with thin limestone. Shale: dark gray green to black and maroon; very fine grained; laminated. Mica flakes. skeletal debris, trilobites and echinoderms. Calcareous, often well indurated. Limestone (mudstone to grainstone): fine to coarse grained; laminated to thin bedded, planar and cross stratified; irregular and even bedded. Thin (< 2 centimeters), laterally discontinuous laminated to cross laminated pellet? packstone and grainstone. Loading. Pseudonodules. Pseudomudcracks? Convoluted bedding. Fining upward sequences. Sharp bases. Sharp to diffuse tops. Stylolites. Hardgrounds. Limestone clast conglomerates with mono- and polymictic clast associations, rounded to angular clasts, clasts float in shale, and darkened micritic rinds around clasts. Oolitic. Locally glauconitic. Burrows. Samples: J-2 1020, 168.7 mbM; J-2 1019, 168.4 mbM; J-2 1015.5, 167.3 mbM; J-2 1012, 166.2 mbM; J-2 1005, 164.1 mbM; J-2 997.5, 161.8 mbM; J-2 995, 161.0 mbM; J-2 985.5, 158.1 mbM; J-2 980, 156.5 mbM.

2	1.0	17.0	Limestone and shale, fossiliferous limestone interbedded with thin shale. Limestone (packstone and grainstone): medium to coarse grained; very thin bedded, irregular and even. Sharp bases with diffuse to scoured tops. Pseudonodules. Loading. Contorted bedding. Shale: maroon; very fine grained.
3	46.0	63.0	Shale and limestone, thin to thick shale interbedded with thin limestone beds. Shale: gray green and maroon; faintly laminated. Disseminated skeletal debris in shale. Rare limestone clasts. Limestone (mudstone to grainstone): fine to coarse grained, thinly laminated to medium bedded, planar and low angle cross stratigication; irregular and even bedded. Fossils include: inarticulate brachiopods, trilobites, echinoderms. Limestone clast conglomerates with shale and limestone (mudstone to grainstone) matrix, clasts projecting into overlying shale, random to subparallel clast orientation, and long dimension of clasts commonly exceeding diameter of core (approximately 8 centimeters). Stylolites. Hardgrounds. Pseudonodules. Pseudomudcracks? Loading. Contorted bedding. Oolitic. Glauconitic. Pelletal? Sharp base, planar and irregular. Sharp to diffuse tops. Burrows. Fining upward sequences. Coarsening upward sequences. Microhummocky cross stratification. Samples: J-2 972.5, 1 54.2 mbM; J-2 969, 153.1 mbM; J-2 963, 151.3 mbM; J-2 954, 148.5 mbM; J-2 952, 147.9 mbM; J-2 950, 147.3 mbM; J-2 947, 146.4 mbM; J-2 941, 144.6 mbM; J-2 930, 141.2 mbM; J-2 926, 140.0 mbM; J-2 918, 137.6 mbM; J-2 913, 136.0 mbM; J-2 904.5, 133.4 mbM; J-2 898, 131.5 mbM; J-2 889.5, 128.9 mbM; J-2 885.5, 127.6 mbM; J-2 878, 125.4 mbM; J-2 874.5, 124.3 mbM; J-2 873.5, 124.0 mbM; J-2 864, 121.1 mbM; J-2 856.5, 118.8 mbM; J-2 847.5, 116.1 mbM; J-2 847, 115.9 mbM; J-2 844.5, 115.1 mbM; J-2 835, 112.2 mbM; J-2 26.5, 109.7 mbM.

4	1.0	64.0	Limestone and shale, pellet? and oolitic limestone interbedded with thin shale. Limestone (packstone and grainstone): fine to coarse grained; laminated to medium bedded, planar and cross stratified; irregular and even bedded. Glauconitic. Stylolites. Loading. Sharp irregular base and top, also diffuse tops. Pseudonodules. Shale: dark gray green; very fine grained; faintly laminated. Sample: J-2 824, 108.9 mbM.
5	1.0	65.0	Shale and limestone, thin to thick shale interbedded with thin limestone. Shale: dark gray green; very fine grained; faintly laminated. Limestone (packstone and grainstone): fine grained; laminated to thin bedded, planar and cross stratified; irregular bedded. Skeletal lags. Sharp planar bases and diffuse tops. Loading. Convoluted bedding. Sample: J-2 819, 107.4 mbM.
6	1.0	66.0	Limestone and shale, pellet? and oolitic limestone interbedded with thin shale. Limestone (packstone and grainstone): fine to coarse grained; very thin to thick bedded, planar and low angle cross stratification. Coarsening upward sequence. Stylolites. Quartz silt? Shale: dark gray green, very fine grained; faintly laminated. Sample: J-2 816.5, 106.6 mbM.
7	3.0	69.0	Shale and limestone, thin to thick shale interbedded with thin pelletal?, oolitic, and fossiliferous limestone. Shale: dark gray green and maroon; very fine grained; faintly laminated. Limestone (packstone and grainstone): fine to coarse grained; very thin bedded to medium bedded, planar and low angle cross stratified. Sharp scoured bases and diffuse tops. Basal grainstone lags. Oolitic intervals coarsen upward. Trilobites and echinoderms. Stylolites. Glauconite. Samples: J-2 812, 1 05.2 mbM; J-2 805, 103.1 mbM.

8	1.0	70.0	Limestone and shale, oolitic, intraclastic, and pellet? limestone interbedded with shale. Limestone (packstone and grainstone): fine to coarse grained; very thin to medium bedded, rare low angle cross stratified intervals. Locally fossiliferous. Glauconitic. Pseudonodules. Loading. Hardgrounds. Shale: dark gray green and maroon; very fine grained; laminated. Mica flakes.
9	9.0	79.0	Shale and limestone, thin and thick bedded shale interbedded with intraclastic, oolitic, and pelletal limestone. Shale: dark gray green and maroon; very fine grained; faintly laminated. Limestone (packstone and grainstone): fine to coarse grained; very thin to medium bedded, rare low angle cross stratification. Scoured surfaces. Rare fossils. Stylolites. Loading. Convoluted bedding. Limestone clast conglomerates show polymictic clast associations, subparallel to random clast orientation, and a wide variety of clast sizes (< 1 to > 8 centimeters in long dimension). Quartz silt lenses. Amalgamated bedding. Samples: J-2 795, 100.0 mbM; J-2 789.5, 98.4 mbM; J-2 778.5, 95.0 mbM; J-2 775, 93.90 mbM.
10	1.0	80.0	Limestone and shale, oolitic, intraclastic, and rare pelletal? limestone interbedded with thin shale. Limestone (packstone and grainstone): medium to coarse grained; very thin to thick bedded; planar stratification. Oolitic intervals show vague coarsening upward sequences. Stylolites. Shale: maroon and dark gray green; very fine grained; faintly laminated. Rare fossils.
11	15.0	95.0	Shale and limestone, thin to thick shale interbedded with fossiliferous, intraclastic, oolitic, and pelletal? limestone. Shale: maroon and dark gray green; very fine grained; faintly laminated. Limestone (packstone and grainstone): fine to coarse grained;

			very thin to medium bedded, planar and low angle cross stratification. Limestone clast conglomerates show monomicitic and polymicitic clast associations, subparallel clast orientation, darkened rinds around clasts, clasts which project into overlying rock unit, and a wide size range of clasts. Loading. Sharp scoured bases and diffuse to sharp tops. Vertical and horizontal burrows. Pseudonodules. Hardgrounds. Skeletal lags. Samples: J-2 768, 91.8 mbM; J-2 762, 90.0 mbM; J-2 755, 87.8 mbM; J-2 749, 86.0 mbM; J-2 743, 84.2 mbM; J-2 735.5, 81.9 mbM; J-2 734, 81.4 mbM; J-2 723, 78.1 mbM.
12	1.0	96.0	Limestone and shale, pellet? limestone interbedded with thin shale. Limestone (packstone and grainstone): fine grained; very thin to thin bedded, planar and low angle cross stratification. Sharp base with diffuse to sharp scoured upper bed surfaces. Rare fossil and intraclastic lenses. Pseudonodules. Loading. Burrows. Shale: dark gray green; very fine grained; faintly laminated. Sample: J-2 718, 76.6 mbM.
13	2.0	98.0	Shale and limestone, thin to thick shale interbedded with pellet?, oolitic, fossiliferous, and intraclastic limestone lenses. Shale: maroon and dark gray green; very fine grained, faintly laminated. Locally fossiliferous. Limestone (packstone and grainstone): fine to coarse grained; very thin to medium bedded. Coarsening upward sequences in pellet? rocks. Loading. Pseudonodules. Contorted bedding. Glauconitic. Burrows. Amalgamated bedding. Sample: J-2 711, 74.4 mbM.
14	1.0	99.0	Limestone and shale, pellet? limestone interbedded with shale. Limestone (packstone): fine grained; very thin to thin bedded, planar to cross stratified. Rare fossil lenses. Locally oolitic. Coarsening upward within thin oolitic lenses. Shale: maroon; very fine

			grained; faintly laminated. Limestone clasts float in shale. Sample: J-2 707.5, 73.4 mbM.
15	4.0	103.0	Shale and limestone, thin and thick shale interbedded with rare fossil, intraclastic, and oolitic limestone. Pellet? limestone is somewhat more abundant. Shale: dark gray green and maroon; very fine grained; faintly laminated. Trilobites. Clasts float in shale. Limestone (packstone and grainstone): fine to coarse grained; very fine to medium bedded, planar and low angle cross stratification. Fossil lags. Fining upward sequences. Pseudonodules. Coarsening sequences. Sharp bases and tops. Amalgamated scours. Limestone clast conglomerates with polymictic and multigeneration clast associations. Samples: J-2 706, 72.9 mbM; J-2 695.5, 69.7 mbM.
16	1.0	104.0	Limestone and shale, intraclastic and oolitic limestone interbedded with thin shale. Limestone (packstone and grainstone): coarse grained; very thin to medium bedded. Predominantly oolitic. Stylolites. Coarsening upward sequences. Glauconitic. Shale: maroon to dark gray green; very fine grained; faintly laminated.
17	3.0	107.0	Shale and limestone, thin to thick shale interbedded with oolitic, pelletal?, and intraclastic limestone. Shale: maroon and dark gray green; very fine grained; faintly laminated. Limestone (packstone and grainstone): fine to coarse grained; very thin to medium bedded, low angle cross stratification. Glauconite. Hardgrounds. Pelletal limestone show fining upward sequences. Limestone clast conglomerates with polymictic clast association, darkened rinds, and clasts generally less than 5 centimeters in long dimension. Loading. Pseudonodules. Scoured bases. Amalgamated bedding. Oolitic limestone show common coarsening

			upward sequences. Stylolites. Sample: J-2 685, 66.5 mbM.
18	1.0	108.0	Limestone and shale, oolitic limestone interbedded with shale. Limestone (packstone and grainstone): coarse grained; thin to thick bedded. Oolitic beds coarsen upward. Stylolites. Fossiliferous, mainly trilobites. Hardgrounds. Shale: dark gray green; very fine grained; faintly laminated. Very thin pellet? limestone interlayers show fining upward sequences.
19	5.0	113.0	Shale and limestone, thin to thick shale interbedded with oolitic limestone. Shale: dark gray green and maroon; very fine grained; faintly laminated. Rare, thin fossiliferous layers in shale. Limestone (packstone and grainstone): fine to coarse grained; very thin to thick bedde, planar and cross stratification. Intraclastic. Hardgrounds. Fossiliferous, trilobites, echinoderms, and *Chancelloria*. Sharp abses and diffuse tops. Stylolites. Limestone clast conglomerates with darkened micritic rims, coarse grainstone matrix, polymictic clast association, and random to subparallel clast orientation. Loading. Pseudomudcracks. Pseudonodules. Rare skeletal lags. Samples: J-2 674, 63.1 mbM; J-2 666, 60.7 mbM.
20	1.0	114.0	Limestone and shale, oolitic limestone interbedded with thin shale. Limestone (packstone and grainstone): medium to coarse grained; thin to thick bedded. Coarsening upward sequences. Fossils locally abundant, especially trilobites. Stylobrecciation. Sharp bases and diffuse tops. Loading. Pseudonodules. Rare intraclasts. Shale: dark gray green; very fine grained; faintly laminated.
21	22.0	136.0	Shale and limestone, thin to thick shale interbedded with intraclastic limestone. Shale: maroon and dark gray green; very fine grained; faintly laminated. Rare

			fossil debris. Clasts randomly oriented in shale. Limestone interbeds in shale typically less than 1 centimeter in thickness. Limestone (mudstone and packstone to grainstone): very fine to coarse grained; very thin to thick bedded, planar and low angle cross stratification. Loading. Pseudonodules. Contorted beds. Amalgamated bedding. Hardgrounds. Stylolites, stylobrecciation. Burrows. Sharp bases and diffuse tops. Fossil debris, trilobites and echinoderms. Limestone clast conglomerates with monomictic clast associations primarily, random clast orientations, clasts projecting into overlying shale beds, darkened rinds around many clasts, and multigeneration clasts Oolitic. Nodular and lenticular mudstone interbedded with shale. Quartz siltstone beds in middle of unit. Oncoids? Samples: J-2 655, 57.3 mbM; J-2 647.5, 55.1 mbM; J-2 641, 53.1 mbM; J-2 635, 51.2 mbM; J-2 623, 47.6 mbM; J-2 618, 46.1 mbM; J-2 612, 44.2 mbM; J-2 599.5, 40.4 mbM; J-2 595, 39.0 mbM; J-2 590.5, 37.7 mbM.
22	7.0	143.0	Limestone and shale, nodular and lenticular mudstone along with rare pelletal? limestone interbedded with thin shale. Limestone(mudstone and packstone to grainstone): very fine to fine grained, thin bedded, low angle cross stratification. Rare fossil packstone interlayers. Sharp bases and tops, sometimes diffuse tops. Loading. Pseudonodules. Contorted bedding. Intraclastic. Oolitic. Microhummocky cross stratification. Shale: dark gray green; very fine grained; otherwise nondescript. Samples: J-2 585, 36.0 mbM; J-2 582.5, 35.2 mbM; J-2 571.5, 31.9 mbM; J-2 570, 31.4 mbM; J-2 566, 30.2 mbM.
23	2.0	145.0	Limestone and shale, pelletal? limestone and lime mudstone interbedded with thin shale. Limestone (packstone to grainstone and mudstone): very fine to fine grained; thin to thick bedded, planar and

			low angle cross lamination. Rare skeletal lags. Sharp bases and diffuse tops. Microhummocky cross stratification. Loading. Pseudonodules. Burrows. Shale: dark gray green, very fine grained; faintly laminated. Samples: J-2 565, 29.9 mbM; J-2 560.5, 28.5 mbM.
24	2.0	147.0	Limestone (oncolitic and oolitic packstone): fine to coarse grained; medium to very thick bedded. Rare mudstone and quartz siltstone interlayers. Stylolites. Hardgrounds. Algal boundstone toward top.Samples: J-2 555, 26.8 mbM; J-2 553.5, 26.4 mbM.
25	7.0	154.0	Limestone (algal boundstone with oncoids, ooids, intraclasts, fossils, and shale occupying interalgal areas): very fine to coarse grained; thin to very thick bedded. Thrombolitic. Stylolites. Graptolites. Pseudomudcracks. Syneresis cracks? Burrows. Algal peloids. Samples: J-2 545, 23.8 mbM; J-2 540.5, 22.4 mbM; J-2 535, 20.7 mbM; J-2 534.5, 20.6 mbM; J-2 531.5, 19.7 mbM.
26	1.0	155.0	Limestone (nodular mudstone): very fine to fine grained; medium bedded. Rare shale drapes. Algal peloids. Pellets? Stylolites. Sample: J-2 529, 18.9 mbM.
27	2.0	157.0	Shale and limestone (thin to thick shale interbedded with intraclastic and pelletal limestone): Shale: green gray to dark gray green; very fine grained; faintly laminated. Some fossiliferous interlayers. Limestone clasts in shale are randomly oriented. Limestone (packstone to grainstone and mudstone): very fine to coarse grained; thin to thick bedded, planar to low angle cross stratification. Oolitic. Hardgrounds. Lime mudstone interlayers. Limestone clast conglomerates with ooid an d peloid matrix, subparallel to random clast orientation, clasts from 7 to 8 centimeters in long dimension, and common

			multigeneration clasts. Samples: J-2 524, 17.4 mbM; J-2 520, 16.2 mbM.
28	1.0	158.0	Limestone and shale, pelletal? limestone interbedded with thin shale. Limestone (packstone and grainstone): fine grained; thin to medium bedded, with planar and low angle cross stratification. Intraclastic. Pseudomudcracks. Sharp bases and tops. Loading. Pseudonodules. Nodular mudstone interlayers. Shale: dark gray green; very fine grained; faintly laminated. Limestone clasts float in shale matrix. Sample: J-2 518, 15.6 mbM.
29	3.0	161.0	Shale and limestone, thin shale interbedded with intraclastic and oolitic limestone and lime mudstone. Shale: dark gray green; very fine grained; faintly laminated. Limestone clasts float in shale matrix. Rare fossiliferous interlayers. Limestone (packstone to grainstone and mudstone): fine to coarse grained; very thin to thick bedded. Sharp bases and tops. *Renalcis*? clasts. Oncoids? Samples: J-2 513, 14.0 mbM; J-2 509, 12.8 mbM.
30	8.0	169.0	Limestone and shale, pellet? and algal peloidal limestone interbedded with shale. Limestone (packstone and grainstone): fine to medium grained; very thin to medium bedded, with planar and cross stratification. Rare lime mudstone, fossiliferous, oolitic, and intraclastic lenses. Stylolites. Pseudomudcracks. Hardgrounds. Oncoids. Loading. Pseudonodules. Burrows. Microhummocky cross stratification? Skeletal lags. Contorted bedding. Shale: dark gray green; very fine grained; faintly laminated. Limestone clasts and discontinuous interlayers? randomly oriented in shale. Samples: J-2 504, 11.3 mbM; J-2 502.5, 10.8 mbM; J-2 499, 9.8 mbM; J-2 498.5, 9.5 mbM; J-2 497, 9.5 mbM; J-2 493, 7.9 mbM; J-2 492, 7.6 mbM; J-2 491, 7.3 mbM; J-2 485, 5.5

			mbM; J-2 483.5, 5.0 mbM; J-2 482, 4.6 mbM.
31	4.0	173.0	Shale and limestone, thin to thick shale interbedded with intraclastic and pelletal limestone. Shale: dark gray green; very fine grained; faintly laminated. Limestone clasts randomly oriented in shale matrix. Limestone (packstone and grainstone): fine to coarse grained; thin to medium bedded, planar and cross stratification. Limestone clast conglomerates with monomictic clast associations, coarse peloidal and oolitic matrix, and darkened rinds around clasts. Loading. Pseudonodules. Sharp bases and scoured tops. Samples: J-2 478.5, 3.5 mbM; J-2 473, 1.8 mbM; J-2 470.5, 1.1 mbM; J-2 468, 0.3 mbM.
32	5.0	178.0	MAYNARDVILLE LIMESTONE. Limestone and shale, intraclastic and pelletal? limestone interbedded with thin shale drapes. Limestone (packstone and grainstone): fine to coarse grained; very thin to medium bedded, low angle cross stratification. Limestone clast conglomerates with polymictic clast associations, small clast size (2-3 centimeters), and peloidal matrix. Loading. Pseudonodules. Pseudomudcracks. Rare fossiliferous interlayers and basal lags. Shale: dark gray green; very fine grained; faintly laminated. Samples: J-2 461.5, 1.7 maN; J-2 459, 2.4 maN; J-2 455, 3.7 maN; J-2 453, 4.3 maN.
33	8.0	186.0	Limestone (packstone and grainstone): fine to coarse grained; thin to very thick bedded. Oncolitic. Oolitic, normal and superficial ooids. Quartz silt? Algal peloids. Rare mudstone lenses. Stylolites. Rare glauconite. Hardgrounds. Samples: J-2 438, 8.9 maN; J-2 428, 11.9 maN; J-2 426.5, 12.4 maN.
34	1.0	187.0	Limestone (packstone): coarse grained; thick bedded. Oncolitic. Oolitic. Hardgrounds. Stylolites. Numerous coarsening upward sequences.

35	3.0	190.0	Limestone (packstone and grainstone): fine to coarse grained; thick to very thick bedded. Oncolitic. Algal peloidal. Oolitic. Sample: J-2 417, 15.3 maN.
36	1.0	191.0	Limestone (packstone and grainstone): coarse grained; thick bedded. Stylolites. Oncolitic, oncoids up to 1 centimeter in diameter. Oolitic, ooids exceed 2 millimeters in diameter. Hardgrounds. Sample: J-2 409.5, 17.5 maN.
37	2.0	193.0	Limestone (packstone and grainstone): fine to medium grained; thick to very thick bedded. Peloidal. Oolitic. Rare argillaceous interlayers. Stylolites. Hardgrounds. Burrows. Superficial ooids. Fossiliferous, trilobites. Sample: J-2 404, 19.2 maN.
38	1.0	194.0	Limestone (packstone and grainstone): coarse grained; thick bedded. Oolitic, Oncolitic. Rare argillaceous and quartz silt? interlayers. Fossiliferous horizons, mainly trilobites.
39	1.0	195.0	Limestone (packstone and grainstone): fine grained; thick bedded perhaps cross stratified? Superficial ooids. Algal peloids. Stylolites. Hardgrounds. Dolomitized mudstone. Burrowed? Stylocummulate. Sample: J-2 397.5, 21.2 maN.
40	2.0	197.0	Limestone (packstone and grainstone): coarse grained; thick to very thick bedded. Oncoids. Ooids. Stylolites. Hardgrounds.
41	11.0	208.0	Limestone (packstone and grainstone): fine grained; very thick bedded. Superficial ooids? Algal peloids. Samples: J-2 382.5, 25.8 maN; J-2 372.5, 28.8 maN; J-2 359, 32.9 maN; J-2 356, 33.9 maN.
42	2.0	210.0	Limestone (boundstone and packstone to grainstone): fine to coarse grained; thick bedded. Thrombolite with algal

			peloidal, oolitic, oncolitic, and mudstone filling interalgal areas. Renalcis? Stylocummulate. Sample: J-2 350, 35.7 maN.
43	1.0	211.0	Limestone (packstone and grainstone): coarse grained; thick bedded. Stylolites. Oncoids less than 1 centimeter in diameter. Ooids generally less than 2 millimeters. High amplitude stylolites.
44	7.0	218.0	Limestone (boundstone and packstone to grainstone): fine to coarse grained; very thick bedded. Thrombolite. Oncoid, ooid, and algal peloidal grainstone to packstone fills interalgal areas. Clotted fabric. Dolomitized in part. Burrowed? Samples: J-2 338, 39.4 maN; J-2 334, 40.6 maN; J-2 330.5, 41.6 maN; J-2 321.5, 44.4 maN.
45	3.0	221.0	Limestone and dolostone (boundstone and packstone to grainstone): medium grained; very thick bedded. Cryptalgal laminites. Algal peloidal packstone and grainstone alternating with algally? bound algal peloids. Stylolites. Wavy ultra thin laminations. Samples: J-2 319, 45.1 maN; J-2 312, 47.3 maN; J-2 310.5, 47.7 maN.
46	7.0	228.0	Limestone and dolostone (boundstone and packstone to grainstone): fine to coarse grained; very thick bedded. Renalcis? Stylobrecciated. Oncoids. Numerous stylolites. Oolitic interlayers. Algal peloids. Samples: J-2 307.5, 48.7 maN; J-2 305, 49.4 maN; J-2 300.5, 50.8 maN; J-2 296, 52.2 maN; J-2 287, 54.9 maN.
47	1.0	229.0	Limestone and dolostone (boundstone and packstone to grainstone): medium grained; thick bedded. Cryptalgal laminites. Dolomitized interlayers. Stylolites.
48	20.0	249.0	Limestone (boundstone and packstone to grainstone): fine to coarse grained; very thick bedded. Thrombolite. Oolitic grainstone fills interalgal areas.

			Aggregate grains. Oncoids. Dolomitized interlayers (mudstone). Stylocummulate. Fossil debris, trilobites common throughout. Samples: J-2 282.5, 56.3 maN; J-2 268, 60.7 maN; J-2 264, 61.9 maN; J-2 255, 64.7 maN; J-2 250.5, 66.0 maN; J-2 238, 69.9 maN; J-2 234.5, 70.9 maN; J-2 232.5, 71.5 maN; J-2 224, 74.1 maN.
49	2.0	251.0	Dolostone (boundstone and grainstone): fine to medium grained; very thick bedded. Laterally linked hemispheroids. Perhaps grades laterally into cryptalgal laminites. Sample: J-2 217, 76.3 maN.
50	7.0	258.0	Limestone and dolostone (boundstone and packstone to grainstone): fine to coarse grained; very thick bedded. Thrombolotic. Fenestral fabric. Oolitic grainstone fills interalgal areas. Stylolites. Samples: J-2 211, 78.1 maN; J-2 205, 79.9 maN; J-2 204.5, 80.1 maN; J-2 193.5, 83.4 maN; J-2 189, 84.8 maN.
51	2.0	260.0	Dolostone and limestone (boundstone and grainstone): fine to medium grained; very thick bedded. Laterally linked hemispheroids. Domal stromatolites? Fenestral fabric.
52	1.0	261.0	Limestone (boundstone and packstone to grainstone): fine to medium grained; thick bedded. Thrombolitic. Oolitic and oncolitic? packstone and grainstone. Algal peloids occur sporatically.
53	2.0	263.0	Dolostone and limestone (boundstone): fine grained; very thick bedded. Fenestral fabric. Stromatolitic. Laterally linked hemispheroids? Sample: J-2 176, 88.8 maN.
54	4.0	267.0	Limestone and dolostone (boundstone and packstone to grainstone): fine to medium grained; thick to very thick bedded. Thrombolitic. Rare ooids and oncoids. Fenestral fabric. Vuggy porosity. Algal peloids. Thrombolites interfinger with thin cryptalgal laminites. Samples: J-2

			168.5, 91.0 maN; J-2 166.5, 91.7 maN; J-2 162, 93.0 maN.
55	4.0	271.0	Dolostone and limestone (boundstone and packstone to grainstone): medium grained; very thick bedded. Cryptalgal laminites. Wavy, ultra thin laminations. Antigravitational sedimentation. Stylolites. Fenestral fabric. Samples: J-2 151.5, 96.2 maN; J-2 150, 96.7 maN; J-2 147, 97.6 maN.
56	3.0	274.0	Limestone and dolostone (boundstone and packstone to grainstone): fine to medium grained; very thick bedded. Thrombolitic? Algal peloids bound together exhibiting an overall fenestral fabric. Vuggy porosity. Samples: J-2 143, 98.8 maN; J-2 140.5, 99.6 maN.
57	3.0	277.0	Dolostone (boundstone and packstone to grainstone): medium grained; very thick bedded. Rare limestone interlayers. Cryptalgal laminites. Wavy, ultrathin laminations. Samples: J-2 135, 101.3 maN; J-2 133, 101.9 maN; J-2 131, 102.5 maN.
			COPPER RIDGE DOLOSTONE.

SCARBORO ROAD SECTION

The Scarboro Road subsurface drill core (ORNL GW 130 and GW 131) is located at the east end of the Y-12 weapons plant adjacent to Scarboro Road along grid line E64,500. A complete Nolichucky and Maynardville section is represented.

ORNL GW 130 (590 ft. east--offset from grid line)

UNIT	TKN. (m.)	CUM. TKN. (m.)	DESCRIPTION
			MARYVILLE LIMESTONE.
1	1.0	1.0	NOLICHUCKY SHALE. Shale: dark gray green; very fine grained; faintly laminated. Rare thin intraclastic lenses.
2	2.0	3.0	Limestone and shale, pelletal? limestone interbedded with thin to thick shale. Limestone (packstone and grainstone): fine grained; very thin to thin bedded, planar and low angle cross lamination. Pseudonodules. Loading. Shale: dark gray green and maroon; very fine grained; faintly laminated.
3	43.0	46.0	Shale and limestone, thin to thick shale interbedded with pelletal?, intraclastic, fossiliferous, and oolitic limestone. Shale: dark gray green and maroon; very fine grained; laminated. Rare fossils? Contact between dark gray green and maroon colored shale is sharp and planar. Limestone (packstone to grainstone and rare mudstone): fine to coarse grained; very thin to medium bedded, planar and low angle cross lamination. Loading. Pseudonodules. Contorted bedding. Sharp bases and sharp to diffuse tops.

			Limestone clast conglomerates show variable clast sizes (< 8 centimeters), clasts which project into overlying rock units, a wide variety of clast types (pellet grainstone is most common), and shale as the dominant matrix type. Ooid and lime mudstone lenses are rare.
4	1.0	47.0	Limestone and shale, pellet? limestone interbedded with thin shale. Limestone (packstone and grainstone): fine grained, thin to medium bedded, low angle cross lamination. Loading. Pseudonodules. Stylolites. Sharp scoured bases and scoured to diffuse tops. Shale: dark gray green and maroon, very fine grained; faintly laminated.
5	2.0	49.0	Shale and limestone, thin to thick shale interbedded with pellet? and oolitic limestone. Shale: dark gray green; very fine grained; faintly laminated. Limestone (packstone and grainstone): fine to coarse grained, very thin to medium bedded, planar and low angle cross lamination. Fossiliferous, trilobites and echinoderms.
6	2.0	51.0	Limestone and shale, pelletal? and intraclastic limestone interbedded with thin shale. Limestone (packstone and grainstone): fine to coarse grained; very thin to medium bedded, pellet? limestone shows low angle cross lamination. Pseudonodules. Loading. Stylolites. Rare oolitic lenses. Limestone clast conglomerates with clasts from 1 to 6 centimeters in long dimension. Shale: dark gray green and maroon; very fine grained; faintly laminated.
7	1.0	52.0	Shale and limestone, thin to thick shale interbedded with pellet? limestone. Shale: dark gray green and maroon; very fine grained. Calcareous. MIca flakes. Limestone (packstone and grainstone): fine grained; very thin to thin bedded, low angle cross laminations. Rarely intraclastic. Loading. Contorted bedding.

8	2.0	54.0	Limestone and shale, pelletal? and oolitic limestone interbedded with thin shale. Limestone (packstone and grainstone): fine to coarse grained, very thin to medium bedded, planar and low angle cross lamination. Rare limestone clast conglomerates. Sharp bases and sharp to diffuse tops. Glauconitic, especially in ooid grainstones. Shale: dark gray green and maroon; very fine grained; faintly laminated.
9	2.0	56.0	Shale and limestone, thin to thick shale interbedded with rare ooid and intraclastic limestone. Shale: dark gray green and maroon; very fine grained; laminated. Dark gray green shale occurs in close stratigraphic proximity to limestone lenses. Limestone (packstone and grainstone): medium to coarse grained; thin to medium bedded. Stylolites. Loading.
10	2.0	58.0	Limestone and shale, oolitic limestone interbedded with thin shale. Limestone (packstone and grainstone): coarse grained; thick bedded. Rare pelletal? lenses. Ooid beds show vague coarsening upward sequences. Fossiliferous, trilobites and echinoderms. Shale: dark gray green and maroon; very fine grained; laminated.
11	4.0	62.0	Shale and limestone, thin to thick shale interbedded with pelletal? and oolitic limestone. Shale: primarily dark gray green; very fine grained; faintly laminated. Locally fossils float in shale. Limestone (packstone and grainstone): fine to coarse grained; very thin to medium bedded, planar and low angle cross laminations. Loading. Pseudonodules. Convoluted bedding. Rare intraclastic lenses.
12	4.0	66.0	Limestone and shale, pelletal? limestone interbedded with thin shale. Limestone (packstone and grainstone): fine grained; very thin to thin bedded, low angle cross laminations. Rare oolitic

			and intraclastic lenses interlayered with shale. Shale: dark gray green; very fine grained; faintly laminated.
13	2.0	68.0	Shale and limestone, thin to thick shale interbedded with pelletal? limestone. Shale: maroon and dark gray green; very fine grained; faintly laminated. Limestone clasts in shale. Limestone (packstone and grainstone): fine grained; very thin to thin bedded, planar and low angle cross lamination. Rare oolitic and intraclastic lenses. Loading. Pseudonodules. Sharp bases and diffuse tops.
14	2.0	70.0	Limestone and shale, pellet? limestone interbedded with thin to thick shale. Limestone (packstone and grainstone): fine grained; very thin to thin bedded, planar and low angle cross laminiation. Rare oolitic and intraclastic lenses. Locally fossiliferous, trilobites. Amalgamated bedding. Sharp bases and scoured sharp tops. Skeletal lags. Shale: maroon and dark gray green; very fine grained; faintly laminated.
15	3.0	73.0	Shale and limestone, thin to thick shale interbedded with pelletal? limestone. Shale: dark gray green; very fine grained; laminated. Limestone nodules. Mica flakes. Quartz silt? Limestone (packstone and grainstone): fine grained; very thin to thin bedded, low angle cross lamination. Intraclastic and oolitic lithologies are rare. Loading. Pseudonodules.
16	4.0	77.0	Limestone and shale, pellet? and oolitic limestone interbedded with thin shale. Limestone (packstone and grainstone): fine to coarse grained; very thin to medium bedded, low angle cross lamination. Sharp bases and diffuse tops. Loading. Shale: dark gray green; very fine grained; laminated.
17	1.0	78.0	Shale and limestone, thin to thick shale interbedded with pelletal? and

			intraclastic limestone. Shale: dark gray green and maroon; very fine grained. Limestone (packstone and grainstone): fine to coarse grained; very thin to medium bedded, planar and low angle cross lamination. Mica flakes. Quartz silt. Rare oolitic lenses.
18	1.0	79.0	Limestone and shale, intraclastic and pelletal? limestone interbedded with thin shale. Limestone (packstone and grainstone): fine to coarse grained; very thin to medium bedded, low angle cross lamination. Limestone clast conglomerates show a wide variety of clast sizes (1-7 centimeters in long dimension), polymictic and monomictic clast association, and clasts which project into overlying rock units. Loading. Pseudonodules. Basal skeletal lags. Sharp bases and diffuse tops. Shale: dark gray green; very fine grained; laminated. Disseminated fossil debris, primarily trilobites.
19	1.0	80.0	Shale and limestone, thin to thick shale interbedded with intraclastic limestone. Shale: dark gray green to maroon; very fine grained; faintly laminated. Limestone (packstone and grainstone): coarse grained; thin to medium bedded. Rare pellet? interlayers.
20	1.0	81.0	Limestone and shale, pellet? and intraclastic limestone interbedded with thin shale. Limestone (packstone and grainstone): fine to coarse grained; very thin to medium bedded, planar and low angle cross lamination. Shale: dark gray green; very fine grained.
21	5.0	86.0	Shale and limestone, thin to thick shale interbedded with pellet? and intraclastic limestone. Shale: dark gray green and maroon; very fine grained; faintly laminated. Disseminated trilobite debris throughout. Limestone (packstone and grainstone): fine to coarse grained; very thin to medium bedded, low angle cross lamination. Loading.

			Pseudonodules. Contorted bedding. Glauconitic. Oolitic. Fossiliferous, trilobites and echinoderms.
22	1.0	87.0	Limestone and shale, pellet? and intraclastic limestone interbedded with thin to thick shale. Limestone (packstone and grainstone): fine to coarse grained; very thin to medium bedded, low angle cross lamination. Shale: dark gray green and maroon; very fine grained; faintly laminated.
23	1.0	88.0	Shale and limestone, thin to thick shale interbedded with intraclastic limestone. Shale: dark gray green and maroon; very fine grained. Limestone (packstone and grainstone): coarse grained; thick bedded. Limestone clast conglomerates show polymictic clast associations, multigeneration clasts, bored and burrowed clasts, subparallel to random clast orientation (with respect to bedding), and a coarse grained fossiliferous matrix supporting clasts.
24	2.0	90.0	Limestone and shale, pellet? limestone interbedded with thin shale. Limestone (packstone and grainstone): fine grained; very thin to thin bedded, low angle cross lamination. Rare intraclastic beds, commonly less than 3 centimeters in thickness. Shale: dark gray green and maroon; very fine grained; faintly laminated.
25	2.0	92.0	Shale and limestone, thin to thick shale interbedded with rare pellet? and intraclastic limestone. Shale: dark gray green and maroon; very fine grained. Limestone (packstone and grainstone): fine to coarse grained; very thin to thin bedded, low angle cross lamination.
26	1.0	93.0	Limestone and shale, pellet? limestone interbedded with thin shale. Limestone (packstone and grainstone): fine grained; very thin to thin bedded, low angle cross lamination. Rare

			intraclastic lenses. Shale: dark gray green; very fine grained; laminated.
27	5.0	98.0	Shale and limestone, thin to very thick shale interbedded with pelletal?, oolitic, and intraclastic limestone. Shale: dark gray green and maroon; very fine grained; faintly laminated. Limestone (packstone and grainstone): fine to coarse grained; very thin to medium bedded, planar and low angle cross lamination. Loading. Stylolites. Pseudonodules.
28	1.0	99.0	Limestone and shale, pelletal? and oolitic limestone interbedded with thin shale. Limestone (packstone and grainstone): fine to coarse grained; very thin to medium bedded, low angle cross lamination. Shale: dark gray green and maroon; very fine grained.
29	1.0	100.0	Shale and limestone, thin to thick shale interbedded with oolitic limestone. Shale: dark gray green and maroon; very fine grained; faintly laminated. Limestone (packstone and grainstone): coarse grained; medium bedded. Rare intraclastic and pellet limestone lenses and thin beds.
30	1.0	101.0	Limestone and shale, oolitic and intraclastic limestone interbedded with thin shale drapes. Limestone (packstone and grainstone): coarse grained; medium to thick bedded. Rare pellet? limestone lenses. Shale: maroon; very fine grained; laminated.
31	1.0	102.0	Shale and limestone, thin to thick shale interbedded with pellet? limestone. Shale: dark gray green and maroon; very fine grained; faintly laminated. Limestone (packstone and grainstone): fine grained; very thin to thin bedded, low angle cross lamination. Rare intraclastic interlayers.
32	1.0	103.0	Limestone and shale, oolitic and pelletal? limestone interbedded with thin

			shale. Limestone (packstone and grainstone): fine to coarse grained; very thin to medium bedded, low angle cross lamination. Shale: dark gray green; very fine grained; faintly laminated. Limestone clasts float in shale matrix.
33	1.0	104.0	Limestone and shale, pelletal? limestone interbedded with thin shale. Limestone (packstone and grainstone): fine grained; very thin to thin bedded, low angle cross lamination. Rare intraclastic interlayers. Shale: dark gray green and maroon; very fine grained.
34	7.0	111.0	Shale and limestone, thin to thick shale interbedded with pelletal?, oolitic, and intraclastic limestone. Shale: dark gray green and maroon, maroon predominates; very fine grained; faintly laminated. Limestone clasts occur randomly oriented in shale matrix. Limestone (packstone and grainstone): fine to coarse grained; very thin to thick bedded, planar and low angle cross lamination. Rare fossiliferous interlayer, trilobites and echinoderms.
35	1.0	112.0	Limestone and shale, pelletal? and oolitic limestone interbedded with thin shale. Limestone (packstone and grainstone): fine to coarse grained; very thin to medium bedded, low angle cross lamination. Shale: maroon and dark gray green; very fine grained.
36	16.0	128.0	Shale and limestone, thin to very thick shale interbedded with pelletal?, oolitic, and intraclastic limestone and lime mudstone. Shale: dark gray green and maroon; very fine grained. Limestone clasts randomly oriented in shale. Limestone (packstone to grainstone and mudstone): fine to coarse grained; very thin to thick bedded, low angle cross lamination in pellet? lithology. Loading. Pseudonodules. Convoluted bedding. Sharp bases and sharp to diffuse tops.

			Lime mudstone most abundant toward top of unit.
37	1.0	129.0	Limestone and shale, pelletal? and intraclastic limestone interbedded with thin shale. Limestone (packstone and grainstone): fine to coarse grained; very thin to medium bedded, low angle cross lamination. Rare lime mudstone and oolitic interlayers and lenses. Shale: dark gray green; very fine grained; laminated.
38	1.0	130.0	Shale and limestone, thin to thick shale interbedded with intraclastic limestone. Shale: dark gray green and maroon; very fine grained; faintly laminated. Limestone (packstone and grainstone): coarse grained; medium bedded. Rare pellet interlayers.
39	1.0	131.0	Limestone and shale, pelletal? and intraclastic limestone interbedded with thin shale. Limestone (packstone and grainstone): fine to coarse grained; very thin to thin bedded. Shale: dark gray green and maroon; very fine grained; faintly laminated.
40	10.0	141.0	Shale and limestone, thin to very thick shale interbedded with peloidal limestone. Shale: dark gray green and maroon; very fine grained; faintly laminated. Limestone (packstone and grainstone): coarse grained; medium to thick bedded. Rare intraclastic, oolitic, pelletal, and lime mudstone lithologies. Superficial ooids. Stylolites. Stylocummulate.
41	6.0	147.0	MAYNARDVILLE LIMESTONE. Limestone and shale, lime mudstone interbedded with very thin dolomitized shale interlayers and drapes. Limestone (mudstone and rare grainstone): fine grained; thick to very thick bedded. Superficial ooids. "Normal" ooids exceed 2 millimeters in diameter. Shale: brown; very fine to fine grained. Burrows. Vugs.

42	2.0	149.0	Limestone (boundstone? and packstone to grainstone): fine grained; thick bedded. Internal and irregular swirled laminations resemble laterally linked hemispheroids. Stylolites. Partial dolomitization.
43	1.0	150.0	Limestone and shale, lime mudstone interbedded with very thin dolomitized shale. Limestone (mudstone to grainstone and boundstone): fine to medium grained; thin to thick bedded. Superficial ooids. Mudstone rip up peloids and small intraclasts. Thrombolitic toward top. Fossiliferous, trilobites, echinoderms, and mollucs fill interalgal areas. Shale: brown; sugary; fine grained; laminated. Burrowed?
44	1.0	151.0	Limestone and shale, peloidal limestone, and lime mudstone interbedded with very thin dolomitized shale. Limestone (mudstone and grainstone): fine to medium grained; thin to thick bedded. Superficial ooids. Mudstone rip up peloids. Stylolites. Burrows. Shale: brown; fine grained; laminated.
45	14.0	165.0	Limestone (boundstone and packstone to grainstone): fine to coarse grained; thick to very thick bedded. Thrombolitic. Fossil debris fills interalgal areas. *Renalcis*, trilobites, echinoderms, and mollucs dominate. Laminated fabric, may be fenestral. Rare oolitic grainstone interlayers.
46	1.0	166.0	Shale: dark gray green; very fine grained; faintly laminated. Thrombolitic at base and top.
47	24.0	190.0	Limestone (boundstone and packstone to grainstone): fine to coarse grained; thick to very thick bedded. Thrombolitic. Similar to unit 45. Superficial ooids toward top.
48	7.0	197.0	Limestone (grainstone): fine to medium grained; very thick bedded. Peloidal. Mud rip up grains and superficial ooids

			in grain to grain contact. Fenestral fabric? Stylolites. Mottled. Partially dolomitized. Dolomite pore filling cement??
49	3.0	200.0	Limestone (boundstone and packstone to grainstone): fine to coarse grained; thick to very thick bedded. Thrombolitic. Similar to unit 45. Oncolitic toward top.
50	2.0	202.0	Limestone (packstone): medium to coarse grained; very thick bedded. Oncolitic. Oolitic. Oncoids may exceed 4 centimeters in long dimension. Oncoids are elongate to subrounded.
51	2.0	204.0	Limestone and dolostone (boundstone and packstone to grainstone): fine to coarse grained; thick to very thick bedded. Thrombolitic. Similar to unit 45.
52	3.0	207.0	Limestone and dolostone (packstone): medium to coarse grained; very thick bedded. Oncolitic. Oolitic. Similar to unit 50.
53	7.0	214.0	Limestone and dolostone (boundstone and packstone to grainstone): fine to medium grained; very thick bedded. Thrombolitic. Mottled fabric. Fenestral fabric? In part laminated, cryptalgal or stromatolitic?
54	3.0	217.0	Limestone and dolostone (packstone and grainstone): coarse grained; very thick bedded. Oncolitic. Oncoids more abundant here than below. Oncoids rarely exceed 2 centimeters in long dimension.
55	3.0	220.0	Limestone and dolostone (boundstone and packstone to grainstone): fine to medium grained; very thick bedded. Thrombolitic.
			Well collared in upper part of MAYNARDVILLE LIMESTONE.

ORNL GW 131 (525 ft. east--offset from grid line)

			Lower ~5 meters of Maynardville limestone not penetrated.
1	21.0	21.0	MAYNARDVILLE LIMESTONE. Limestone (boundstone and packstone to grainstone): fine to coarse grained; very thick bedded. Thrombolitic. Ooids and skeletal debris fill interalgal areas. Stylolitic. Stylobrecciated. Mottled. Burrows? *Renalcis*. Partial dolomitization.
2	6.0	27.0	Limestone (packstone and grainstone): fine to medium grained; very thick bedded. Superficial ooids. Partial to Pervasive dolomitization. Stylolites. Rare oncoids and "normal ooids".
3	1.0	28.0	Limestone (boundstone and packstone to grainstone): fine to coarse grained; thick bedded. Thrombolitic. Stylolites.
4	3.0	31.0	Limestone (grainstone): fine to medium grained; very thick bedded. Superficial ooids. Algal peloids. Dolomitization. Stylolites.
5	2.0	33.0	Limestone (boundstone and packstone to grainstone): fine to coarse grained; thick bedded. Thrombolitic. Stylolites.
6	1.0	34.0	Limestone (grainstone): fine to medium grained; very thick bedded. Superficial ooids. Algal peloids. Fenestral fabric. Dolomitization. Dolomite pore filling cement?
7	9.0	43.0	Limestone and dolostone (boundstone and packstone to grainstone): fine to medium grained; very thick bedded. Thrombolitic. Stylolites. Stylobrecciation. Mottled fabric.
8	1.0	44.0	Limestone (packstone and grainstone): coarse grained; thick bedded. Oncolitic. Stylolites. Blocky pore filling cement. Oncoids irregular in shape.

9	4.0	48.0	Limestone (boundstone and packstone to grainstone): fine to coarse grained; very thick bedded. Thrombolitic. Oncoids and ooids commonly fill interalgal areas. Stylolites.
10	2.0	50.0	Limestone (packstone to grainstone and boundstone): fine to coarse grained; medium to thick bedded. Oncolitic. Oolitic. Thrombolitic at base and top.
11	6.0	56.0	Limestone (boundstone): fine grained; very thick bedded. Thrombolitic. Stylolites and stylocummulate. Mottled fabric.
12	1.0	57.0	Limestone (packstone and grainstone): coarse grained; thick bedded. Oncolitic. Oolitic. Oncoids exceed 1 centimeter in diameter, ooids are much smaller (< 3 millimeters). Stylolitic.
13	3.0	60.0	Limestone and dolostone (boundstone and packstone to grainstone): fine to coarse grained; very thick bedded. Thrombolite. Oncolitic and oolitic at base. Stylobrecciated.
14	8.0	68.0	Limestone (packstone and grainstone): fine to coarse grained; medium to very thick bedded. Oncolitic. Oolitic. Rare shale, pellet?, and intraclastic interlayers.
15	3.0	71.0	Limestone and shale, oolitic and intraclastic limestone and lime mudstone interbedded with very thin shale. Limestone (mudstone and packstone to grainstone): fine to coarse grained; thin to thick bedded. Burrows? Limestone clast conglomerates exhibit coarse ooid rich matrix. Stylolites. Shale: gray green to light gray; very fine grained; laminated.
16	1.0	72.0	Limestone and shale, lime mudstone interbedded with very thin shale. Limestone (mudstone): fine grained; thin bedded. Rare pellets? in mudstone. Burrows. Fossil debris, trilobites and

			perhaps echinoderms. Shale: gray green; very fine grained; very thin bedded.
17	2.0	74.0	Limestone (packstone and grainstone): coarse grained; thick bedded. Oolitic. Normal marine ooids, well formed. Ooids may exceed 2 millimeters in diameter. Lime mudstone interbedded with very thin shale at base.
18	2.0	76.0	Limestone (boundstone and packstone to grainstone): fine to coarse grained; very thick bedded. Thrombolitic. Oncoids and ooids interlayered toward the top of the unit. Stylolites.
19	2.0	78.0	Limestone (packstone and grainstone): coarse grained; very thick bedded. Oncolitic. Oolitic. Carbonate allochems are dark gray to black in color.
20	4.0	82.0	Limestone (boundstone and packstone to grainstone): primarily fine grained, rarely coarse grained; very thick bedded. Thrombolitic. Packstone and grainstone which fill interalgal areas are becoming increasing less common. Stylolites.
21	2.0	84.0	Limestone and dolostone (packstone and grainstone): coarse grained; thick bedded. Oncolitic. Oolitic. Interlayered limestone and dolostone, where whole areas between bedding parallel stylolites may be limestone or dolostone. Limestone is dark gray, dolostone is light brown to beige.
22	13.0	97.0	Limestone and dolostone (boundstone): fine grained; very thick bedded. Thrombolitic. Stylolites. Rare cryptalgal laminations. *Renalcis*?
23	2.0	99.0	Dolostone (boundstone and packstone to grainstone): fine to medium grained; very thick bedded. Ultra thin wavy laminations. Perhaps cross stratified. Algal peloids? Fenestral fabric?

24	2.0	101.0	Limestone and dolostone (boundstone): fine grained; thick bedded. Thrombolitic. Large Vugs. Fenestral fabric.

COPPER RIDGE DOLOSTONE.

S-3 POND SECTION

The S-3 Pond subsurface drill core (ORNL GW 134 and GW 135) is located at the westernmost edge of the Y-12 weapons plant along grid line E52,500. A complete Nolichucky and Maynardville section is represented.

ORNL GW 134 (20 ft. west--offset from grid line)

UNIT	TKN. (m.)	CUM. TKN. (m.)	DESCRIPTION
			MARYVILLE LIMESTONE.
1	1.0	1.0	NOLICHUCKY SHALE. Shale: dark gray green; very fine grained; faintly laminated. Rare thin intraclastic lenses.
2	1.0	2.0	Limestone and shale, intraclastic and pelletal? limestone interbedded with thin shale. Limestone (packstone and grainstone): fine to coarse grained; very thin to thick bedded, planar and low angle cross lamination. Pseudonodules. Loading. Limestone clast conglomerates exhibit wide a variety of clast sizes, monomictic clast association, and clasts floating in a shale matrix. Shale: dark gray green and maroon; very fine grained; faintly laminated.
3	3.0	5.0	Shale and limestone, thin to thick shale interbedded with pelletal? and intraclastic limestone. Shale: dark gray green and maroon; very fine grained; laminated. Abiotic Contact between dark gray green and maroon colored shale is sharp and planar. Color alterations in shale occur often. Limestone (packstone to grainstone): fine to coarse grained; very thin to medium bedded, planar and

			low angle cross lamination. Loading. Pseudonodules. Contorted bedding. Sharp bases and sharp to diffuse tops. Limestone clast conglomerates show variable clast sizes (1-7 centimeters), clasts which project into overlying rock units, a wide variety of clast types (pellet grainstone and lime mudstone is most common), and shale as the dominant matrix type.
4	1.0	6.0	Limestone and shale, pellet? limestone interbedded with thin shale. Limestone (packstone and grainstone): fine grained, thin to medium bedded, low angle cross lamination. Loading. Pseudonodules. Stylolites. Sharp scoured bases and scoured to diffuse tops. Shale: dark gray green, very fine grained; laminated.
5	22.0	28.0	Shale and limestone, thin to very thick shale interbedded with pellet? and intraclastic limestone. Shale: dark gray green and maroon; very fine grained; faintly laminated. Limestone (packstone and grainstone): fine to coarse grained, very thin to medium bedded, planar and low angle cross lamination. Lime mudstone interlayered with thin shale occurs as a 16 centimeter thick bed in the center of this unit. Limestone clast conglomerates exhibit monomictic clast associations, platey and tabular clasts many of which exceed 8 centimeters in long dimension, and random clast orientation with respect to bedded.
6	1.0	29.0	Limestone and shale, pelletal? and intraclastic limestone interbedded with thin shale. Limestone (packstone and grainstone): fine to coarse grained; very thin to medium bedded, pellet? limestone shows low angle cross lamination. Pseudonodules. Loading. Stylolites. Limestone clast conglomerates with clasts from 3 to 5 centimeters in long dimension. Shale: dark gray green and maroon; very fine grained; faintly laminated.

7	29.0	58.0	Shale and limestone, thin to thick shale interbedded with pellet?, intraclastic, and fossiliferous limestone. Shale: dark gray green and maroon; very fine grained. Calcareous. Mica flakes. Limestone (packstone and grainstone): fine grained; very thin to medium bedded, low angle cross laminations in pellet? lithology. Loading. Contorted bedding. Becoming fossiliferous in the upper part of unit. Trilobites and echinoderms.
8	1.0	59.0	Limestone and shale, pelletal? and oolitic limestone interbedded with thin shale. Limestone (packstone and grainstone): fine to coarse grained, very thin to medium bedded, planar and low angle cross lamination in pellet lithology. Rare fossiliferous limestone. Sharp bases and sharp to diffuse tops. Glauconitic, especially in ooid grainstones. Shale: dark gray green and maroon; very fine grained; faintly laminated.
9	2.0	61.0	Shale and limestone, thin to thick shale interbedded with rare ooid and intraclastic limestone. Shale: dark gray green and maroon; very fine grained; laminated. Pellets? or algal peloids occur disseminated in shale. Dark gray green shale occurs in close stratigraphic proximity to limestone lenses. Limestone (packstone and grainstone): medium to coarse grained; thin to medium bedded. Stylolites. Loading.
10	1.0	62.0	Limestone and shale, pellet? and oolitic limestone interbedded with thin shale. Limestone (packstone and grainstone): fine to coarse grained; very thin to medium bedded. Coarsening upward sequences. Shale: dark gray green and maroon; very fine grained; laminated.
11	6.0	68.0	Shale and limestone, thin to thick shale interbedded with pelletal? and oolitic limestone. Shale: dark gray green and maroon; very fine grained; faintly laminated. Limestone (packstone and grainstone): fine to coarse grained;

			very thin to medium bedded, planar and low angle cross laminations in pellet lithology. Loading. Pseudonodules. Convoluted bedding. Rare intraclastic lenses.
12	1.0	69.0	Limestone and shale, oolitic and pelletal? limestone interbedded with thin shale. Limestone (packstone and grainstone): fine to coarse grained; very thin to thick bedded, low angle cross laminations in pellet lithology. Thin discontinuous shale drapes occur throughout oolitic grainstone. Shale: dark gray green; very fine grained; faintly laminated.
13	1.0	70.0	Shale and limestone, thin to thick shale interbedded with oolitic limestone. Shale: maroon and dark gray green; very fine grained; faintly laminated. Limestone clasts in shale. Limestone (packstone and grainstone): coarse grained; thin bedded. Rare pellet? or algal peloidal lenses.
14	1.0	71.0	Limestone and shale, oolitic and pellet? limestone interbedded with very thin shale. Limestone (packstone and grainstone): fine to coarse grained; very thin to medium bedded, planar and low angle cross laminiation in pellet lithology. Sharp bases and scoured sharp tops. Skeletal lags? Shale: maroon and dark gray green; very fine grained; faintly laminated.
15	2.0	73.0	Shale and limestone, thin to thick shale interbedded with oolitic and pelletal? limestone. Shale: dark gray green and maroon; very fine grained; laminated. Limestone nodules. Quartz silt? Limestone (packstone and grainstone): fine to coarse grained; very thin to medium bedded, low angle cross lamination in pellet lithology. Loading. Pseudonodules.
16	1.0	74.0	Limestone and shale, pellet? and oolitic limestone interbedded with thin shale. Limestone (packstone and grainstone):

			fine to coarse grained; very thin to medium bedded, low angle cross lamination. Sharp bases and diffuse tops. Loading. Shale: dark gray green and maroon; very fine grained; laminated.
17	2.0	76.0	Limestone and shale, oolitic and pelletal? limestone interbedded with thin shale. Limestone (packstone and grainstone): fine to coarse grained; thin to medium bedded, planar and low angle cross lamination. Ooids exceed 2 millimeters in diameter. Thin, discontinuous shale drapes in oolitic grainstone Shale: dark gray green and maroon; very fine grained; laminated. Rare intraclastic lenses in shale.
18	5.0	81.0	Limestone and shale, pelletal? limestone interbedded with thin shale. Limestone (packstone and grainstone): fine grained; very thin to thin bedded, low angle cross lamination in pellet lithology. Loading. Pseudonodules. Basal skeletal lags? Sharp bases and diffuse tops. Rare oolitic and intraclastic interlayers. Shale: dark gray green; very fine grained; laminated. Disseminated fossil debris, primarily trilobites.
19	3.0	84.0	Shale and limestone, thin to thick shale interbedded with pelletal? and intraclastic limestone. Shale: dark gray green to maroon; very fine grained; faintly laminated. Limestone (packstone and grainstone): fine to coarse grained; thin to medium bedded. Rare oolitic interlayers.
20	1.0	85.0	Limestone and shale, pellet? and intraclastic limestone interbedded with thin shale. Limestone (packstone and grainstone): fine to coarse grained; very thin to medium bedded, planar and low angle cross lamination in pellet? lithology. Shale: dark gray green and maroon; very fine grained.

21	3.0	88.0	Shale and limestone, thin to thick shale interbedded with pellet? limestone. Shale: dark gray green and maroon; very fine grained; faintly laminated. Disseminated trilobite debris throughout. Limestone (packstone and grainstone): fine grained; very thin to medium bedded, low angle cross lamination. Loading. Pseudonodules. Contorted bedding. Glauconitic. Rare oolitic and intraclastic interlayers.
22	1.0	89.0	Limestone and shale, pellet? limestone interbedded with thin to thick shale. Limestone (packstone and grainstone): fine grained; very thin to medium bedded, low angle cross lamination. Rare intraclastic lenses. Shale: dark gray green and maroon; very fine grained; faintly laminated.
23	2.0	91.0	Shale and limestone, thin to thick shale interbedded with intraclastic limestone. Shale: dark gray green and maroon; very fine grained. Limestone (packstone and grainstone): coarse grained; medium bedded. Limestone clast conglomerates show a wide variety of clast sizes (1-7 centimeters in long dimension), polymictic and monomictic clast association, and clasts which project into overlying rock units. Rare pellet? interlayers.
24	2.0	93.0	Limestone and shale, pellet? and intraclastic limestone interbedded with thin shale. Limestone (packstone and grainstone): fine to coarse grained; very thin to medium bedded, low angle cross lamination in pellet? lithology. Limestone clast conglomerates show polymictic clast associations, multigeneration clasts, bored and burrowed clasts, subparallel to random clast orientation (with respect to bedding), and a coarse grained fossiliferous matrix supporting clasts. Shale: dark gray green and maroon; very fine grained; faintly laminated.

25	16.0	109.0	Shale and limestone, thin to thick shale interbedded with pellet? and intraclastic limestone. Shale: dark gray green and maroon; very fine grained. Limestone (packstone and grainstone): fine to coarse grained; very thin to medium bedded, low angle cross lamination in pellet? lithology. Oolitic interlayers become abundant toward top of unit.
26	1.0	110.0	Limestone and shale, pellet? and oolitic limestone interbedded with thin shale. Limestone (packstone and grainstone): fine to coarse grained; very thin to medium bedded, low angle cross lamination in pellet? lithology. Rare intraclastic lenses. Shale: dark gray green; very fine grained; laminated.
27	3.0	113.0	Shale and limestone, thin to very thick shale interbedded with oolitic,pelletal, and intraclastic limestone. Shale: dark gray green and maroon; very fine grained; faintly laminated. Limestone (packstone and grainstone): fine to coarse grained; very thin to medium bedded, planar and low angle cross lamination. Loading. Stylolites. Pseudonodules.
28	1.0	114.0	Limestone and shale, oolitic limestone interbedded with thin shale. Limestone (packstone and grainstone): coarse grained; thin to medium bedded. Rare intraclastic lenses. Shale: dark gray green and maroon; very fine grained.
29	2.0	116.0	Shale and limestone, thin to thick shale interbedded with intraclastic and pellet? limestone. Shale: dark gray green and maroon; very fine grained; faintly laminated. Limestone (packstone and grainstone): fine to coarse grained; thin to medium bedded. Limestone clast conglomerates show polymictic and monomictic clast associations, bored and burrowed clasts, subparallel to random clast orientation (with respect to bedding), and a coarse grained matrix and shale matrix supporting clasts..

30	1.0	117.0	Limestone and shale, oolitic limestone interbedded with thin shale. Limestone (packstone and grainstone): coarse grained; medium to thick bedded. Rare pellet? and intraclastic limestone lenses. Shale: maroon; very fine grained; laminated.
31	11.0	128.0	Shale and limestone, thin to thick shale interbedded with rare pellet? oolitic, intraclastic, and fossiliferous limestone. Shale: dark gray green and maroon; very fine grained; faintly laminated. Limestone (packstone and grainstone): fine to coarse grained; very thin to medium bedded, low angle cross lamination in pellet? lithology. Very rare lime mudstone interlayers.
32	1.0	129.0	Limestone and shale, pelletal? limestone interbedded with thin shale. Limestone (packstone and grainstone): fine grained; very thin to medium bedded, low angle cross lamination. Shale: dark gray green; very fine grained; faintly laminated. Limestone clasts float in shale matrix.
33	18.0	147.0	Shale and limestone, thin to very thick shale interbedded with lime mudstone and intraclastic limestone. Shale: dark gray green and maroon, maroon; very fine grained; faintly laminated. Limestone clasts occur randomly oriented in shale matrix. Limestone (mudstone and packstone to grainstone): fine to coarse grained; very thin to thick bedded. Rare oolitic, algal peloidal, and pelletal? limestone interlayers. Lime mudstone interbedded with thin shale becomes very abundant toward top of unit. Loading. Pseudonodules. Convoluted bedding. Sharp bases and sharp to diffuse tops.

ORNL GW 135 (710 ft. east--offset from grid line)

34	6.0	153.0	<u>MAYNARDVILLE LIMESTONE</u>. Limestone and shale, lime mudstone interbedded with thin shale. Limestone (mudstone): fine grained; very thin to thin bedded. Rare intraclastic and oolitic lenses. Shale:

			dark green gray and brownish where dolomitized; very fine grained; laminated.
35	1.0	154.0	Limestone (boundstone and packstone to grainstone): fine to coarse grained; thick bedded. Thrombolitic. Oolitic grainstone fills interalgal areas. Stylolites.
36	1.0	155.0	Shale and limestone, thin partially dolomitized shale interbedded with pellet? limestone. Shale: dark gray green, very fine grained. Limestone (packstone and grainstone): fine grained; thin bedded. Thrombolitic at base. Lime mudstone interbedded with shale at top.
37	1.0	156.0	Limestone and shale, lime mudstone interbedded with thin shale. Limestone (mudstone): fine grained; very thin to thin bedded. Burrowed. Mottled. Rare pellet and intraclastic lenses. Shale: dark gray green; very fine grained.
38	38.0	194.0	Limestone (boundstone and packstone to grainstone): fine to coarse grained; very thick bedded. Thrombolitic. Ooids, oncoids, and algal peloids fill interalgal areas. Stylolites. Vugs. Discontinuous algal? laminations. *Renalcis*?
39	2.0	196.0	Limestone (packstone and grainstone): coarse grained; very thick bedded. Oncolitic. Oolitic.
40	4.0	200.0	Limestone (boundstone and packstone to grainstone): fine to coarse grained; very thick bedded. Thrombolitic. Oncoids common throughout. Stylolites.
41	1.0	201.0	Limestone (packstone and grainstone): coarse grained; thick bedded. Oncolitc.
42	3.0	204.0	Limestone (boundstone and packstone to grainstone): fine to coarse grained; very thick bedded. Thrombolitic. Dolomitization. Stylolites.

43	2.0	206.0	Limestone (packstone and grainstone): coarse grained; very thick bedded. Oncolitic. Oolitic. Ooids commonly replaced by ferroan dolomite.
44	2.0	208.0	Limestone (boundstone and packstone to grainstone): fine to coarse grained; very thick bedded. Oncolitic at base. Thrombolitic throughout remainder of unit. Ooids and skeletal debris fill interalgal regions. Stylolites.
45	2.0	210.0	Limestone (packstone and grainstone): coarse grained; very thick bedded. Oncolitic. Oolitic. Stylolitic.
46	6.0	216.0	Limestone (boundstone and packstone to grainstone): fine to coarse grained; very thick bedded. Thrombolitic.
47	1.0	217.0	Limestone (packstone and grainstone): fine to medium grained; thick bedded. Peloidal, superficial ooids, oncoids, and normal marine ooids. Stylolitic. Algal peloids and some mudstone rip up intraclasts.
48	2.0	219.0	Limestone (boundstone and packstone to grainstone): fine to coarse grained; very thick bedded. Thrombolitic. Dolomitization. Finer grained when compared to previous thrombolites.
49	2.0	221.0	Limestone (packstone and grainstone): fine grained; thick bedded. Superficial ooids? and algal peloids? Dolomitization.
50	4.0	225.0	Limestone and dolostone (boundstone): fine grained; very thick bedded. Thrombolitic. Superficial ooids at base and top.
51	1.0	226.0	Limestone (packstone and grainstone): fine grained; thick bedded. Superficial ooids? Dolomite pore filling cement?
52	1.0	227.0	Limestone (boundstone and packstone to grainstone): fine to coarse grained; thick bedded. Thrombolitic. Ooids fill

			interalgal regions. Partial dolomitization.
53	2.0	229.0	Limestone (packstone and grainstone): fine to medium grained; very thick bedded. Superficial ooids and algal peloids. Stylobrecciation.
54	3.0	232.0	Limestone and dolostone (boundstone): fine grained; thick bedded. Thrombolitic. *Renalcis*.
55	1.0	233.0	Limestone and dolostone (packstone and grainstone): fine to medium grained; thick bedded. Superficial ooids and algal peloids.
56	4.0	237.0	Limestone (boundstone and packstone to grainstone): fine to coarse grained; very thick bedded. Thrombolitic. Stylolites. Vugs. Faint laminations.
57	2.0	239.0	Limestone (packstone and grainstone): fine grained; thick bedded. Superficial ooids? Algal peloids? Thrombolitic at base and at top.
58	3.0	242.0	Limestone (packstone and grainstone): coarse grained; very thick bedded. Oncolitic. Oolitic. Superficial ooids at base.
59	2.0	244.0	Limestone (packstone and grainstone): medium grained; very thick bedded. Normal marine ooids. Ooids are much finer grained than in previous units, between 1 and 2 millimeters in diameter. Oncolitic toward top.
60	4.0	248.0	Limestone and dolostone (packstone and grainstone): coarse grained; very thick bedded. Oncolitic. Some ooids. Partial dolomitization.
61	1.0	249.0	Limestone and shale, lime mudstone and intraclastic limestone interbedded with thin shale. Limestone (mudstone and packstone to grainstone): fine to coarse grained; very thin to medium bedded. Shale: green gray; very fine grained. Partially dolomitized.

62	2.0	251.0	Limestone (packstone and grainstone): coarse grained; thick bedded. Oncolitic. Rare intraclastic and lime mudstone interlayers. Thin shale drapes.
63	1.0	252.0	Limestone and shale, lime mudstone and intraclastic limestone interbedded with thin shale drapes. Similar to unit 61.
64	1.0	253.0	Limestone (packstone and grainstone): coarse grained; thick bedded. Oncolitic. Oolitic.
65	12.0	265.0	Limestone and dolostone (boundstone and packstone to grainstone): fine to coarse grained; very thick bedded. Thrombolitic.
66	5.0	270.0	Dolostone and limestone (boundstone and packstone to grainstone): fine to medium grained; very thick bedded. Stromatolitic. Ultra thin wavy laminations forming laterally linked hemispheroids. Stylolites.
67	1.0	271.0	Dolostone (boundstone and packstone to grainstone): fine grained; thick bedded. Cryptalgal laminites. Microtepee structures? Fenestral fabric. Algal peloids. Dolomite pore filling cement?
68	4.0	275.0	Limestone and Dolostone (boundstone and packstone to grainstone): fine grained; very thick bedded. Stromatolitic. Similar to unit 66.
69	1.0	276.0	Limestone and Dolostone (boundstone and packstone to grainstone): fine grained; thick bedded. Thrombolitic. Stylolitic. *Renalcis*? Absence of algal or cryptalgal lamination.
70	1.0	277.0	Limestone and dolostone (boundstone and packstone to grainstone): fine grained, thick bedded. Cryptalgal laminites. Similar to unit 67.

COPPER RIDGE DOLOSTONE.

APPENDIX C

PETROGRAPHIC CONSTITUENT ANALYSIS

Table C.1. Analysis of CL Lithofacies (Volume %).

Constituent	Sample Number			
	I-80-1.3	I-80-4.9	I-82-0.3	J-2 162
Trilobites	0.00	0.50	0.00	0.00
Girvanella	0.00	3.75	0.00	0.00
Fossil allochems, Total	0.00	(4.25)	0.00	0.00
Intraclasts, Total	(1.75)	0.00	0.00	0.00
Mudstone	1.75	0.00	0.00	0.00
Ooids, Total	(0.75)	(4.50)	0.00	0.00
Fibrous/Prismatic	0.75	0.00	0.00	0.00
Superficial	0.00	4.50	0.00	0.00
Peloids	8.00	6.50	0.00	7.50
Micrite/Microspar	50.75	12.00	29.50	49.00
Void Filling Cement, Total	(2.00)	0.00	(5.25)	(21.00)
Blocky	2.00	0.00	5.25	21.00
Detrital quartz silt	3.50	0.00	0.00	0.00
Pyrite	2.00	2.25	0.00	0.00
Dolomite/Stylolite	31.25	70.50	65.25	22.50
Total	100.00	100.00	100.00	100.00

Table C.2. Analysis of Stromatolite Lithofacies (Volume %).

Constituent	Sample Number	
	RS19	J-2 307.5
Trilobites	0.00	0.25
Fossil allochems, Total	0.00	(0.25)
Peloids	34.50	21.50
Micrite/Microspar	31.00	15.75
Void Filling Cement, Total	(9.25)	(5.00)
Blocky	9.25	5.00
Dolomite/Stylolite	25.25	57.50
Total	100.00	100.00

Table C.3. Analysis of Thrombolite Lithofacies (Volume %).

Constituent	Sample Number				
	I-2-2.1	I-3-1.0	I-3-4.2	I-5-2.8	I-14-0.0
Echinoderms	0.25	0.25	1.75	2.75	2.25
Trilobites	2.00	0.25	0.25	2.00	1.50
<u>Girvanella</u>	4.75	4.00	3.50	5.75	11.00
Cyanobacteria	0.00	3.50	3.75	0.75	27.00
Gastropods	0.00	0.00	0.25	0.00	0.00
Sponge spicules	2.00	5.50	3.00	2.00	2.00
Fossil allochems, Total	(9.00)	(13.50)	(12.50)	(13.25)	(43.75)
Intraclasts, Total	0.00	0.00	0.00	0.00	(7.50)
Mudstone	0.00	0.00	0.00	0.00	7.25
Peloidal packstone	0.00	0.00	0.00	0.00	0.25
Ooids, Total	(4.00)	0.00	0.00	0.00	0.00
Polycrystalline	4.00	0.00	0.00	0.00	0.00
Peloids	0.00	0.00	0.00	0.00	5.75
Micrite/Microspar	62.25	66.25	68.25	54.00	37.50
Void Filling Cement, Total	(1.50)	(8.00)	0.00	0.00	(3.00)
Blocky	1.50	8.00	0.00	0.00	3.00
Detrital quartz silt	0.00	0.00	0.00	5.75	0.00
Clay/Mica	0.00	0.00	0.00	11.75	0.00
Pyrite	0.25	0.00	0.00	0.00	0.00
Dolomite/Stylolite	23.00	7.25	16.25	12.75	2.50
Fracture/Fill Veins	0.00	5.00	3.00	2.50	0.00
Total	100.00	100.00	100.00	100.00	100.00

Table C.4. Analysis of NOPG Lithofacies (Volume %).

Constituent	Sample Number					
	I-62-1.2	I-62-1.3	I-74-9.8	A9-T	B9	J-2 300.5
Echinoderms	0.50	2.75	0.75	2.00	2.25	0.25
Trilobites	0.50	6.50	0.25	7.50	1.50	0.75
Girvanella	1.75	0.25	0.00	2.75	0.00	1.00
Gastropods	0.00	0.00	0.00	0.50	0.00	0.00
Molluscs undifferentiated	0.00	1.25	0.00	0.75	0.25	0.00
Sponge spicules	0.00	0.00	0.00	1.50	0.00	0.00
Fossil allochems, Total	(2.75)	(10.75)	(1.00)	(15.00)	(4.00)	(2.00)
Intraclasts, Total	(24.25)	(4.25)	(2.75)	(6.25)	0.00	0.00
Mudstone	0.00	0.75	2.75	0.00	0.00	0.00
Peloidal packstone	15.75	0.25	0.00	4.75	0.00	0.00
Fossiliferous packstone	0.00	1.50	0.00	0.00	0.00	0.00
Oolitic packstone	8.50	1.75	0.00	1.50	0.00	0.00
Ooids, Total	(16.00)	(18.25)	(11.00)	(12.75)	(33.00)	(3.50)
Fibrous/Prismatic	6.75	15.00	3.50	7.75	20.00	3.50
Polycrystalline	5.75	0.75	7.50	2.50	7.25	0.00
Monocrystalline	3.50	2.50	0.00	2.50	5.75	0.00
Oncoids	16.00	24.00	31.00	13.75	17.50	30.75
Peloids	4.25	3.50	3.75	13.00	10.75	11.50
Micrite/Microspar	18.00	32.25	1.50	28.50	6.50	0.00
Void Filling Cement, Total	(11.50)	(0.25)	(35.75)	(10.75)	(26.50)	(38.75)
Fibrous/Bladed	8.00	0.25	34.25	6.75	24.75	38.75
Syntaxial	0.00	0.00	1.50	2.00	1.75	0.00
Blocky	3.50	0.00	0.00	2.00	0.00	0.00
Detrital quartz silt	0.00	0.00	0.00	0.00	0.00	0.00
Clay/Mica	0.00	0.00	0.00	0.00	0.00	0.00
Glauconite	0.00	0.00	0.00	0.00	0.00	0.00
Pyrite	0.00	0.00	0.00	0.00	0.00	0.00
Dolomite/Stylolite	7.25	4.25	9.75	0.00	0.75	13.50
Fracture/Fill Veins	0.00	2.50	3.50	0.00	1.00	0.00
Total	100.00	100.00	100.00	100.00	100.00	100.00

Table C.5. Analysis of EPG Lithofacies (Volume %).

Constituent	Sample Number					
	I-76-24.6	I-77-2.0	I-78-0.5	I-79-0.0	I-79-6.2	I-81-1.4
Echinoderms	0.00	0.25	0.25	13.00	0.00	0.00
Trilobites	0.00	0.25	0.75	5.00	0.00	0.00
Sponge spicules	0.00	0.00	0.00	0.00	2.25	0.00
Fossil allochems, Total	0.00	(0.50)	(1.00)	(18.00)	(2.25)	0.00
Intraclasts, Total	(1.00)	0.00	0.00	(10.50)	(13.75)	0.00
Mudstone	0.25	0.00	0.00	7.25	13.75	0.00
Peloidal packstone	0.75	0.00	0.00	0.00	0.00	0.00
Fossiliferous packstone	0.00	0.00	0.00	3.25	0.00	0.00
Ooids, Total	(8.50)	(4.50)	(33.50)	0.00	0.00	(2.75)
Fibrous/Prismatic	0.00	0.00	0.00	0.00	0.00	0.00
Superficial	8.50	4.50	33.50	0.00	0.00	2.75
Peloids	57.50	58.50	21.50	28.25	48.25	64.00
Micrite/Microspar	0.00	0.00	0.00	27.00	0.00	0.00
Void Filling Cement, Total	(19.75)	(27.25)	(20.75)	(7.25)	(21.50)	(23.50)
Fibrous/Bladed	0.00	0.00	0.00	0.00	0.00	21.00
Syntaxial	0.00	0.25	2.50	1.25	0.00	0.00
Blocky	19.75	27.00	18.25	6.00	21.50	2.50
Pyrite	0.00	0.00	0.00	0.00	0.00	3.50
Dolomite/Stylolite	13.25	3.00	23.25	9.00	14.25	0.00
Fracture/Fill Veins	0.00	6.25	0.00	0.00	0.00	6.25
Total	100.00	100.00	100.00	100.00	100.00	100.00

Table C.5. (continued).

Constituent	Sample Number
	I-81-5.9
Echinoderms	0.00
Trilobites	0.00
Sponge spicules	3.75
Fossil allochems, Total	(3.75)
Intraclasts, Total	0.00
Mudstone	0.00
Peloidal packstone	0.00
Fossiliferous packstone	0.00
Ooids, Total	(2.00)
Fibrous/Prismatic	2.00
Superficial	0.00
Peloids	37.50
Micrite/Microspar	16.00
Void Filling Cement, Total	(32.50)
Fibrous/Bladed	0.00
Syntaxial	0.00
Blocky	32.50
Pyrite	0.00
Dolomite/Stylolite	6.00
Fracture/Fill Veins	2.25
Total	100.00

Table C.6. Analysis of MWS Lithofacies (Volume %).

Constituent	Sample Number					
	I-1-11.6	I-1-15.5	I-4-0.9	I-7-0.0	I-50-0.5	I-58-2.5
Echinoderms	0.00	0.00	0.00	0.00	0.00	0.25
Inarticulate brachiopods	0.00	0.00	0.00	0.00	0.00	0.25
Trilobites	0.50	0.25	0.00	0.00	5.50	2.25
Girvanella	2.25	4.25	8.25	4.25	8.25	2.75
Sponge spicules	0.00	0.50	0.00	0.00	0.50	0.00
Fossil allochems, Total	(2.75)	(5.00)	(8.25)	(4.25)	(14.25)	(5.50)
Intraclasts, Total	0.00	0.00	0.00	(7.50)	(6.00)	(3.75)
Mudstone	0.00	0.00	0.00	7.50	6.00	0.00
Peloidal packstone	0.00	0.00	0.00	0.00	0.00	3.75
Peloids	0.00	0.00	6.25	22.50	11.00	23.50
Micrite/Microspar	75.75	53.00	73.75	50.75	45.75	42.25
Void Filling Cement, Total	0.00	0.00	0.00	(2.50)	(3.00)	0.00
Fibrous/Bladed	0.00	0.00	0.00	0.00	0.00	0.00
Syntaxial	0.00	0.00	0.00	0.00	0.00	0.00
Blocky	0.00	0.00	0.00	2.50	3.00	0.00
Detrital quartz silt	0.00	3.25	0.00	0.25	0.00	0.25
Clay/Mica	7.50	32.00	8.25	5.00	11.50	11.50
Glauconite	0.00	0.25	0.00	0.00	0.50	0.00
Pyrite	0.75	1.25	0.25	0.25	2.25	1.50
Dolomite/Stylolite	10.00	5.25	3.00	7.00	3.75	6.75
Fracture/Fill Veins	3.25	0.00	0.25	0.00	2.00	5.00
Total	100.00	100.00	100.00	100.00	100.00	100.00

Table C.6. (continued).

Constituent	Sample Number		
	I-63-8.9	I-69-4.9	BG-6-86.9
Echinoderms	0.25	0.00	0.00
Inarticulate brachiopods	0.00	1.00	0.00
Trilobites	0.25	3.75	2.25
Girvanella	1.50	6.00	9.25
Sponge spicules	0.00	0.00	0.00
Fossil allochems, Total	(2.00)	(10.75)	(11.50)
Intraclasts, Total	0.00	0.00	0.00
Mudstone	0.00	0.00	0.00
Peloidal packstone	0.00	0.00	0.00
Peloids	8.50	4.50	4.50
Micrite/Microspar	61.00	35.00	63.00
Void Filling Cement, Total	(2.00)	(7.25)	0.00
Fibrous/Bladed	0.00	3.00	0.00
Syntaxial	0.00	2.25	0.00
Blocky	2.00	2.00	0.00
Detrital quartz silt	0.00	0.00	0.00
Clay/Mica	9.50	17.25	6.50
Glauconite	0.25	0.00	0.00
Pyrite	0.25	2.75	0.25
Dolomite/Stylolite	11.50	15.50	11.00
Fracture/Fill Veins	5.00	7.00	3.25
Total	100.00	100.00	100.00

Table C.7. Analysis of OPG Lithofacies (Volume %).

Constituent	Sample Number					
	I-1-0.0	I-8-4.0	I-9-2.8	I-16-0.4	I-21-0.0	I-26-Core
Echinoderms	0.25	0.75	0.50	1.25	0.25	0.00
Inarticulate brachiopods	0.00	0.00	0.00	0.00	0.00	0.00
Trilobites	1.75	0.75	2.00	1.75	0.25	0.00
Girvanella	0.00	0.00	0.00	0.00	3.25	0.50
Gastropods	0.00	0.00	0.00	0.00	0.00	0.00
Pelecypods	0.00	0.00	0.00	0.00	0.00	0.00
Chancelloria	0.00	0.00	0.00	0.00	0.00	5.75
Fossil allochems, Total	(2.00)	(1.50)	(2.50)	(3.00)	(3.75)	(6.25)
Intraclasts, Total	(1.50)	(13.50)	(2.75)	(8.75)	(4.25)	0.00
Mudstone	0.00	12.25	0.00	2.25	0.00	0.00
Peloidal packstone	1.50	0.00	0.00	0.00	4.25	0.00
Oolitic packstone	0.00	1.25	0.00	6.50	0.00	0.00
Other types	0.00	0.00	2.75	0.00	0.00	0.00
Ooids, Total	(49.00)	(41.25)	(41.75)	(44.00)	(46.00)	(37.00)
Fibrous/Prismatic	46.25	5.50	22.75	32.00	15.25	19.50
Polycrystalline	0.00	34.00	17.75	8.50	0.00	2.25
Monocrystalline	2.75	1.75	1.25	3.50	30.75	15.25
Peloids	14.00	6.75	3.75	5.75	4.00	2.50
Micrite/Microspar	25.75	0.00	37.50	28.25	10.50	12.75
Void Filling Cement, Total	(7.75)	(22.75)	(11.75)	(10.25)	(31.50)	(26.25)
Fibrous/Bladed	5.50	19.25	8.25	5.75	25.00	15.25
Syntaxial	0.00	0.00	0.00	0.00	0.00	0.00
Blocky	2.25	3.50	3.50	4.50	6.50	11.00
Detrital quartz silt	0.00	0.00	0.00	0.00	0.00	0.00
Clay/Mica	0.00	0.00	0.00	0.00	0.00	0.00
Glauconite	0.00	0.00	0.00	0.00	0.00	0.00
Pyrite	0.00	0.00	0.00	0.00	0.00	0.50
Dolomite/Stylolite	0.00	11.75	0.00	0.00	0.00	12.00
Fracture/Fill Veins	0.00	2.50	0.00	0.00	0.00	2.75
Total	100.00	100.00	100.00	100.00	100.00	100.00

Table C.7. (continued).

Constituent	Sample Number					
	I-26-Flank	I-31-1.3	I-35-1.0	I-55-0.8	I-72-1.2	BG-0
Echinoderms	1.50	7.25	0.25	5.75	0.25	1.50
Inarticulate brachiopods	0.00	0.00	0.00	0.00	0.25	0.00
Trilobites	0.00	4.50	7.25	2.50	2.50	1.75
Girvanella	0.00	0.00	6.50	5.25	2.50	0.00
Gastropods	0.00	0.00	0.00	0.00	0.00	0.00
Pelecypods	0.00	0.00	0.00	0.00	0.00	0.00
Chancelloria	0.00	0.00	2.75	0.00	0.00	0.00
Fossil allochems, Total	(1.50)	(11.75)	(16.75)	(13.50)	(5.50)	(3.25)
Intraclasts, Total	0.00	(6.25)	(3.75)	(13.00)	(1.25)	0.00
Mudstone	0.00	0.00	0.00	1.50	1.25	0.00
Peloidal packstone	0.00	6.25	0.00	9.25	0.00	0.00
Oolitic packstone	0.00	0.00	3.75	2.25	0.00	0.00
Other types	0.00	0.00	0.00	0.00	0.00	0.00
Ooids, Total	(47.50)	(29.75)	(32.50)	(19.00)	(52.50)	(54.50)
Fibrous/Prismatic	35.25	4.75	18.75	18.75	35.50	47.25
Polycrystalline	3.75	23.00	11.00	0.00	16.75	0.00
Monocrystalline	8.50	2.00	2.75	0.25	0.25	7.25
Peloids	3.00	5.50	6.25	6.25	8.25	7.50
Micrite/Microspar	0.00	3.75	37.00	22.00	4.00	19.50
Void Filling Cement, Total	(42.00)	(35.75)	(3.75)	(12.75)	(20.50)	(2.25)
Fibrous/Bladed	42.00	22.00	3.00	3.50	9.25	2.25
Syntaxial	0.00	7.50	0.00	4.00	0.00	0.00
Blocky	0.00	6.25	0.75	5.25	11.25	0.00
Detrital quartz silt	0.00	0.00	0.00	0.00	0.00	0.00
Clay/Mica	0.00	0.00	0.00	0.00	0.00	5.00
Glauconite	0.00	0.00	0.00	0.00	0.00	0.00
Pyrite	0.00	0.00	0.00	0.00	0.00	0.00
Dolomite/Stylolite	6.00	7.25	0.00	11.25	8.00	8.00
Fracture/Fill Veins	0.00	0.00	0.00	2.25	0.00	0.00
Total	100.00	100.00	100.00	100.00	100.00	100.00

Table C.7. (continued).

Constituent	Sample Number					
	BG-3-28.8	BG-3-55.5	BG-4-25.5	IOA 0.0	IOA 0.3	IOA 0.9
Echinoderms	0.00	33.00	8.75	2.50	2.50	0.50
Inarticulate brachiopods	0.00	0.00	0.00	0.00	0.00	0.00
Trilobites	4.00	2.25	8.50	0.75	0.50	0.50
Girvanella	0.00	0.00	0.00	0.00	0.00	0.00
Gastropods	0.00	0.00	0.00	0.00	0.00	0.00
Pelecypods	0.00	0.00	0.00	0.00	0.00	0.00
Chancelloria	0.00	0.00	0.25	0.00	0.00	0.00
Fossil allochems, Total	(4.00)	(35.25)	(17.50)	(3.25)	(3.00)	(1.00)
Intraclasts, Total	0.00	0.00	0.00	(23.25)	(1.25)	(0.50)
Mudstone	0.00	0.00	0.00	0.00	0.00	0.00
Peloidal packstone	0.00	0.00	0.00	0.00	0.00	0.00
Oolitic packstone	0.00	0.00	0.00	23.25	1.25	0.50
Other types	0.00	0.00	0.00	0.00	0.00	0.00
Ooids, Total	(37.00)	(27.00)	(31.25)	(30.50)	(36.00)	(55.50)
Fibrous/Prismatic	37.00	27.00	31.25	2.75	5.75	14.00
Polycrystalline	0.00	0.00	0.00	0.00	16.50	38.00
Monocrystalline	0.00	0.00	0.00	27.75	13.75	3.50
Peloids	7.50	9.25	5.50	1.00	0.75	0.25
Micrite/Microspar	41.25	0.00	17.75	0.00	0.00	0.00
Void Filling Cement, Total	(5.50)	(26.25)	(17.75)	(29.00)	(52.25)	(41.25)
Fibrous/Bladed	1.75	2.50	5.50	23.75	52.25	41.25
Syntaxial	0.00	22.50	8.75	2.50	0.00	0.00
Blocky	3.75	1.25	3.50	2.75	0.00	0.00
Detrital quartz silt	0.00	2.25	0.00	0.00	0.00	0.00
Clay/Mica	0.00	0.00	0.00	0.00	0.00	0.00
Glauconite	0.00	0.00	8.25	0.25	0.00	0.00
Pyrite	0.00	0.00	0.00	0.00	0.00	0.00
Dolomite/Stylolite	4.75	0.00	2.00	12.75	2.25	0.25
Fracture/Fill Veins	0.00	0.00	0.00	0.00	4.50	1.25
Total	100.00	100.00	100.00	100.00	100.00	100.00

Table C.7. (continued).

Constituent	Sample Number					
	10A 1.00	10A 1.5	10A 1.8	10A 2.6	10A 2.8	10A 3.75
Echinoderms	2.25	0.25	0.75	0.25	0.25	1.25
Inarticulate brachiopods	0.00	0.00	0.00	0.00	0.00	0.00
Trilobites	1.00	0.00	0.00	0.25	0.50	0.25
Girvanella	0.00	0.00	0.00	0.00	0.00	0.00
Gastropods	0.00	0.00	0.00	0.00	0.00	0.00
Pelecypods	0.00	0.00	0.00	0.00	0.00	0.00
Chancelloria	0.00	0.00	0.00	0.00	0.00	0.00
Fossil allochems, Total	(3.25)	(0.25)	(0.75)	(0.50)	(0.75)	(1.50)
Intraclasts, Total	(1.00)	0.00	0.00	0.00	0.00	0.00
Mudstone	0.00	0.00	0.00	0.00	0.00	0.00
Peloidal packstone	0.00	0.00	0.00	0.00	0.00	0.00
Oolitic packstone	1.00	0.00	0.00	0.00	0.00	0.00
Other types	0.00	0.00	0.00	0.00	0.00	0.00
Ooids, Total	(50.25)	(50.75)	(54.75)	(53.00)	(57.00)	(50.25)
Fibrous/Prismatic	12.50	17.00	10.00	17.50	17.50	13.75
Polycrystalline	20.25	29.25	42.75	29.25	33.00	31.50
Monocrystalline	17.50	4.50	2.00	6.25	6.50	5.00
Peloids	0.75	2.50	1.75	4.25	2.50	2.50
Micrite/Microspar	0.00	1.25	0.00	1.50	0.75	16.75
Void Filling Cement, Total	(36.00)	(44.00)	(40.50)	(36.50)	(39.00)	(22.00)
Fibrous/Bladed	36.00	44.00	50.50	36.50	39.00	22.00
Syntaxial	0.00	0.00	0.00	0.00	0.00	0.00
Blocky	0.00	0.00	0.00	0.00	0.00	0.00
Detrital quartz silt	0.00	0.00	0.00	0.00	0.00	0.00
Clay/Mica	0.00	0.00	0.00	0.00	0.00	0.00
Glauconite	0.00	0.00	0.00	0.00	0.00	0.00
Pyrite	0.00	0.00	0.00	0.00	0.00	0.00
Dolomite/Stylolite	0.75	0.00	0.00	0.50	0.00	0.75
Fracture/Fill Veins	8.00	1.25	2.25	3.75	0.00	6.25
Total	100.00	100.00	100.00	100.00	100.00	100.00

Table C.7. (continued).

Constituent	Sample Number					
	IOA 3.9	IOA 4.5	IOA 4.9	IOA 5.1	IOA 5.3	IOA 5.4
Echinoderms	1.25	0.75	1.50	2.00	2.50	6.75
Inarticulate brachiopods	0.00	0.00	0.00	0.00	0.00	0.00
Trilobites	0.25	0.00	0.50	3.50	4.00	2.00
<u>Girvanella</u>	0.00	0.00	0.00	0.00	0.00	0.00
Gastropods	0.00	0.00	0.00	0.00	0.00	0.00
Pelecypods	0.00	0.00	0.00	0.00	0.00	0.00
<u>Chancelloria</u>	0.00	0.00	0.00	0.00	0.00	0.00
Fossil allochems, Total	(1.50)	(0.75)	(2.00)	(5.50)	(6.50)	(8.75)
Intraclasts, Total	0.00	0.00	0.00	(1.25)	0.00	0.00
Mudstone	0.00	0.00	0.00	0.00	0.00	0.00
Peloidal packstone	0.00	0.00	0.00	0.00	0.00	0.00
Oolitic packstone	0.00	0.00	0.00	1.25	0.00	0.00
Other types	0.00	0.00	0.00	0.00	0.00	0.00
Ooids, Total	(52.75)	(52.75)	(49.25)	(49.50)	(42.75)	(43.75)
Fibrous/Prismatic	10.75	7.50	10.25	37.25	37.00	27.75
Polycrystalline	37.50	41.00	29.00	5.00	5.00	14.75
Monocrystalline	4.50	4.25	10.00	7.25	0.75	1.25
Peloids	5.50	1.75	2.00	0.25	1.50	0.75
Micrite/Microspar	1.75	20.50	20.25	40.75	42.75	27.00
Void Filling Cement, Total	(30.75)	(19.25)	(20.50)	(1.25)	(3.50)	(7.00)
Fibrous/Bladed	30.75	19.25	20.50	1.25	3.50	7.00
Syntaxial	0.00	0.00	0.00	0.00	0.00	0.00
Blocky	0.00	0.00	0.00	0.00	0.00	0.00
Detrital quartz silt	0.00	0.00	0.00	0.00	0.00	0.00
Clay/Mica	0.00	0.00	0.00	0.00	0.00	0.00
Glauconite	0.00	0.00	0.00	0.00	0.00	0.00
Pyrite	0.00	0.00	0.00	0.00	0.00	0.00
Dolomite/Stylolite	0.75	0.50	6.00	1.50	3.00	12.75
Fracture/Fill Veins	7.00	4.50	0.00	0.00	0.00	0.00
Total	100.00	100.00	100.00	100.00	100.00	100.00

Table C.7. (continued).

Constituent	Sample Number					
	IOA 5.75	IOA 5.9	A2-1	A2-2	A6-2	A11-0
Echinoderms	6.00	17.50	4.00	2.25	1.50	5.00
Inarticulate brachiopods	0.00	0.00	0.00	0.00	0.00	0.25
Trilobites	4.75	3.50	5.50	1.50	3.75	6.25
Girvanella	0.00	0.00	0.00	0.00	0.00	0.00
Gastropods	0.00	0.00	0.00	0.00	0.00	0.25
Pelecypods	0.75	0.00	0.00	0.00	0.00	0.00
Chancelloria	0.00	0.00	0.00	0.00	0.00	0.50
Fossil allochems, Total	(11.50)	(21.00)	(9.50)	(3.75)	(5.25)	(12.25)
Intraclasts, Total	(0.75)	0.00	(9.00)	(1.75)	(1.75)	0.00
Mudstone	0.00	0.00				
Peloidal packstone	0.00	0.00				
Oolitic packstone	0.75	0.00				
Other types	0.00	0.00				
Ooids, Total	(37.75)	(35.50)	(18.00)	(38.00)	(45.00)	(24.50)
Fibrous/Prismatic	34.75	20.25				
Polycrystalline	0.00	0.25				
Monocrystalline	3.00	15.00				
Peloids	0.00	0.50	19.75	3.25	0.00	14.75
Micrite/Microspar	49.50	41.50	6.75	12.25	4.00	11.50
Void Filling Cement, Total	0.00	(0.75)	(34.50)	(41.00)	(43.75)	(31.75)
Fibrous/Bladed	0.00	0.75				
Syntaxial	0.00	0.00				
Blocky	0.00	0.00				
Detrital quartz silt	0.00	0.00	0.00	0.00	0.00	0.00
Clay/Mica	0.00	0.00	0.00	0.00	0.00	0.00
Glauconite	0.00	0.00	0.00	0.00	0.00	0.00
Pyrite	0.00	0.00	0.00	0.00	0.25	1.00
Dolomite/Stylolite	0.25	0.75	2.50	0.00	0.00	4.00
Fracture/Fill Veins	0.25	0.00	0.00	0.00	0.00	0.25
Total	100.00	100.00	100.00	100.00	100.00	100.00

Table C.8. Analysis of FPG Lithofacies (Volume %).

Constituent	Sample Number					
	I-28-1.6	I-34-2.5	I-39-1.5	I-60-3.0	BG-3-24.0	BG-5-4.8
Echinoderms	31.25	5.25	6.25	2.75	46.75	6.75
Inarticulate brachiopods	0.00	0.25	0.00	1.00	1.50	0.00
Trilobites	6.00	13.25	9.00	21.25	2.00	4.25
Girvanella	0.00	11.00	1.50	0.00	0.00	2.75
Gastropods	0.00	0.25	0.00	0.00	0.00	0.25
Pelecypods	0.00	1.25	0.25	0.00	0.00	0.25
Chancelloria	0.00	3.75	12.50	0.00	0.00	14.00
Sponge spicules	0.00	0.25	0.25	0.00	0.00	0.00
Fossil allochems, Total	(37.25)	(35.25)	(29.75)	(25.00)	(50.25)	(28.25)
Intraclasts, Total	0.00	0.00	0.00	0.00	0.00	0.00
Peloidal packstone	0.00	0.00	0.00	0.00	0.00	0.00
Ooids, Total	0.00	(5.75)	(3.50)	0.00	(11.75)	0.00
Fibrous/Prismatic	0.00	3.75	1.50	0.00	0.00	0.00
Monocrystalline	0.00	0.00	2.00	0.00	11.75	0.00
Superficial	0.00	2.00	0.00	0.00	0.00	0.00
Peloids	0.00	15.50	16.00	15.75	0.00	11.75
Micrite/Microspar	30.50	8.00	26.25	20.50	0.00	15.25
Void Filling Cement, Total	(20.25)	(16.50)	(14.50)	(26.00)	(22.50)	(7.75)
Fibrous/Bladed	9.00	2.00	4.75	19.25	2.75	0.00
Syntaxial	11.25	7.00	6.50	2.00	19.75	1.50
Blocky	0.00	7.50	3.25	4.75	0.00	6.25
Detrital quartz silt	0.00	0.75	0.00	0.00	0.00	0.00
Glauconite	0.00	0.25	0.00	0.00	0.00	0.00
Pyrite	0.00	0.00	0.50	0.00	0.00	0.00
Dolomite/Stylolite	12.00	18.00	9.50	8.75	15.50	31.25
Fracture/Fill Veins	0.00	0.00	0.00	4.00	0.00	5.75
Phosphate	0.00	0.00	0.00	0.00	0.00	0.00
Total	100.00	100.00	100.00	100.00	100.00	100.00

Table C.8. (continued).

Constituent	Sample Number			
	BG-5-22.5	BG-6-50.6	C39	C60
Echinoderms	3.50	2.75	11.50	0.25
Inarticulate brachiopods	0.25	0.25	0.00	4.50
Trilobites	6.00	45.50	7.25	12.50
Girvanella	0.00	0.50	2.50	8.25
Gastropods	0.00	0.00	0.00	0.00
Pelecypods	0.00	0.00	0.00	0.00
Chancelloria	18.00	0.00	16.75	0.00
Sponge spicules	0.00	0.25	2.75	0.00
Fossil allochems, Total	(27.75)	(49.25)	(40.75)	(25.50)
Intraclasts, Total	0.00	(5.00)	0.00	0.00
Peloidal packstone	0.00	5.00	0.00	0.00
Ooids, Total	(4.75)	0.00	0.00	0.00
Fibrous/Prismatic	3.25	0.00	0.00	0.00
Monocrystalline	1.50	0.00	0.00	0.00
Superficial	0.00	0.00	0.00	0.00
Peloids	8.75	2.75	14.75	33.50
Micrite/Microspar	35.50	19.00	26.75	6.75
Void Filling Cement, Total	(5.75)	0.00	(9.50)	(32.00)
Fibrous/Bladed	3.50	0.00	2.00	27.25
Syntaxial	0.00	0.00	4.75	0.00
Blocky	2.25	0.00	2.75	4.75
Detrital quartz silt	0.00	0.00	0.00	0.00
Glauconite	1.75	0.00	0.00	0.00
Pyrite	0.00	3.75	0.00	0.00
Dolomite/Stylolite	12.25	15.50	8.25	2.25
Fracture/Fill Veins	3.50	0.00	0.00	0.00
Phosphate	0.00	4.75	0.00	0.00
Total	100.00	100.00	100.00	100.00

Table C.9. Analysis of FPGWS Lithofacies (Volume %).

Constituent	Sample Number					
	I-1-7.4	I-60-12.6	I-65-5.7	BG-4-17.5	J-2 878	C43-0
Echinoderms	14.00	0.00	6.00	11.50	36.00	8.00
Inarticulate brachiopods	1.50	2.75	2.00	0.25	0.00	1.00
Trilobites	21.25	15.50	14.25	9.75	0.00	13.75
Girvanella	0.00	0.00	7.50	5.50	0.00	4.25
Chancelloria	0.00	0.00	0.00	2.00	0.00	0.00
Fossil allochems, Total	(36.75)	(18.25)	(29.75)	(29.00)	(36.00)	(27.00)
Peloids	3.75	4.50	12.25	28.00	5.75	24.50
Micrite/Microspar	0.00	0.00	19.50	19.50	0.00	13.50
Void Filling Cement, Total	(53.50)	(17.00)	(14.25)	(13.00)	0.00	(24.25)
Fibrous/Bladed	35.00	17.00	13.75	3.75	0.00	15.75
Syntaxial	18.50	0.00	1.50	2.00	0.00	4.25
Blocky	0.00	0.00	0.00	7.25	0.00	4.25
Detrital quartz silt	0.00	1.50	0.00	3.00	0.00	0.00
Clay/Mica	0.00	31.00	8.00	2.00	10.00	9.00
Glauconite	0.00	0.00	0.00	0.25	17.25	0.00
Pyrite	0.00	2.75	1.25	2.50	3.75	0.25
Dolomite/Stylolite	6.00	15.25	12.75	0.00	6.75	1.25
Fracture/Fill Veins	0.00	0.75	0.00	2.75	20.50	0.25
Phosphate	0.00	9.00	2.25	0.00	0.00	0.00
Total	100.00	100.00	100.00	100.00	100.00	100.00

Table C.9. (continued).

Constituent	Sample Number
	C43-1
Echinoderms	6.50
Inarticulate brachiopods	0.00
Trilobites	5.25
Girvanella	0.00
Chancelloria	12.75
Fossil allochems, Total	(24.50)
Peloids	20.75
Micrite/Microspar	26.75
Void Filling Cement, Total	(2.50)
Fibrous/Bladed	1.50
Syntaxial	1.00
Blocky	0.00
Detrital quartz silt	0.25
Clay/Mica	8.75
Glauconite	0.00
Pyrite	0.75
Dolomite/Stylolite	9.75
Fracture/Fill Veins	6.00
Phosphate	0.00
Total	100.00

Table C.10. Analysis of XPG Lithofacies (Volume %).

Constituent	Sample Number					
	I-6-2.5	I-11-1.1	J-2 819	J-2 812	BG-4-0.5	BG-4-1.5
Echinoderms	3.25	0.00	0.00	0.00	4.00	11.25
Inarticulate brachiopods	1.50	0.50	0.25	0.25	0.25	0.25
Trilobites	0.50	0.00	0.00	0.00	7.25	8.25
Girvanella	0.00	0.00	0.00	0.00	4.00	0.00
Fossil allochems, Total	(5.25)	(0.50)	(0.25)	(0.25)	(15.50)	(19.75)
Intraclasts, Total	0.00	0.00	0.00	0.00	0.00	(6.50)
Mudstone	0.00	0.00	0.00	0.00	0.00	6.50
Peloidal packstone	0.00	0.00	0.00	0.00	0.00	0.00
Ooids, Total	0.00	0.00	0.00	0.00	0.00	0.00
Fibrous/Prismatic	0.00	0.00	0.00	0.00	0.00	0.00
Monocrystalline	0.00	0.00	0.00	0.00	0.00	0.00
Superficial	0.00	0.00	0.00	0.00	0.00	0.00
Peloids	6.50	17.75	8.50	2.50	56.75	38.00
Micrite/Microspar	0.00	0.00	4.50	0.00	0.00	7.25
Void Filling Cement, Total	0.00	0.00	0.00	0.00	(8.75)	(15.50)
Fibrous/Bladed	0.00	0.00	0.00	0.00	0.00	1.50
Syntaxial	0.00	0.00	0.00	0.00	2.25	9.25
Blocky	0.00	0.00	0.00	0.00	6.50	4.75
Detrital quartz silt	13.75	1.25	39.25	55.00	0.25	1.75
Clay/Mica	11.00	6.00	20.00	14.75	0.75	0.00
Glauconite	4.25	3.75	4.25	7.50	0.50	0.00
Pyrite	1.50	0.00	0.00	0.25	0.00	0.00
Dolomite/Stylolite	57.75	70.75	17.75	16.00	17.00	8.25
Fracture/Fill Veins	0.00	0.00	5.50	3.75	0.50	3.00
Total	100.00	100.00	100.00	100.00	100.00	100.00

Table C.10. (continued).

Constituent	Sample Number			
	A1-1	A6-1	B5	C44
Echinoderms	3.75	3.25	0.25	2.50
Inarticulate brachiopods	0.00	0.75	1.50	0.25
Trilobites	0.25	8.50	7.25	1.75
Girvanella	0.00	2.25	4.00	0.00
Fossil allochems, Total	(4.00)	(14.75)	(13.00)	(4.50)
Intraclasts, Total	(1.50)	0.00	0.00	0.00
Mudstone	0.00	0.00	0.00	0.00
Peloidal packstone	1.50	0.00	0.00	0.00
Ooids, Total	(8.00)	(0.50)	(1.00)	(10.75)
Fibrous/Prismatic	6.75	0.25	1.00	10.75
Monocrystalline	1.25	0.00	0.00	0.00
Superficial	0.00	0.25	0.00	0.00
Peloids	52.00	53.75	59.75	51.50
Micrite/Microspar	6.75	3.75	4.50	1.75
Void Filling Cement, Total	(18.25)	(21.75)	(19.75)	(31.50)
Fibrous/Bladed	5.50	3.00	5.25	2.75
Syntaxial	1.50	4.25	0.00	7.25
Blocky	11.25	14.50	14.50	21.50
Detrital quartz silt	0.00	0.00	0.75	0.00
Clay/Mica	0.00	0.00	0.00	0.00
Glauconite	0.00	0.00	0.00	0.00
Pyrite	0.00	0.00	0.00	0.00
Dolomite/Stylolite	2.50	0.00	0.00	0.00
Fracture/Fill Veins	7.00	5.50	1.25	0.00
Total	100.00	100.00	100.00	100.00

Table C.11. Analysis of XPGWS Lithofacies (Volume %).

Constituent	Sample Number					
	I-32-1.9	I-32-2.0	I-42-0.3	I-57-1.6	I-74-0.3	BG-4-9.7
Echinoderms	3.25	11.25	6.25	1.00	1.25	1.50
Inarticulate brachiopods	0.00	0.00	0.00	0.25	0.25	0.25
Trilobites	16.00	3.25	6.00	17.25	5.50	12.25
Girvanella	3.00	0.00	0.00	0.00	3.25	0.00
Chancelloria	0.25	0.00	6.50	0.00	0.00	0.00
Sponge spicules	0.50	0.00	0.00	0.00	0.00	0.00
Fossil allochems, Total	(23.00)	(14.50)	(18.75)	(18.50)	(10.25)	(14.00)
Intraclasts, Total	(9.00)	(2.00)	(7.25)	0.00	0.00	(4.00)
Mudstone	4.25	0.00	0.00	0.00	0.00	4.00
Peloidal packstone	4.75	2.00	7.25	0.00	0.00	0.00
Ooids, Total	0.00	(1.75)	0.00	0.00	0.00	0.00
Fibrous/Prismatic	0.00	1.75	0.00	0.00	0.00	0.00
Peloids	21.25	20.25	13.50	24.25	21.00	31.25
Micrite/Microspar	15.00	32.00	8.25	8.75	33.50	6.25
Void Filling Cement, Total	(15.25)	(10.25)	(33.50)	(10.50)	(5.75)	(21.25)
Fibrous/Bladed	2.75	0.00	2.00	2.25	0.00	1.50
Syntaxial	0.00	4.00	20.25	0.00	0.00	0.00
Blocky	12.50	6.25	11.25	8.25	5.75	19.75
Detrital quartz silt	0.00	1.00	0.00	0.25	0.00	3.50
Clay/Mica	15.25	7.50	17.25	25.50	6.50	19.00
Glauconite	0.00	0.25	0.00	0.00	0.00	0.00
Pyrite	0.00	3.25	0.25	1.50	0.00	0.25
Dolomite/Stylolite	1.25	3.00	1.25	6.25	18.75	10.25
Fracture/Fill Veins	0.00	4.25	0.00	4.50	4.25	0.25
Phosphate	0.00	0.00	0.00	0.00	0.00	0.00
Total	100.00	100.00	100.00	100.00	100.00	100.00

Table C.11. (continued).

Constituent	Sample Number	
	BG-4-31.5	BG-6-27.4
Echinoderms	6.25	3.00
Inarticulate brachiopods	0.50	2.25
Trilobites	8.25	16.50
Girvanella	0.00	0.00
Chancelloria	0.00	0.00
Sponge spicules	0.00	0.00
Fossil allochems, Total	(15.00)	(21.75)
Intraclasts, Total	(5.50)	0.00
Mudstone	0.00	0.00
Peloidal packstone	5.50	0.00
Ooids, Total	0.00	0.00
Fibrous/Prismatic	0.00	0.00
Peloids	29.00	20.50
Micrite/Microspar	4.50	5.75
Void Filling Cement, Total	(20.75)	(27.75)
Fibrous/Bladed	0.25	2.75
Syntaxial	3.25	0.25
Blocky	17.25	24.75
Detrital quartz silt	2.25	0.25
Clay/Mica	6.25	11.50
Glauconite	0.00	0.75
Pyrite	0.00	0.00
Dolomite/Stylolite	11.25	9.50
Fracture/Fill Veins	5.50	0.25
Phosphate	0.00	2.00
Total	100.00	100.00

Table C.12. Analysis of SWXPG Lithofacies (Volume %).

Constituent	Sample Number					
	I-25-3.9	I-66-5.6	I-68-2.2	I-68-2.2	I-71-7.6	I-73-3.1
Echinoderms	0.00	0.00	0.00	0.25	2.50	1.50
Inarticulate brachiopods	1.50	0.25	0.00	0.00	5.75	0.50
Trilobites	0.50	2.50	3.25	4.25	2.25	6.25
Fossil allochems, Total	(2.00)	(2.75)	(3.25)	(4.50)	(10.50)	(8.25)
Intraclasts, Total	0.00	0.00	0.00	0.00	0.00	0.00
Peloidal packstone	0.00	0.00	0.00	0.00	0.00	0.00
Peloids	18.00	52.25	36.75	25.75	35.75	4.00
Micrite/Microspar	0.00	6.25	11.00	13.50	25.25	25.00
Void Filling Cement, Total	0.00	(12.00)	(11.50)	(5.25)	(1.50)	(11.50)
Fibrous/Bladed	0.00	0.00	0.00	1.75	1.50	11.50
Blocky	0.00	12.00	11.50	3.50	0.00	0.00
Detrital quartz silt	21.50	0.25	0.00	0.25	0.00	6.25
Clay/Mica	49.75	14.00	24.00	27.25	16.00	25.00
Glauconite	2.50	0.00	0.25	0.00	0.00	0.00
Pyrite	0.00	0.00	0.25	0.00	1.75	1.75
Dolomite/Stylolite	0.00	12.50	13.00	20.75	9.25	8.25
Fracture/Fill Veins	6.25	0.00	0.00	2.75	0.00	0.00
Phosphate	0.00	0.00	0.00	0.00	0.00	10.00
Total	100.00	100.00	100.00	100.00	100.00	100.00

Table C.12. (continued).

Constituent	Sample Number		
	J-2 997.5	J-2 612	J-2 459
Echinoderms	0.00	14.50	0.25
Inarticulate brachiopods	0.25	2.75	1.50
Trilobites	0.00	5.00	0.00
Fossil allochems, Total	(0.25)	(22.25)	(1.75)
Intraclasts, Total	0.00	0.00	(28.50)
Peloidal packstone	0.00	0.00	28.50
Peloids	3.75	6.25	0.00
Micrite/Microspar	0.00	9.25	0.00
Void Filling Cement, Total	0.00	0.00	0.00
Fibrous/Bladed	0.00	0.00	0.00
Blocky	0.00	0.00	0.00
Detrital quartz silt	21.25	0.25	1.50
Clay/Mica	62.25	47.25	54.00
Glauconite	3.50	0.00	0.25
Pyrite	2.00	2.50	3.50
Dolomite/Stylolite	2.50	12.25	10.50
Fracture/Fill Veins	4.50	0.00	0.00
Phosphate	0.00	0.00	0.00
Total	100.00	100.00	100.00

Table C.13. Analysis of Shale Lithofacies (Volume %).

Constituent	Sample Number					
	I-1-0.3	I-10-0.8	I-21-2.2	I-29-4.8	I-36-2.9	I-48-3.7
Echinoderms	1.50	0.00	3.00	0.00	0.00	0.00
Inarticulate brachiopods	2.75	6.25	1.25	1.75	1.75	0.25
Trilobites	0.25	0.50	0.25	0.25	0.00	0.00
Fossil allochems, Total	(4.50)	(6.75)	(4.50)	(2.00)	(1.75)	(0.25)
Intraclasts, Total	(3.50)	0.00	0.00	0.00	0.00	0.00
Mudstone	3.25	0.00	0.00	0.00	0.00	0.00
Peloidal packstone	0.25	0.00	0.00	0.00	0.00	0.00
Fossiliferous packstone	0.00	0.00	0.00	0.00	0.00	0.00
Peloids	16.25	36.25	27.50	44.25	61.25	49.75
Detrital quartz silt	0.25	0.50	2.25	0.25	0.50	0.75
Clay/Mica	71.50	53.25	54.00	45.50	31.00	45.75
Glauconite	0.00	0.75	0.00	0.75	0.00	0.00
Pyrite	0.00	0.00	0.25	4.25	0.00	1.75
Dolomite/Stylolite	4.00	2.25	11.50	3.00	5.50	1.75
Fracture/Fill Veins	0.00	0.25	0.00	0.00	0.00	0.00
Total	100.00	100.00	100.00	100.00	100.00	100.00

Table C.13. (continued).

Constituent	Sample Number					
	I-67-0.5	BG-4-4.5	B10	J-2 941	J-2 904.5	J-2 816.5
Echinoderms	0.00	0.00	0.25	2.25	0.25	0.00
Inarticulate brachiopods	1.50	2.75	1.75	2.75	12.50	6.50
Trilobites	0.00	0.00	5.00	0.25	0.50	0.00
Fossil allochems, Total	(1.50)	(2.75)	(7.00)	(5.25)	(13.25)	(6.50)
Intraclasts, Total	0.00	0.00	(2.25)	0.00	0.00	0.00
Mudstone	0.00	0.00	0.00	0.00	0.00	0.00
Peloidal packstone	0.00	0.00	2.25	0.00	0.00	0.00
Fossiliferous packstone	0.00	0.00	0.00	0.00	0.00	0.00
Peloids	43.25	39.25	11.75	43.75	32.75	8.75
Detrital quartz silt	1.25	0.50	3.50	9.25	4.25	1.25
Clay/Mica	50.25	56.25	45.25	37.00	46.00	82.25
Glauconite	0.75	0.25	0.00	0.50	1.25	0.75
Pyrite	1.50	0.00	1.50	2.50	2.00	0.25
Dolomite/Stylolite	1.50	1.00	28.75	1.75	0.50	0.25
Fracture/Fill Veins	0.00	0.00	0.00	0.00	0.00	0.00
Total	100.00	100.00	100.00	100.00	100.00	100.00

Table C.13. (continued).

Constituent	Sample Number			
	J-2 711	J-2 595	J-2 509	J-2 468
Echinoderms	0.00	0.00	3.75	2.25
Inarticulate brachiopods	4.75	11.75	9.00	1.25
Trilobites	0.00	0.00	1.25	0.00
Fossil allochems, Total	(4.75)	(11.75)	(14.00)	(3.50)
Intraclasts, Total	0.00	0.00	0.00	(2.00)
Mudstone	0.00	0.00	0.00	0.00
Peloidal packstone	0.00	0.00	0.00	1.75
Fossiliferous packstone	0.00	0.00	0.00	0.25
Peloids	21.25	15.00	19.00	9.75
Detrital quartz silt	3.25	2.00	6.25	1.50
Clay/Mica	69.00	53.50	56.25	79.75
Glauconite	1.50	0.25	3.25	1.25
Pyrite	0.25	3.00	0.00	1.50
Dolomite/Stylolite	0.00	6.00	1.25	0.75
Fracture/Fill Veins	0.00	8.50	0.00	0.00
Total	100.00	100.00	100.00	100.00

Table C.14. Analysis of IPG Lithofacies (Volume %).

Constituent	Sample Number					
	I-1-17.0	I-2-0.5	I-5-0.0	I-12-0.5	I-22-0.0	I-23-0.4
Echinoderms	0.25	6.25	2.00	0.25	15.25	3.50
Inarticulate brachiopods	0.00	0.00	0.00	0.00	0.00	0.00
Trilobites	2.00	4.00	2.50	1.75	8.75	2.25
Girvanella	0.00	0.00	0.00	3.50	3.25	0.00
Molluscs undifferentiated	0.00	0.00	0.00	0.00	0.00	0.00
Chancelloria	0.00	0.25	0.00	0.00	0.00	0.00
Sponge spicules	0.00	0.75	0.00	0.00	0.00	0.00
Other fossil allochems	0.00	0.00	0.00	0.00	0.00	0.00
Fossil allochems, Total	(2.25)	(11.25)	(4.50)	(5.50)	(27.25)	(5.75)
Intraclasts, Total	(62.25)	(37.50)	(50.25)	(53.00)	(42.50)	(46.25)
Mudstone	33.50	22.50	38.50	41.75	3.50	30.75
Peloidal packstone	28.75	11.50	0.25	11.25	39.00	15.50
Fossiliferous packstone	0.00	0.00	0.00	0.00	0.00	0.00
Oolitic packstone	0.00	0.00	0.00	0.00	0.00	0.00
Quartz siltstone	0.00	0.00	0.00	0.00	0.00	0.00
Other types	0.00	3.50	11.50	0.00	0.00	0.00
Ooids, Total	0.00	0.00	0.00	0.00	0.00	0.00
Fibrous/Prismatic	0.00	0.00	0.00	0.00	0.00	0.00
Peloids	0.25	16.00	22.00	11.75	5.25	22.75
Micrite/Microspar	0.00	9.00	9.25	9.25	2.75	8.50
Void Filling Cement, Total	0.00	(14.25)	(6.25)	(12.25)	(11.00)	(7.25)
Micrite	0.00	0.00	0.00	0.00	0.00	0.00
Fibrous/Bladed	0.00	8.25	1.75	2.75	4.50	3.75
Syntaxial	0.00	2.50	0.00	0.00	6.50	0.00
Blocky	0.00	3.50	4.50	9.50	0.00	3.50
Detrital quartz silt	2.25	0.00	0.00	0.00	0.00	0.00
Clay/Mica	28.00	0.00	0.00	0.00	0.00	0.00
Glauconite	0.75	0.00	0.00	0.00	0.00	0.00
Pyrite	1.50	0.00	0.00	0.00	4.75	2.00
Dolomite/Stylolite	1.75	9.00	6.25	4.25	6.50	7.50
Fracture/Fill Veins	1.00	3.00	1.50	4.00	0.00	0.00
Total	100.00	100.00	100.00	100.00	100.00	100.00

Table C.14. (continued).

Constituent	Sample Number					
	I-29-5.7	I-44-1.5	I-50-1.2	I-51-0.5	I-59-0.4	I-61-2.0
Echinoderms	9.00	1.50	6.25	1.75	4.50	0.25
Inarticulate brachiopods	0.00	0.00	0.00	0.00	0.25	0.00
Trilobites	2.50	4.75	3.00	10.50	9.50	2.00
Girvanella	0.00	2.25	2.25	0.00	1.50	0.00
Molluscs undifferentiated	0.00	0.00	0.00	0.00	0.00	0.00
Chancelloria	0.00	3.00	0.00	0.00	0.00	0.00
Sponge spicules	0.25	0.75	0.00	1.50	0.00	0.00
Other fossil allochems	0.00	0.00	0.00	0.00	0.00	0.00
Fossil allochems, Total	(11.75)	(12.25)	(11.50)	(13.75)	(15.75)	(2.25)
Intraclasts, Total	(27.00)	(31.25)	(36.75)	(38.75)	(57.50)	(65.25)
Mudstone	14.50	14.25	0.00	4.25	0.00	0.00
Peloidal packstone	10.00	10.25	32.25	34.50	27.25	65.25
Fossiliferous packstone	0.00	4.50	4.50	0.00	30.25	0.00
Oolitic packstone	0.00	2.25	0.00	0.00	0.00	0.00
Quartz siltstone	0.00	0.00	0.00	0.00	0.00	0.00
Other types	2.50	0.00	0.00	0.00	0.00	0.00
Ooids, Total	(9.75)	(6.50)	0.00	0.00	0.00	0.00
Fibrous/Prismatic	9.75	6.50	0.00	0.00	0.00	0.00
Peloids	12.00	22.50	16.50	4.50	11.50	2.50
Micrite/Microspar	16.50	3.75	2.75	12.50	3.75	2.75
Void Filling Cement, Total	(10.00)	(13.75)	(24.25)	(10.00)	(11.00)	(0.50)
Micrite	2.50	0.00	0.00	0.00	0.00	0.00
Fibrous/Bladed	6.00	4.50	3.75	7.50	2.75	0.25
Syntaxial	1.50	3.00	12.00	0.00	3.75	0.00
Blocky	0.00	6.25	8.50	2.50	4.50	0.25
Detrital quartz silt	0.50	0.00	0.00	0.00	0.00	0.00
Clay/Mica	0.00	0.00	0.00	3.75	0.00	0.25
Glauconite	0.25	0.00	0.00	0.00	0.00	0.00
Pyrite	2.00	4.25	5.00	0.00	0.25	0.00
Dolomite/Stylolite	10.25	2.75	3.25	16.75	0.25	26.50
Fracture/Fill Veins	0.00	3.00	0.00	0.00	0.00	0.00
Total	100.00	100.00	100.00	100.00	100.00	100.00

Table C.14. (continued).

Constituent	Sample Number					
	I-64-0.7	I-68-7.4	BG-1-17.1	BG-1-25.2	BG-2-6.2	BG-3-35.5
Echinoderms	11.25	5.50	2.50	0.25	13.75	3.75
Inarticulate brachiopods	0.00	0.00	0.00	0.00	0.00	0.00
Trilobites	6.25	15.25	1.50	3.25	4.75	0.25
Girvanella	1.50	0.00	0.00	0.00	0.25	0.00
Molluscs undifferentiated	0.00	0.00	0.00	0.00	0.00	0.00
Chancelloria	0.00	0.00	0.00	0.00	0.00	0.00
Sponge spicules	0.00	0.00	0.00	1.25	0.00	0.00
Other fossil allochems	0.00	0.00	0.00	0.00	0.00	0.00
Fossil allochems, Total	(19.00)	(20.75)	(4.00)	(4.75)	(18.75)	(4.00)
Intraclasts, Total	(46.50)	(44.75)	(66.50)	(65.50)	(51.50)	(70.00)
Mudstone	12.50	5.50	66.50	46.00	0.00	0.00
Peloidal packstone	5.50	6.25	0.00	19.50	51.50	6.75
Fossiliferous packstone	12.25	33.00	0.00	0.00	0.00	4.75
Oolitic packstone	0.00	0.00	0.00	0.00	0.00	0.00
Quartz siltstone	0.00	0.00	0.00	0.00	0.00	58.50
Other types	16.25	0.00	0.00	0.00	0.00	0.00
Ooids, Total	(0.25)	0.00	0.00	0.00	(0.25)	0.00
Fibrous/Prismatic	0.25	0.00	0.00	0.00	0.25	0.00
Peloids	2.50	5.50	7.75	3.75	2.75	2.50
Micrite/Microspar	0.00	0.00	12.00	18.50	0.00	0.00
Void Filling Cement, Total	(18.50)	(16.50)	0.00	(3.75)	(14.25)	0.00
Micrite	0.00	0.00	0.00	0.00	0.00	0.00
Fibrous/Bladed	1.50	2.75	0.00	0.00	1.75	0.00
Syntaxial	11.50	6.75	0.00	0.00	9.75	0.00
Blocky	5.50	7.00	0.00	3.75	2.75	0.00
Detrital quartz silt	0.00	0.00	0.00	0.00	0.00	5.50
Clay/Mica	0.00	0.00	3.25	0.00	0.00	17.00
Glauconite	0.00	0.00	0.00	0.00	0.00	0.00
Pyrite	0.50	0.75	0.00	0.00	0.00	0.00
Dolomite/Stylolite	12.75	11.75	6.50	3.75	10.50	1.00
Fracture/Fill Veins	0.00	0.00	0.00	0.00	2.00	0.00
Total	100.00	100.00	100.00	100.00	100.00	100.00

Table C.14. (continued).

Constituent	Sample Number					
	BG-3-41.0	BG-4-8.0	BG-5-0.0	BG-6-2.0	BG-6-28.2	BG-6-56.8
Echinoderms	16.75	3.50	11.25	0.25	6.75	1.75
Inarticulate brachiopods	0.50	0.50	0.25	0.00	0.75	0.50
Trilobites	6.75	8.50	6.00	4.25	7.00	4.25
Girvanella	0.50	6.75	0.25	0.00	0.75	0.25
Molluscs undifferentiated	0.00	0.00	0.00	0.00	0.50	0.25
Chancelloria	0.00	0.25	0.75	0.00	0.00	0.00
Sponge spicules	0.75	1.75	1.75	0.00	0.50	0.00
Other fossil allochems	0.00	0.00	0.00	0.00	0.00	0.00
Fossil allochems, Total	(25.25)	(21.25)	(20.25)	(4.50)	(16.25)	(7.00)
Intraclasts, Total	(44.25)	(45.00)	(34.25)	(70.50)	(47.75)	(77.00)
Mudstone	6.00	0.00	6.25	30.25	0.00	0.00
Peloidal packstone	38.25	45.00	28.00	40.25	31.25	0.00
Fossiliferous packstone	0.00	0.00	0.00	0.00	16.50	77.00
Oolitic packstone	0.00	0.00	0.00	0.00	0.00	0.00
Quartz siltstone	0.00	0.00	0.00	0.00	0.00	0.00
Other types	0.00	0.00	0.00	0.00	0.00	0.00
Ooids, Total	0.00	0.00	0.00	0.00	0.00	0.00
Fibrous/Prismatic	0.00	0.00	0.00	0.00	0.00	0.00
Peloids	5.50	18.00	5.50	5.75	12.00	0.00
Micrite/Microspar	2.75	0.00	20.50	0.00	6.00	4.50
Void Filling Cement, Total	(14.00)	(1.50)	(11.50)	(2.25)	(11.00)	0.00
Micrite	0.00	0.00	0.00	0.00	0.00	0.00
Fibrous/Bladed	3.50	0.00	1.75	0.00	2.75	0.00
Syntaxial	9.50	0.00	5.75	0.00	4.00	0.00
Blocky	1.00	1.50	4.00	2.25	4.25	0.00
Detrital quartz silt	0.00	0.00	0.00	0.00	0.00	0.00
Clay/Mica	0.00	3.50	0.00	8.00	0.00	5.25
Glauconite	0.00	0.00	0.00	0.00	0.00	0.00
Pyrite	1.50	0.00	0.75	0.00	0.50	0.00
Dolomite/Stylolite	6.75	10.75	6.25	9.00	6.50	6.25
Fracture/Fill Veins	0.00	0.00	1.00	0.00	0.00	0.00
Total	100.00	100.00	100.00	100.00	100.00	100.00

Table C.14. (continued).

Constituent	Sample Number					
	BG-6-65.2	J-2 1005	J-2 972.5	A3-1	A4-0	A7-1
Echinoderms	0.75	7.50	1.75	8.00	2.00	5.75
Inarticulate brachiopods	0.00	0.25	0.00	0.75	0.00	0.00
Trilobites	3.25	1.50	0.75	5.50	7.75	5.50
Girvanella	0.00	0.00	0.00	0.00	0.00	0.00
Molluscs undifferentiated	0.00	0.00	0.00	0.00	0.00	0.00
Chancelloria	0.00	0.00	0.00	0.00	0.00	0.00
Sponge spicules	0.00	0.00	0.00	0.00	0.00	0.00
Other fossil allochems	0.00	0.00	0.00	3.25	0.00	1.00
Fossil allochems, Total	(4.00)	(9.25)	(2.50)	(17.50)	(9.75)	(12.25)
Intraclasts, Total	(77.75)	(77.50)	(92.00)	(20.25)	(25.75)	(54.50)
Mudstone	0.00	0.00	0.00			
Peloidal packstone	8.00	0.00	0.00			
Fossiliferous packstone	69.75	0.00	92.00			
Oolitic packstone	0.00	0.00	0.00			
Quartz siltstone	0.00	77.50	0.00			
Other types	0.00	0.00	0.00			
Ooids, Total	0.00	0.00	0.00	0.00	0.00	0.00
Fibrous/Prismatic	0.00	0.00	0.00			
Peloids	0.00	6.50	0.75	16.75	31.25	9.50
Micrite/Microspar	0.00	0.00	0.00	10.25	6.25	0.25
Void Filling Cement, Total	0.00	(3.25)	0.00	(29.25)	(9.00)	(18.50)
Micrite	0.00	0.00	0.00			
Fibrous/Bladed	0.00	1.50	0.00			
Syntaxial	0.00	1.75	0.00			
Blocky	0.00	0.00	0.00			
Detrital quartz silt	0.00	1.75	1.25	0.00	0.00	0.00
Clay/Mica	14.00	0.25	3.25	0.00	0.00	0.00
Glauconite	0.00	0.50	0.25	0.00	0.00	0.00
Pyrite	0.00	0.75	0.00	1.75	0.75	0.00
Dolomite/Stylolite	4.25	0.00	0.00	4.25	17.25	5.00
Fracture/Fill Veins	0.00	0.25	0.00	0.00	0.00	0.00
Total	100.00	100.00	100.00	100.00	100.00	100.00

Table C.14. (continued).

Constituent	Sample Number				
	A13-1	A14-1	A18	B1	B13
Echinoderms	2.50	1.50	0.00	0.00	0.00
Inarticulate brachiopods	0.25	1.25	0.75	0.75	0.00
Trilobites	6.75	7.75	13.00	19.00	4.75
Girvanella	0.00	0.00	0.00	0.00	0.00
Molluscs undifferentiated	0.00	0.00	0.00	0.00	0.00
Chancelloria	0.00	0.00	0.00	0.00	0.00
Sponge spicules	0.00	0.00	0.00	0.00	0.00
Other fossil allochems	0.00	0.00	0.00	0.00	0.00
Fossil allochems, Total	(9.50)	(10.50)	(13.75)	(19.75)	(4.75)
Intraclasts, Total	(31.00)	(37.50)	(35.00)	(34.00)	(35.00)
Mudstone					
Peloidal packstone					
Fossiliferous packstone					
Oolitic packstone					
Quartz siltstone					
Other types					
Ooids, Total	0.00	0.00	0.00	0.00	0.00
Fibrous/Prismatic					
Peloids	16.75	14.25	30.00	26.00	0.75
Micrite/Microspar	11.00	12.00	11.00	7.00	50.75
Void Filling Cement, Total	(29.00)	(20.00)	(2.00)	(2.00)	(1.75)
Micrite					
Fibrous/Bladed					
Syntaxial					
Blocky					
Detrital quartz silt	0.00	0.00	0.00	0.00	0.25
Clay/Mica	0.00	0.00	0.00	0.00	0.00
Glauconite	0.00	0.00	0.00	0.00	0.00
Pyrite	0.00	0.00	0.00	0.00	0.00
Dolomite/Stylolite	1.50	3.00	5.00	8.00	6.75
Fracture/Fill Veins	1.25	2.75	3.25	3.25	0.00
Total	100.00	100.00	100.00	100.00	100.00

APPENDIX D

X-RAY DIFFRACTION ANALYSIS OF SHALE

EXPERIMENTAL PROCEDURE AND DISCUSSION

Twenty-two shale samples from the Nolichucky Shale were selected for X-ray analysis (Table D.1). Each sample was excavated and carefully bagged. Every practical precaution was taken to acquire uncontaminated and nonweathered samples. In the laboratory, approximately 10 gm of each sample was weighed out and ground down for 30 minutes to a fine powder using a mortar and pestle. Then, each 10 gm sample was suspended in a 1000 ml beaker filled with deionized water. The sediment was stirred vigorously for 5 minutes. After 30 minutes of particle settling, the upper 500 ml of water were pipetted into a 600 ml beaker. Deionized water was added to fill the 600 ml beaker; the water level (column) in the beaker was 10 cm deep. The sediment was suspended by stirring for 3 minutes. The sample which remained in the 1000 ml beaker was discarded. The fine-grained sediment in the 600 ml beaker settled for 3 hours, after which time the upper 5 cm of the water column was pipetted to another beaker. The pipetted mixture represents the < 2 micron size fraction. One week (7 days) was allotted for the clay-sized particles to settle out of suspension. From the accumulation of sediment on the bottom of the beaker, 1 elutriated slide mount was prepared. An elutriated slide was prepared for each of the 22 samples using the procedure described above.

A Philips diffractometer was used to analyze each slide; the diffractometer was set up for Cu K alpha radiation at 35 kv and 17 ma. Three analyses were conducted on each sample: (1) untreated, (2) treated with ethylene glycol at 60 degrees C for 12 hours, and (3) heated to 550 degrees C for 1 hour. Each analysis was performed with the normal scale set at 100 counts with a time constant of 2 seconds. The goniometer drive was set at 1 degree 2 theta per minute.

Results of the X-ray diffraction analysis are shown in Tables D.2 and D.3. It is important to note that virtually no temporal or spatial variability is observed in the clay mineral suite. That is, individual samples reveal identical clay mineral assemblages. Figure D.1 shows a typical X-ray diffractogram from the Nolichucky Shale.

Table D.1. Samples used in XRD analysis of shale.

Section Locality	Unit Number (keyed to units in Appendix B)	Feet Above Base Of Unit	Meters Below Base Of Maynardville (mbM)
I-75	1	3.0	99
I-75	6	1.2	87
I-75	15	3.4	82
I-75	20	3.0	76
I-75	29	4.8	64
I-75	36	7.1	53
I-75	46	1.0	44
I-75	56	1.0	33
I-75	63	12.4	18
I-75	71	7.6	2
I-75	73	2.4	1
BG	1	1.7	90
BG	1	21.3	83
BG	3	17.5	74
BG	3	57.5	61
BG	4	5.0	50
BG	4	26.0	44
BG	4	32.0	42
BG	5	19.7	35
BG	6	20.8	28
BG	6	38.7	18
BG	6	82.1	5

Table D.2. D-spacings (in Angstrom units) of the observed X-ray diffraction peaks.

Peak	Untreated	Glycolated	Heated
1	14.5(22)	15.5(19)B	14.2(22)
2	10.1(22)A	10.0(22)A	10.1(22)
3	7.14(20)	7.13(19)	
4	4.99(22)	5.00(22)	5.02(22)
5	4.25(22)	4.25(22)	4.25(22)
6	3.54(14)	3.55(18)	3.53(11)
7	3.34(22)	3.34(22)	3.34(22)

Numbers in parentheses indicate the number of samples in which the peak was observed (maximum is 22). Broad peaks are labelled B; asymmetrical peaks are labelled A.

Table D.3. Identification of the principal clay minerals and quartz in the Nolichucky.

Peak	Untreated	Glycolated	Heated	Identified Minerals
1	14.5	expands	dehydrates	Fe-chlorite
2	10.1	no change	no change	Mixed layer illite-Vermiculite; hydrated illite-chlorite
3	7.14	no change	disappears	Fe-chlorite; kaolinite (?)
4	4.99	no change	no change	Illite
5	4.25	no change	no change	Quartz
6	3.54	no change	no change	Chlorite; kaolinite (?); illite
7	3.34	no change	no change	Illite; quartz

Values are expressed in Angstrom units.

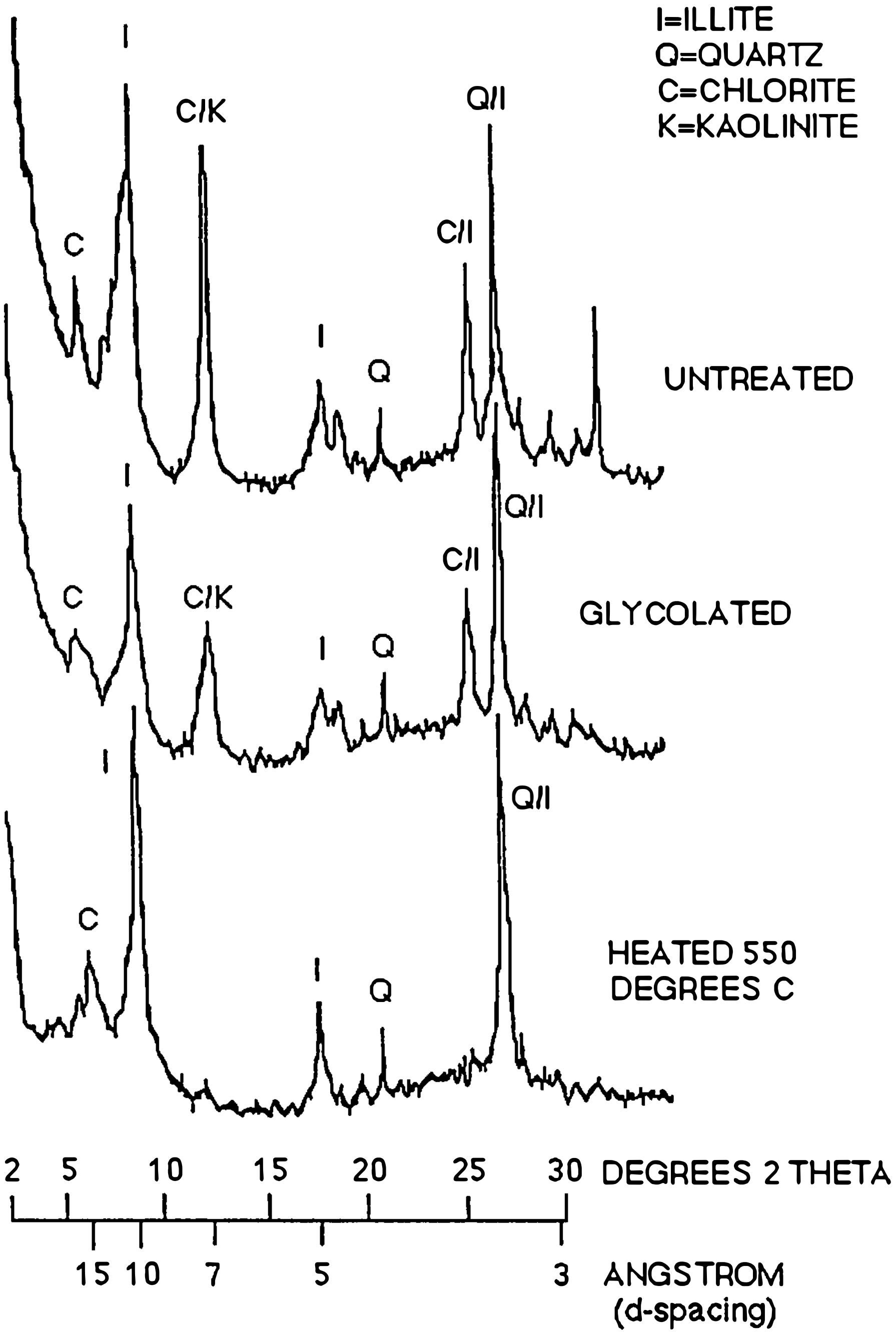

Figure D.1. Typical X-ray diffractogram of the Nolichucky Shale.

VITA

Lawrence James Weber Jr. was born on January 25, 1959 in Fulton, Missouri. After living in Missouri, Texas, Ohio, and Indiana for several years, Jim's family settled down in Olney, Illinois. There he attended public school and was graduated from East Richland High School in May 1977. The following Fall he entered DePauw University in Greencastle, Indiana, where he studied Liberal Arts. In May, 1981, Jim received a Bachelor of Arts degree from DePauw with a major in Geology.

In the Fall of 1981, Jim accepted a Teaching Assistantship at the Department of Geosciences, The New Mexico Institute of Mining and Technology (NMIMT), and began study toward a Master of Science. In December, 1983 he was awarded the M.S. degree in Geology from the NMIMT.

In September of 1983, Jim entered the Graduate School of The University of Tennessee. From 1983 to 1985 he was employed by the Geology Department as a Graduate Teaching Assistant and Course Instructor. In 1985, Jim was awarded a Graduate Research Fellowship with the Environmental Sciences Division, Oak Ridge National Laboratories. In August 1988 Jim received the Doctor of Philosophy degree with a major in geology.

Mr. Weber is a member of the American Association of Petroleum Geologists, the Canadian Society of Petroleum Geologists, the Geological Society of America, the Society of Economic Paleontologists and Mineralogists, and Sigma Xi. He is married to the former Teresa Lyn Mizer; they had their first child, Taylor Elizabeth Weber, on January 25, 1988. Jim is currently employed as a Reservoir Geologist by Mobil Oil in Midland, Texas.